Implications of ocean acidification for microbial life and for microbial interactions

Dissertation zur Erlangung des Doktorgrades der Naturwissenschaften

- Dr. rer. nat. -

dem Fachbereich 2 Biologie/Chemie der Universität Bremen

vorgelegt von

Christiane Hassenrück

Bremen, April 2016

Die vorliegende Arbeit wurde in der Zeit von Februar 2013 bis April 2016 am Max-Planck-Institut für Marine Mikrobiologie angefertigt.

1. Gutachterin: Prof. Dr. Antje Boetius

2. Gutachter: Prof. Dr. Michael Friedrich

Tag des Promotionskolloquiums: 13. Juni 2016

“The more clearly we can focus our attention on the wonders and realities of the universe around us, the less taste we shall have for destruction.” – Rachel Carson

Summary

Ocean acidification (OA) is a major threat to marine systems impacting many aspects of marine life. Microbial communities are a crucial component of marine systems, and are involved in several important processes necessary to support ecosystem functioning. Despite their importance, very little is known about how OA will affect microbial communities and the services they provide to the ecosystem. In particular the long-term impact of OA on microbial life in natural systems is poorly understood. Previous studies were largely based on laboratory or short-term experiments, and often reported inconsistent results regarding the response of microbial communities and processes to OA. To go beyond the limited scope of such experiments, study sites that are naturally exposed to elevated CO_2 concentration are increasingly being studied as analogues for future OA. Here, shallow-water hydrothermal CO_2 vents in a tropical coral reef were investigated as model system to provide an ecosystem perspective on OA effects on reef microbial communities. The diversity and function of microbial communities, as well as interactions with other reef organisms were characterized in different reef environments at the CO_2 vents to estimate potential OA effects and to assess the suitability of this model system for OA research.

In **chapter 1**, a detailed environmental characterization of the study sites was conducted. The results showed that sediments at the CO_2 vents can be affected by factors other than CO_2 such as temperature, organic matter content or alterations in pore water element concentrations. Hence, a comprehensive description of the environment is necessary when using hydrothermal CO_2 vents as OA analogues. Indeed, the investigation of microbial communities in the sediment (**chapter 2**) showed that pH was among the factors significantly, yet not mainly, explaining changes in microbial community composition. Therefore, changes in OA-related variables may often not be the primary cause of microbial changes in a complex environment such as hydrothermal CO_2 vents. Furthermore, changes in microbial taxa were identified, which may alter biogeochemical cycling in the sediment at the CO_2 vents. In **chapter 3**, sediment microbial processes related to carbon, nitrogen and sulfur cycling at the CO_2 vents were further explored. Whereas some processes, such as photosynthesis and carbohydrate degradation, did not appear to be strongly affected, sulfate reduction and nitrogen cycling

seemed to be impacted at the CO_2 vents. This indicates that some remineralization functions in reef sediments may be influenced by CO_2 venting.

Microbial communities on seagrass leaves (**chapter 4**) showed pronounced differences at the CO_2 vents compared to reference sites, with a higher prevalence of bacteria associated with coral diseases. This suggests a potential role of seagrasses as vectors for coral pathogens, thus supporting predictions about decreased reef health under increased CO_2 conditions. A settlement experiment, described in **chapter 5**, revealed only a minor effect of pH on the development of bacterial communities, with other factors, such as light exposure or close interactions with other organisms, potentially being more important in shaping bacterial communities.

In conclusion, microbial communities, functions and interactions with other reef organisms were fundamentally altered at the CO_2 vents. However, the strength of the influence of the CO_2 vents seemed to depend on the investigated reef environment. The changes in microbial communities and processes may contribute to a general decline of the reef ecosystem at hydrothermal CO_2 vents. This thesis offers new insights into microbial life at shallow-water hydrothermal CO_2 vents, as well as predictions about potential OA impacts. Yet, it also emphasizes the challenge of estimating future OA effects based on observation at OA analogues that exhibit such high environmental complexity as shallow-water hydrothermal CO_2 vents.

Zusammenfassung

Ozeanversauerung stellt eine große Bedrohung für marine Systeme dar, die viele Aspekte des Lebens im Meer beeinflusst. Mikrobielle Gemeinschaften sind ein bedeutender Bestandteil mariner Systeme und tragen zu vielen Prozessen bei, die notwendig sind, um das Ökosystem zu erhalten. Trotz ihrer Bedeutung ist wenig darüber bekannt, wie Ozeanversauerung mikrobielle Gemeinschaften und ihre Funktion im Ökosystem beeinflusst. Insbesondere Langzeiteffekte von Ozeanversauerung auf mikrobielles Leben in natürlichen Systemen sind kaum erforscht. Vorherige Studien basierten größtenteils auf Labor- oder Kurzzeitexperimenten und berichteten oft widersprüchliche Ergebnisse bezüglich der Reaktion von mikrobiellen Gemeinschaften und Prozessen auf Ozeanversauerung. Um den begrenzten Umfang solcher Experimente zu erweitern, werden vermehrt Standorte untersucht, die natürlich erhöhten CO_2-Konzentrationen ausgesetzt sind, und somit als Modell für zukünftige Ozeanversauerung dienen. In dieser Arbeit wurden hydrothermale CO_2-Quellen im Flachwasser eines tropischen Korallenriffs als Modellsystem erforscht, um die Auswirkungen von Ozeanversauerung auf mikrobielle Gemeinschaften in einem ökosystemweiten Zusammenhang zu untersuchen. Die Diversität und Funktion von mikrobiellen Gemeinschaften auf dem Riff und ihre Interaktionen mit anderen Rifforganismen wurden in verschiedenen Lebensräumen an den CO_2-Quellen charakterisiert, um auf mögliche Auswirkungen von Ozeanversauerung zu schließen und die Tauglichkeit dieses Modellsystems für die Forschung über Ozeanversauerung zu bewerten.

In **Kapitel 1** wurden die Umweltbedingungen in dem Untersuchungsgebiet detailliert charakterisiert. Die Ergebnisse zeigten, dass Sedimente an den CO_2-Quellen auch von anderen Faktoren als CO_2 beeinflusst werden können, wie z.B. Temperatur, dem Gehalt organischen Materials oder Veränderungen in der Elementzusammensetzung des Porenwassers. Deswegen ist eine umfangreiche Beschreibung der Umweltbedingungen notwendig, wenn hydrothermale CO_2-Quellen als Modell für Ozeanversauerung benutzt werden. Tatsächlich zeigte die Untersuchung der mikrobiellen Gemeinschaften im Sediment (**Kapitel 2**), dass der pH-Wert zwar zu den Faktoren gehörte, die Veränderungen in der Zusammensetzung mikrobieller Gemeinschaften erklären konnten, aber nicht die größte Bedeutung hatte. Deshalb sind Änderungen von

Faktoren, die mit Ozeanversauerung in Verbindung stehen, möglicherweise nicht die vorwiegende Ursache von mikrobiellen Veränderungen in der komplexen Umgebung der hydrothermalen CO_2-Quellen. Weiterhin wurden Veränderungen mikrobieller Taxa festgestellt, die Auswirkungen auf biogeochemische Kreisläufe im Sediment an den CO_2-Quellen haben könnten. In **Kapitel 3** wurden mikrobielle Prozesse im Sediment näher untersucht, die an Kohlenstoff-, Stickstoff- und Schwefelkreisläufen an den CO_2-Quellen beteiligt sind. Während einige Prozesse wie z.B. Photosynthese und Kohlenhydratabbau nicht stark betroffen waren, schienen die CO_2-Quellen Auswirkungen auf Sulfatreduktion und Stickstoffkreislauf zu haben. Dies lässt vermuten, dass einige Remineralisierungsprozesse in Riffsedimenten von den CO_2-Quellen beeinflusst werden.

Mikrobielle Gemeinschaften auf Seegrasblättern, die in **Kapitel 4** untersucht wurden, zeigten deutliche Unterschiede an den CO_2-Quellen im Vergleich zu Referenzstandorten mit einer vermehrten Häufigkeit von Bakterien, die mit Korallenkrankheiten in Verbindung gebracht wurden. Dieses Ergebnis deutet auf eine potenzielle Rolle von Seegräsern als Überträger von Korallenpathogenen hin und unterstützt Hypothesen zu einem verschlechterten Zustand von Riffen unter erhöhten CO_2-Bedingungen. Ein Besiedlungsexperiment (**Kapitel 5**) zeigte, dass der pH-Wert nur einen vernachlässigbaren Einfluss auf die Entwicklung bakterieller Gemeinschaften hatte, während andere Faktoren wie z.B. Lichteinwirkung oder Wechselwirkungen mit anderen Organismen potenziell einen größeren Effekt hatten.

Diese Arbeit zeigte, dass mikrobielle Gemeinschaften, Funktionen und Interaktionen mit anderen Rifforganismen grundlegende Unterschiede an den CO_2-Quellen aufweisen. Die Intensität des Einflusses der CO_2-Quellen schien jedoch von dem untersuchten Lebensraum abhängig zu sein. Die Veränderungen an mikrobiellen Gemeinschaften und Prozessen tragen möglicherweise zu einer allgemeinen Verarmung des Riffökosystems an den CO_2-Quellen bei. Weiterhin bietet diese Arbeit neue Einblicke in mikrobielles Leben an hydrothermalen CO_2-Quellen im Flachwasser und mögliche Prognosen über potentielle Auswirkungen von Ozeanversauerung. Dennoch bleibt es eine Herausforderung, von den Beobachtungen an Modellsystemen, die eine so komplexe Umwelt aufweisen wie hydrothermale CO_2-Quellen, auf Effekte zukünftiger Ozeanversauerung zu schließen.

Contents

Abbreviations xi

1. Introduction 1

1.1 Ocean acidification 1

1.1.1 Ocean acidification effects on marine microbes 3

1.1.2 Shallow-water hydrothermal CO_2 *vents as ocean acidification analogues* 5

1.2 Role of microbial communities in coral reef ecosystems 12

1.3 Thesis objectives 14

1.4 Methods 16

1.4.1 Sampling area 16

1.4.2 Molecular community analysis 19

1.4.3 Bioinformatic sequence processing 22

1.4.4 Statistical approaches to microbial ecology 24

1.5 Publication outline 25

2. Thesis chapters 29

Chapter 1 31

Chapter 2 67

Chapter 3 109

Chapter 4 165

Chapter 5 193

3. Discussion and outlook 211

3.1 Effect of hydrothermal CO_2 venting on microbial communities in different reef environments 211

3.2 Whole ecosystem effects of hydrothermal CO_2 venting in a coral reef 213

3.3 Suitability of hydrothermal CO_2 vents as OA analogues 216
3.4 Future of microbial research at natural OA analogues 217
Bibliography 221
Acknowledgements 231
Appendix 233
Additional co-author publications 233
Conference presentations 235
Cruise Participation 236
Teaching and Tutoring 237
Erklärung 239

Abbreviations

OA	Ocean acidification
PNG	Papua New Guinea
HI	Hydrothermal influence
ARISA	Automated Ribosomal Intergenic Spacer Analysis
TRFLP	Terminal Restriction Fragment Length Polymorphism
NGS	Next generation sequencing
OTU	Operational taxonomic unit
metaG	Metagenomic
metaT	Metatranscriptomic
PCA	Principal Component Analysis
RDA	Redundancy analysis
NMDS	Non-metric multidimensional scaling
ANOSIM	Analysis of similarity
TA	Total alkalinity

1. Introduction

1.1 Ocean acidification

Ocean acidification (OA) is defined as a decrease in ocean water pH caused by increased atmospheric CO_2 concentrations (Caldeira & Wickett 2003). The concentration of CO_2 in the world's oceans is in a chemical equilibrium with the CO_2 concentrations in the atmosphere. Therefore, an increase in atmospheric CO_2 partial pressure (pCO_2) leads to an elevated dissolution of CO_2 in the ocean. In the water, CO_2 dissociates into bicarbonate and carbonate releasing protons, which influences seawater pH (Figure 1A). Over the last 800 000 years, there have been periodic fluctuations in atmospheric and seawater pCO_2 ranging from approximately 180 ppm to 280 ppm with pH fluctuations between approximately 8.3 and 8.1 (Pelejero et al. 2010). However, within the last decades climate change has led to an increase in atmospheric CO_2 far exceeding the speed of natural fluctuations with levels unprecedented in recent earth history (Figure 1B; Pelejero et al. 2010). Since preindustrial times about 30% of the anthropogenically released CO_2 in the atmosphere has been taken up by the ocean, causing a decrease in seawater pH by 0.1 units from approximately 8.2 to 8.1, corresponding to an increase in protons by 26% (IPCC 2013). The decreasing trend in seawater pH is expected to continue, reaching pH 7.8 by the year 2100 under the current and predicted CO_2 emissions trajectories (IPCC 2013). As a consequence of the pH change the composition of the inorganic carbon pool in the ocean is shifting towards an increased availability of CO_2 and a reduced availability of carbonate, and therefore a decrease of the saturation state of calcium carbonate (Figure 1C; Barker & Ridgwell 2012).

These changes in the carbonate system are expected to have dramatic effects on marine life (see Doney et al. 2009, and Kroeker et al. 2013). Since many calcifying pelagic and benthic organisms use calcium carbonate to build up skeletal features, they are considered to be among the most vulnerable to OA and have long been the main focus of OA studies. Indeed, increased pCO_2 negatively affected benthic calcifiers such as corals (Hoegh-Guldberg et al. 2007), crustose coralline algae (Ragazzola et al. 2012, Fabricius et al. 2015), molluscs (Gazeau et al. 2007), echinoderms (Dupont et al. 2010),

and pelagic calcifiers such as coccolithophores (Ziveri et al. 2014) and pteropods (Orr et al. 2005). However, increased pCO_2 also has effects on non-calcifying organisms and can e.g. alter fish sensory perception (Munday et al. 2014), and increase algal and seagrass growth (Koch et al. 2013). Marine microbial communities have only recently been studied in the context of OA, but are expected to respond to OA with far-reaching consequences for marine ecosystems (Liu et al. 2010, Joint et al. 2011).

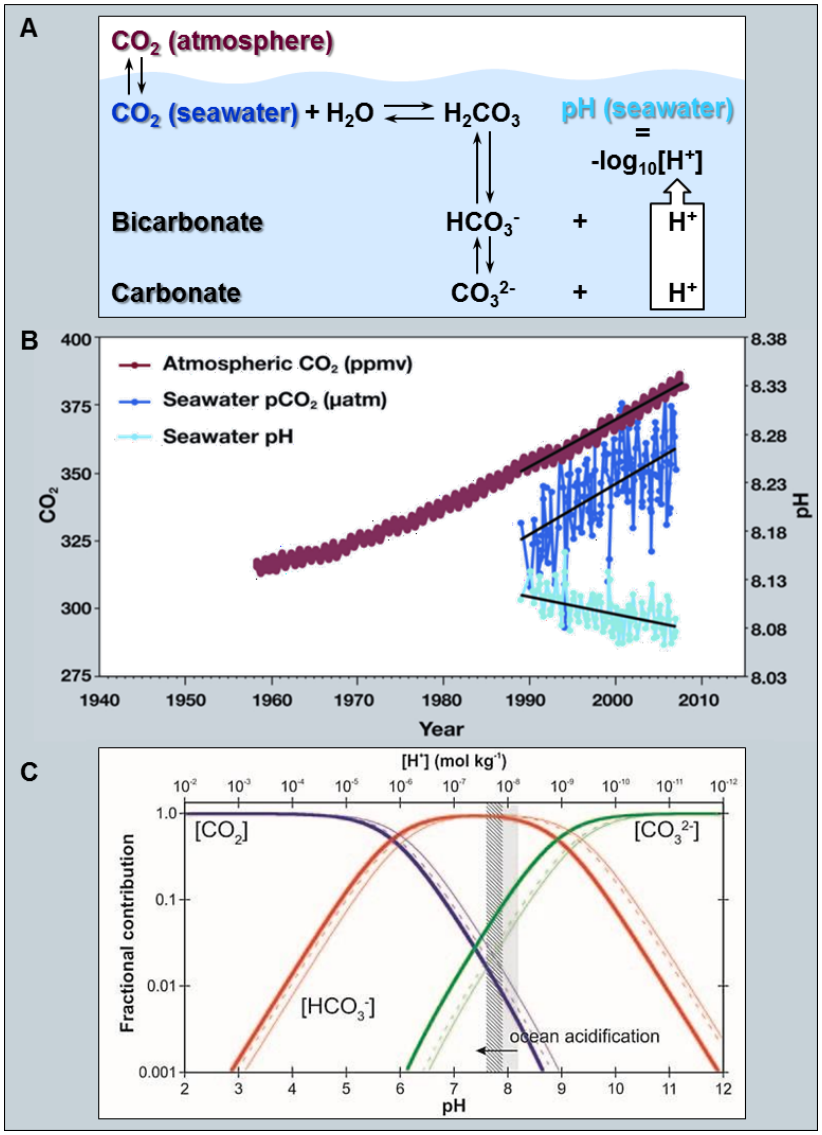

Figure 1: Carbonate chemistry. A: The carbonate system in the ocean showing the dissolution of CO_2 from the atmosphere, the different forms of dissociation and effects on seawater pH. B: Trends in atmospheric and seawater CO_2 concentrations and seawater pH measured at Mauna Loa, Hawai'i (source: http://www.pmel.noaa.gov; accessed 27.01.2016). C: Bjerrum plot showing the relative proportions of bicarbonate, carbonate and CO_2 in the dissolved inorganic carbon pool in seawater at different temperature, salinity and pressure conditions (heavy curves: S = 35‰, T = 25ºC, P = 0 bar; narrow curves: S = 35, T = 0ºC, P = 0 bar; dashed curves: S = 35, T = 0ºC, P = 300 bar). The shaded region indicates the range of modern (annual average) ocean surface pH, while the hashed region indicates the projected range for the year 2100 (modified after Barker & Ridgwell 2012).

1.1.1 Ocean acidification effects on marine microbes

Marine microbial communities generally include bacteria and archaea as well as small eukaryotes (protists) such as diatoms (Liu et al. 2010), and their versatile activities provide important ecosystem services. Marine microbial communities play a major role in global element cycles, where they are involved in primary production and remineralization, nitrogen and sulfur cycling. Besides, they mediate colonization and biofouling processes, as well as diseases and symbioses. Therefore, microbial communities constitute an integral component of ecosystem functioning in pelagic, benthic, biofilm or host-associated environments. It is crucial to understand how microbial communities, their abundance, diversity, composition, function and interactions will be affected by OA to estimate how the services they provide may change in the future ocean.

Laboratory studies about OA effects on microbial communities were so far mainly focused on water column communities from temperate and polar systems. Of particular interest were the microbial communities contributing to primary production, carbon degradation and nitrogen cycling (Table 1A). Under increased pCO_2 conditions dominant cyanobacterial strains show elevated carbon and nitrogen fixation rates with the potential to fundamentally alter nutrient cycles in the open ocean (Hutchins et al. 2007, Fu et al. 2008). Fu et al. (2008) further emphasized the importance of the interaction of OA effects with other environmental factors, such as nutrient limitation, since under iron-limited conditions increased pCO_2 did not affect nitrogen fixation rates of a cyanobacterial *Crocosphaera* strain. Furthermore, the response of cyanobacterial strains to pCO_2 increases was not uniform with some strains showing decreased nitrogen fixation rates (Czerny et al. 2009, Gradoville et al. 2014). Nitrification processes in the water column declined at high pCO_2 leading to the hypothesis that OA may reduce the availability of oxidized nitrogen compounds (Hutchins et al. 2009, Beman et al. 2011). The hydrolytic degradation of organic carbon compounds was stimulated under increased pCO_2 conditions suggesting an increase in carbon turnover under future OA (Piontek et al. 2010, Maas et al. 2013).

To increase the scope of OA experiments beyond the limits of laboratory studies, mesocosm experiments were conducted to investigate whole community responses to OA

by manipulating pCO_2 in a close-to-natural setting. Phytoplankton communities, especially pico- and nanoeukaryotes, benefitted most from an increased pCO_2, most likely as a consequence of the increased availability of dissolved CO_2 leading to a reduced cost of converting bicarbonate to CO_2 during photosynthetic carbon fixation (Newbold et al. 2012, Brussaard et al. 2013, Sala et al. 2016). On the contrary, the response of the bacterioplankton community was not uniform across different mesocosm experiments. Many studies did not report strong OA effect on bacterial abundance, diversity and community composition (Table 1B), although in some cases increases in bacterial abundance (Grossart et al. 2006, Endres et al. 2014), decreases in bacterial diversity (Zhang et al. 2012) and shifts in bacterial community composition were observed (Allgaier et al. 2008). Increased carbon degradation rates by bacterioplankton, as demonstrated by laboratory studies, were observed in most but not all mesocosm experiments (Grossart et al. 2006). Despite these inconsistencies, the mesocosm studies concluded that seasonal dynamics, such as phytoplankton blooms, have a stronger effect on bacterioplankton communities than OA, and that OA effects may indeed depend on such temporal patterns (Grossart et al. 2006, Allgaier et al. 2008, Piontek et al. 2013, Endres et al. 2014).

Microbial communities in other environments than the water column are far less studied. Current knowledge from laboratory experiments suggests that microbes in surface biofilms or host-associated communities show a more pronounced response to increased pCO_2, which consistently caused a shift in microbial community composition (Table 1A+B). However, the taxa contributing to this shift varied according to environment and experimental setting, e.g. in coral-associated bacterial communities, disease-related taxa increased at increased pCO_2 (Vega Thurber et al. 2009, Meron et al. 2011). Laboratory experiments on sediment microbial communities focused mostly on microbial remineralization rates rather than community composition, with variable results (Kitidis et al. 2011, Laverock et al. 2013, Braeckman et al. 2014, Gazeau et al. 2014). Whereas most argue that remineralization in the sediment will not be affected by OA (Kitidis et al. 2011, Laverock et al. 2013, Gazeau et al. 2014), others reported decreased oxygen consumption and nitrification rates (Braeckman et al. 2014). Tait et al. (2013)

further emphasized the importance of archaea in sediment communities, since they may respond differently to increased pCO_2 than bacteria.

Despite an increasing effort to disentangle the effects of OA on microbial communities, the above observations revealed many inconsistencies regarding the response of marine microbes to increased pCO_2. However, most of these studies were based on short-term perturbation experiments that required an active manipulation of the carbonate system, although long-term OA effects under natural conditions are often of more interest to the scientific community (Liu et al. 2010). Furthermore, laboratory and mesocosm studies are biased towards observations on planktonic microbial communities, while other environments remain vastly underexplored. To address these issues, naturally CO_2-rich sites are increasingly being used as natural analogues for OA. They offer the opportunity to study whole ecosystem effects in a system that is acclimatized to high pCO_2. Shallow-water hydrothermal CO_2 vents constitute such naturally CO_2-rich sites (Hall-Spencer et al. 2008).

1.1.2 Shallow-water hydrothermal CO_2 vents as ocean acidification analogues

Shallow-water hydrothermal vents (or seeps, which is used as synonym here) are distributed worldwide and are mostly associated with active tectonic plate margins (Tarasov et al. 2005). They are found e.g. in the Mediterranean Sea (Molari et al. in preparation, Wenzhöfer et al. 2000, Hall-Spencer et al. 2008, Vizzini et al. 2013), in the Atlantic around the Azores (Cardigos et al. 2005), in the Pacific off Mexico (Prol-Ledesma et al. 2004) and Taiwan (Tang et al. 2013), around New Zealand (Burrell et al. 2015) and off Papua New Guinea (Fabricius et al. 2011). In general, shallow-water hydrothermal vents are characterized by active gas venting and hydrothermal fluid discharge, however, physico-chemical conditions vary between different vents (Tang 2013). The expelled gases consist mainly of CO_2 (range: 45 to > 99%), N_2 (range: < 1 to 54%), CH_4 (range: < 1 to 10%), H_2S (range: < 1 to 8%), and H_2 (range: < 1 to 3%). Vent fluid geochemistry shows an enrichment of Mn, Si, Li and Fe, and a depletion of Mg, Na, Cl and SO_4 comparable to deep-sea hydrothermal vent fluids (German & von Damm 2003). Furthermore, the temperature in the vicinity of the shallow-water hydrothermal vents is often severely increased reaching values of more than 100°C (Tang 2013).

Shallow-water hydrothermal vents therefore constitute extreme environments. Because pCO_2 is often not the only factor that is different at the vent compared to ambient conditions, not all shallow-water hydrothermal vents can readily be used as OA analogues.

Most OA studies at shallow-water hydrothermal vents are focused on the vents in the Mediterranean Sea, specifically around Ischia, Vulcano and Panarea Island, and the Milne Bay area in Papua New Guinea. At all these sites, the gas composition is dominated by CO_2 (> 90%), with only traces of components that may confound CO_2 effects such as H_2S (Molari et al. in preparation, Hall-Spencer et al. 2008, Fabricius et al. 2011, Vizzini et al. 2013). The localized venting of CO_2 creates a pCO_2/pH gradient in the water column that includes pCO_2/pH values projected for the future ocean under current climate change models (Hall-Spencer et al. 2008, Fabricius et al. 2011). Since seawater temperature is often not noticeably increased at these sites, the CO_2 vents have also been referred to as volcanic instead of hydrothermal (Hall-Spencer et al. 2008).

Recent studies on microbial communities at CO_2 vents used as OA analogues reported variable results regarding OA effects on microbial abundance, diversity and community composition (Table 1C). In the water column, total bacterial communities seem to be resistant to the reduced pH conditions at the CO_2 vents (Molari et al. in preparation), although increases in bacterial abundance and shifts in community composition have also been reported (Burrell et al. 2015, Chauhan et al. 2015). Burrell et al. (2015) further detected a shift in the active bacterial community, which was however not investigated in the other studies. As observed in short-term experiments, microbial biofilms and host-associated microbial communities often responded more strongly to the reduced pH conditions at the CO_2 vents than water column communities, although the response in host-associated communities appears to be host-specific (Lidbury et al. 2012, Meron et al. 2012, 2013, Morrow et al. 2014). Unlike in laboratory and mesocosm experiments, sediment microbial communities have received more attention at CO_2 vents. Previous studies have so far consistently reported a shift in microbial community composition including microphytobenthos (Table 1C). Nevertheless, they disagree to some extent on which taxa are responsible for that shift, and whether the shift is accompanied by a decrease or increase in microbial diversity (Molari et al. in preparation,

Kerfahi et al. 2014, Taylor et al. 2014, Raulf et al. 2015). Only little data are available on microbial functions at CO_2 vents. First results suggest that trends in the organic carbon degradation potential of microbial communities are largely consistent with laboratory and mesocosm studies (Burrell et al. 2015), whereas nitrification seems rather unaffected at CO_2 vents (Kitidis et al. 2011). Molari et al. (in preparation) further reported decreases in sulfate reduction rates under the reduced pH conditions.

The investigation of hydrothermal CO_2 vents as OA analogues has yielded valuable insights into microbial communities under increased pCO_2/reduced pH conditions. However, the research at these OA analogues is still in its infancy and many open questions remain. Although hydrothermal CO_2 vents have been carefully selected as OA analogues based on their gas composition, the pCO_2/pH gradient is likely confounded by other parameters related to the reduced pH conditions, e.g. concentrations of major and trace elements, or temperature (Vizzini et al. 2013). It is therefore important to keep in mind that the conditions at hydrothermal CO_2 vents are only an approximation of future OA scenarios. Furthermore, there is a considerable lack of data regarding microbial functions at OA analogues. Previous studies investigated microbial community composition and diversity using trends in specific microbial taxa as proxy for changes in microbial functions (Morrow et al. 2014, Raulf et al. 2015). However, apart from a few studies (Molari et al. in preparation, Kitidis et al. 2011, Burrell et al. 2015), measurements of whole community metabolic rates are rare. Additionally, observations at OA analogues are 'patchy' in terms of study location, environment type, applied methods, observed environmental parameters and microbial target group. This makes it difficult to find a consensus among studies regarding OA effects on microbial communities.

Table 1: Summary of OA studies on microbial communities in short-term laboratory (A) and mesocosm experiments (B) as well as at shallow-water hydrothermal CO_2 vents as OA analogues (C). Arrows indicate increase (↑) or decrease (↓). No observed changes are indicated by a hyphen (–).

	pCO_2/pH	Effect at reduced pH	Reference
A: Laboratory experiments			
Trichodesmium (Atlantic and Pacific strains)	pCO_2 150 – 1500 ppm	Nitrogen fixation ↑ Carbon fixation ↑	(Hutchins et al. 2007)
Trichodesmium (North Pacific)	pCO_2 180 – 1600 ppm	Carbon fixation – Nitrogen fixation –	(Gradoville et al. 2014)
Crocosphaera (North Pacific strain)	pH 8.5 –7.9	Fe-replete: Growth rates ↑ Nitrogen fixation ↑ Carbon fixation ↑ Fe-limited: Growth rates ↑ Nitrogen fixation – Carbon fixation ↑	(Fu et al. 2008)
Nodularia (Baltic Sea)	pH 8.6 – 7.9	Cell division rates ↓ Nitrogen fixation ↓	(Czerny et al. 2009)
Planktonic cyanobacteria (subtropical North Atlantic)	pH 8.4 – 7.8	*Trichodesmium*: N_2 fixation ↑ C fixation ↑ *Prochlorococcus*/*Synechococcus*: minor	(Lomas et al. 2012)
Bacterioplankton (North Sea)	pH 8.2 – 7.7	Bacterial abundance – Bacterial diversity ↑– Shift in bacterial community OA effects modulated by season	(Krause et al. 2012)
Bacterio- and phytoplankton (Antarctica)	pH 7.8 – 7.7	Bacteria: Abundance ↑ Active fraction ↓ Diversity ↓ Hydrolysis ↑ Phytoplankton: Growth rates ↑ Diatoms ↑	(Maas et al. 2013)
Bacterioplankton polysaccharide degraders (North Atlantic)	pH 8.3 – 7.7	Polysaccharide degradation ↑ Enzymatic activity ↑	(Piontek et al. 2010)
Planktonic nitrifiers (North Atlantic, North Pacific)	pH 8.1 – 7.4	Nitrification ↓	(Beman et al. 2011)
Water column nitrifiers (Coastal North Pacific)	pH 8.0 – 6.0	Nitrification ↓	(Huesemann et al. 2002)
Bacterial and algal biofilm (Great Barrier Reef)	pH 8.1 – 7.6	Shift in algal community O_2 production/consumption – Carbon and nitrogen content ↑ Shift in bacterial community	(Witt et al. 2011)

	pCO_2/pH	Effect at reduced pH	Reference
Various reef-associated bacterial biofilms (Great Barrier Reef)	pH 8.1 – 7.5	Shift in bacterial community	(Webster et al. 2012)
CCA-associated bacterial biofilm (Great Barrier Reef)	pH 8.1 – 7.5	Shift in bacterial community	(Webster et al. 2013)
Coral-associated microbes (Hawai'i)	pH 8.1 – 6.7	Shift in community composition and genetic potential: Disease-associated ↑ Antibiotics resistance ↑	(Vega Thurber et al. 2009)
Coral-associated bacteria (Red Sea)	pH 8.2 – 7.3	Bacterial diversity ↑ Shift in bacterial community: Disease-associated ↑	(Meron et al. 2011)
Active sediment bacterial and archaeal communities (Arctic)	pH 8.1 – 7.2	Shift in active community	(Tait & Laverock 2013)
Sediment communities (Arctic)	pH 8.1 – 7.2	Mineralization − Denitrification −	(Gazeau et al. 2014)
Sediment nitrifiers and denitrifiers[a] (Arctic)	pH 8.1 – 7.2	AOB *amoA* transcripts ↓ Shift in active AOB community AOA *amoA* transcripts ↑ AOA community – Anammox ↑	(Tait et al. 2014)
Sediment and water column nitrifiers (English Channel)	pH 8.0 – 6.1	Sediment: Nitrification − Water column: Nitrification ↓	(Kitidis et al. 2011)
Sediment communities (North Sea)	pH 8.0 – 7.7	Oxygen consumption ↓ Nitrification ↓ Total N mineralization –	(Braeckman et al. 2014)
B: Mesocosms			
Bacterio- and phytoplankton (Mediterranean)	pH 8.1 – 7.8	Phototrophic pico- and nanoeukaryotes ↑ Bacterial picoplankton and phototrophic microplankton ↓↑ OA effects modulated by nutrient regime and season	(Sala et al. 2016)
Phytoplankton (Arctic)	pH 8.2 – 7.5	picoeukaryotic photoautotrophs ↑ nanophytoplankton ↑	(Brussaard et al. 2013)
Bacterioplankton (Arctic)	pH 8.3 – 7.8	Enzymatic activity ↑ Primary production ↑ Response of bacteria coupled to bloom dynamics	(Piontek et al. 2013)
Bacterioplankton (Norway)	pH 8.1 – 7.5	Bacterial abundance ↑ Protein hydrolysis ↑ Response of bacteria coupled to bloom dynamics	(Endres et al. 2014)
Bacterioplankton (Arctic)	pH 8.4 – 7.5	Bacterial community composition: minor	(Roy et al. 2013)

	pCO_2/pH	Effect at reduced pH	Reference
Bacterio- and phytoplankton (Norway)	pH 8.3 – 7.8	Bacteria: Abundance – Community composition – Shift in eukaryotic community	(Newbold et al. 2012)
Bacterio- and phytoplankton (Baltic)	pH 7.6 – 6.7	Bacterial abundance – Bacterial community composition: minor	(Lindh et al. 2013)
Bacterioplankton (Arctic)	pH 8.3 – 7.5	Bacterial diversity ↓ Bacterial community composition: minor	(Zhang et al. 2012)
Bacterioplankton (Norway)	pH 8.3 – 7.8	Bacterial abundance – Bacterial community composition: minor	(Oliver et al. 2014)
Bacterioplankton (Norway)	pCO_2 190 – 700 ppm	Bacterial abundance ↑ Bacterial protein production ↑ Protease activity ↑ Glucosidase activity – Response of bacteria coupled to bloom dynamics	(Grossart et al. 2006)
Bacterioplankton (Norway)	pCO_2 350 – 1050 ppm	Bacterial abundance – Bacterial protein production – Shift in free-living bacterial community Response of bacteria coupled to bloom dynamics	(Allgaier et al. 2008)
Sediment nitrifiers (Plymouth Sound)	pH 8.1 – 6.8	Surface sediment: Nitrification − Burrow wall: Nitrification ↓	(Laverock et al. 2013)
C: Natural systems			
Ischia			
Sediment and water column nitrifiers	pH 8.2 – 7.6	Nitrification −	(Kitidis et al. 2011)
Coral-associated bacteria	pH 8.1 – 7.3	Bacterial community composition: minor	(Meron et al. 2012)
Coral-associated bacteria	pH 8.1 – 7.0	Bacterial diversity ↑ Shift in bacterial community	(Meron et al. 2013)
Vulcano Island			
Bacterioplankton	pH 8.0 – 6.7	Shift in community	(Chauhan et al. 2015)
Bacterial and eukaryotic biofilm	pH 8.2 – 7.7	Bacterial diversity ↑ Shift in bacterial and eukaryotic community	(Lidbury et al. 2012)
Microalgal biofilm	pH 8.2 – 7.7	Shift in diatom community Cyanobacterial abundance –	(Johnson et al. 2011)
Epilithic and sediment microphytobenthos	pH 8.2 – 6.8	Shift in diatom community	(Johnson et al. 2015)

	pCO_2/pH	Effect at reduced pH	Reference
Sediment bacteria	pH 8.2 – 7.7	Carbon and nitrogen content – Bacterial diversity ↑ Shift in rare bacterial community	(Kerfahi et al. 2014)
Intertidal epilithic bacteria	pH 8.2 – 7.7	Bacterial diversity ↓ Shift in bacterial community	(Taylor et al. 2014)
Panarea			
Sediment, seagrass, water column communities	pH 8.1 – 7.5	Sulfate reduction ↓ Bacterial abundance – Shift in sediment bacterial community	(Molari et al. in preparation)
New Zealand			
Bacterioplankton	pH 8.0 – 7.7	Aminopeptidase activity – Glucosidase activity ↑ Bacterial abundance ↑ Bacterial diversity ↑ Shift in active bacterial community	(Burrell et al. 2015)
Papua New Guinea			
Coral and sponge-associated bacteria	pH 8.1 – 7.3	Bacterial diversity: Coral-associated ↓ Sponge-associated ↑ Shift in bacterial community	(Morrow et al. 2014)
Sediment bacteria and archaea	pH 8.3 – 6.9	Bacterial diversity ↑ Rare bacteria ↑ Shift in bacterial community: Archaeal diversity – Rare archaea ↑ Shift in archaeal community	(Raulf et al. 2015)

[a] AOB: ammonia oxidizing bacteria, AOA: ammonia oxidizing archaea, *amoA*: ammonia monooxygenase gene subunit A, Anammox: anaerobic ammonium oxidation.

1.2 Role of microbial communities in coral reef ecosystems

Coral reefs are among the most diverse ecosystems on the planet, but also belong to the ecosystems most threatened by OA (Hoegh-Guldberg et al. 2007). One of the most studied natural OA analogues is a hydrothermal CO_2 vent system in a coral reef in Papua New Guinea. These vents have been extensively used to investigate long-term OA effects on reef communities in their natural environment, e.g. corals (Strahl, Francis, et al. 2015, Strahl, Stolz, et al. 2015), seagrass (Russell et al. 2013, Takahashi et al. 2015), macroalgae (Johnson et al. 2012, Vogel et al. 2015), foraminifera (Uthicke et al. 2013), reef fishes (Munday et al. 2014), macroinvertebrates (Fabricius et al. 2014), crustose coralline algae (Fabricius et al. 2015), as well as first observations on microbial communities (Morrow et al. 2014, Raulf et al. 2015).

Coral reefs are a highly productive system despite their occurrence in ultra-oligotrophic waters. Microbial remineralization processes are crucial in maintaining the high productivity by facilitating efficient nutrient recycling. Especially reef sediments, which can occupy up to ten times as much area as the coral reef framework, are majorly involved in biogeochemical cycling and the remineralization of organic matter (Gattuso et al. 1998, Rasheed et al. 2002). Microbial remineralization processes include the aerobic respiration of organic carbon compounds in the oxygenated layers of the sediment, as well as the anaerobic degradation in deeper, anoxic sediment layers coupled to denitrification and sulfate reduction (Fenchel & Jorgensen 1977). Microbes are further key players in all steps of the nitrogen cycle, an element which is usually depleted in coral reef waters and requires rapid recycling (Rusch & Gaidos 2013). Photosynthetic microbes, predominantly cyanobacteria and small eukaryotes, such as diatoms, are also involved in carbon fixation, although their contribution is minor compared to corals, specifically their dinoflagellate symbionts, and macroalgae (Boucher et al. 1998). Apart from remineralization processes, microbial communities mediate colonization processes, such as coral larval settlement (Webster et al. 2004) or the establishment of biofouling communities (Dang & Lovell 2000), and are also implicated in coral diseases (Bourne et al. 2008, Sato et al. 2010). Therefore microbial communities play a major role in reef maintenance and health (Ainsworth et al. 2010, Garren & Azam 2012).

Given the versatile role of microbial communities in various aspects of coral reef ecosystem functioning, it is crucial to understand how microbial communities and the services they provide will be affected by OA in an ecosystem context. There is a still limited but growing number of studies available on OA effects on microbial communities in coral reefs at natural OA analogues. Observations from the hydrothermal CO_2 vent system in Papua New Guinea are so far restricted to a study on coral-associated microbes (Morrow et al. 2014) and a first description of the bacterial and archaeal community in the sediment (Raulf et al. 2015). Furthermore, very little is known about microbial functions and processes at this hydrothermal CO_2 vent system.

1.3 Thesis objectives

Microbial communities in different reef environments play a crucial role in various processes on coral reefs, such as remineralization, nutrient cycling and colonization, which are necessary to maintain coral reef ecosystems. To predict how coral reef ecosystems will be impacted by climate change stressors, such as OA, it is therefore necessary to understand how microbial communities may respond to OA, and how microbial functions and interactions with other reef organisms may be affected. To assess OA effects on microbes in their natural environment, investigations should go beyond the limited scope of laboratory experiments and include the study of natural analogues for OA such as hydrothermal CO_2 vents. So far little is known about microbial communities at naturally CO_2-rich coral reefs, and previous results are often contradictory. Furthermore, besides the advantage of studying whole ecosystem effects, natural OA analogues pose a challenge to scientists because of the inherent complexity of natural systems, which may confound OA effects and requires a detailed characterization of the environment.

The overall objective of this PhD study was to provide an ecosystem perspective on ocean acidification effects on reef microbial communities using a shallow-water hydrothermal CO_2 vent system in Papua New Guinea as a model system. The aims were (I) to better understand the diversity and function of reef microbial communities as well as interactions with other reef organisms at the hydrothermal CO_2 vents, (II) to compare the effect of CO_2 venting on microbial communities in different reef environments, and finally (III) to estimate ocean acidification effects on microbial communities based on the observations at the hydrothermal vents and assess the suitability of this model system for OA research.

To address these aims the chapters of this PhD thesis focus on the following research questions:

- How does the CO_2 venting change the physico-chemical conditions in the reef sediment, and how does this in turn affect its inhabiting biota and remineralization functions? (Chapter 1)

- To which extend is the composition of the microbial community in the sediment influenced by the changes in the biogeochemical conditions described in chapter 1, and which microbial taxa may benefit or suffer from these changes? (Chapter 2)
- Does the CO_2 venting influence element cycling in the reef sediment? (Chapter 3)
- To which extend are the composition and succession of biofilm bacterial communities exposed to the water column affected by the CO_2 venting? (Chapter 4 and 5) Is there an interaction between the bacterial and eukaryotic microbial community? (Chapter 4)

1.4 Methods

1.4.1 Sampling area

Papua New Guinea is located on the junction of two major tectonic plates, the Australian and Pacific plates, as well as several smaller plates, creating a tectonically very active area (Tregoning et al. 1998). The sampling sites for this PhD study were located in the Milne Bay province, Papua New Guinea, on Normanby and Dobu Island (Figure 2A). These two islands are aligned with the Woodlark Basin Spreading Center, which marks the transition from the Australian to the Woodlark plate. As a consequence of the tectonic activity, the islands are characterized by active volcanism and gas seepage (Little et al. 2011). These gas seeps have been known to the local population for several generations and can be found at multiple places along the coasts of Normanby and Dobu Island (Fabricius et al. 2011). The work for this PhD study was conducted at two different gas seeps (Figure 2B): Upa Upasina (Reef 1) and Dobu (Reef 2). The gas composition of these seeps is almost pure CO_2, which creates a natural pCO_2/pH gradient in the water column (Figure 2C; Fabricius et al. 2011).

Generally, the CO_2 seeps were in 0.5 to 4 m water depth. At Upa Upasina reef (Figure 3A) the CO_2 seepage was mostly diffuse with only occasional concentrated bubble streams (Figure 3B). Reference sites were approximately 500 m distant from the main seepage area (Figure 3C). A detailed description of the environmental conditions in the sediment at Upa Upasina reef was the focus of chapter 1. At Dobu Island the gas seepage was spatially more constrained with several strong bubble streams, which were also characterized by a sulfidic smell and white microbial mats (Figure 3D). The seepage area was furthermore enclosed by a ring of Porites corals, which resulted in very steep pH gradients. The sampling at the seep sites at Dobu Island was conducted within the Porites ring, but not directly adjacent to the main seeps (Figure 3E). Reference sites at Dobu Island were located 2 km away from the seeps (Figure 3F).

In this PhD study, I investigated microbial communities in different reef environments: associated with reef sediments (Upa Upasina and Dobu; chapters 2 and 3), and exposed to the water column on seagrass leaves (Dobu; chapter 4) and on settlement tiles (Upa Upasina and Dobu; chapter 5). The microbial communities in these different

reef environments were subject to the pCO_2/pH gradient at different temporal scales. Whereas the sediment has been exposed to the CO_2 vents for decades, the period biofilm communities on seagrass leaves and settlement tiles were exposed to the pCO_2/pH gradient depended on leave age and deployment time, respectively.

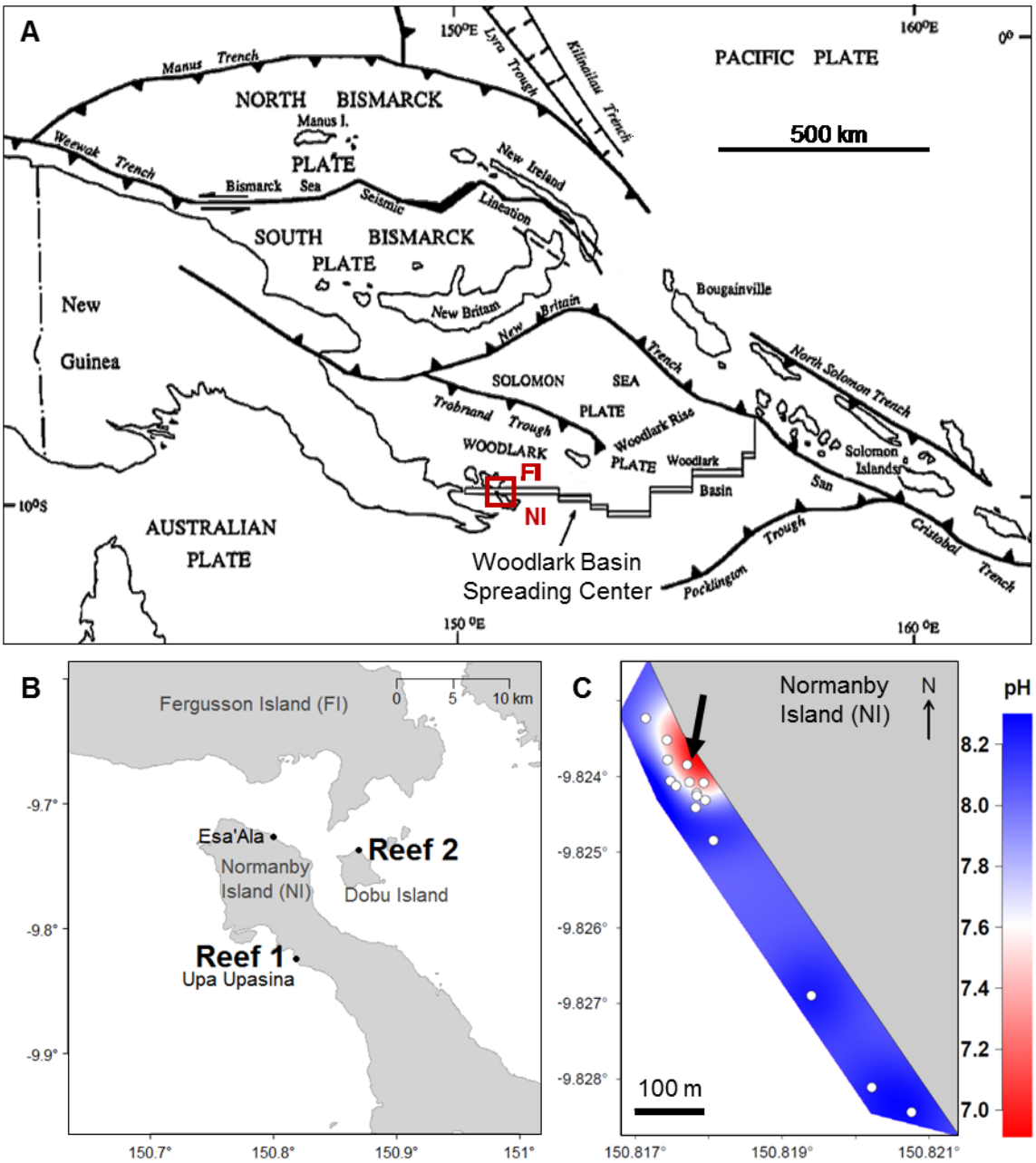

Figure 2: Sampling area in Papua New Guinea. A: Major fault lines and trenches between Pacific and Australian tectonic plates around Papua New Guinea (modified after Tregoning et al. 1998). The red square is highlighting the sampling area on Normanby and Dobu Island (B). C: Water column pH gradient at Upa Upasina (Reef 1), white points mark pH measurements, the arrow shows the location of main vent (see also Figure 3).

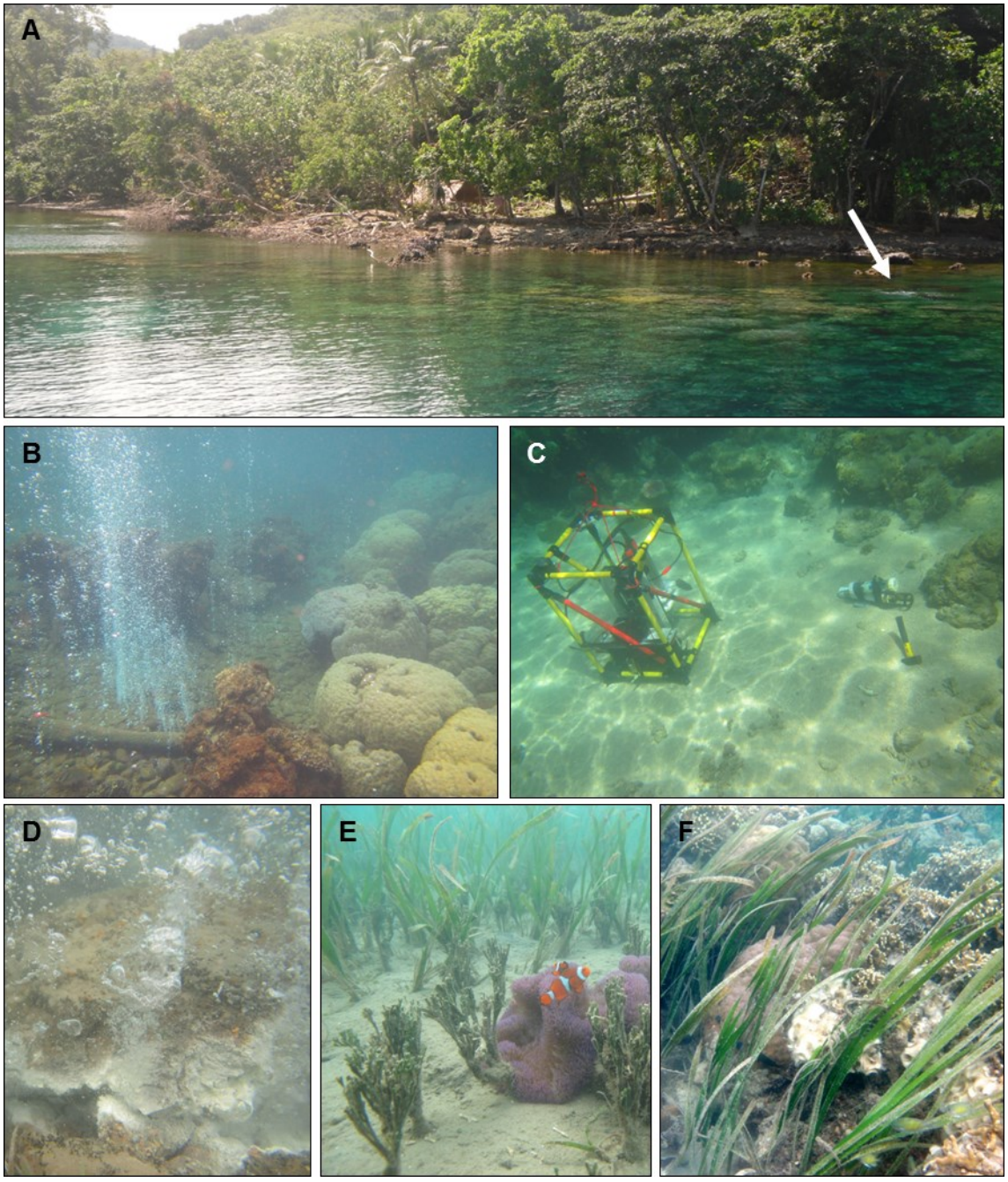

Figure 3: Environmental conditions at Normanby (A-C) and Dobu Island (E-D). A: Upa Upasina reef (Reef 1), arrow: location of main seep site. B: Underwater image of the main seep site at Upa Upasina reef (courtesy of K. Fabricius). C: Microprofiler deployment at the reference site at Upa Upasina reef (courtesy of A. Fink). D: CO_2 seep at Dobu Island containing sulfide (courtesy of K. Fabricius). E: *Enhalus* seagrass at the CO_2-impacted site at Dobu Island (courtesy of L. C. Hofmann). F: *Enhalus* seagrass at the reference site at Dobu Island (courtesy of L. C. Hofmann).

1.4.2 Molecular community analysis

Since the majority of the microbial diversity cannot be captured by classical cultivation-dependent methods, cultivation-independent molecular techniques, such as community fingerprinting and DNA sequencing, are increasingly being used to characterize microbial communities. Environmental studies on microbial communities further require a large number of samples to accurately describe patterns in community structure and diversity (Zinger et al. 2011). Molecular community fingerprinting via Terminal Restriction Fragment Length Polymorphisms (TRFLP) or Automated Ribosomal Intergenic Spacer Analysis (ARISA) can yield a reliable overview of the microbial community structure at a high sample throughput and low time and financial costs (Gobet et al. 2014). Both techniques are PCR-based and rely on DNA sequence length rather than sequence base content.

TRFLP was developed by Avaniss-Aghajani et al. (1994) for the 16S rRNA gene, but the technique can also be adapted to any other gene. Here, TRFLP was used in chapter 3 to characterize the total and active bacterial community in the sediment based on 16S rRNA (active) and the 16S rRNA gene (total), and the sulfate reducing community based on the dissimilatory sulfate reductase (*dsr*) gene. The general workflow starts with the PCR amplification of the target gene using fluorescently labeled primers. The PCR fragments are then cut by a restriction enzyme and the lengths of the resulting terminal restriction fragments are analyzed via capillary electrophoresis. The restriction fragments of different microbial types will vary in length due to differences in the location of the restriction sites caused by differences in the gene sequence (Figure 4A). The microbial community can therefore be described by operational taxonomic units (OTUs) based on restriction fragment lengths.

ARISA was developed to use the length variability of the intergenic spacer between the bacterial 16S and 23S rRNA genes (Fisher & Triplett 1999) and was applied here to screen microbial communities in all investigated reef environments. The amplification of the intergenic spacer results in a pool of DNA fragments of variable lengths that can be used to approximate community structure without the need for a restriction enzyme digest (Figure 4A). ARISA is not restricted to bacteria, but can also be applied to eukaryotes (Wolf et al. 2013). However, since both TRFLP and ARISA only use DNA sequence

length to define OTUs, they do not offer information on taxonomic affiliation and have a limited taxonomic resolution. To address these issues DNA sequencing is required.

The development of next generation sequencing (NGS) techniques has revolutionized microbial ecology, facilitating the generation of millions of DNA sequences within a short amount of time and at a low cost. This development marked the start of the 'omics' era: the large-scale sequencing of community DNA (metagenomics) and RNA (metatranscriptomics). The optimization of NGS techniques is ongoing, and the current trend suggests that screening techniques, such as TRFLP and ARISA, may become obsolete as sequencing costs decrease given the superior amount of information provided by DNA sequencing.

In recent years, 454 pyrosequencing and Illumina sequencing were among the most frequently used NGS techniques. The major advantage of 454 pyrosequencing over Illumina has been the length of the generated sequences of more than 700 bp per read (454 GS FLX Titanium system, Branford, CT, USA), compared to 300 bp with Illumina sequencing (Illumina MiSeq, San Diego, CA, USA). However, with paired-end sequencing, i.e. the sequencing of DNA fragments from both ends, Illumina can now generate sequences of more than 500 bp, comparable to the length of 454 pyrosequencing reads (Fadrosh et al. 2014). Considering the much higher throughput and lower sequencing cost per base of Illumina sequencing (Liu et al. 2012), it has become the preferred technique for DNA sequencing within the last years. Following this shift in sequencing technology, the DNA sequence generation for this PhD study was based on 454 sequencing for the early projects (Chapter 4) and Illumina sequencing for the majority of the projects (Chapters 2 and 3).

I employed two different sequencing approaches to characterize microbial communities at the CO_2 seeps in Papua New Guinea: amplicon sequencing and metagenomic/metatranscriptomic shotgun sequencing. Amplicon (also called tag) sequencing is based on the amplification of a specific DNA region, usually the 16S or 18S rRNA gene, to study the taxonomic composition and diversity of a microbial community. However, because of the amplification step, amplicon data sets are subject to PCR bias. Additionally, since only one specific DNA region of interest is sequenced, amplicon approaches do not include information on the full functional potential of the

community. Shotgun sequencing, on the other hand, generates sequences from the whole DNA (or RNA) pool of an environmental sample without prior amplification of a specific DNA region and can therefore also recover information on functional genes. Unlike amplicon sequencing, shotgun sequencing requires much deeper sequencing with millions of sequences per sample to cover the complete gene content of a microbial community.

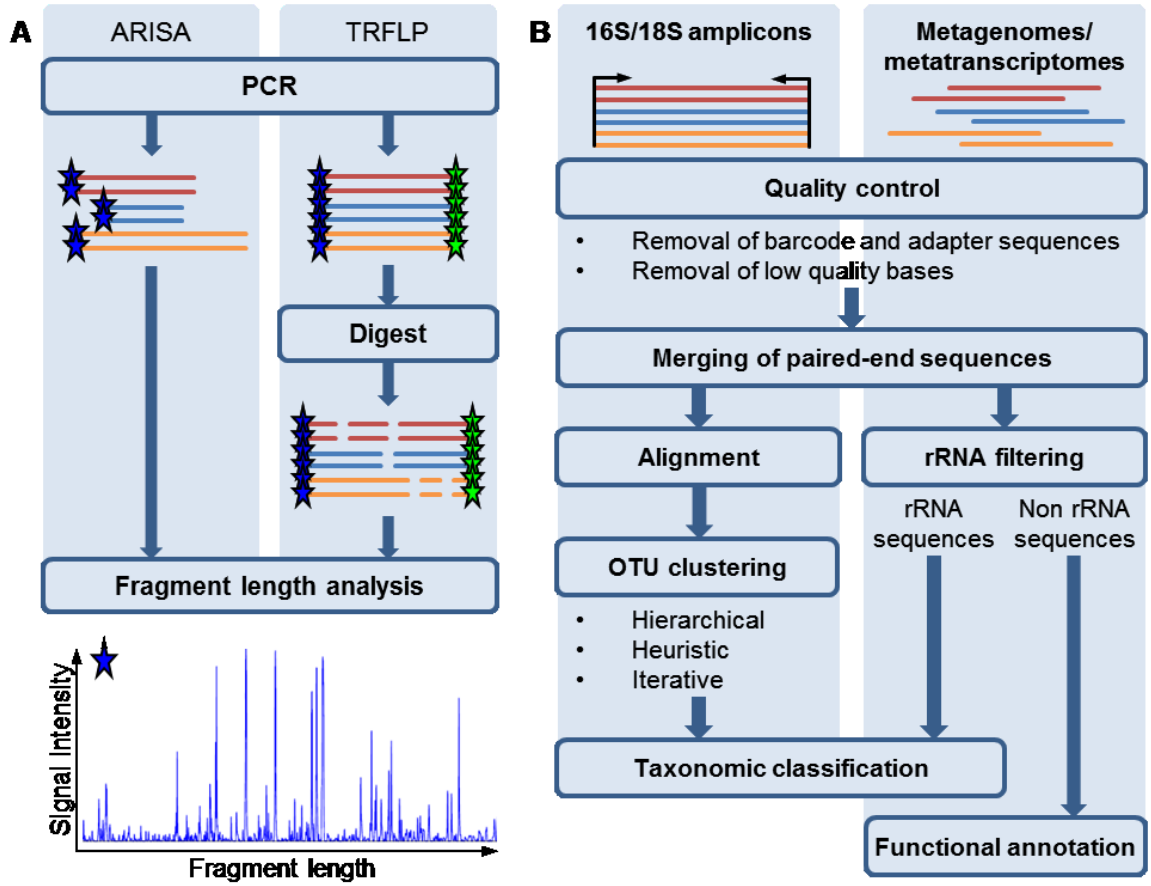

Figure 4: Molecular techniques applied in this thesis. A: Schematic workflow for generating molecular community fingerprints with ARISA (Automated Ribosomal Intergenic Spacer Analysis) and TRFLP (Terminal Restriction Fragment Length Polymorphism). B: Schematic workflow for the analysis of 16S and 18S ribosomal NGS amplicon sequences and metagenomic (metatranscriptomic) shotgun sequencing libraries.

1.4.3 Bioinformatic sequence processing

The bioinformatic analysis of NGS data is a very fast-evolving field following the advances in sequencing technologies and aiming to cope with the increased amount of sequencing data. There is a multitude of bioinformatic tools available for the analysis of NGS data, and new programs are constantly developed. The evolution of sequence analysis tools is also reflected in this PhD thesis, where I continuously aimed at using state-of-the-art analysis methods. An overview of the bioinformatics workflow for sequence analyses is provided in Figure 4B, which highlights the major steps in the analyses. Here, I want to explain in more detail the OTU clustering step in the analysis of amplicon data and the analysis of the shotgun sequencing data.

It is common practice to cluster amplicon sequences into OTUs as units of highest taxonomic resolution. I employed three different approaches for OTU clustering: hierarchical and heuristic clustering, and swarming. In hierarchical OTU clustering, pairwise distances are calculated between all sequences, which are then grouped into OTUs based on a fixed distance threshold, e.g. 97% similarity. Because the computational requirements for the calculation of the pairwise distances is non-linearly increasing with the number of input sequences (Schloss et al. 2009), this approach is not suited for large sequencing data sets such as those generated by Illumina. Therefore, only the bacterial 454 sequences presented in chapter 4 were clustered into OTUs using hierarchical clustering.

Heuristic OTU clustering is computationally less intensive than hierarchical clustering, because it does not require calculation of all pairwise distances. In heuristic clustering, one sequence is chosen as ‘seed’ for an OTU, usually the most abundant or longest sequence in the data set (Li et al. 2012, Edgar 2013). Then, all sequences within a certain distance radius are grouped into this OTU and are removed from the remaining sequence pool. However, the shape and size of the OTUs generated with heuristic clustering as well as the affiliation of a specific sequence to an OTU depends strongly on the selection of the ‘seed’ sequence and may not be very reproducible over several analysis runs with the same data set (Mahé et al. 2014). Heuristic OTU clustering therefore constitutes a trade-off between accuracy and computation speed and was used here with the eukaryotic Illumina sequences presented in chapter 4.

A recently published new OTU clustering tool, called swarm, offers a solution to this trade-off (Mahé et al. 2014). Unlike hierarchical or heuristic clustering programs, swarm does not use a fixed global distance threshold for OTU clustering, but rather builds OTUs in an iterative approach with a local distance threshold. OTUs generated by swarm do not have a uniform similarity radius, but differ in shape based on the input data. Since 16S sequence similarity between different species is also variable (Kim et al. 2014), swarm OTUs may constitute a closer approximation of true units of diversity. The computation time with swarm is comparable to heuristic clustering programs, while the shape of the OTUs is much more robust (Mahé et al. 2014). In this thesis, swarming was used for the analysis of the bacterial and archaeal Illumina sequences presented in chapter 2.

Additionally to amplicon sequencing, three of the samples presented in chapter 2 were selected for metagenomic/metatranscriptomic shotgun sequencing (chapter 3). Since the depth of the shotgun sequencing data was insufficient given the high diversity of the microbial community to be assembled into larger contigs, each sequence was either taxonomically classified (rRNA sequences) or functionally annotated (non-rRNA sequences; Figure 4B). This approach was shown to be similarly reliable compared to sequence assembly in capturing patterns in the taxonomic and functional composition of a microbial community, and it is therefore implemented in the metagenomics portal of the European Bioinformatics Institute (EBI; Hunter et al. 2014).

Despite the tremendous advances of NGS technologies and bioinformatic data processing, ‘omics’ approaches are not the solution to answer all questions in microbial ecology. Both amplicon and shotgun sequencing data are limited in their ability to characterize microbial communities that should be considered in the interpretation of such data: (i) Sequence affiliation is not equal to species identification, even on 16S level. The taxonomic classification of a DNA sequence may be biased by sequence length and the completeness of the taxonomic reference database. (ii) DNA sequences do not contain information on whether an organism is active. To address this issue, further analyses on RNA basis may be conducted to differentiate between the total (DNA) and active community (RNA). (iii) Gene transcription does not necessarily reflect enzyme activity. Translation rates and protein turnover are just two examples of processes, which may

decouple transcription from metabolic rates. To gain a comprehensive understanding of the composition and function of microbial communities it is therefore advisable to combine 'omics' data with additional methods, e.g. biogeochemical data and metabolic rate measurements.

1.4.4 Statistical approaches to microbial ecology

Many molecular methods, such as community fingerprinting and NGS, produce semi-quantitative, compositional data. This means that the range of possible sequence counts for an OTU is constrained by a grand total per sample, e.g. the maximum number of sequences in a sample, also referred to as library size (Fernandes et al. 2014). On the one hand, this phenomenon prevents the direct comparison of OTU abundances based on sequence counts between different samples with different library sizes. On the other hand, it may cause spurious correlations between OTUs. If one OTU is suddenly absent from the DNA pool, the sequences that would have belonged to this OTU will be 'filled' by sequences of other OTUs, which will give the wrong impression of increased abundance. Therefore, OTU abundances are not independent anymore, which is a prerequisite of statistical tests. To solve the first issue, it has been common practice to use proportions (relative sequence abundance) or rarefied data (subsampled to an equal library size) for statistical comparisons (Schloss et al. 2009). However, these approaches have been strongly criticized, especially when applied to test for differential OTU abundance (McMurdie & Holmes 2014). Furthermore, they did not address the issue of inter-OTU dependence. Recent advances in biological data analysis recommend applying centered-log-ratio (clr) transformation to sequencing data sets to address the issue of compositionality (Fernandes et al. 2014). Clr transformation maintains the relative difference between OTU abundances regardless of the grand total and if calculated on $\log_2$, shows differences between OTUs that represent fold-changes (Fernandes et al. 2014). While I employed the classical rarefying approach in chapter 4, the data analysis based on clr transformation was implemented here in chapters 2, 3 and 5.

1.5 Publication outline

In the following five chapters I will focus mainly on microbial communities in the sediment at the CO_2 seeps in Papua New Guinea, presenting first a description of the environmental conditions in the sediment coupled with information on microbial and meiofaunal abundance and major metabolic processes. Subsequently, I will describe the microbial communities in the sediment in more detail, focusing on environmental factors that may influence community structure, trends in taxonomic community composition, and the functional potential of the microbial communities in relation to biogeochemical measurements. I will end with two pilot studies describing the bacterial and eukaryotic biofilm community on seagrass leaves and the bacterial community on settlement tiles exposed to the pH gradient created by the CO_2 seeps in the water column.

Chapter 1: Sediment biogeochemistry at hydrothermal CO_2 seeps within a coral reef

Artur Fink, Katja Guilini, Christiane Hassenrück, Anna Lichtschlag, Sergey M. Borisov, Dirk de Beer

Limnology and Oceanography (submitted).

This study investigates physico-chemical parameters in the sediment at volcanic CO_2 seeps as well as the abundance of benthic meio- and microfauna and remineralization processes. It shows that reductions in permeability caused by OA-driven dissolution of reef carbonates may decrease the biocatalytic filtration function of future reef sediments. Furthermore, the study emphasizes that sediments at volcanic CO_2 seeps can be affected by factors other than CO_2, thus highlighting the need for comprehensive measurements of environmental parameters within the sediments.

The study was designed by A. Fink and D. de Beer. K. Guilini provided meiofauna data. C. Hassenrück contributed data on microbial cell counts. A. Lichtschlag provided pore water data. S. Borisov was involved in the measurements of oxygen consumption rates. All co-authors were involved in data interpretation and discussion as well as proof-

reading of the manuscript. This chapter is included in this thesis to provide background information for chapters 2 and 3.

Chapter 2: Quantification of the effects of ocean acidification on sediment microbial communities in the environment: the importance of ecosystem approaches

Christiane Hassenrück, Artur Fink, Anna Lichtschlag, Halina E. Tegetmeyer, Dirk de Beer, Alban Ramette

FEMS Microbiology Ecology (in press).

This study used molecular and statistical methods to quantify the influence of various environmental parameters on microbial communities in the sediment along a pH gradient at CO_2 vents in Papua New Guinea. It was shown that pH was among the factors significantly, yet not mainly, explaining changes in microbial community composition, and that therefore pH variation may often not be the primary cause of microbial changes when sampling is done along complex environmental gradients. Furthermore, the study discusses the potential for bacterial and archaeal taxa affected by the CO_2 vents to alter biogeochemical cycles in the sediment.

The study was designed by C. Hassenrück and A. Ramette. C. Hassenrück was involved in sample collection, laboratory work, data analysis, and manuscript preparation. A. Fink and A. Lichtschlag contributed biogeochemical data and provided input for the manuscript preparation. H. Tegetmeyer performed the DNA sequencing. D. de Beer and all other co-authors contributed to data interpretation and discussion as well as proof-reading of the manuscript.

Chapter 3: Metatranscriptomic and biogeochemical investigations of sediment microbial processes at a shallow-water hydrothermal CO_2 vent in Papua New Guinea

Christiane Hassenrück, Artur Fink*, Pierre Offre, Pier Luigi Buttigieg, Halina E. Tegetmeyer, Alban Ramette, Dirk de Beer*

Frontiers in Aquatic Microbiology (in preparation).

This study provides an overview of microbial processes involved in major element cycles and how they may be affected by CO_2 venting. The active microbial community as well as metabolic rates are investigated using molecular and biogeochemical methods focusing on the carbon, sulfur and nitrogen cycle. Furthermore, hypotheses for future research on microbial processes at shallow-water hydrothermal CO_2 vents are presented.

The study was designed by C. Hassenrück and A. Fink, who conducted the sample collection, laboratory work and data analysis. H. Tegetmeyer performed the DNA and RNA sequencing. P. Offre and P. Buttigieg were involved in the analysis and interpretation of the metagenomic and metatranscriptomic data. A. Ramette, D. de Beer and all other co-authors contributed to data interpretation and discussion as well as proof-reading of the manuscript.
* The manuscript was prepared by A. Fink and C. Hassenrück as joint first authors.

Chapter 4: Seagrass biofilm communities at a naturally CO_2-rich vent

Christiane Hassenrück, Laurie C. Hofmann, Kai Bischof, Alban Ramette

Environmental Microbiology Reports 7: 516–525.

This study uses molecular methods to describe the bacterial and eukaryotic biofilm community associated with the leaves of the seagrass *Enhalus acroides* growing at a coral reef under ambient conditions and at a CO_2 vent. An increased relative sequence abundance of bacteria associated with coral diseases was detected at the CO_2 vent, as well as a decreased diversity of crustose coralline algae. The result suggest a potential role of seagrasses as vectors of coral pathogens, thus supporting predictions about decreased reef health under increased CO_2 conditions.

The study was designed by C. Hassenrück and L. Hofmann, who also completed the sampling and laboratory work for the characterization of the microbial communities. L.C. Hofmann measured carbon and nitrogen content of the seagrass leaves as well as epiphyte cover. C. Hassenrück conducted the data analysis and prepared the manuscript. K. Bischof, A. Ramette and all other co-authors contributed to data interpretation and discussion as well as proof-reading of the manuscript.

Chapter 5: Bacterial biofilm composition on settlement tiles along natural pH gradients at two CO_2 seeps in Papua New Guinea

Christiane Hassenrück, Katharina Fabricius, Alban Ramette

In preparation.

This study used a high sample throughput molecular fingerprinting approach to characterize the bacterial community on settlement tiles along two natural pH gradients. The results suggest that changes in seawater pH did not have a strong impact on the development of the bacterial biofilms on settlement tiles, and that other abiotic and biotic factors, such as light exposure or close interactions with other organisms on the settlement tiles, may be more important in shaping bacterial biofilm communities.

This study was designed by K. Fabricius. C. Hassenrück completed the laboratory work and the data analysis related to the characterization of the microbial community. These results are presented here in a short report prepared by C. Hassenrück. K. Fabricius and A. Ramette contributed to data interpretation and discussion as well as proof-reading of the report.

2. Thesis chapters

Chapter 1

Sediment biogeochemistry at hydrothermal CO_2 seeps within a coral reef

Artur Fink[1], Katja Guilini[2], Christiane Hassenrück[1], Anna Lichtschlag[3], Sergey M. Borisov[4], Dirk de Beer[1]

[1] Max Planck Institute for Marine Microbiology, Celsiusstraße 1, 28359 Bremen, Germany

[2] Ghent University, Krijgslaan 281, S8, 9000 Gent, Belgium

[3] National Oceanography Centre, University of Southampton, Waterfront Campus, European Way, Southampton SO14 3ZH, United Kingdom

[4] Institute for Analytical Chemistry and Food Chemistry, Graz University of Technology, Stremayrgasse 9/III, 8010 Graz, Austria

Limnology and Oceanography (submitted).

Abstract: Due to their high permeability, coarse carbonate sediments allow advective pore water exchange and function as biocatalytic filters of organic matter retaining nutrients within coral reefs. Ocean acidification (OA) reduces the production and increases the dissolution of reef carbonates. This could decrease sediment grain sizes and reduce their permeability with potentially severe consequences for element cycling on reefs. We investigated the main processes controlling carbon cycling in sediments of a fringing reef subjected to hydrothermal CO_2 seepage off Papua New Guinea. The coarse and highly permeable carbonate sediments of the control sites buffered the pore water pH at 7.5 - 7.9. In contrast, seep sediments had a lower pore water pH of < 6 - 7, reduced redox conditions and elevated temperature. Here, no accumulation of coarse carbonates occurred so that finer and less permeable silicate sediments dominated. A reduced sediment-water exchange due to decreased advection coincided with a reduced oxygen penetration, organic carbon content, oxygen consumption and sulfate reduction rates. Strikingly, seep sediments that likely received seagrass-derived organic matter showed high remineralization rates. However, the adverse chemical environment in seep sediments likely met or surpassed physiological limits of sediment inhabiting organisms and could explain a drastic decline in meiofauna abundance. Thus sediments at hydrothermal CO_2 seeps can be affected by factors other than CO_2 emphasizing the need for comprehensive measurements of environmental parameters within the sediments. Reductions in permeability caused by OA-driven reduction of reef carbonates may decrease the biocatalytic filtration function of future reef sediments with unprecedented consequences for reef productivity.

Keywords: ocean acidification, permeable coral reef sediments, carbonate dissolution, shallow-water hydrothermal vents, natural laboratories, remineralization

Introduction

Ocean acidification (OA) due to the uptake of anthropogenic carbon dioxide (CO_2) by the oceans is recognized as a major threat to marine ecosystems. Recent CO_2 emission scenarios project an increase from the current ~400 µatm to more than 750 µatm by 2100, leading to a projected reduction of the global average seawater pH by up to 0.4 units (Caldeira and Wickett 2003; Feely et al. 2004). The accompanying decrease in carbonate ions (CO_3^{2-}) will lower the saturation state (Ω) of carbonate minerals (Zeebe and Wolf-Gladrow 2001), which are produced by calcifying organisms to build up complex carbonate structures.

Coral reefs harbor an immense biodiversity and provide important ecosystem services, but their existence directly depends on the net production of calcium carbonate over time (Hallock 1997). The major site of calcium carbonate production is the coral reef framework, which upon gradual breakdown accumulates forming the reef sediments. Due to their high permeabilities, both act as biocatalytic filters, which effectively recycle dissolved and particulate organic matter (OM) from the water column and in this way retain nutrients within the reef (Richter et al. 2001; Rasheed et al. 2002; Wild et al. 2004; Werner et al. 2006; Rao et al. 2012; Rix et al. 2016). This allows coral reefs to maintain a high biomass and gross primary productivity within oligotrophic environments (Muscatine and Porter 1977).

The rate of OM remineralization in sediments is tightly linked to transport processes that supply electron donors (OM) and electron acceptors (oxygen, sulfate, etc.). While solute exchange in fine cohesive sediments is mediated by molecular diffusion, large-grained permeable sediments additionally allow for pore water advection, i.e. the fast circulation of bottom water through sediments driven by pressure gradients caused by tides, waves, currents, sediment topography and density gradients (Huettel et al. 2014). Moreover, porewater advection efficiently brings particulate OM (bacteria, unicellular algae, detritus) to deeper sediment layers (Pilditch et al. 1997; Huettel et al. 2007), where it is degraded and remineralized by highly active communities of microorganisms, meiofauna and macrofauna (Huettel et al. 2014). In coral reef sediments this results in very high remineralization rates significantly contributing to the element cycling in coral reefs (Wild et al. 2004, 2005; Werner et al. 2006; Rao et al. 2012).

OA is expected to significantly alter the carbonate budget of coral reefs with potentially severe consequences for the reef ecosystem. On the one hand, OA reduces the rate of reef calcification (Leclercq et al. 2002; Langdon et al. 2003; Andersson et al. 2009; Dove et al. 2013). On the other hand, it increases the dissolution of existing carbonate structures, including reef sediments (Andersson et al. 2009; Cyronak et al. 2013; Comeau et al. 2014, 2015; Eyre et al. 2014). We hypothesize that a reduced production and increased dissolution of carbonate sediments due to OA will directly reduce their grains size and on the long term may lead to lower permeability limiting pore water advection. This could reduce the biocatalytic filtration function of reef sediments and negatively affect the element cycling and primary production of future coral reefs.

To study how long-term acidification affects coral reefs sediments, hydrothermal CO_2 seeps located within coral reefs provide a unique opportunity (Fabricius et al. 2011; Inoue et al. 2013; Enochs et al. 2015). The CO_2 seeps off Papua New Guinea (Normanby Island, Milne Bay) have been active for at least 80 years and are extensively being used as natural OA analogs (Fabricius et al. 2011). Under reduced pH conditions (water column pH 7.8) structurally complex corals were out-competed by more robust, but structurally simpler corals, resulting in an overall loss in structural complexity and biodiversity of the ecosystem (Fabricius et al. 2011, 2013). Reef development entirely ceased at a water column pH of < 7.7, a condition that instead favored the growth of dense seagrass meadows. Sediments around the CO_2 seeps were significantly reduced in carbonates and in the abundance and diversity of calcareous sediment organisms and their remains (Fabricius et al. 2011; Uthicke et al. 2013). Also, sediment microbial communities showed significant changes in richness and community composition (Raulf et al. 2015; Hassenrück et al. 2016).

While bottom water pH conditions at hydrothermal CO_2 seeps fall within the range of projected OA scenarios, so far there is a limited understanding of abiotic conditions in the sediments (Vizzini et al. 2013). In other shallow-water hydrothermal seeps the input of hydrothermal fluids causes abiotic conditions in sediments, which can be substantially different from background sediments. Seep sediments often show a severely reduced pH, increased temperature and high levels of reducing compounds (e.g. H_2S, Fe^{2+}), nutrients and trace elements (Wenzhöfer et al. 2000; German and Von Damm

2003; Price et al. 2007), which may confound studies investigating the effects of acidification on ecosystems (Vizzini et al. 2013).

In the present study, we characterize the abiotic conditions and properties of coral reef sediments at CO_2 seeps off Papua New Guinea. We describe patterns in sediment-inhabiting microorganisms and meiofauna and remineralization rates of reef sediments and relate them to changes in abiotic factors and OA-caused ecosystem shifts.

Material and Methods

Site description and sampling strategy

The investigated CO_2 seeps were situated within a fringing coral reef off Upa Upasina (Normanby Island, PNG; Figure 1). Sampling and measurements were performed in May and June 2013, and April 2014. Diffuse gas seeping occurred through sediments covering an area of approximately 200 m x 40 m, while the most intense discharge of gases occurred through cracks in basalt rocks at the Main seep (Figure S1, Fabricius et al. 2011). In the seepage area, we investigated sediments from six different sites named Seep 1 - 6 at a water depth between 2.5 and 6 m. Seep 5 and Seep 6 were located next to a dense seagrass bed of *Cymodocea*. The sediment at Seep 6 was colonized by the seagrass *Halophila ovalis* and covered an area of approximately 2 m × 2 m. Sediments located approximately 350 and 500 m south-east of the seeping area were selected as Control sites and treated as replicates. For ex-situ measurements, vertical sediment cores were taken by snorkelers using plastic core liners, which were sealed underwater and processed within one hour after sampling.

Water column parameters

At each site water samples were collected approximately 5 cm above the sediment surface using closeable plastic syringes (n = 3 - 4). Immediately after collection the samples were analyzed for pH using a Mettler Toledo pH probe, which was calibrated with NBS buffers. To account for variable bottom water parameters, we used four *in situ* loggers (XR-420, RBR Ltd., Ottawa, Canada), which quantified pH. Temperature was measured using HOBO Pendant temperature loggers (Onset, MA, USA), which were attached to the RBR loggers. The pH sensors (AMT Analysenmesstechnik GmbH, Rostock, Germany) were calibrated with NBS buffers (pH 7.00, 9.21, Mettler Toledo AG, Schwerzenbach, Switzerland), and pH was cross-calibrated with a CTD (Seabird, SBE 19v2) equipped with a pH sensor (SBE 18), which was calibrated at the total pH scale (pH_T) using a TRIS buffer (Dickson et al. 2007). The loggers were placed on the sediments of the Control site and Seep 1 - 4, recording data over 5 to 14 days.

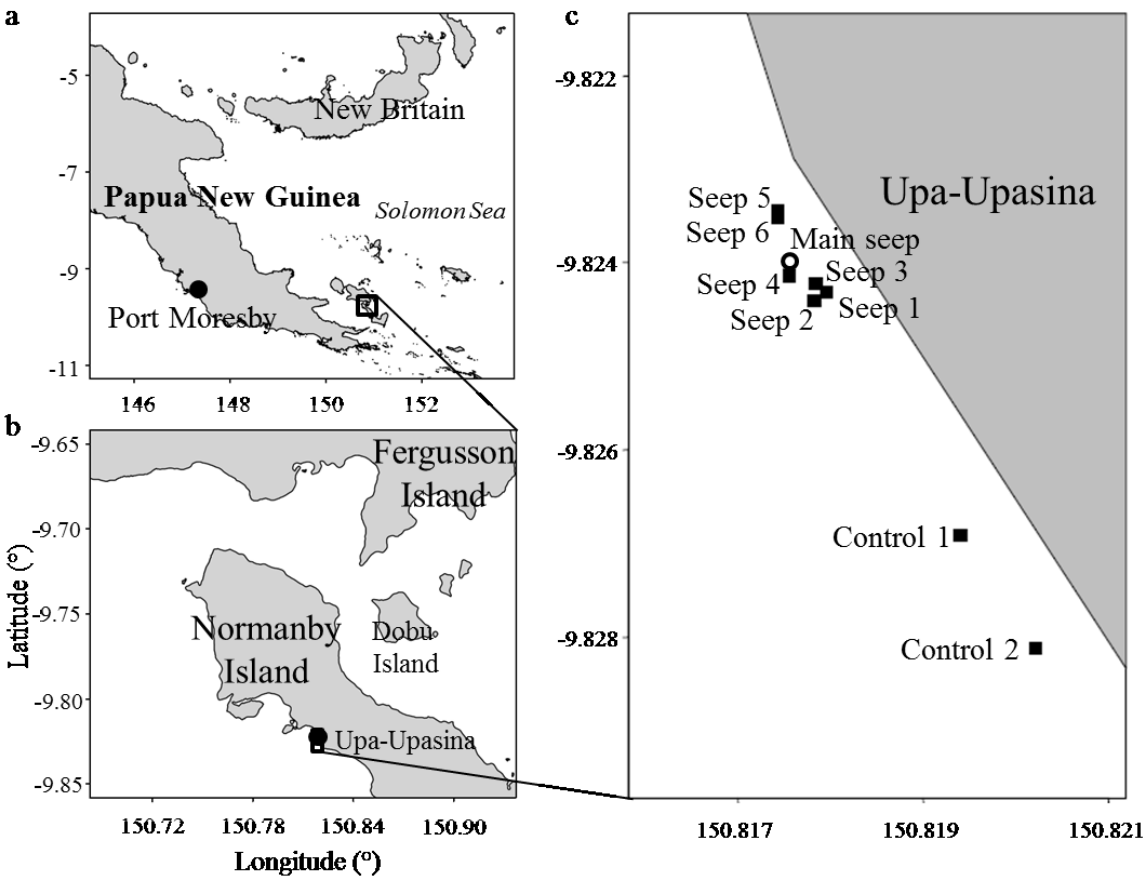

Figure 1: (a) Map of Papua New Guinea, (b) the northern part of Normanby Island, and (c) the location of the investigated sites and the Main seep off Upa Upasina.

Sediment characteristics

Sediments were obtained using core liners of 36 mm inner diameter, sliced into 2 cm intervals and frozen at -20°C until analysis. Sediment porosity of the upper two centimeters was determined as the weight loss of a known volume of sediment after freeze-drying (n = 3). The same samples were pulverized and used for total carbon (TC), total nitrogen (TN) and total organic carbon (TOC) determination using an elemental analyzer (Euro EA 3000, EuroVector). Prior to measurement of TOC, the samples were decalcified in silver cups by the addition of HCl. Total inorganic carbon (TIC) was calculated as the difference between TC and TOC.

Additional cores were collected for the analysis of grain size and permeability. Grain size was measured by sieving dried sediments (60°C, until constant weight) using a

calibrated sieve stack (n = 3). Median grain sizes were determined graphically using the program GSSTAT (Poppe et al. 2004). Sediment permeability of the upper 4 cm was measured with the falling-head method (n = 3, Klute and Dirksen 1986).

In situ profiles

Microsensors for O_2, H_2S and redox potential were built, calibrated, and used as described previously (Revsbech 1989; Jeroschewski et al. 1996; de Beer et al. 2013). The tip size of the microsensors was 150-300 µm with an actual measuring surface of 5 µm and a response time (t_{90}) of < 5 s. The oxygen microsensors were two-point calibrated *in situ* using the bottom water oxygen concentration and the typically anoxic pore water of deeper sediments. Redox potential microsensors were calibrated with standard redox buffers (191 mV and 468 mV, Omnilab-Laborzentrum GmbH & Co. KG). Commercially available temperature sensors (Pt1000, UST Umweltsensortechnik GmbH, Geschwenda, Germany) and needle-type microelectrodes for pH (MI-407, 0.8 mm needle diameter, t_{90} = 10 - 15 s, Microelectrodes, Inc., NH, USA) were also used. The pH microelectrodes were calibrated with pH 7.00 and 9.21 NBS buffers (Mettler Toledo AG) at 29°C. All sensors were mounted on a profiling lander (maximum distance between sensors was 11 cm) and were calibrated before deployment. Per investigated site 1 - 4 deployments were made. The lander was programmed to obtain 10 cm deep vertical profiles in 250 µm steps. Each profile started and ended with a logging period (13 min) above the sediment. Due to irregular sediment topography, profiles were manually aligned, and the typical transition from a stable water column signal to a steep change within the diffusive boundary layer was defined as the sediment surface (Gundersen and Jørgensen 1990).

Oxygen consumption rates (OCR)

Oxygen consumption rates in sediments were measured *ex situ* using the percolation method of de Beer et al. (2005) as modified by Polerecky et al. (2005). Pore water oxygen concentrations were monitored using planar oxygen optodes designed for ratiometric read-out with an RGB camera (Larsen et al. 2011) with a sensing area of 50 × 10 mm that were glued vertically to the inside of an acrylic core liner (5 cm inner diameter) using electrical tape. Intact sediment cores (n = 3) were retrieved and closed

from below using a rubber stopper that was fitted with a valve. Bottom water at the respective site was collected using a Niskin bottle. The sediment cores and the bottom water were submerged in a water bath kept at 29°C prior to the start of the measurements. In order to create a diffusive boundary layer at the sediment surface, we used an air pump connected to a Pasteur pipette to create a thin stream of air, which was blowing onto the water surface. Bottom water from the respective location (see Table S1 for initial pH) was drained through the sediment core using a peristaltic pump (30 mL min^{-1}). Upon stopping the percolation, the initial decrease of oxygen concentration over time was monitored in 1 mm depth intervals down to a maximum depth of 4.5 cm. The planar optode was calibrated by percolating seawater of known oxygen concentration (covering 0 - 100% air saturation) through the sediment. The measured volumetric OCR was corrected for porosity and represents potential OCR. To estimate the areal OCR, the potential OCR were integrated over the oxygen penetration depth measured *in situ* (de Beer et al. 2005). The areal OCR may underestimate the *in situ* rates, because this method does not account for the oxidation of chemically reduced compounds that are dissolved in the pore water and are flushed out by the percolation.

Sulfate reduction rates (SRR)

Sulfate reduction rates were measured *ex situ* with the whole core injection method according to Jørgensen (1978). Sediment was sampled with acrylic core liners (26 mm diameter) and pre-incubated in a water bath at 29°C for 6 h before the start of the experiment in the dark (n = 2 - 4). At 1 cm depth intervals cores were injected with 10 - 20 µL of $^{35}SO_4^{2-}$ (approximately 200 kBq) through silicone-filled ports. After incubation for 6 - 7 hours in the dark, sediment cores were sliced in two centimeter depth intervals and fixed in an equal volume of 20% (w/v) zinc acetate. SRR were determined by the single-step chromium distillation technique after Kallmeyer et al. (2004) as modified by Røy et al. (2014). Pore water sulfate concentrations were determined by non-suppressed anion exchange chromatography (Metrohm 761 Compact IC, Herisau, Switzerland). Areal SRR were calculated by integrating the volumetric SRR over the upper 10 cm of the sediment. Since the SRR were measured *ex situ*, they must be considered as potential.

Meiofauna abundance

Sediment samples were collected using core liners with an inner diameter of 5 cm, which were pre-cut in 2 cm steps and taped (n = 3). The sediments were vertically sectioned in 2 cm slices, down to a maximum depth of 8 cm. All sample sections were preserved in a 4% seawater-buffered formalin solution. Meiofauna was extracted from the samples through triple density centrifugation with the colloidal silica polymer LUDOX TM 40 (Heip et al. 1985) and rinsed with freshwater on stacked 1 mm and 32 µm mesh sieves. The fraction retained on the 32 µm mesh sieve was preserved in 4% Li_2CO_3-buffered formalin and stained with Rose Bengal. All metazoan meiobenthic organisms were classified at higher taxon level and counted under a stereoscopic microscope (Leica MZ 8, 16x5x).

Microbial abundance

Microbial cells from 0 - 2 and 2 - 4 cm of the sediments were counted using acridine orange direct counts (AODC, Hobbie et al. 1977; Meyer-Reil 1983). Sediment samples (1 mL wet sediment) were preserved in formaldehyde/seawater (2 - 4%, sterile-filtered). Cells were dislodged from the sediment particles by 6 subsequent ultrasonication treatments (30% for 5min, Bandelin MD72) with 2 mL formaldehyde/ seawater. Cells were counted on Nucleopore polycarbonate filters in duplicates (pore size: 0.2 µm, stained with Irgalan black), stained with acridine orange (0.01%) for 3 min, and rinsed with citrate buffer (pH 4) for 1 min. For each sample approximately 2000 cells were counted on each duplicate filter, of which the mean was used for the statistical analysis.

Statistical analysis

The investigated sites were grouped based on similar characteristics. Control 1 and 2 were grouped as Control. The group Seep included Site 1 - 4. Due to their association with seagrasses, Site 5 and 6 constituted the distinct group Seagrass at Seep. Non-parametric tests (Kruskal-Wallis) and subsequent multiple comparisons (with false discovery rate correction) were used to detect significant differences between groups. The

data were analyzed using the open-source statistical software R (R Core Team 2015) with the package PMCMR. Distance-based linear model (DISTLM) analyses, based on a forward selection procedure and the R^2 selection criterion (Anderson et al. 2008), were performed to test, which predictor variables explain the variance of meiofauna abundance and richness best. Only variables that were available for all depth intervals (O_2 concentration, temperature, pH, porosity, median grain size and sulfate) were used for analysis. Due to the lack of replication, averages of predictor and biological variables were used for analysis. Prior to the analyses, the predictor variables were diagnosed for collinearity with Draftsman plots and Spearman correlations. These analyses were performed with PRIMER v6 and PERMANOVA+ add-on software (Clarke and Gorley 2006; Anderson et al. 2008).

Results

Bottom water parameters

The median pH at the Control site was 8.23. In contrast, at Seep 1 - 4 the bottom water pH was reduced with median values ranging between 7.85 - 8.05, showing a high temporal variability and reaching extreme values of pH 7.5 or lower (Table 1). Due to logger malfunction, no data are available for Seep 5 and 6, but the pH ranged between 7.1 - 7.3 in discrete samples. The average bottom water temperature at the seep sites was slightly higher (28.6 - 29.1°C) compared to the Control site (28.1°C).

Table 1: Bottom water pH and temperature at the study sites. Loggers deployed *in situ* recorded pH on the total scale (pH_T) and temperature. pH_T is presented as median with 5% and 95% percentiles in parentheses. The other parameters are shown as mean ± standard deviation. n = 3 for discrete pH_{NBS} samples. No pH logger data is available for Seep 5 and 6.

Site	Water depth (m)	pH_{NBS} (discrete)	pH_T (loggers)	Temperature (°C)
Control	3	8.24 ± 0.01	8.23 (8.19-8.28)	28.2 ± 0.1
Seep 1	2.5	7.98 ± 0.03	8.05 (7.53-8.24)	29.1 ± 0.4
Seep 2	4	7.92 ± 0.03	8.05 (7.78-8.20)	29.1 ± 0.4
Seep 3	3	7.57 ± 0.07	7.96 (7.50-8.11)	28.9 ± 0.3
Seep 4	5	8.03 ± 0.06	7.85 (7.56-8.02)	28.6 ± 0.2
Seep 5	2.5	7.19 ± 0.13		28.9 ± 0.1
Seep 6	2.5	7.94 ± 0.02		28.9 ± 0.1

Sediment characteristics

Whereas Control sediments were typical reef sediments, consisting of coarse whitish coral fragments, the seep sediments were finer silicate sands (Lichtschlag, personal communication), which could appear reddish (Seep 4; Figure S2). The sediment characteristics are shown in Table 2. The porosity was similar between the three groups (Kruskal-Wallis, $p < 0.5$). The Control sediments showed the highest carbonate content (average TIC = 8.63% dry weight [dw]), while carbonates were significantly reduced in both seep groups (TIC = 0 - 1.21% dw; Kruskal-Wallis, $p < 0.01$). The median grain size of sediments was largest at the Control site (0.71 mm) and reduced in both seep groups by 32 - 72% (Kruskal-Wallis, $p < 0.01$). The Control sediments showed the highest permeability (10.01×10^{-11} m^2), which was 1.9 to 5.2 times lower in seep sediments (Kruskal-Wallis, $p < 0.01$). Generally, all sediments showed a low TOC and TN content.

Sediments of the group Seep had significantly lower TOC and TN content (TOC = 0.05 - 0.07% dw, TN = 0.01 - 0.03% dw) when compared to the groups Control (TOC = 0.16% dw, TN = 0.03% dw) and Seep with seagrass (TOC = 0.07 - 0.21% dw, TN = 0.03 - 0.04% dw; Kruskal-Wallis, $p < 0.05$ for TOC, $p < 0.01$ for TN). The highest TOC and TN content were found in Seep 6 sediments.

Table 2: Sediment characteristics at the investigated sites. MGS: median grain size, TIC: total inorganic carbon, TOC: total organic carbon, TN: total nitrogen, dw: dry weight. Data are average ± standard deviation, n = 3.

Site	Porosity	Permeability (10^{-11} m^2)	MGS (mm)	TIC (% dw)	TOC (% dw)	TN (% dw)
Control	0.48 (±0.00)	10.0 (±1.3)	0.71 (±0.04)	8.63 (±0.83)	0.16 (±0.00)	0.03 (±0.00)
Seep 1	0.48 (±0.01)	5.4 (±0.8)	0.33 (±0.02)	0.14 (±0.13)	0.05 (±0.01)	0.01 (±0.00)
Seep 2	0.44 (±0.03)	5.3 (±0.3)	0.48 (±0.10)	0	0.06 (±0.00)	0.01 (±0.00)
Seep 3	0.45 (±0.05)	3.0 (±0.1)	0.20 (±0.01)	0	0.05 (±0.00)	0.01 (±0.00)
Seep 4	0.46 (±0.01)	3.0 (±0.0)	0.24 (±0.02)	0.02 (±0.01)	0.07 (±0.01)	0.02 (±0.00)
Seep 5	0.49 (±0.05)	2.3 (±0.5)	0.21 (±0.01)	0.05 (±0.00)	0.07 (±0.01)	0.03 (±0.00)
Seep 6	0.50 (±0.03)	1.9 (±0.3)	0.19 (±0.01)	0.73 (±0.54)	0.21 (±0.04)	0.04 (±0.01)

In situ profiles

The *in situ* profiles of the overlaying water and the upper 7 cm of the sediments are shown in Figure 2. The profiles in Seep and Seagrass sediments showed clear signs of hydrothermal influence. Generally, the profiles displayed steeper slopes compared to the Control sites. In all Seep sediments the pore water pH decreased strongly with depth, reaching values of < 6 - 7. However, at Seep 6 the pore water pH was spatially heterogeneous and could also be elevated to 7.9. The temperature increased with depth at a rate of 0.3 - 1.2°C cm^{-1} and could even reach 37°C with depth at Seep 3 (data not shown). The redox potential showed a sharp decline just below the sediment surface and often decreased to negative values within the upper centimeters of the sediment. H_2S was detectable at Seep 1 - 3, where it increased with depth reaching 10 - 20 µmol L^{-1}. At the Control sites, the pore water pH ranged between 7.5 - 7.9, while temperature was similar to water column values and constant with depth. H_2S was not detected and the redox potential was either close to bottom water levels or decreased moderately. The *in situ* oxygen penetration (Figure 3) of both seep groups (2.0 - 10.1 mm) was significantly reduced compared to the Control group (7.3 - 13.5 mm; Kruskal-Wallis, $p < 0.05$).

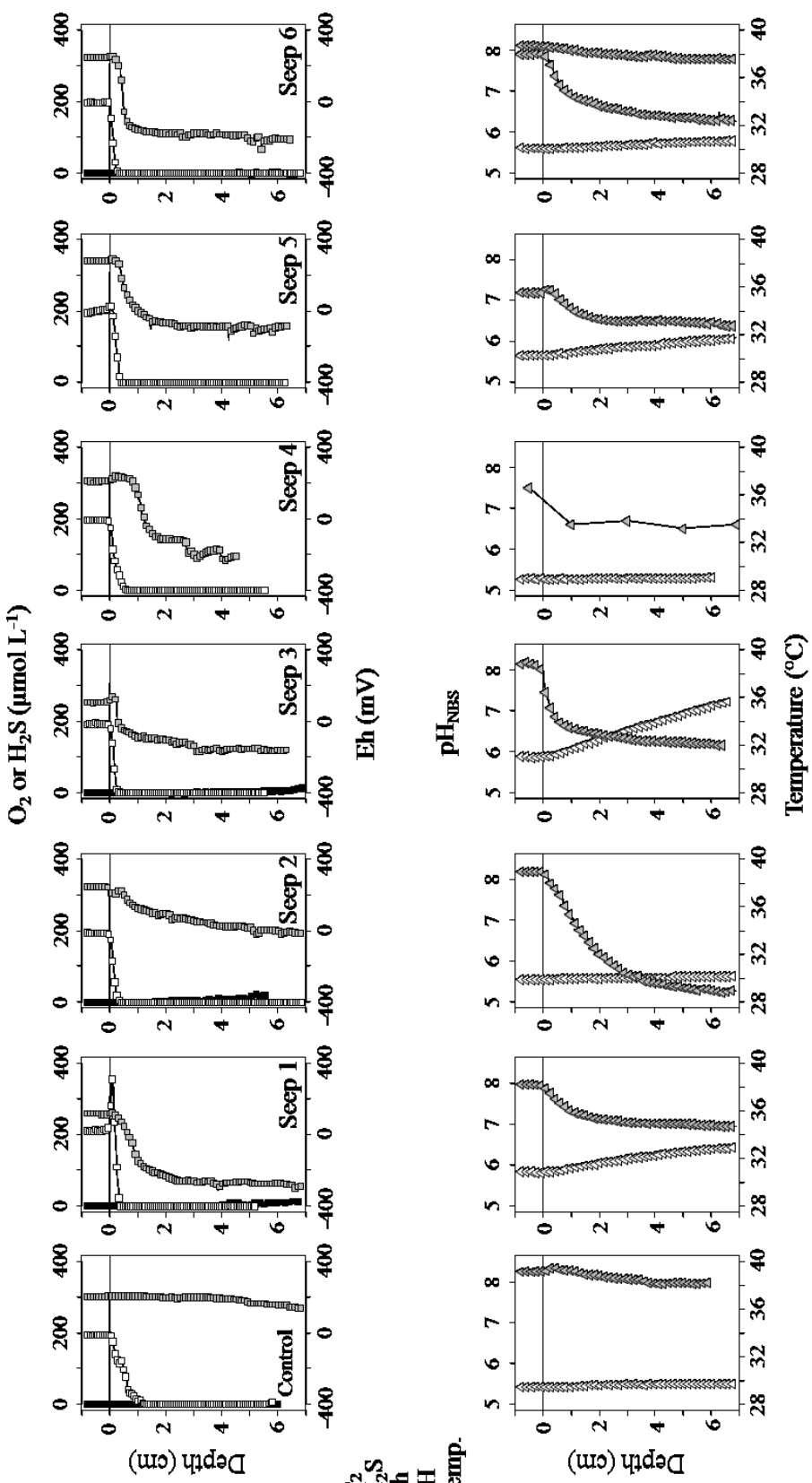

Figure 2: Vertical sediment profiles of *in situ* measurements of oxygen (O_2), hydrogen sulfide (H_2S) and redox potential (Eh; upper panel), and of pH_{NBS} and temperature (lower panel). Due to spatial heterogeneity of pore water pH in sediments of Seep 6 two contrasting profiles are shown. Due to sensor breakage no *in situ* pH profile is available at Seep 4, and the displayed pH profile was measured in discrete pore water samples (Lichtschlag et al. in preparation). The horizontal line at 0 cm depth indicates the sediment surface.

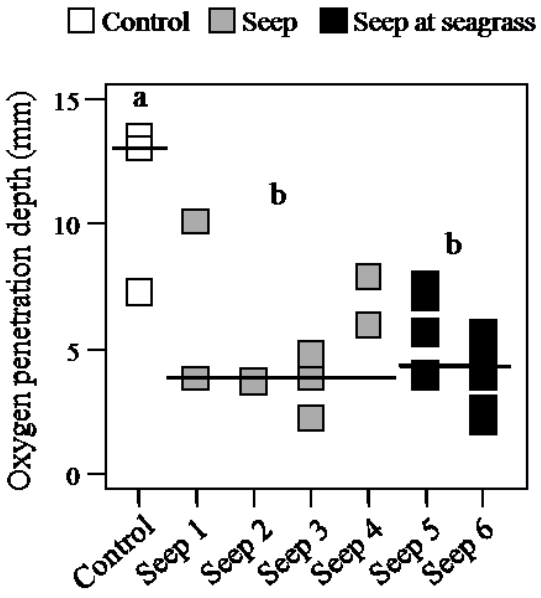

Figure 3: Oxygen penetration depth measured *in situ* at each study site, n = 1 - 6. Horizontal lines indicate the group median. Different letters indicate statistically significant differences between groups ($p < 0.05$).

Oxygen consumption rates

The Control sediments showed the overall lowest potential OCR, which were similar in the upper 4 cm of the sediment, ranging between 2 - 5 µmol cm^{-3} d^{-1} (Figure 4). The potential OCR of Seep and Seagrass sediments were often higher but spatially heterogeneous with depth, between replicates and between sites, with maximum values reaching 24 µmol cm^{-3} d^{-1} at Seep 6. Areal OCR were significantly different between groups (Kruskal-Wallis, $p < 0.05$). Compared to the Control group, which showed the highest median areal OCR (43 mmol m^{-2} d^{-1}; Figure 5a), rates of the Seep group were reduced by 30 - 63% ($p < 0.05$). The group Seep at seagrass showed the overall highest areal OCR (53 mmol m^{-2} d^{-1}). The reduced areal OCR despite high potential OCR in most sediments at the seep sites were due to a reduced oxygen penetration *in situ* (Figure 2 and 3).

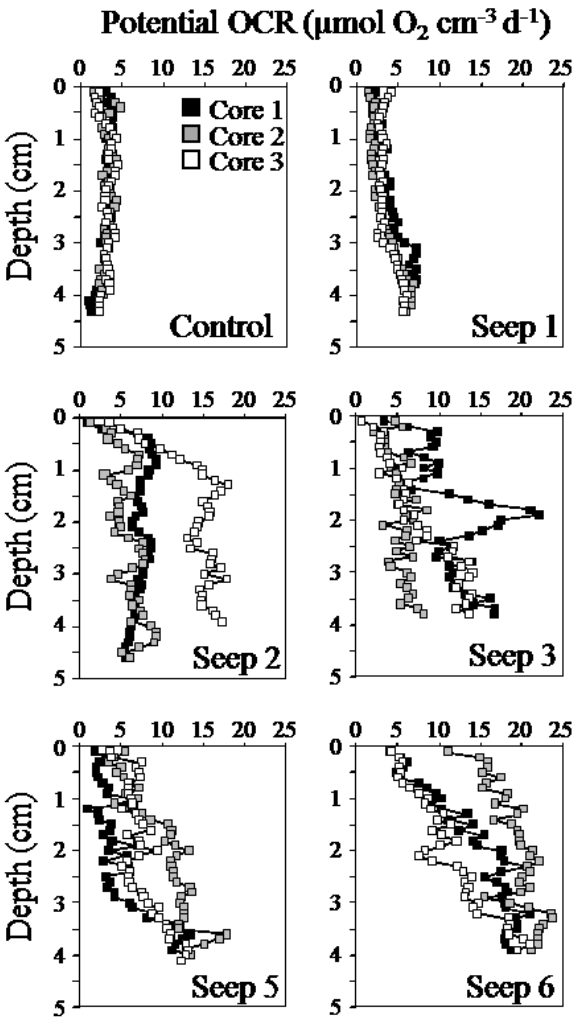

Figure 4: Potential volumetric oxygen consumption rates (OCR) of the investigated sediments, n = 3. No measurements are available for Seep 4.

Sulfate reduction rates

Pore water sulfate concentrations at the Control site were close to water column concentrations of 29 mmol L^{-1}, while the seep sites showed generally lower concentrations (Figure 6). Several seep sediments were characterized by a decreasing sulfate concentration with depth, with Seep 4 showing minimum values as low as 10 mmol L^{-1}. Volumetric SRR were highest in the upper sediment layer and either decreased or remained similar with increasing sediment depth in control and seep sediments. The SRR integrated over the upper 10 cm (areal SRR) were 1 - 2 orders of magnitude lower than the areal OCR (Figure 5b) and differed between groups (Kruskal-

Wallis, $p < 0.01$). Sediments of the Seep group showed significantly lower rates (0 - 1.1 mmol m^{-2} d^{-1}) when compared to the groups Control (1.9 - 2.6 mmol m^{-2} d^{-1}; Kruskal-Wallis, $p < 0.01$) and Seep with seagrass (0.6 - 5.6 mmol m^{-2} d^{-1}; Kruskal-Wallis, $p < 0.01$).

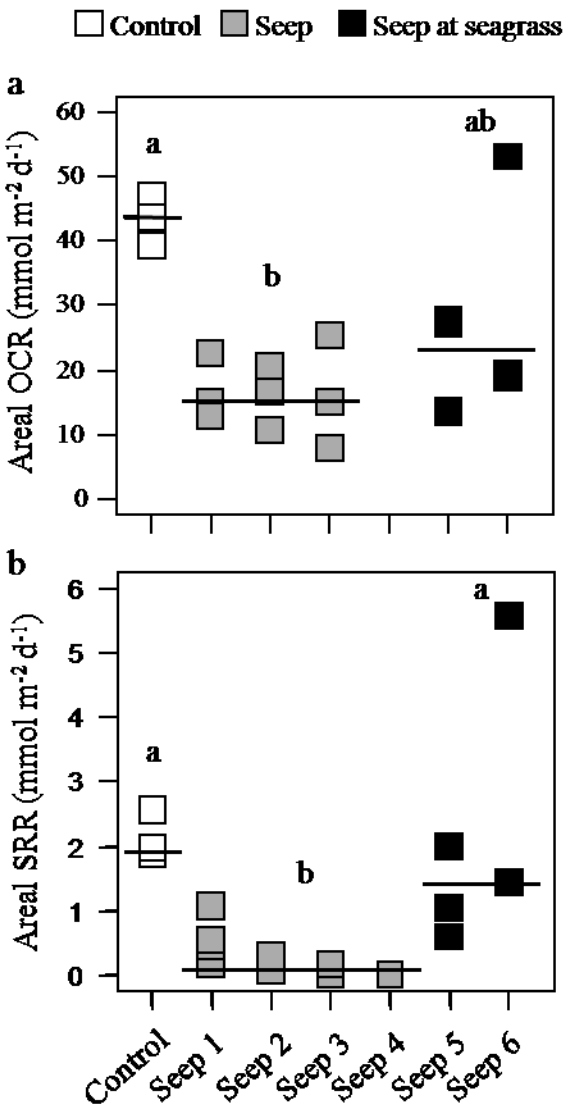

Figure 5: (a) Areal oxygen consumption rates (OCR) of the investigated sediments calculated by integrating potential OCR over the oxygen penetration depth, n = 3. No measurements are available for Seep 4. (b) Areal sulfate reduction rates (SRR) calculated by integration of volumetric SRR over the upper 10 cm of the sediments. n = 2 - 3. Horizontal bars indicate the group median. Different letters indicate statistically significant differences between groups ($p < 0.05$ in a, $p < 0.01$ in b).

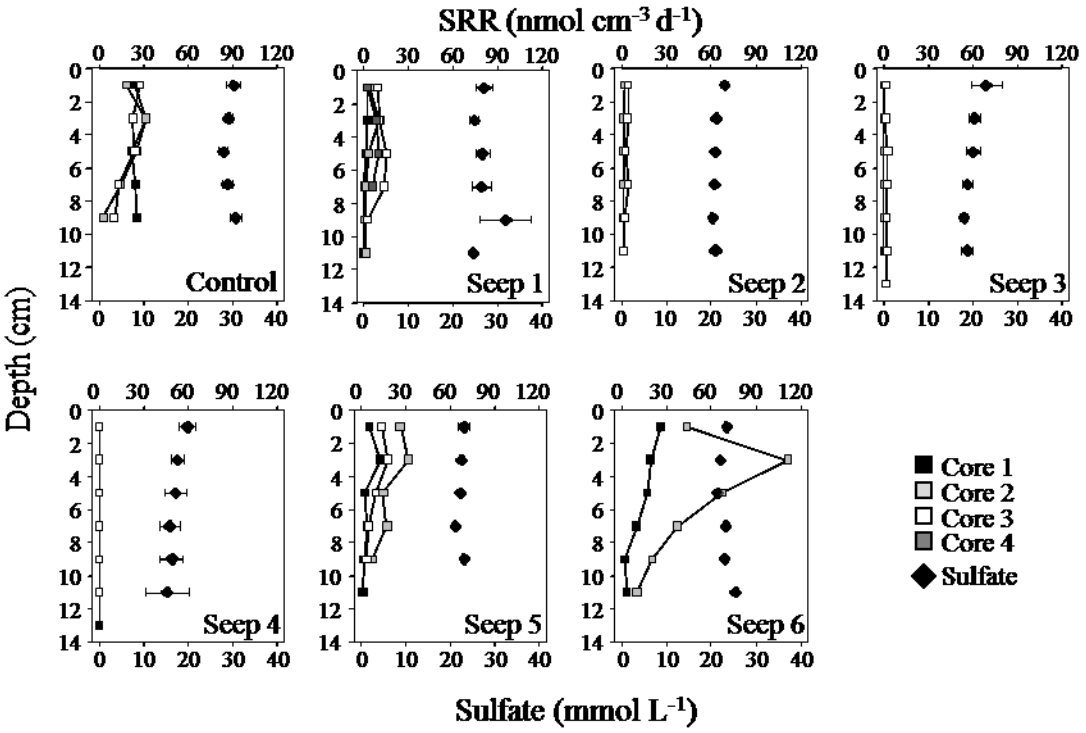

Figure 6: Volumetric sulfate reduction rates (SRR) and sulfate concentrations (mean ± standard error, horizontal error bars) in sediment cores from the investigated sites. n = 3, except n = 4 for Seep 2 and n = 2 for Seep 6 sediments.

Meiofauna abundance and diversity

The abundance of meiofauna in the upper 0 - 8 cm of the sediment was highest in Control sediments (1474 - 2118 individuals per 10 cm^2) and was significantly reduced in the Seep group (56 - 385 individuals per 10 cm^2; Kruskal-Wallis, $p < 0.05$; Figure 7). Meiofauna was most abundant in the upper two centimeters of the sediment and decreased with increasing sediment depth. In Control sediments this decrease was gradual, while seep sediments showed steep declines of 77 - 95% between 0 - 2 and 2 - 4 cm depth, remaining similar below. In the upper 0 - 8 cm of the sediment the taxonomic richness ranged between 9 - 15 taxa and was similar between the Control and Seep group (Kruskal-Wallis, $p > 0.05$), but showed distinct trends with depth. While richness decreased with depth in the Seep sediments, it remained similar in Control sediments over the investigated depth.

Several factors were correlated with each other (Table S2), particularly sulfate concentration, pH and median grain size ($r > 0.85$). The factors sulfate concentration, pH, and median grain size were significantly correlated with meiofauna abundance (Table S3). Sulfate concentrations best explained the variability in meiofauna abundance (82%). Meiofauna richness was significantly correlated with pH, temperature and median grain sizes, which together explained 95% of the variability.

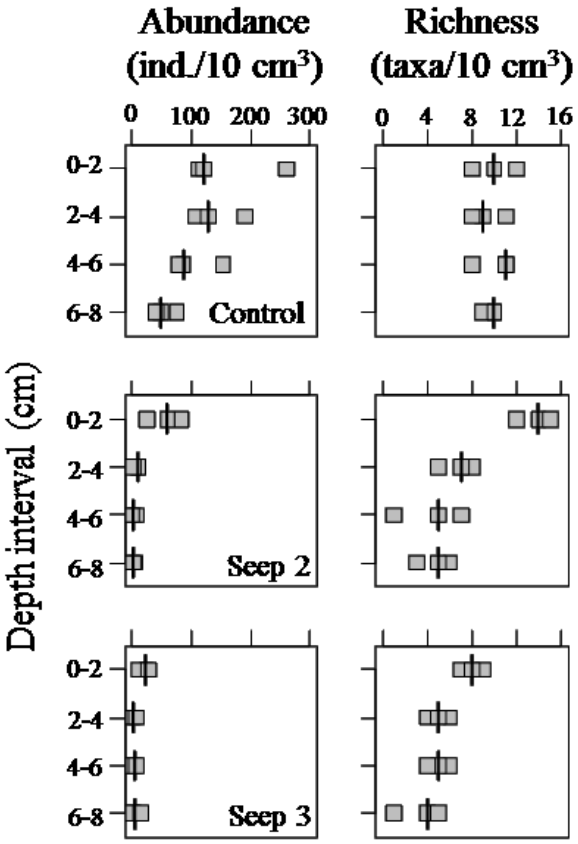

Figure 7: Depth profiles of meiofauna abundance and taxonomic richness in sediments from Control, Seep 2 and Seep 3. Vertical bars indicate the median of n = 3.

Microbial abundance

Microbial abundances were in the same order of magnitude and were not significantly different between groups (Kruskal-Wallis, $p > 0.1$ for 0-2 cm and $p > 0.7$ for 2 - 4 cm depth, Figure 8). They ranged between 6.5 - 10.6 x 10^8 cells cm^{-3} in the upper 0 - 2 cm and were slightly reduced to 5.4 - 9.5 x 10^8 cells cm^{-3} at 2 - 4 cm depth.

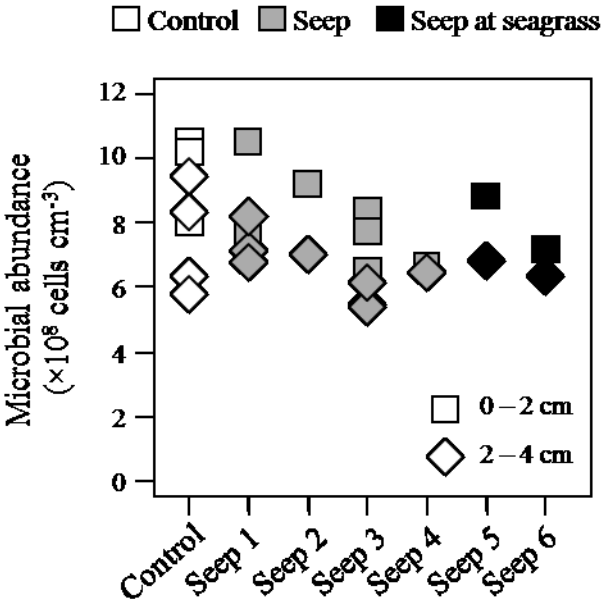

Figure 8: Microbial abundance from 0 - 2 cm (squares) and 2 - 4 cm (diamonds). n = 4 for Control, n = 3 for Seep 2 and Seep 3, n = 1 for all other sites.

Discussion

Sediment abiotic conditions

Our results demonstrate that hydrothermal activity at the seep sites profoundly changed the sediment habitat. The sediments of the Control sites (water column pH = 8.1) were typical permeable coral reef sediments (Rao et al. 2012; Yamamoto et al. 2015) not influenced by hydrothermal activity. The redox potential was only moderately decreased, while temperature (29°C) and pH (7.9) were similar to levels of the water column. As reported by other studies (Fabricius et al. 2011, 2013; Uthicke et al. 2013), water column conditions at the seep sites covered a realistic pH range of projected OA scenarios for the end of the century (average pH 7.7 - 8.0). However, abiotic conditions in the seep sediments were similar to sediments of other shallow-water hydrothermal vents (e.g. Wenzhöfer et al. 2000; Karlen et al. 2010). Pore water pH in most seep sediments decreased to values between < 6 and 7 with depth, likely surpassing the range for pore water pH under future OA. The only exception was a sediment patch inhabited by the seagrass *Halophila ovalis* (Seep 6), in which one profile showed an elevated pH, likely due to locally elevated inorganic carbonate content. Also, temperatures were often significantly higher than the respective water column values, indicating geothermal heating at some depth. The reduced redox potential found in seep sediments suggested that the pore water also contained elevated concentrations of chemically reducing compounds. Indeed, at some seep sites we detected elevated levels of hydrogen sulfide and reduced metals (Fe^{2+}, Mn^{2+}, Lichtschlag personal communication), which are often enriched in hydrothermal fluids (German and Von Damm 2003).

As a consequence of the reduced pore water pH, the seep sediments were largely decalcified (Fabricius et al. 2011; Uthicke et al. 2013) and consisted of finer silicate sands with 2 - 5 fold reduced permeabilities. The advective supply of organic matter and oxygen into the seep sediments is likely to be reduced due to the lower permeabilities. Indeed, the lower oxygen penetration at the seeps sites indicates a reduced oxygen supply, but this may also be due to the oxidation of reduced compounds with oxygen at the sediment-water interface (Wenzhöfer et al. 2000).

Thus, the seep sediments are influenced by other potentially habitat-shaping

factors, which co-occur with reduced pore water pH and which may complicate their use for ocean acidification research (Vizzini et al. 2013; Hassenrück et al. 2016). The described changes in abiotic parameters in sediments and pore water agree very well with data reported from other coral reef sediments located in Papua New Guinea (Ambitle Island), which are also influenced by hydrothermal seeping (Karlen et al. 2010). This suggests that similar changes may also be expected in sediments at other hydrothermal CO_2 seeps that are used as OA analogs and emphasizes the need to assess their suitability for OA research by characterizing their abiotic parameters.

Biotic responses

While the abundance of meiofauna in Control sediments was in the upper range of abundances found in other coral reef sediments (Boucher and Gourbault 1990), it was drastically reduced in seep sediments. This is a common finding at hydrothermal systems and is explained by the adverse environmental conditions in the sediments (Thiermann et al. 1997; Zeppilli and Danovaro 2009; Karlen 2010; Gollner et al. 2010). In contrast, meiofauna richness pooled over the entire sampling depth was similar between Control and Seep sediments. Identification on higher taxon level might, however, have masked differential vulnerability to exposure to hydrothermal conditions between different, even closely related species, genera and populations. However, both richness and abundance showed a marked decrease with increasing depth in Seep sediments, while in Control sediments richness and abundance were similar or decreased only moderately with depth, respectively. Abundance patterns were best explained by sulfate concentration, while pH, temperature and grain size explained the variability in richness. As in our study, sulfate concentrations are often reduced in sediments at hydrothermal seeps (German and Von Damm 2003) and used as a conservative tracer for hydrothermal fluids (Price et al. 2013), implying its high correlation with other hydrothermal fluid parameters. Indeed, sulfate concentration was correlated with pH and median grain size, suggesting an interplay of these factors in determining the observed patterns in meiofauna abundance and richness. While low pH and elevated temperature are directly associated with hydrothermal seepage, the reduced median grain size in seep sediments likely coincides with a reduced OM supply due to lower pore water advection in the less permeable seep sediments. This

is in agreement with the highest meiofauna abundance and richness close to the sediment-water interface of seep sediments, where relatively moderate environmental chemical conditions are present and where OM supply is typically the highest.

In contrast to meiofauna, the abundance of microorganisms remained similar between the investigated sediments and in the range of other coral reef sediments (Hansen et al. 1987; Rasheed et al. 2003). However, microbial communities significantly changed towards a reduced diversity, i.e. a lower evenness in the seep sediments (Hassenrück et al. 2016). Furthermore, the taxonomic composition of the microbial communities was strongly affected, with several factors responsible for the shifts in microbial community composition, including pore water pH, temperature and permeability (Hassenrück et al. 2016). This indicates that particularly the combination of several factors may meet or exceed physiological limits and support only tolerant organisms in sediments at hydrothermal CO_2 seeps.

Remineralization rates

We found a clear reduction in areal oxygen consumption and sulfate reduction rates in most seep sediments. Since the remineralization of organic matter in coral reef sediments is typically dominated by oxygen respiration and sulfate reduction (Werner et al. 2006), this suggests that OM remineralization was reduced in most seep sediments.

The lower areal OCR in seep sediments were not due to decreased volumetric OCR, but caused by a reduced oxygen penetration. Oxygen consumption is the sum of oxygen consumed by aerobic respiration and by the oxidation of reduced substances (e.g. H_2S, Fe^{2+}, Mn^{2+}) from anaerobic respiration (Fenchel and Jørgensen 1977) or from hydrothermal origin (Jannasch and Mottl 1985). Because of the low sulfate reduction rates and thus low production of H_2S in most seep sediments, the often high volumetric OCR were likely caused by the oxidation of reduced compounds of hydrothermal origin. The high volumetric OCR did not result in higher areal OCR, because oxygen consumption was limited by the oxygen availability. This can be explained by a combination of the oxidation of reduced compounds of hydrothermal origin, as also found in other vents systems (Wenzhöfer et al. 2000; de Beer et al. 2013), and a reduced advective supply of oxygen due to lower permeabilities. A reduced oxygen availability

can limit aerobic respiration in higher organisms and may also explain the decrease in the relative abundance of certain *Flavobacteria* (Hassenrück et al. 2016), many of which are known aerobic degraders of complex organic compounds (Bernardet et al. 2002).

In contrast to higher organisms, which are obligate aerobes, many microorganisms are able to use alternative electron acceptors (e.g. SO_4^{2-}, Fe^{3+}), particularly when oxygen is not available (Fenchel and Jørgensen 1977). However, sulfate reduction rates declined at most seep sites and even reached detection limit at Seep 4. This is consistent with a decrease in the relative abundance of known sulfate reducers of the deltaproteobacterial family *Desulfobacteriaceae* (Hassenrück et al. 2016) and the reduced expression of marker genes in the sediments (Hassenrück & Fink et al., in preparation). The patterns in SRR could not be explained by electron acceptor limitation since sulfate never reached limiting concentrations. The relatively moderate increase in temperature of seep sediments also seemed unlikely to have affected sulfate reduction.

Although we cannot exclude any negative effects of potentially toxic trace elements, our data point towards low pH and low organic matter supply as the main factors affecting SRR. Most sites with a reduced pore water pH also showed lower SRR. However, sediments at Seep 6 were spatially heterogeneous in TIC content and pore water pH was either similarly low as in the other seep sediments or reached levels of Control sediments (pH 7.9; Figure 2). Strikingly, one sediment core from this site showed the highest overall SRR. This observation may indicate a possible relationship between elevated pH and high SRR. Also in other shallow-water hydrothermal seeps a reduction of SRR (Bayraktarov et al. 2013) and the abundance of sulfate reducers (Sievert et al. 1999) were mainly attributed to low pH. Microbial adaptations to high CO_2 and low pH involve energy-costly processes to keep circumneutral pH in the cytoplasm (Baker-Austin and Dopson). Particularly, metabolic types with low energy yields, as sulfate reducers, may therefore be inhibited by high CO_2/low pH when energy supply is not sufficient.

We suggest that differences in organic matter supply can also explain the observed patterns in SRR. Compared to the Control sediments, filtration of organic matter mediated by pore water advection is likely reduced in the less permeable seep

sediments. In support of this, SRR in our study decreased with organic carbon content of the sediments (Figure S3d) and furthermore showed a decreasing trend with depth, where typically less degradable OM is present. The low organic carbon content of the sediments implies that most OM supplied to the sediments is remineralized so that no accumulation of OM occurs. This suggests that most easily degradable OM is remineralized aerobically at the sediment surface, not leaving enough substrate to support high sulfate reduction rates in deeper layers.

Interestingly, SRR were enhanced in seep sediments that were in the proximity of or colonized by seagrasses. Despite showing the smallest grain sizes and lowest permeabilities, SRR in sediments of Seep 5 and Seep 6 were only slightly reduced or even higher than in Control sediments, respectively. Both sites were located close to a dense bed of the seagrass *Cymodocea,* while Seep 6 sediments were also colonized by the seagrass *Halophila ovalis.* Seagrasses live in close association with sediments and are known to fuel sulfate reduction in sediments by supplying organic matter (Pollard and Moriarty 1991) via mechanisms, which do not necessarily require permeable sediments. These include the direct supply of seagrass parts as detritus (Gacia et al. 2002), the exudation of organic matter via leafs, roots and rhizomes (Barrón et al. 2014), and the gravitational settling of suspended organic material by reduction of local hydrodynamics by seagrass canopies (Gacia and Duarte 2001). Likely as a result of immediate organic matter supply from *H. ovalis,* sediments of Seep 6 showed the overall highest TOC content and SRR, while Seep 5 sediments rather received seagrass-derived OM via the water column.

OA effects on future coral reefs

This study confirms our hypothesis that a reduced production and an increased dissolution of reef carbonates due to OA could result in finer and, thus, less permeable sediments. The sediments at the seep sites were indeed finer and less permeable and were dominated by presumably land-derived silicate sands almost free of carbonates. Strikingly, this was also evident at moderately reduced bottom water and pore water pH (Seep 1), and suggests that even moderate acidification can severely impact the calcium carbonate budget of coral reefs.

A decline in the permeability of reef sediments will likely decrease the infiltration of organic matter by pore water advection and may reduce the role of sediments in retaining nutrients within future coral reefs. In a similar way and with similar results, reductions in the structural complexity of the reef framework as found at high CO_2 sites (Fabricius et al. 2011, 2013) are likely to coincide with lower framework permeability leading to less trapping, filtration and remineralization of OM. These indirect OA effects may thus have far reaching consequences for coral reef productivity and functions.

Strikingly, a progressive shift from coral-dominated towards seagrass-dominated benthic communities due to OA may enhance element cycling in sediments again. This is because seagrasses are able to supply colonized and adjacent sediments with organic matter via mechanisms that do not rely on high sediment permeability. In turn, due to the close association of seagrasses with sediments via their roots, nutrients released within sediments can efficiently be recycled for growth (de Boer 2007). These mechanisms may constitute a competitive advantage for seagrasses when future sediments get finer and may contribute to the CO_2 induced change from coral- to seagrasses-dominated benthic communities.

Conclusions

This study demonstrates that sediments at hydrothermal CO_2 seeps can be affected by extreme abiotic conditions and complex interactions of several habitat-shaping factors. These can impact sediment inhabiting organisms and important biogeochemical processes. Therefore, a careful characterization of the sediment habitat at hydrothermal CO_2 seeps is necessary, and great care has to be taken when such sites are used to study OA effects on sediments. Furthermore, our findings suggest that a reduced accumulation of carbonate sediments under OA could lead to finer sands of lower permeability, which may decrease their role as biocatalytic filters of organic matter. This indirect OA effect may decrease the efficient recycling of nutrients and thereby limit reef productivity, with potentially severe consequences for reef organisms and functions. This may contribute to the CO_2 induced change of benthic communities from corals to seagrasses, which possess more efficient ways to recycle nutrients from fine sediments.

Acknowledgements

The local owners of Upa Upasina are thanked for allowing our work on their reef. We are very grateful to captain R. van de Loos and the crew of the MV Chertan for assistance in the field. We would like to thank the cruise leaders K. Fabricius and S. Uthicke, and all participants of the cruises to PNG. The HGF-MPG Joint Research Group for Deep-Sea Ecology is thanked for provision of the *in situ* microprofiler and M. Wall for sharing CTD logger data. We thank the MPI Microsensor group technicians for the preparations of the excellent microsensors. For technical support with instruments we would like to acknowledge L. Polerecky, K. Imhoff, P. Färber, H. Osmers, V. Meyer, M. Alisch, V. Asendorf and A. Nordhausen. T. Ferdelman is deeply thanked for fruitful discussions and advice during all stages of the study. This study was funded by the German Ministry for Research and Education (BMBF) project on the Biological Impacts of Ocean Acidification (BIOACID II).

References

Anderson, M. J., R. Gorley, and K. Clarke. 2008. PERMANOVA+ for PRIMER: Guide to software and statistical methods. Primer-E Plymouth UK.

Andersson, A. J., I. B. Kuffner, F. T. Mackenzie, P. L. Jokiel, K. S. Rodgers, and A. Tan. 2009. Net Loss of $CaCO_3$ from a subtropical calcifying community due to seawater acidification: mesocosm-scale experimental evidence. Biogeosciences **6**: 1811–1823. doi:10.5194/bg-6-1811-2009.

Baker-Austin, C., and M. Dopson. Life in acid: pH homeostasis in acidophiles. Trends Microbiol. **15**: 165–171. doi:10.1016/j.tim.2007.02.005.

Barrón, C., E. T. Apostolaki, and C. M. Duarte. 2014. Dissolved organic carbon fluxes by seagrass meadows and macroalgal beds. Mar. Biogeochem. **1**: 42. doi:10.3389/fmars.2014.00042.

Bayraktarov, E., R. E. Price, T. G. Ferdelman, and K. Finster. 2013. The pH and pCO_2 dependence of sulfate reduction in shallow-sea hydrothermal CO_2 – venting sediments (Milos Island, Greece). Extreme Microbiol. **4**: 111. doi:10.3389/fmicb.2013.00111.

de Beer, D., M. Haeckel, J. Neumann, G. Wegener, F. Inagaki, and A. Boetius. 2013. Saturated CO_2 inhibits microbial processes in CO2-vented deep-sea sediments. Biogeosciences **10**: 5639–5649. doi:10.5194/bg-10-5639-2013.

de Beer, D., F. Wenzhofer, T. G. Ferdelman, and others. 2005. Transport and mineralization rates in North Sea sandy intertidal sediments, Sylt-Romo Basin, Wadden Sea. Limnol. Oceanogr. **50**: 113–127.

de Boer, W. F. 2007. Seagrass–sediment interactions, positive feedbacks and critical thresholds for occurrence: a review. Hydrobiologia **591**: 5–24. doi:10.1007/s10750-007-0780-9.

Boucher, G., and N. Gourbault. 1990. Sublittoral meiofauna and diversity of nematode assemblages off Guadeloupe Islands (French West Indies). Bull. Mar. Sci. **47**: 448–463.

Caldeira, K., and M. E. Wickett. 2003. Oceanography: Anthropogenic carbon and ocean pH. Nature **425**: 365–365. doi:10.1038/425365a.

Clarke, K. R., and R. Gorley. 2006. V6: User manual/tutorial. Primer-E Plymouth UK.

Comeau, S., R. C. Carpenter, C. A. Lantz, and P. J. Edmunds. 2015. Ocean acidification accelerates dissolution of experimental coral reef communities. Biogeosciences **12**: 365–372. doi:10.5194/bg-12-365-2015.

Comeau, S., P. J. Edmunds, C. A. Lantz, and R. C. Carpenter. 2014. Water flow modulates the response of coral reef communities to ocean acidification. Sci. Rep. **4**: 6681. doi:10.1038/srep06681.

Cyronak, T., I. R. Santos, and B. D. Eyre. 2013. Permeable coral reef sediment dissolution driven by elevated pCO_2 and pore water advection. Geophys. Res. Lett. **40**: 4876–4881. doi:10.1002/grl.50948.

Dickson, A. G., C. L. Sabine, and J. R. Christian. 2007. Guide to Best Practices for Ocean CO_2 Measurements, North Pacific Marine Science Organization.

Dove, S. G., D. I. Kline, O. Pantos, F. E. Angly, G. W. Tyson, and O. Hoegh-Guldberg. 2013. Future reef decalcification under a business-as-usual CO2 emission scenario. Proc. Natl. Acad. Sci. U. S. A. **110**: 15342–15347. doi:10.1073/pnas.1302701110.

Eyre, B. D., A. J. Andersson, and T. Cyronak. 2014. Benthic coral reef calcium carbonate dissolution in an acidifying ocean. Nat. Clim Change **4**: 969–976. doi:10.1038/nclimate2380.

Fabricius, K. E., G. De'ath, S. Noonan, and S. Uthicke. 2013. Ecological effects of ocean acidification and habitat complexity on reef-associated macroinvertebrate communities. Proc. R. Soc. Lond. B Biol. Sci. **281**. doi:10.1098/rspb.2013.2479.

Fabricius, K. E., C. Langdon, S. Uthicke, and others. 2011. Losers and winners in coral reefs acclimatized to elevated carbon dioxide concentrations. Nat. Clim. Change **1**: 165–169.

Feely, R. A., C. L. Sabine, K. Lee, W. Berelson, J. Kleypas, V. J. Fabry, and F. J. Millero. 2004. Impact of Anthropogenic CO_2 on the $CaCO_3$ System in the Oceans. Science **305**: 362–366. doi:10.1126/science.1097329.

Fenchel, T. M., and B. B. Jørgensen. 1977. Detritus Food Chains of Aquatic Ecosystems: The Role of Bacteria, p. 1–58. *In* M. Alexander [ed.], Advances in Microbial Ecology. Springer US.

Gacia, E., and C. M. Duarte. 2001. Sediment Retention by a Mediterranean Posidonia oceanica Meadow: The Balance between Deposition and Resuspension. Estuar. Coast. Shelf Sci. **52**: 505–514. doi:10.1006/ecss.2000.0753.

Gacia, E., C. M. Duarte, and J. J. Middelburg. 2002. Carbon and nutrient deposition in a Mediterranean seagrass (Posidonia oceanica) meadow. Limnol. Oceanogr. **47**: 23–32. doi:10.4319/lo.2002.47.1.0023.

German, C. R., and K. L. Von Damm. 2003. 6.07 - Hydrothermal Processes, p. 181-222, p. 181–222. *In* H.D.H.K.K. Turekian [ed.], Treatise on geochemistry. Pergamon.

Gollner, S., B. Riemer, P. Martínez Arbizu, N. Le Bris, and M. Bright. 2010. Diversity of Meiofauna from the 9°50´N East Pacific Rise across a Gradient of Hydrothermal Fluid Emissions. PLoS ONE **5**: e12321. doi:10.1371/journal.pone.0012321.

Gundersen, J. K., and B. B. Jørgensen. 1990. Microstructure of diffusive boundary layers and the oxygen uptake of the sea floor. Nature **345**: 604–607. doi:10.1038/345604a0.

Hallock, P. 1997. Reefs and reef limestones in Earth history, p. 13–42. *In* Life and Death of Coral Reefs. Chapman & Hall.

Hansen, L. A., D. M. Alongi, D. J. W. Moriarty, and P. C. Pollard. 1987. The dynamics of benthic microbial communities at Davies Reef, central Great Barrier Reef. Coral Reefs **6**: 63–70. doi:10.1007/BF00301375.

Hassenrück, C., A. Fink, A. Lichtschlag, H. E. Tegetmeyer, D. de Beer, and A. Ramette. 2016. Quantification of the effects of ocean acidification on sediment microbial

communities in the environment: the importance of ecosystem approaches. FEMS Microbiol. Ecol. doi:10.1093/femsec/fiw027.

Heip, C., M. Vincx, and G. Vranken. 1985. The ecology of marine nematodes. Oceanogr. Mar. Biol. Ann. Rev. **23**: 399–489.

Hobbie, J. E., R. J. Daley, and S. Jasper. 1977. Use of nuclepore filters for counting bacteria by fluorescence microscopy. Appl. Environ. Microbiol. **33**: 1225–1228.

Huettel, M., P. Berg, and J. E. Kostka. 2014. Benthic Exchange and Biogeochemical Cycling in Permeable Sediments. Annu. Rev. Mar. Sci. **6**: 23–51. doi:10.1146/annurev-marine-051413-012706.

Huettel, M., P. Cook, F. Janssen, G. Lavik, and J. J. Middelburg. 2007. Transport and degradation of a dinoflagellate bloom in permeable sublittoral sediment. Mar. Ecol. Prog. Ser. **340**: 139–153. doi:10.3354/meps340139.

Jannasch, H. W., and M. J. Mottl. 1985. Geomicrobiology of Deep-Sea Hydrothermal Vents. Science **229**: 717–725. doi:10.1126/science.229.4715.717.

Jeroschewski, P., C. Steuckart, and M. Kühl. 1996. An Amperometric Microsensor for the Determination of H_2S in Aquatic Environments. Anal. Chem. **68**: 4351–4357. doi:10.1021/ac960091b.

Jørgensen, B. B. 1978. A comparison of methods for the quantification of bacterial sulfate reduction in coastal marine sediments: I. Measurement with radiotracer techniques. Geomicrobiol. J. **1**: 11–27.

Kallmeyer, J., T. G. Ferdelman, A. Weber, H. Fossing, and B. B. Jørgensen. 2004. A cold chromium distillation procedure for radiolabeled sulfide applied to sulfate reduction measurements. Limnol Ocean. Methods **2**: 171–180.

Karlen, D. J. 2010. The Biocomplexity of Benthic Communities Associated with a Shallow-water Hydrothermal System in Papua New Guinea. Ph.D. thesis. Univ. of South Florida.

Karlen, D. J., R. E. Price, T. Pichler, and J. R. Garey. 2010. Changes in Benthic Macrofauna Associated with a Shallow-Water Hydrothermal Vent Gradient in Papua New Guinea. Pac. Sci. **64**: 391–404. doi:10.2984/64.3.391.

Klute, A., and C. Dirksen. 1986. Hydraulic conductivity and diffusivity: Laboratory methods. Methods Soil Anal. Part 1—Physical Mineral. Methods 687–734.

Langdon, C., W. S. Broecker, D. E. Hammond, and others. 2003. Effect of elevated CO_2 on the community metabolism of an experimental coral reef. Glob. Biogeochem. Cycles **17**: n/a-n/a. doi:10.1029/2002gb001941.

Larsen, M., S. M. Borisov, B. Grunwald, I. Klimant, and R. N. Glud. 2011. A simple and inexpensive high resolution color ratiometric planar optode imaging approach: application to oxygen and pH sensing. Limnol. Oceanogr. Methods **9**: 348–360. doi:10.4319/lom.2011.9.348.

Leclercq, N., J.-P. Gattuso, and J. Jaubert. 2002. Primary production, respiration, and calcification of a coral reef mesocosm under increased CO_2 partial pressure. Limnol. Oceanogr. **47**: 558–564. doi:10.4319/lo.2002.47.2.0558.

Meyer-Reil, L.-A. 1983. Benthic response to sedimentation events during autumn to spring at a shallow water station in the Western Kiel Bight. Mar. Biol. **77**: 247–256.

Muscatine, L., and J. W. Porter. 1977. Reef Corals: Mutualistic Symbioses Adapted to Nutrient-Poor Environments. BioScience **27**: 454–460. doi:10.2307/1297526.

Pilditch, C. A., C. W. Emerson, and J. Grant. 1997. Effect of scallop shells and sediment grain size on phytoplankton flux to the bed. Cont. Shelf Res. **17**: 1869–1885. doi:10.1016/S0278-4343(97)00050-2.

Polerecky, L., U. Franke, U. Werner, B. Grunwald, and D. de Beer. 2005. High spatial resolution measurement of oxygen consumption rates in permeable sediments. Limnol Ocean. Methods **3**: 75–85.

Pollard, P. C., and D. J. W. Moriarty. 1991. Organic carbon decomposition, primary and bacterial productivity, and sulphate reduction, in tropical seagrass beds of the Gulf of Carpentaria, Australia. Mar. Ecol. Prog. Ser. Oldendorf **69**: 149–159.

Poppe, L. J., A. H. Eliason, and M. E. Hastings. 2004. A visual basic program to generate sediment grain-size statistics and to extrapolate particle distributions. Comput. Geosci. **30**: 791–795. doi:10.1016/j.cageo.2004.05.005.

Price, R. E., J. P. Amend, and T. Pichler. 2007. Enhanced geochemical gradients in a marine shallow-water hydrothermal system: Unusual arsenic speciation in horizontal and vertical pore water profiles. Appl. Geochem. **22**: 2595–2605. doi:10.1016/j.apgeochem.2007.06.010.

Price, R. E., I. Savov, B. Planer-Friedrich, S. I. Bühring, J. Amend, and T. Pichler. 2013. Processes influencing extreme As enrichment in shallow-sea hydrothermal fluids of Milos Island, Greece. Chem. Geol. **348**: 15–26. doi:10.1016/j.chemgeo.2012.06.007.

Rao, A. M. F., L. Polerecky, D. Ionescu, F. J. R. Meysman, and D. de Beer. 2012. The influence of pore-water advection, benthic photosynthesis, and respiration on calcium carbonate dynamics in reef sands. Limnol. Oceanogr. **57**: 809–825.

Rasheed, M., M. I. Badran, and M. Huettel. 2003. Particulate matter filtration and seasonal nutrient dynamics in permeable carbonate and silicate sands of the Gulf of Aqaba, Red Sea. Coral Reefs **22**: 167–177. doi:10.1007/s00338-003-0300-y.

Rasheed, M., M. I. Badran, C. Richter, and M. Huettel. 2002. Effect of reef framework and bottom sediment on nutrient enrichment in a coral reef of the Gulf of Aqaba, Red Sea. Mar. Ecol. Prog. Ser. **239**: 277–285. doi:10.3354/meps239277.

Raulf, F. F., K. Fabricius, S. Uthicke, D. de Beer, R. M. M. Abed, and A. Ramette. 2015. Changes in microbial communities in coastal sediments along natural CO_2 gradients at a volcanic vent in Papua New Guinea. Environ. Microbiol. **17**: 3678–3691. doi:10.1111/1462-2920.12729.

Revsbech, N. P. 1989. An oxygen microsensor with a guard cathode. Limnol. Oceanogr. **34**: 474–478.

Richter, C., M. Wunsch, M. Rasheed, I. Kotter, and M. I. Badran. 2001. Endoscopic exploration of Red Sea coral reefs reveals dense populations of cavity-dwelling sponges. Nature **413**: 726–730. doi:10.1038/35099547.

Rix, L., J. M. de Goeij, C. E. Mueller, and others. 2016. Coral mucus fuels the sponge loop in warm- and cold-water coral reef ecosystems. Sci. Rep. **6**: 18715.

Røy, H., H. S. Weber, I. H. Tarpgaard, T. G. Ferdelman, and B. B. Jørgensen. 2014. Determination of dissimilatory sulfate reduction rates in marine sediment via radioactive 35S tracer. Limnol. Oceanogr. Methods **12**: 196–211. doi:10.4319/lom.2014.12.196.

Sievert, S. M., T. Brinkhoff, G. Muyzer, W. Ziebis, and J. Kuever. 1999. Spatial Heterogeneity of Bacterial Populations along an Environmental Gradient at a Shallow Submarine Hydrothermal Vent near Milos Island (Greece). Appl. Environ. Microbiol. **65**: 3834–3842.

Thiermann, F., I. Akoumianaki, J. A. Hughes, and O. Giere. 1997. Benthic fauna of a shallow-water gaseohydrothermal vent area in the Aegean Sea (Milos, Greece). Mar. Biol. **128**: 149–159. doi:10.1007/s002270050078.

Uthicke, S., P. Momigliano, and K. E. Fabricius. 2013. High risk of extinction of benthic foraminifera in this century due to ocean acidification. Sci Rep **3**. doi:10.1038/srep01769.

Vizzini, S., R. Di Leonardo, V. Costa, C. D. Tramati, F. Luzzu, and A. Mazzola. 2013. Trace element bias in the use of CO_2-vents as analogues for low-pH environments: Implications for contamination levels in acidified oceans. Estuar. Coast. Shelf Sci. 2013: **134**:19–30.

Wenzhöfer, F., O. Holby, R. N. Glud, H. K. Nielsen, and J. K. Gundersen. 2000. In situ microsensor studies of a shallow water hydrothermal vent at Milos, Greece. Mar. Chem. **69**: 43–54. doi:10.1016/S0304-4203(99)00091-2.

Werner, U., P. Bird, C. Wild, and others. 2006. Spatial patterns of aerobic and anaerobic mineralization rates and oxygen penetration dynamics in coral reef sediments. Mar. Ecol. Prog. Ser. **309**: 93–105.

Wild, C., M. Rasheed, C. Jantzen, P. Cook, U. Struck, M. Huettel, and A. Boetius. 2005. Benthic metabolism and degradation of natural particulate organic matter in carbonate and silicate reef sands of the northern Red Sea. Mar. Ecol. Prog. Ser. **298**: 69–78. doi:10.3354/meps298069.

Wild, C., M. Rasheed, U. Werner, U. Franke, R. Johnstone, and M. Huettel. 2004. Degradation and mineralization of coral mucus in reef environments. Mar. Ecol. Prog. Ser. **267**: 159–171.

Yamamoto, S., H. Kayanne, T. Tokoro, T. Kuwae, and A. Watanabe. 2015. Total alkalinity flux in coral reefs estimated from eddy covariance and sediment pore-water profiles. Limnol. Oceanogr. **60**: 229–241. doi:10.1002/lno.10018.

Zeebe, R. E., and D. Wolf-Gladrow. 2001. CO_2 in Seawater: Equilibrium, Kinetics, Isotopes. Elsevier Oceanogr. Ser. 65 Amsterdam.

Zeppilli, D., and R. Danovaro. 2009. Meiofaunal diversity and assemblage structure in a shallow-water hydrothermal vent in the Pacific Ocean. Aquat Biol **5**: 75–84.

Supporting information

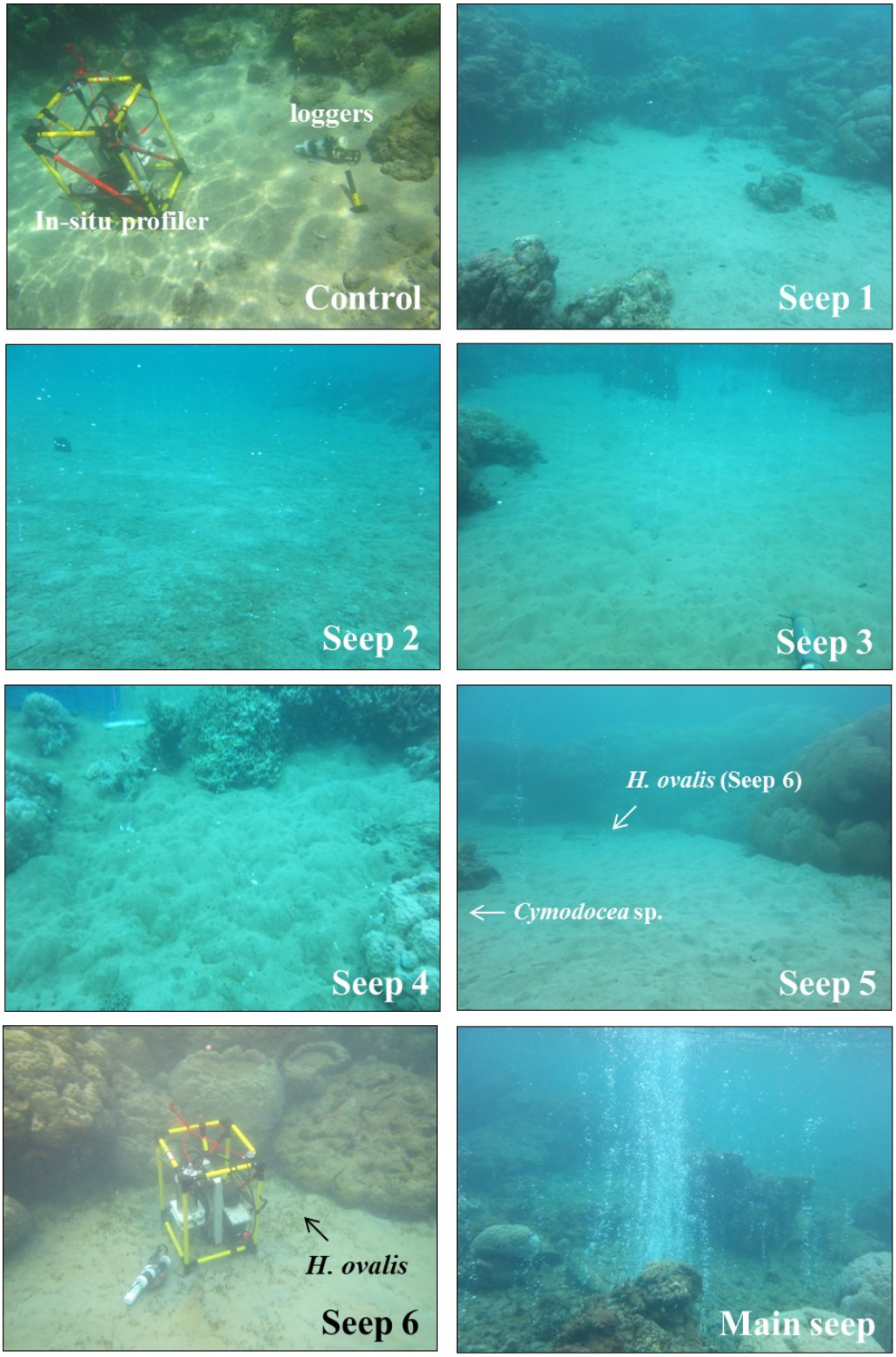

Figure S1: Photographs of investigated sites and the Main seep.

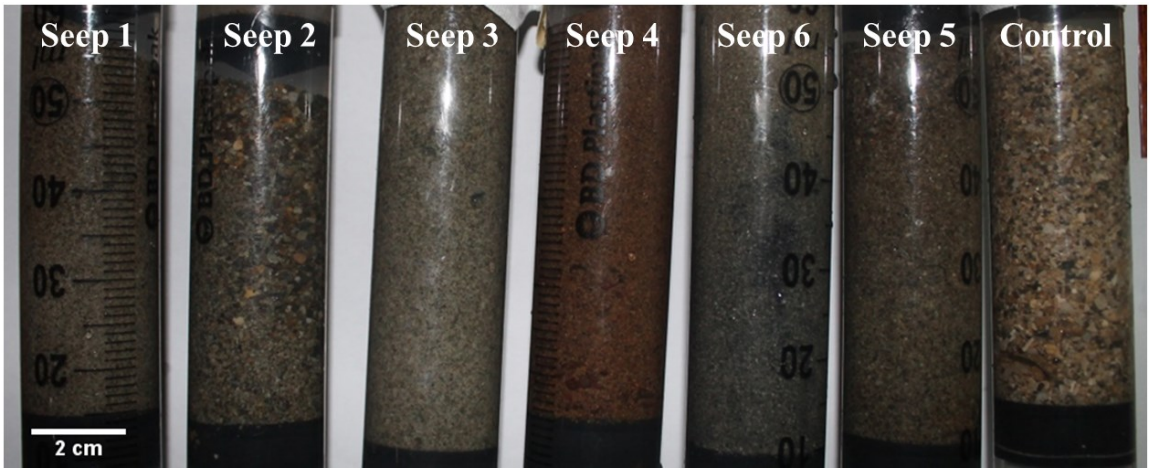

Figure S2: Photographs of sediment cores from the investigated sites.

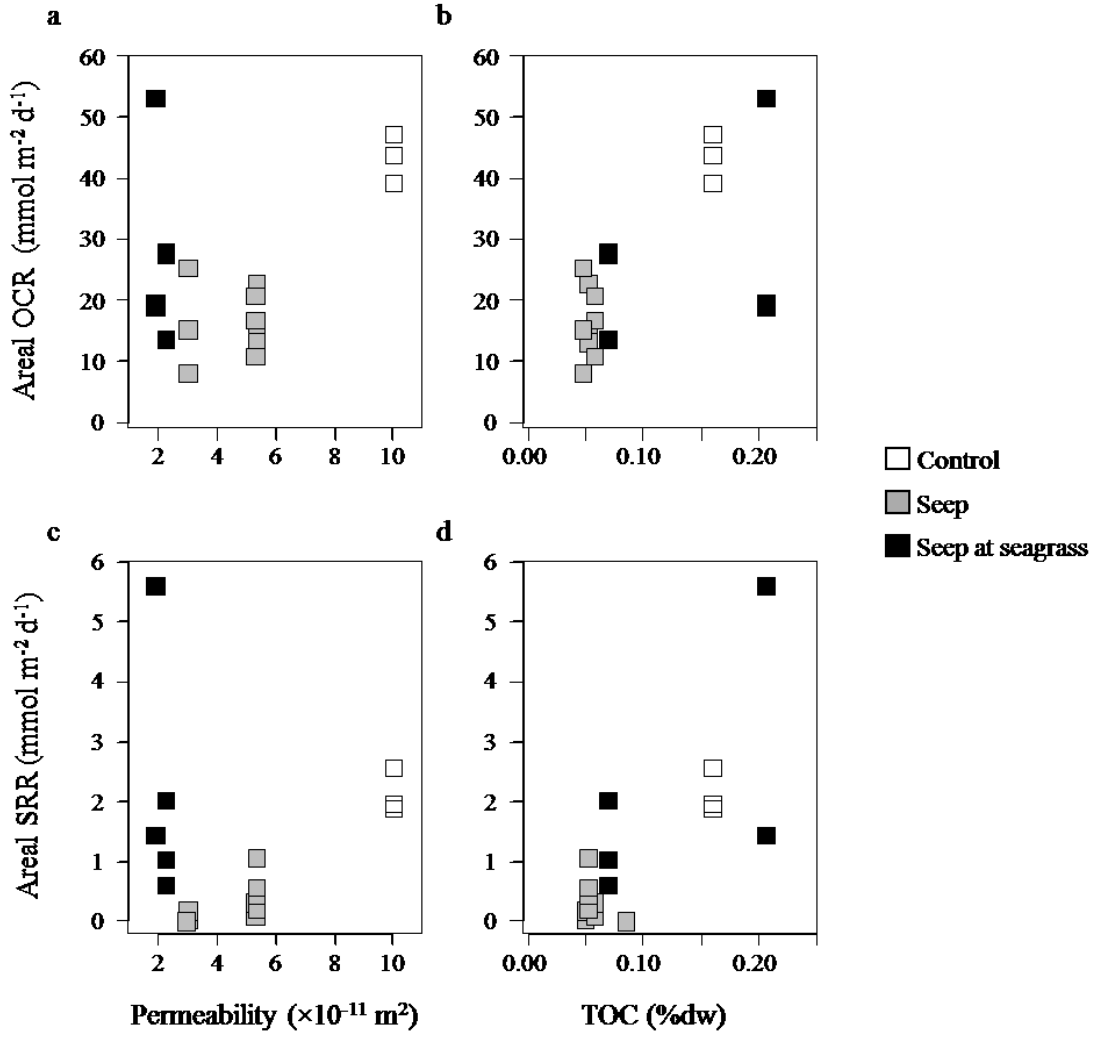

Figure S3: Areal oxygen consumption rates (OCR) and areal sulfate reduction rates (SRR) in relation to average (a,c) permeability and (b,d) average total organic carbon content (TOC) of the investigated sediments.

Table S1: Initial pH_{NBS} (mean ± SD) of percolated water during measurements of potential oxygen consumption, n = 3.

Site	pH_{NBS}
Control	8.15 ± 0.02
Seep 1	8.09 ± 0.03
Seep 2	8.00 ± 0.05
Seep 3	7.73 ± 0.04
Seep 5	7.39 ± 0.06
Seep 6	7.37 ± 0.03

Table S2: Correlation matrix showing the Spearman correlation coefficients between environmental factors used for DistLM analysis of meiofauna data.

Environmental factor	O_2	Temperature	pH	Median grain size	Porosity	Sulfate
O_2						
Temperature	-0.22					
pH	0.44	-0.33				
Median grain size	0.31	-0.55	0.85			
Porosity	0.19	0.023	0.75	0.63		
Sulfate	0.46	-0.61	0.90	0.96	0.63	

Table S3. Results of the DistLM analyses of meiofauna abundance and richness. Marginal tests show significant correlations between each individual variable on abundance (a) and richness (c). Sequential tests (b,d) are based on forward-selected variables, where the explained covariation by each variable depends on variables already in the model.

Variable	R^2	SS(trace)	Pseudo-F	P	Prop.	Cumul.	res.df
a) Marginal tests (abundance)							
O_2		26518	3.6	0.0778	0.26		
Temperature		25134	33.3	0.0792	0.25		
pH		80078	39.0	0.0001	0.80		
Median grain size		76970	32.6	0.0021	0.77		
Porosity		28052	38.7	0.0784	0.28		
Sulfate		82503	45.6	0.0004	0.82		
b) Sequential tests (abundance)							
Sulfate	0.820	82503	45.6	0.001	0.8	0.82	10
pH	0.852	3223	19.5	0.198	320.4	0.85	9
Porosity	0.886	3453	24.2	0.171	343.2	0.89	8
Median grain size	0.891	432	0.3	0.585	42.9	0.89	7
O_2	0.901	1067	0.6	0.414	106.0	0.90	6
Temperature	0.901	0	0.6	0.995	0.0	0.90	5
c) Marginal tests (richness)							
O_2		17	19	0.1876	0.16		
Temperature		40	60	0.0328	0.38		
pH		64	15	0.0041	0.61		
Median Grain size		39	58	0.0363	0.37		
Porosity		16	17	0.2167	0.15		
Sulfate		51	91	0.0138	0.48		
d) Sequential tests (richness)							
pH	0.61	64	15.4	0.004	0.6	0.61	10
Temperature	0.75	15	49.9	0.050	0.1	0.75	9
Sulfate	0.95	22	34.5	0.007	0.2	0.95	8
O_2	0.96	1	13.8	0.259	78.3	0.96	7
Median Grain size	0.96	211	301.0	0.840	2.0	0.96	6
Porosity	0.96	52	61.9	0.940	0.5	0.96	5

Table S4: Abundance of meiofaunal taxa and the median grain sizes at different depths of the investigated sediment. Due to its size this table was not included in this thesis.

Chapter 2

Quantification of the effects of ocean acidification on sediment microbial communities in the environment: the importance of ecosystem approaches

Christiane Hassenrück[1], Artur Fink[1], Anna Lichtschlag[2], Halina E. Tegetmeyer[1,3], Dirk de Beer[1], Alban Ramette[1,4]

[1] Max Planck Institute for Marine Microbiology, Celsiusstraße 1, 28359 Bremen, Germany

[2] National Oceanography Centre, University of Southampton, Waterfront Campus, European Way, Southampton SO14 3ZH, United Kingdom

[3] University of Bielefeld, Center for Biotechnology – CeBiTec, Universitätsstraße 27, 33615 Bielefeld, Germany

[4] Institute of Social and Preventive Medicine, Bern University, Finkenhubelweg 11, 3012 Bern, Switzerland

FEMS Microbiology Ecology (in press).

Abstract: To understand how ocean acidification (OA) influences sediment microbial communities, naturally CO_2-rich sites are increasingly being used as OA analogues. However, the characterization of these naturally CO_2-rich sites is often limited to OA-related variables, neglecting additional environmental variables that may confound OA effects. Here, we used an extensive array of sediment and bottom water parameters to evaluate pH effects on sediment microbial communities at hydrothermal CO_2 seeps in Papua New Guinea. The geochemical composition of the sediment pore water showed variations in the hydrothermal signature at seeps sites with comparable pH, allowing the identification of sites which may better represent future OA scenarios than others. At these sites, we detected a 60% shift in the microbial community composition compared to reference sites, mostly related to increases in *Chloroflexi* sequences. pH was among the factors significantly, yet not mainly, explaining changes in microbial community composition. pH variation may therefore often not be the primary cause of microbial changes when sampling is done along complex environmental gradients. Thus, we recommend an ecosystem approach when assessing OA effects on sediment microbial communities under natural conditions. This will enable a more reliable quantification of OA effects via a reduction of potential confounding effects.

Keywords: ocean acidification, microbial community composition, shallow-water hydrothermal vents, natural laboratories, next generation sequencing

Introduction

The increase in atmospheric CO_2 concentrations has led to a continuous increase in the partial pressure of CO_2 and decrease in pH in the oceans since pre-industrial times, a process called ocean acidification (OA). Since then, the ocean water pH has declined from approximately 8.2 to 8.1, reaching pH 7.8 by the year 2100 if we continue on the current and predicted CO_2 emissions trajectories (IPCC 2013). Such changes in the carbonate chemistry can have dramatic effects on marine organisms, e.g. reducing biogenic calcification (Hofmann *et al.* 2010), modifying fish sensory perception (Munday *et al.* 2014), or enhancing seagrass and macroalgal growth (Koch *et al.* 2013). Marine microbial populations are also expected to respond to OA. As key players in nutrient cycling and remineralization of organic matter, changes in marine microbial communities and in the services they provide have the potential for far-reaching consequences (Liu *et al.* 2010; Joint, Doney and Karl 2011).

Previous work on the effects of OA on marine microbes focused mostly on planktonic microbes, and has so far reported rather variable and inconsistent outcomes. Several incubation experiments documented a change in bacterial community composition, involving e.g. *Gammaproteobacteria* and *Flavobacteria*, as well as function under decreased pH conditions, e.g. increased nitrogen fixation rates and decreased nitrification (Beman *et al.* 2011; Kitidis *et al.* 2011; Krause *et al.* 2012; Lomas *et al.* 2012). There is also evidence that OA may increase microbial carbon degradation rates by increasing enzyme activity (Piontek *et al.* 2010). On the other hand, in many mesocosm studies the composition of the planktonic microbial community was mostly stable over varying pH levels without changes in biogeochemical functions (Newbold *et al.* 2012; Lindh *et al.* 2013; Roy *et al.* 2013; Oliver *et al.* 2014). Similarly divergent results were obtained from incubation experiments with microbial biofilms or marine sediments, which predicted either rapid responses of the microbial community to OA (Witt *et al.* 2011; Laverock *et al.* 2013; Tait, Laverock and Widdicombe 2013; Braeckman *et al.* 2014), or only minor impacts of OA on community composition and function (Tait and Laverock 2013; Gazeau *et al.* 2014).

To venture beyond the limited scope of incubation experiments and to assess long-term OA effects on microbial community composition and functions in their natural

environment, the usage of naturally CO_2-rich sites as OA analogues has become increasingly popular. Previous observations on microbial communities in sediments at naturally CO_2-rich sites focused mostly on sites in the Mediterranean Sea and in Papua New Guinea (Kerfahi *et al.* 2014; Taylor *et al.* 2014; Raulf *et al.* 2015). Pronounced changes in microbial richness and community composition were observed along acidification gradients. However, studies disagreed on the direction of the change in microbial richness: Kerfahi *et al.* (2014) and Raulf *et al.* (2015) detected an increase, whereas Taylor *et al.* (2014) observed a decrease of microbial richness with decreasing pH. Furthermore, reports on the prevalence of dominant microbial taxa in marine sediments (i.e. *Gammaproteobacteria*, *Alphaproteobacteria*, *Bacteroidetes*) under acidified conditions were inconsistent, with evidence pointing towards both increases and decreases as well as no changes in relative abundances (Kerfahi *et al.* 2014; Taylor *et al.* 2014; Raulf *et al.* 2015). So far these contrasting results have not been reconciled.

Many naturally CO_2-rich sites are associated with hydrothermal activity, which is the primary source of CO_2 at these sites (Hall-Spencer *et al.* 2008). However, the hydrothermal character often introduces confounding factors that make it difficult to specifically assess the impact of high pCO_2 and reduced pH (Vizzini *et al.* 2013). For instance, most CO_2-rich sites exhibit increased levels of methane, sulfide, temperature and various trace elements (Wenzhöfer *et al.* 2000; Meyer-Dombard *et al.* 2012; Vizzini *et al.* 2013; Burrell *et al.* 2015). Especially the sediments at naturally CO_2-rich sites may be strongly affected as they are influenced from above by the acidified water as well as from below by the hydrothermal fluids (Wenzhöfer *et al.* 2000). The increased temperatures and altered chemical composition of hydrothermal fluids, compared to seawater, can change pore water geochemistry and affect geochemical gradients in the sediment (Wenzhöfer *et al.* 2000; German and von Damm 2003). As such, sediments at naturally CO_2-rich sites constitute a highly complex system with a multitude of environmental parameters that shape microbial habitats and influence microbial community composition and associated functions.

In general, research on microbial communities at shallow-water hydrothermal seeps, including naturally CO_2-rich sites that were used as OA analogues, is very limited (Giovannelli *et al.* 2013) and often environmental measurements are not paired spatially

and temporally with microbiological characterizations. Apart from recent work by Molari *et al.* (unpublished), previous conclusions were based on a limited number of samples and recorded environmental parameters (Kerfahi *et al.* 2014; Taylor *et al.* 2014; Raulf *et al.* 2015). In several instances, water column parameters were used to describe microbial communities without comprehensively assessing the environmental conditions in the sediment, which the microbes were subjected to (Kitidis *et al.* 2011, Kerfahi *et al.* 2014; Raulf *et al.* 2015). Insufficient environmental characterization and subsequent poor selection of naturally CO_2-rich sites as OA analogues may constitute a potential cause for the diverging results regarding the impact of OA on sediment microbial communities.

Here, we quantified the impact of OA on sediment microbial communities at hydrothermal CO_2 seeps, while taking the complex environment associated with the CO_2 seepage into account. For this, we investigated natural shallow-water CO_2 seeps in Papua New Guinea, which have been extensively used in OA research (Fabricius *et al.* 2011; Morrow *et al.* 2014; Raulf *et al.* 2015). We used molecular community fingerprinting (Automated Ribosomal Intergenic Spacer Analysis) of more than 100 samples as well as next generation amplicon sequencing of the 16S rRNA gene to assess bacterial and archaeal community composition. We accompanied the molecular analyses with a comprehensive characterization of environmental conditions, including bottom and pore water chemistry, sediment permeability as well as carbon and nitrogen content. Through these analyses we further identified microbial taxa that may constitute 'losers' and 'winners' under the conditions at the CO_2 seeps.

Materials and Methods

Sampling

Sediment samples were collected at two CO_2 seeps at Upa Upasina, Normanby Island (Reef 1: S 9.82, W 150.82) and Dobu Island (Reef 2: S 9.74, W 150.86), Papua New Guinea (SI figure 1). Both reefs were characterized by a pH gradient created by hydrothermal CO_2 seepage and have been previously used as OA analogues to study sediment microbial communities (Raulf *et al.* 2015). Along this pH gradient, 14 sites were sampled at Reef 1 and six sites at Reef 2. At each site three independent replicate cores (diameter: 2.5 cm) were taken and the sediment of the first 2 cm (0 – 2 cm) and the next lower 2 cm (2 – 4 cm) was preserved in RNAlater Solution (Ambion) for molecular analysis.

To characterize the environmental conditions in the sediment along the pH gradient at Reef 1 the following parameters were measured: *in situ* oxygen concentrations, temperature, redox potential and pH using microsensor profiles (temperature sensor: UST Umweltsensortechnik GmbH, Geschwenda, Germany; pH sensor: Microelectrodes Inc., Bedford, NH, USA; http://doi.pangaea.de/10.1594/PANGAEA.858091); total organic and inorganic carbon and total nitrogen content of the sediment; grain size, porosity and permeability (http://doi.pangaea.de/10.1594/PANGAEA.858091); and pore water geochemistry analyzed from 6 ml pore water (http://doi.pangaea.de/10.1594/PANGAEA.858033). These parameters will be referred to as 'sediment parameters'. Additionally, bottom water samples were collected approximately 5 cm above each of the sediment cores at Reef 1 and 2 to measure carbonate chemistry (pH, dissolved inorganic carbon (DIC), total alkalinity (TA)) and nutrient concentrations (SiO_4, PO_4, NO_x, NH_4). Data on bottom water carbonate chemistry and nutrient concentrations will further be referred to as 'bottom water parameters' and is available in the Pangaea database (http://doi.pangaea.de/10.1594/PANGAEA.854018). An overview of the sampling design and the measured parameters is provided in SI table 1.

Automated Ribosomal Intergenic Spacer analysis

From each sample DNA was extracted from 1 g of sediment using the UltraClean Soil DNA extraction kit according to the manufacturer's instructions (MoBio Laboratories Inc., Carlsbad, CA, USA). The DNA was eluted in TE buffer (100 mmol L^{-1} Tris-HCl, 10m mmol L^{-1} EDTA) and quantified photometrically with a NanoQuant (Tecan, Crailsheim, Germany). To screen for changes in microbial community structure we used Automated Ribosomal Intergenic Spacer analysis (ARISA) with universal bacterial primers (Fisher and Triplett 1999). As previously described in Ramette (2009), triplicate reactions of the ARISA-PCR were run for each sample in an Eppendorf MasterCycler using the PeqLab PCR kit (PeqLab Biotechnology GmbH, Erlangen, Germany). Each PCR reaction contained 10 – 15 ng DNA, 1× buffer S, 0.25 mmol L^{-1} dNTPs, 0.1 g L^{-1} bovine serum albumin (BSA), 0.4 µmol L^{-1} fluorescently labeled forward primer (ITSF: 5'-GTCGTAACAAGGTAGCCGTA-3') and reverse primer (ITSReub: 5'-GCCAAGGCATCCACC-3'), an additional 1 mmol L^{-1} $MgCl_2$ and 0.05 U μL^{-1} Taq polymerase in a total reaction volume of 25 µL. PCR conditions were 3 min at 94°C followed by 30 cycles of 45 seconds denaturation at 94°C, 45 seconds annealing at 55°C, and 90 seconds elongation at 72°C, with a final elongation step for 5 min at 72°C. Fragment sizes were determined on a capillary sequencer. Fragments between 100 base pairs (bp) and 1000 bp were binned into operational taxonomic units (OTUs) using custom R scripts available at http://www.mpi-bremen.de/en/Software_4.html.

Amplicon sequencing and sequence processing

To taxonomically classify the microbial community, we sequenced the hypervariable regions V3-V4 and V4-V6 of the bacterial and archaeal 16S rRNA gene, respectively, using the bacterial primers S-D-Bact-0341-b-S-17 (5'-CTACGGGNGGCWGCAG-3') and S-D-Bact-0785-a-A-21 (5'-GACTACHVGGGTATCTAATCC-3'), and the archaeal primers Arch349F (5'-GYGCASCAGKCGMGAAW-3') and Arch915R (5'-GTGCTCCCCCGCCAATTCCT-3'; Amann *et al.* 1990; Klindworth *et al.* 2013). The community of the upper sediment layer of one replicate core was sequenced from 13

sampling sites at Reef 1. Sequences were generated on the Illumina MiSeq platform (CeBiTec Bielefeld, Germany), in a 2x300 bp paired-end run. Primer sequences were removed from the raw paired-end reads with *cutadapt* (Martin 2011). The primer-trimmed sequences are available on *ENA* (PRJEB11384). Sequences were quality trimmed with a sliding window of 4 bases and a minimum average quality of 15 with *trimmomatic* v0.32 (Bolger, Lohse and Usadel 2014), merged with *PEAR* v0.9.5 (Zhang *et al.* 2014), clustered into OTUs using *swarm* v2.0 (Mahé *et al.* 2014) and taxonomically classified with *SINA* (SILVA Incremental Aligner) v1.2.10 using the SILVA rRNA project reference database (release 119) at a minimum alignment similarity of 0.9 and a last common ancestor consensus of 0.7 (Pruesse, Peplies and Glöckner 2012). OTUs that were unclassified on domain level as well as those matching chloroplast and mitochondrial sequences were excluded from the analysis. The final OTU tables are accessible at http://doi.pangaea.de/10.1594/ PANGAEA.854018. Throughout the manuscript taxon names are used to designate sequence affiliation to the respective taxon and 'abundance' of bacterial and archaeal taxa is referring to the sequence abundance of Illumina amplicons.

Statistical analysis

Principal Component Analysis (PCA) was used to classify the sampling sites at Reef 1 into categories of hydrothermal influence based on observed sediment parameters. To assess the covariation among environmental parameters, pairwise Pearson correlation coefficients were calculated.

Alpha diversity indices were calculated based on repeated random subsampling of the amplicon data sets to assess richness and evenness of the microbial community, namely OTU number, Chao1 and abundance-based coverage estimator (ACE), inverse Simpson, percentage of absolute (occurring only once in the complete data set) and relative singletons (occurring only once in the sample) as well as absolute doubletons (occurring twice in only one sample in the complete data set). Significant differences in alpha diversity indices between hydrothermal influence categories were determined by analysis of variance (ANOVA) using permutation tests. P-values of subsequent pairwise

tests were adjusted using the Benjamini-Hochberg (BH; Benjamini and Hochberg 1995) correction procedure at the significance level of $p = 0.05$.

The change in community structure (beta diversity) between samples was quantified by calculating Bray-Curtis and Jaccard dissimilarity from relative OTU abundances. The former was used to produce non-metric multidimensional scaling (NMDS) plots and to test for community similarity between hydrothermal influence categories (ANOSIM tests); the latter was used to calculate the number of shared OTUs between samples. For the amplicon data sets, we excluded the rare biosphere by retaining only those OTUs that were present with more than two sequences in more than 10% of the samples. This reduction of the data sets did not change beta diversity patterns (Mantel test, $r > 0.9$, $p < 0.001$).

The contribution of environmental parameters to explaining the variation in community structure was calculated using redundancy analysis (RDA) and variation partitioning of centered log-transformed relative OTU abundances. Prior to significance testing, parameters were excluded using forward model selection until the minimum value of the Akaike Information Criterion (AIC) was reached. Of highly correlated parameters only one parameter was kept in the final models. Differentially abundant OTUs were detected using the *R* package *ALDEx2* (Fernandes *et al.* 2014) at a significance threshold of 0.05 for BH-adjusted parametric and non-adjusted non-parametric p-values. The significance threshold for planned parametric post-hoc tests was 0.1 (BH-adjusted).

All statistical analyses were conducted in R using the core distribution with the additional packages: *vegan* (Oksanen *et al.*, 2015), *compositions* (van den Boogaart *et al.,* 2014), *ALDEx2* (Fernandes *et al.* 2014) and *FactoMineR* (Husson *et al.*, 2015).

Results

Environmental conditions at sampling sites

The bottom water pH gradients created by the CO_2 seeps at Normanby and Dobu Island ranged from approximately 6.8 to 8.3 at both Reefs (Table 1). In addition to the changes in pH, bottom water silicate concentrations were increasing with decreasing distance to the main CO_2 seepage area from approximately 4 μmol L^{-1} at reference sites and more than 10-50 μmol L^{-1} at the seep sites. Reef 2 was further characterized by the presence of microbial mats in close proximity to the CO_2 seeps and by a strong sulfidic smell emanating from the CO_2 seeps. The presence of sulfide at the CO_2 seeps at Reef 2 convinced us to focus our sampling effort on Reef 1 as more likely OA analogue.

At Reef 1, the median pore water pH in the first 2 cm of the sediment and the following 2 cm calculated from *in situ* microprofiles ranged from 8.1 at reference sites to 5.9 at seep sites. Generally, median sediment pH was lower than bottom water pH and declined more rapidly when moving towards the main CO_2 seepage area. However, at a seagrass patch influenced by CO_2 seepage this relationship was reversed with a bottom water pH (7.1) that was lower than the median pore water pH (7.8). With decreasing sediment pH, median permeability dropped from approximately 8E-11 m^2 to 3E-11 m^2. Temperature profiles further showed increased temperatures at some of the seep sites, especially in the sediment layer from 2 – 4 cm, where maximum temperatures of more than 34°C were reached compared to approximately 30°C at the majority of the sites (Table 1). Pore water geochemistry of sediments with active fluid seepage showed increases in cations that are typically present in hydrothermal fluids, such as lithium, silicon and manganese, and decreases in cations that are typically depleted in hydrothermal fluids such as magnesium.

Table 1: Environmental conditions at the sampling sites on Normanby and Dobu Island, Papua New Guinea. Values are given as mean ± standard error. For pH, oxygen concentration and temperature microprofiles mean values per hydrothermal influence category were calculated based on median values per sediment layer (0 – 2 cm, 2 – 4 cm).

	Sediment layer	Reef 1			Reef 2		
		Reference	Medium	High	Reference	Medium	High
Water depth [m]		3.87 ± 0.08	4.30 ± 0.48	3.74 ± 0.56	3.50 ± 0.00	2.50 ± 0.08	2.30 ± 0.23
pH	0 – 2 cm	7.86 ± 0.23	7.15 ± 0.24	6.67 ± 0.21			
	2 – 4 cm	7.75 ± 0.20	6.64 ± 0.40	6.53 ± 0.31			
O_2 [µmol L^{-1}]	0 – 2 cm	16.28 ± 2.25	5.78 ± 4.70	0.41 ± 0.33			
	2 – 4 cm	0.17 ± 0.42	0.12 ± 0.08	0			
T [°C]	0 – 2 cm	29.80 ± 0.35	30.26 ± 0.14	30.49 ± 1.55			
	2 – 4 cm	29.86 ± 0.38	30.69 ± 0.20	31.56 ± 2.57			
Porosity	0 – 2 cm	0.49 ± 0.01	0.46 ± 0.02	0.47 ± 0.01			
	2 – 4 cm	0.45 ± 0.01	0.44 ± 0.02	0.45 ±0.03			
Permeability [m^2]	0 – 4 cm	8.24E-11 ± 0.81E-11	3.57E-11 ± 0.87E-11	2.96E-11 ± 0.02E-11			
pH	Bottom water	8.24 ± 0.02	7.83 ± 0.08	7.53 ± 0.13	8.33 ± 0.00	7.56 ± 0.05	6.78 ± 0.02
TA [mmol L^{-1}]	Bottom water	2.51 ± 0.02	2.50 ± 0.02	2.60 ± 0.03	2.42 ± 0.02	2.47 ± 0.02	2.52 ± 0.03
SiO_4 [µmol L^{-1}]	Bottom water	3.06 ± 0.18	5.17 ± 0.97	14.92 ± 3.17	4.26 ± 0.04	20.06 ± 3.48	50.95 ± 4.90
PO_4 [µmol L^{-1}]	Bottom water	0.04 ± 0.01	0.07 ± 0.01	0.08 ± 0.01	1.16 ± 0.65	0.10 ± 0.02	1.69 ± 0.72
NO_3 [µmol L^{-1}]	Bottom water	0.28 ± 0.02	0.46 ± 0.08	0.48 ± 0.07	3.37 ± 1.59	0.50 ± 0.17	0.96 ± 0.29
NO_2 [µmol L^{-1}]	Bottom water	0.02 ± 0.01	0.02 ± 0.00	0.03 ± 0.01	0.03 ± 0.01	0.02 ± 0.01	0.05 ± 0.01
NH_4 [µmol L^{-1}]	Bottom water	3.15 ± 2.55	2.47 ± 0.73	1.27 ± 0.79	0.76 ± 0.25	2.56 ± 1.56	1.33 ± 0.20

Sediment parameters were used to conduct a PCA to identify sampling sites at Reef 1 with similar characteristics based on all of the following parameters: pH, TA, oxygen concentration (O_2), redox potential (redox), temperature, porosity, grain size, permeability, total nitrogen (TN), total organic carbon (TOC), total inorganic carbon (TIC), nutrients (NH_4, NO_x), anions (Cl, Br, SO_4) and cations (Na, Li, Si, B, Mg, K, Fe, Mn, Sr, Rb, Ba, Ca, Cs). We identified three main clusters of sampling sites: reference and seep sites were separated along principal component 2 (PC2). The seep sites were further separated along PC1. The parameters contributing to PC1, which accounted for 40% of the variation in the data, were mostly concentrations of signature elements for hydrothermal activity such as lithium, silicon and manganese. Permeability, grain size, pH, nitrogen and organic carbon content of the sediment were among the parameters that contributed to PC2 (16% of the total variance in the data; Figure 1; SI figure 2). Based on the pattern in the PCA the sampling sites were classified into three categories: (I) reference sites characterized by ambient pH, (II) sites characterized by low pH and low hydrothermal influence, (III) and sites characterized by low pH and high hydrothermal influence, including pronounced temperature increases. Sampling sites falling within these three hydrothermal influence (HI) categories will be referred to as 'reference', 'medium HI' and 'high HI' sites thereafter.

Only sediment parameters where data were available for at least eight of the 14 sampling sites at Reef 1 were included in the RDA models to explain the variation in microbial community structure. Together with bottom water parameters and spatial information these were reef, position along the reef, water depth, bottom water silicate, phosphate, nitrate, nitrite, ammonium concentrations, TA and pH, sediment porosity, permeability, temperature, pH, redox potential and oxygen concentrations. Pairwise linear correlations among environmental parameters that were used for the RDA models revealed a complex pattern of covariation. Several parameters were highly correlated, e.g. bottom water silicate concentrations and bottom water pH, or permeability and the position of the sampling sites along the reef where absolute correlation coefficients were approximately 0.8. On the other hand, bottom water and sediment pH did not show any linear correlation (SI figure 3).

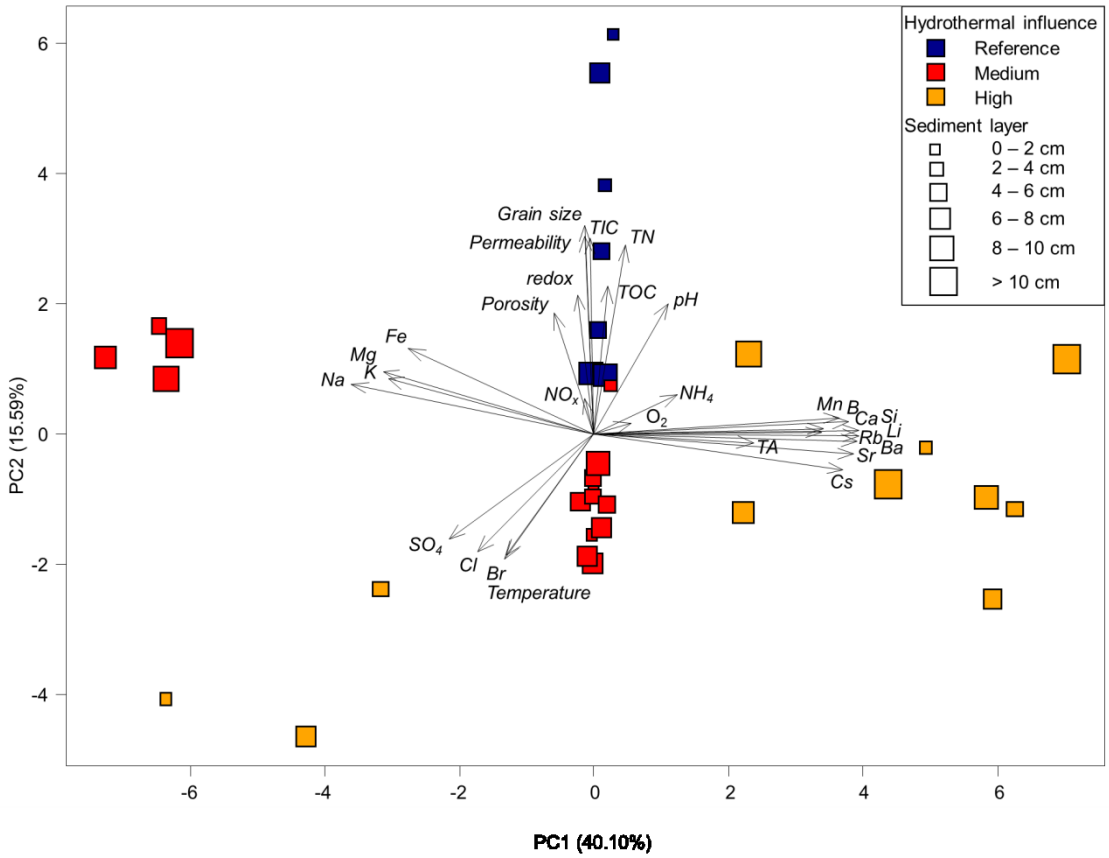

Figure 1: Principal Component Analysis (PCA) of the environmental conditions in the sediment at the sampling site at Reef 1 on Normanby Island to classify the sampling sites according to hydrothermal influence. The data are available at Pangaea (http://doi.pangaea.de/10.1594/PANGAEA.858033, http://doi.pangaea.de/10.1594/PANGAEA.858091). For oxygen, pH, temperature and redox potential microprofiles the PCA was calculated with median values for each sediment layer. Missing values were replaced by the mean of the respective parameter for the calculation of the PCA. The arrows show the loadings of the environmental parameters scaled to 4 times their value for better visualization. TIC: total inorganic carbon, TOC: total organic carbon, DIC: dissolved inorganic carbon, TN: total nitrogen, TA: total alkalinity.

Variation in microbial community structure

A total of 117 sediment samples were analyzed with ARISA to identify overall changes in microbial community structure (Figure 2). Microbial community structure showed distinct clusters associated with hydrothermal influence categories. Those clusters were confirmed to be significantly different from each other by ANOSIM (SI table 2). Whereas the microbial community structure of reference samples from both reefs was quite similar, there was a divergent trend at each of the two reefs from reference to medium to high HI sites. The microbial communities at the seep sites at Reef 1 and 2 were significantly different from each other (ANOSIM, R > 0.8, BH-adjusted

$p < 0.05$). Furthermore, there was no apparent influence of sediment layer on the microbial community composition (Figure 2). The average number of shared OTUs between samples from different hydrothermal influence categories at each reef was in most cases less than 40%. Generally more OTUs were shared between reference and medium HI sites or between medium and high HI sites, compared to reference and high HI sites (SI table 2). Even among samples within hydrothermal influence categories, the microbial community was very heterogeneous with about 50% shared OTUs between any two samples. The patterns of change in bacterial and archaeal community composition in the first 2 cm of the sediment based on 16S sequences were very consistent with ARISA results (SI table 2). The number of shared 16S OTUs was slightly lower with on average 12% to 28% shared OTUs between hydrothermal influence categories and about 30 to 50% within categories.

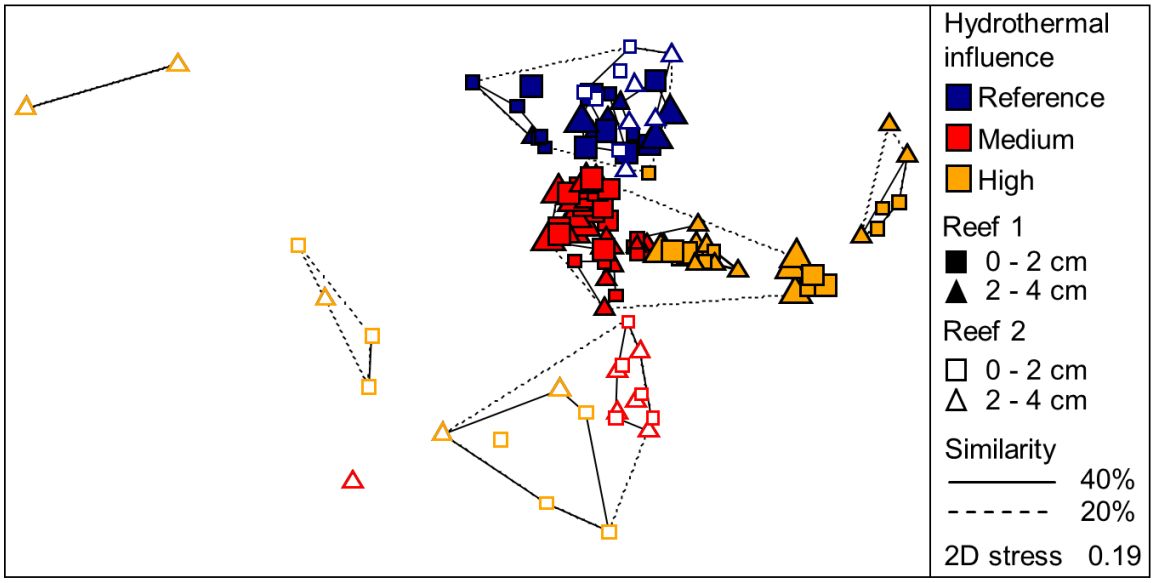

Figure 2: Non-metric multidimensional scaling (NDMS) plot based on the Bray-Curtis dissimilarity matrix of the microbial community based on Automated Ribosomal Intergenic spacer Analysis (ARISA). Larger symbols mark the subset of samples which was used in the redundancy analysis (RDA) models with sediment parameters (Table 2).

To estimate and compare the contribution of different sets of environmental parameters to explaining the patterns in microbial community composition, the ARISA data were analyzed with several RDA models: (i) the complete ARISA data set using bottom water parameters, (ii) a subset of the ARISA data set from Reef 1, where sediment parameters were available, that was also analyzed with (iii) bottom water parameters for comparability, (iv) the complete data set and (v) the ARISA subset using solely hydrothermal influence categories as explanatory variable (Table 2).

All ARISA RDA models as well as their individual factors significantly explained variation in microbial community structure, with the exception of bottom water nitrite concentration in the complete ARISA model, which was not significant but retained in the model selection procedure. The total amount of explained variation (R^2) varied from 20% to 44% between the RDA models based on the ARISA dataset. The models based only on hydrothermal influence categories explained approximately 10% less variation than the models based on numeric environmental parameters. The model with the ARISA subset from Reef 1 and bottom water parameters explained more variation than the model with the complete ARISA data set that also included samples from Reef 2 with an R^2 of 35% compared to 28%. Including sediment parameters further increased the total amount of explained variation, resulting in by far the best model with a R^2 of 44% and the lowest AIC of the models with the ARISA subset. pH alone was able to explain 4.5% (total R^2) in the bottom water models and almost 9% when pore water pH was used. Accounting for the variation explained by the other parameters in the models (pure R^2), pH explained much less of the changes in community structure due to covariation with the other parameters in the model. Despite the high degree of covariation, the contribution of pH to explaining the microbial community composition was significant in all models (Table 2). The variation explained by the other factors in the models was similar to that of pH ranging from a R^2 of 1.1 to 11.7%. Water depth, silicate concentrations, temperature and permeability were among the factors with the highest effects on community changes. For the amplicon data sets, only the significance of hydrothermal influence categories was tested due to the reduced number of samples. For both bacterial and archaeal communities, hydrothermal influence significantly explained the variation in community structure with a R^2 of 38% and 27%, respectively (Table 2).

Table 2: Contribution of observed environmental parameters to explaining the variation in microbial community structure based on redundancy analysis (RDA)-based variation partitioning. To compare the explanatory power of different sets of environmental parameters, several RDA models were tested: the complete ARISA data set was analyzed using bottom water parameters and hydrothermal influence categories; a subset of the ARISA data was analyzed using bottom water, sediment parameters and hydrothermal influence categories. The bacterial and archaeal amplicon data sets were analyzed using hydrothermal influence categories.

Data set	Model[a]	Source of variation	Total R^2 adjusted	Pure R^2 adjusted	F	df	p-value[b]	Covariation[c]
ARISA complete	Bottom water (AIC = 574.1)	All	0.277		5.126	9,88	< 0.001	
		Reef	0.067	0.037	5.555	1,88	< 0.001	0.030
		Position along reef	0.051	0.034	5.163	1,88	< 0.001	0.017
		Water depth	0.049	0.034	5.149	1,88	< 0.001	0.015
		SiO_4	0.055	0.029	4.540	1,88	< 0.001	0.026
		PO_4	0.028	0.025	4.068	1,88	< 0.001	0.003
		NO_3	0.017	0.015	2.827	1,88	0.028	0.002
		NO_2	0.018	0.008	1.962	1,88	0.272	0.010
		TA	0.033	0.015	2.900	1,88	0.025	0.017
		pH	0.041	0.029	4.547	1,88	< 0.001	0.012
	Categories (AIC = 638.5)	All	0.198		9.789	3,104	< 0.001	
		Reef	0.059	0.061	8.999	1,104	< 0.001	-0.002
		Hydrothermal influence	0.137	0.139	10.185	2,104	< 0.001	-0.002
ARISA subset	Bottom water (AIC = 248.6)	All	0.352		5.665	5,38	< 0.001	
		Position along reef	0.080	0.056	4.378	1,38	0.005	0.024
		Water depth	0.068	0.059	4.531	1,38	< 0.001	0.009
		SiO_4	0.097	0.066	4.994	1,38	< 0.001	0.031
		NO_3	0.066	0.041	3.442	1,38	0.024	0.025
		pH	0.045	0.043	3.579	1,38	0.025	0.003
	Sediment (AIC = 244.84)	All	0.436		5.156	8,35	< 0.001	
		Water depth	0.068	0.057	4.632	1,35	< 0.001	0.011
		SiO_4[d]	0.097	0.117	8.486	1,35	< 0.001	-0.020
		Porosity	0.029	0.043	3.728	1,35	< 0.001	-0.014
		Permeability	0.069	0.043	3.721	1,35	< 0.001	0.026
		O_2	0.016	0.012	1.763	1,35	0.002	0.004
		Redox potential	0.038	0.011	1.693	1,35	0.037	0.027
		Temperature	0.051	0.052	4.314	1,35	< 0.001	-0.001
		pH	0.088	0.038	3.457	1,35	< 0.001	0.050

Data set	Model[a]	Source of variation	Total R^2 adjusted	Pure R^2 adjusted	F	df	p-value[b]	Covariation[c]
	Categories (AIC = 251.8)	Hydrothermal influence	0.259		8.500	2,41	< 0.001	
16S Bacteria	Categories (AIC = 120.5)	Hydrothermal influence	0.375		4.606	2,10	< 0.001	
16S Archaea	Categories (AIC = 100.2)	Hydrothermal influence	0.267		3.188	2,10	< 0.001	

[a] The Akaike Information Criterion (AIC) is given for each model as goodness-of-fit statistic.
[b] Only the significance of the whole model (all) and the pure effects of the respective parameters (accounting for the effects of all other factors in the model) were tested. P-values were calculated based on restricted permutations.
[c] Covariation constitutes the amount of variation that can be explained by more than the parameter of interest.
[d] Bottom water silicate concentration were used as proxy for pore water concentrations, because of a high correlation based on point measurements of selected samples.

Taxonomic composition of microbial communities

The sediment at the CO_2 seeps hosted a very diverse community: estimated species richness based on 16S OTUs ranged from 13 000 to 48 000 for bacteria and 475 to 4100 for archaea (SI figure 4). Median Chao1 richness was highest in samples from reference sites with 42 000 for bacteria and 2700 for archaea, followed by 35 000 and 2000 at medium HI sites, and 14 000 and 960 at high HI sites, respectively. However, within each hydrothermal influence category, Chao1 estimates varied considerably over a range of more than 20 000 bacterial and 2000 archaeal species, without significant difference between groups. Bacterial and archaeal inverse Simpson index showed a weak decreasing trend from reference to medium and high HI sites. Both bacterial and archaeal communities consisted of a large proportion of rare OTUs, which made up approximately 40% (absolute singletons), 25% (relative singletons) and 10% (absolute doubletons) of all OTUs in each sample (SI figure 4).

The bacterial community was dominated by *Gamma*- and *Deltaproteobacteria* with a total relative abundance of 18% and 17%, respectively (Figure 3A). The next most abundant bacterial phyla were *Bacteroidetes* (9%), *Actinobacteria* (9%) and *Chloroflexi* (7%). Even at low taxonomic resolution levels, several bacterial taxa were identified as being differentially abundant between hydrothermal influence categories. The number of differentially abundant bacterial taxa increased as higher taxonomic resolution levels were considered (SI table 3). Generally between 20% and 70% of the sequences per sample belonged to differentially abundant bacterial taxa. In the next sections, we will focus on dominant bacterial taxa. The full list of the differentially abundant bacterial taxa is provided in SI table 4.

Among the dominant differentially abundant phyla, *Chloroflexi*, *Chlorobi* and *Deferribacteres* increased at medium and high HI sites compared to reference sites. The changes in relative abundance within the *Chlorobi* and *Chloroflexi* were caused by several taxa within these phyla, i.e. of the classes *Ignavibacteria* for *Chlorobi* and *Anaerolineae*, *Ardenticatenia* and *Caldilineae* for *Chloroflexi*. The genus *Caldithrix* was mostly responsible for the increase of *Deferribacteres* towards the seep sites. The difference in the relative abundance of *Chloroflexi* was most apparent towards high HI sites and was not statistically significant between reference and medium HI sites.

Chlorobi and *Caldithrix* also showed significant increases between reference and medium HI sites.

Although not detected as differentially abundant on phylum level, *Cyanobacteria*, predominantly of the *Subsections I* and *II*, were significantly less abundant at the seep sites than at reference sites. In all cases, this decrease was significant between reference and medium HI sites. The genus *Pleurocapsa* of *Subsection II* showed the strongest decrease among the *Cyanobacteria* from on average 2.3% at reference sites and disappearing almost completely at the seep sites. *Alphaproteobacteria* decreased towards the seep sites. This decrease was not uniform in all differentially abundant taxa of the *Alphaproteobacteria*, e.g. *Rhodobacteriaceae* increased from on average 1.7 to 3.4% at medium and high HI sites, whereas *Rhodospirillaceae* decreased from 8 to 3% and 1.5%, respectively. *Flavobacteria* were most abundant at reference and medium HI sites with on average 6% and 4%, respectively, and decreased toward high HI sites (1.8%). Similar to the case of *Alphaproteobacteria* this trend was not uniform, e.g. *Zeaxanthinibacter* already decreased significantly from reference sites (1.7%) to about 0.3% at medium and high HI sites. Within the *Deltaproteobacteria* several subgroups were differentially abundant, exhibiting divergent trends: whereas the order *Desulfuromonadales* (reference: 0.6%, medium HI: 1.1%, high HI: 2.9%) increased towards the seep sites with the strongest increase towards high HI sites, the family *Desulfobacteraceae* decreased severely towards high HI sites with an average relative abundance of 1.4% as compared to 6% at both reference and medium HI sites.

Differentially abundant OTUs largely fell into the previously mentioned differentially abundant bacterial taxa. Additionally, a large number of differentially abundant OTUs belonged to the actinobacterial *OM1 clade* (15 OTUs) and the gammaproteobacterial family *JTB255* (25 OTUs) with a total relative abundance of 4% and 1.4%, respectively. Yet, these OTUs did not follow a consistent trend with highest relative abundance at sites of any of the three hydrothermal influence categories.

The archaeal community was dominated by the *Marine Group I* archaeon *Candidatus* Nitrosopumilus, which accounted for 36% of the total number of sequences in the archaeal 16S data set (Figure 3B). The next most abundant groups were *Deep Sea Hydrothermal Vent Group 6* (18%), other *Marine Group I* archaea (15%), *Marine*

Benthic Group E (10%) and the genus *Cenarchaeum* (9%), also of the *Marine Group I*. The candidate genus Nitrosopumilus was generally more abundant at high HI sites where they reached maximum relative abundances of more than 60%. At reference and medium HI sites, they were much less abundant with on average 21% and 13%, respectively. A full list of the differentially abundant archaeal taxa is proved in SI table 5.

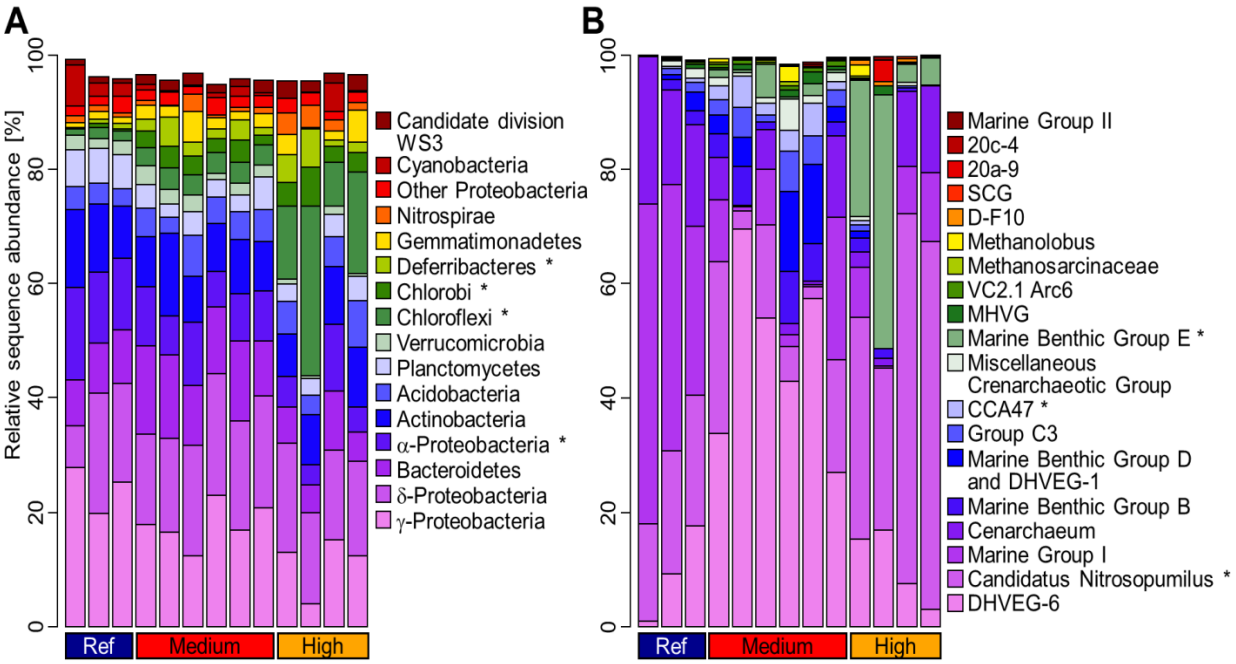

Figure 3: Taxonomic composition of the 10 most abundant bacterial phyla (A) and archaeal genera (B) per sample at reference, medium and high HI (hydrothermal influence) sites. For *Proteobacteria* class-level resolution is shown; for taxa that were unclassified on the respective level of resolution, the next higher-level classified taxonomic rank is shown. Asterisks mark significantly differentially abundant taxa between hydrothermal influence categories. SCG: *Soil Crenarchaeotic Group*, MHVG: *Marine Hydrothermal Vent Group*, DHVEG-6: *Deep Sea Hydrothermal Vent Group 6*.

Discussion

Usage of naturally CO_2*-rich sites as OA analogues*

We used sampling sites at the CO_2 seeps in PNG as analogues for OA research. The detailed characterization of the sediment based on 29 different environmental parameters showed that carbonate chemistry alone, specifically the pH gradient, was insufficient to describe the environmental conditions at these sites. Whereas some of the observed environmental parameters, e.g. sediment permeability, grain size, nitrogen, organic and inorganic carbon content, supported the classification of sites along the pH gradient, mainly pore water element concentrations varied among sampling sites with comparable pH. The enrichment or depletion of certain elements in the pore water can be used as an indicator of hydrothermal activity (German and von Damm 2003). Here, the increased concentrations of lithium, manganese and silicon pointed towards a stronger hydrothermal influence in several of the sampling sites associated with the CO_2 seeps, which were therefore termed 'high HI' sites.

The hydrothermal character of natural CO_2 seeps has been recognized before as potentially confounding influence for OA research (Vizzini *et al.* 2013). Vizzini *et al.* (2013) suggest referring to natural CO_2 seeps as low pH environments rather than analogues for OA. Here, the distinction between medium and high HI sites allowed us to define a level of hydrothermal influence that may still be considered a reasonable OA scenario. Because of their strong hydrothermal character, we propose that high HI sites exhibit conditions, which are less likely to occur under future OA than those at medium HI sites. Consequently, changes in the microbial communities that were only specific to high HI sites should be interpreted with caution because they may bias the assessment of OA impacts. Especially in cases where the community analysis is based on categories and not numerical environmental variables, accounting for the hydrothermal influence at naturally CO_2-rich sites is of paramount importance.

Because of logistic constraints, environmental data in OA studies on sediment microbial communities are often collected from the water column and rarely from the pore water and sediment directly (Kerfahi *et al.* 2014, Raulf *et al.* 2015). Here, particularly at the CO_2 seep sites, we observed strong deviations of the same parameters,

such as pH, between bottom and pore water measurements. Additionally, we detected pronounced differences in pore water element concentration between sampling sites, which were not recorded in previous observations on water column chemistry (Fabricius *et al.* 2011). Such deviations question the usage of bottom water measurements as proxy for conditions in the sediment at such sites, and will strongly affect our ability to accurately assess the driving environmental forces behind patterns of microbial richness and community composition in marine sediments. In this study, the divergence between bottom water and pore water parameters is evident in their explanatory power regarding the variation in microbial community composition. Noteworthy, basing the description of the microbial community on sediment rather than bottom water parameters increased the model fit and the percentage of explained variation of the microbial community composition by approximately 25%.

In both bottom water and sediment models, pH was among the factors significantly explaining changes in microbial community composition, which in case of bottom water pH was also observed previously in PNG (Raulf *et al.* 2015). Yet, many of the other observed parameters were statistically equally important, e.g. temperature and permeability. Furthermore, as commonly found in natural systems, it was difficult to account completely for confounding factors and to isolate the effects of interest due to a high degree of covariation among environmental parameters (Sunagawa *et al.* 2015). Therefore, it is possible that changes in the microbial community that were related to pH, as observed by RDA, could also be related, directly or indirectly, to silicate concentrations or organic carbon content, since these factors were strongly correlated. Only a small, although significant, percentage of explained variation was attributed to pH alone when accounting for covariation. These circumstances make the interpretation of the data in a biological context more difficult because changes in microbial community structure can often be assigned to several factors (Hanson *et al.* 2012).

Furthermore, there may be causal relationships between environmental parameters. Long-term acidification may reduce the accumulation of coarse carbonate sediments, resulting in finer sediments composed of silicate sands (Artur Fink, personal communication). The lower permeability of finer sediments may limit water circulation and the supply of oxygen and organic matter into the sediment and may thus change the

microbial habitat immensely, e.g. in terms of energy availability (Schöttner *et al.* 2011). Therefore, changes in the microbial community attributed to permeability may constitute indirect pH effects. The interdependencies of environmental factors may also help to explain the contrasting results regarding the effects of reduced pH on sediment microbial communities from different natural CO_2-rich sites: before the onset of pH decrease, the initial conditions in the sediment may have varied among naturally CO_2-rich sites even if present pH values are similar. To improve the comparability of naturally CO_2-rich sites, and to reconcile divergent microbiological results from different naturally CO_2-rich sites, knowledge of sediment parameters, such as permeability, is therefore required.

As alternative to the detailed analysis based on measured environmental parameters, the analysis of sediment microbial communities can be based on acidification categories, which summarize the conditions at the sampling sites (Kerfahi *et al.* 2014; Taylor *et al.* 2014). This approach was implemented here by using hydrothermal influence categories to describe the sediment microbial community. Although hydrothermal influence categories had generally less explanatory power than numeric environmental parameters, we were still able to explain about 20 to 38% of the total variation in microbial community composition. Values within this range of explained variation are not uncommon in microbial ecology (Hanson *et al.* 2012).

Changes in microbial community composition

The present study constitutes the second time the same sampling area in PNG was investigated to assess OA impacts on sediment microbial communities, with the initial exploration taking place in 2010 – 11 (Raulf *et al.* 2015). By using a larger sample size and a more comprehensive environmental characterization, we were able to confirm the general observations made in the previous study, thus underlying the reproducibility of the results obtained under natural conditions. Indeed, we found a similar overall taxonomic composition of the bacterial and archaeal communities as well as consistent shifts in microbial community composition and similar turnover rates of ARISA OTUs from reference to seep sites (Raulf *et al.* 2015). However, we showed that the composition of the microbial community at the seep sites was not comparable between Reef 1 and Reef 2, which was not detected previously (Raulf *et al.* 2015). Furthermore,

trends in alpha diversity of the microbial community here and from Raulf *et al.* (2015) diverged markedly: in Raulf *et al.* (2015) estimated bacterial richness and the percentage of rare bacterial OTUs increased as pH decreased, whereas here we detected a decreasing trend in richness that was, however, not statistically significant. A decrease in microbial richness would be consistent with similar observations in the Mediterranean (Taylor *et al.* 2014). Whether those contrasting results from PNG were caused by technical biases or by natural, temporal variation, still needs to be further investigated.

We used differential sequence abundance of bacterial and archaeal taxa to identify potential "winners" and "losers" under low pH conditions. In many samples, the relative abundance of differentially abundant taxa accounted for the majority of sequences in the sample, suggesting a large impact of hydrothermal influence on the microbial community. Among potential winners were the bacterial phyla *Chloroflexi*, *Chlorobi* and *Deferribacteres*. The mostly thermophilic *Chloroflexi* only showed a pronounced increase at high HI sites. Isolates of the three dominant differentially abundant classes *Anaerolineae*, *Ardenticatenia* and *Caldilineae* have been shown to prefer pH conditions around 7 or below (Yamada *et al.* 2006; Kawaichi *et al.* 2013), which were observed at the seep sites. Unlike other *Chloroflexi*, these three classes most likely do not photosynthesize and grow chemoheterotrophically (Yamada *et al.* 2006; Kawaichi *et al.* 2013). *Chloroflexi* have also previously been found to be more abundant at decreased pH in sediments and associated with corals and sponges in PNG (Morrow *et al.* 2014; Raulf *et al.* 2015).

Chlorobi, which are also known as green sulfur bacteria, have previously been detected at shallow-water hydrothermal seeps exhibiting decreased pH (Maugeri *et al.* 2009; Giovannelli *et al.* 2013). Unlike other *Chlorobi*, representatives of the class *Ignavibacteria*, which contained the most dominant differentially abundant OTU in our data set, were characterized as chemoheterotrophic, strictly anaerobic bacteria lacking genes for photosynthesis and sulfur oxidation (Iino *et al.* 2010; Liu *et al.* 2012). Bacteria of the *Deferribacteres*, specifically the genus *Caldithrix*, are most likely anaerobic chemoorganotrophs known to be associated with hydrothermal seeps and decreased pH (Miroshnichenko *et al.* 2003, 2010). *Chloroflexi*, *Chlorobi* and *Deferribacteres* may constitute important carbon degraders at PNG seep sites.

The alphaproteobacterial family *Rhodobacteraceae* was another potential winner at lower pH. *Rhodobacteraceae*, also called purple sulfur bacteria, have previously been reported to increase in abundance at the seep sites in PNG as well as other naturally CO_2-rich sites (Taylor *et al.* 2014; Raulf *et al.* 2015). The most abundant OTU of the *Rhodobacteraceae* was closely related to *Rhodovulum* species, which are able to oxidize iron and reduced sulfur compounds for anoxygenic photosynthesis preferably around pH 7 or lower (Straub, Rainey and Widdel 1999). Both dissolved iron and sulfide were present at the seep sites in PNG, although elevated sulfide concentrations were only detected in sediment layers deeper than 3 cm (Artur Fink, personal communication). These conditions might have facilitated the increased abundance of *Rhodobacteraceae* in general and *Rhodovulum* in particular. In coral reef ecosystems *Rhodobacteraceae* have been implicated in coral and seaweed diseases and their abundance in these associations was even higher at lower pH, supporting the hypothesis of a decline in reef health under OA (Meron *et al.* 2011; Bourne *et al.* 2013; Egan *et al.* 2013).

Rhodospirillaceae, an alphaproteobacterial family known as purple non-sulfur bacteria, were among the potential losers at decreased pH, with some OTUs disappearing completely already at medium HI sites. *Rhodospirillaceae* constitute a physiologically very diverse bacterial family with many uncultured types, complicating the functional classification of the *Rhodospririllaceae* in general. Among the OTUs which could be classified on genus level, *Defluviicoccus* is a chemoheterotroph that grows at temperatures below 30°C and at a variable pH range (Maszenan *et al.* 2005), which suggests that temperature might be the limiting factor for this genus at the seep sites.

Other potential losers were the cyanobacterial genus *Pleurocapsa* and the deltaproteobacterial family *Desulfobacteriaceae*. Although OA is expected to boost photosynthesis, *Cyanobacteria* in general are expected to benefit less from the increased availability of CO_2 when co-occurring with eukaryotic photosynthetic organisms (Koch *et al.* 2013). Preliminary data indicated that bulk net photosynthesis did not vary significantly between sampling sites in PNG (Artur Fink, personal communication), suggesting that there might be a replacement of cyanobacterial photosynthetic taxa at the seep sites by other photosynthetic organisms. Given the increased silicate concentration, diatoms are likely to dominate primary production at the seep sites. The genus

Pleurocapsa is further capable of calcification (Krumbein and Giele 1979; Rippka *et al.* 1979), which may increase its sensitivity to decreased pH.

Desulfobacteraceae reduce sulfate to degrade organic carbon anoxically (Kuever, Rainey and Widdel 2005). Although *Desulfobacteraceae* are expected to be able to adapt to decreased pH (Koschorreck 2008), they have been shown to decrease at CO_2 seeps (Raulf *et al.* 2015). This decrease was also observed here in the abundance of *Desulfobacteraceae* with the strongest decrease towards high HI sites. Measurements of sulfate reduction rates further documented a strong decline in sulfate reduction from reference to high HI sites (Artur Fink personal communication). The decrease in *Desulfobacteraceae* is accompanied by an increase in *Desulfuromonadales*, which can reduce iron or manganese as alternative electron acceptors to sulfate (Vandieken and Thamdrup 2013). Since iron and manganese were enriched at the seep sites, *Desulfuromonadales* may outcompete *Desulfobacteraceae* as carbon degraders.

Other bacterial taxa did not show a consistent trend, either in the monotony of the trend from reference to medium to high HI sites, or when considering the trends at higher taxonomic resolution levels. *Flavobacteria*, with OTUs mostly related to aerobic carbon degraders (Bernardet, Nakagawa and Holmes 2002), were most abundant at reference and medium HI sites and decreased severely towards high HI sites. At higher taxonomic resolution levels, divergent trends emerged between reference and medium HI sites with several flavobacterial taxa either increasing or decreasing. The strong decrease at high HI sites was common to most differentially abundant flavobacterial taxa and may be attributed to the lower oxygen availability at these sites resulting from a shallower oxygen penetration depth as compared to reference sites. The flavobacterial genus *Zeaxanthinibacter* was among the taxa that displayed a continuous decrease from reference to medium and high HI sites. The decrease in *Zeaxanthinibacter* may also be related to decreased Zeaxanthin pigment concentrations at the seep sites (Artur Fink, personal communication; Asker, Beppu and Ueda 2007). Members of this genus are characterized as strictly aerobic bacteria, which grow at a range of pH values and can degrade long-chain carbohydrates (Asker, Beppu and Ueda 2007). Their aerobic lifestyle supports the hypothesis that oxygen may be the limiting factor restricting the distribution of at least some *Flavobacteria*. At high HI sites, *Flavobacteria* might be replaced by

Chlorobi, *Chloroflexi* and *Deferribacteres* as major carbon degraders under anoxic conditions. Our results were only partially consistent with previous studies at naturally CO_2-rich sites, which have so far unanimously supported an increase in *Flavobacteria* at decreased pH potentially linked to an increased availability of organic matter (Kerfahi *et al.* 2014; Taylor *et al.* 2014). However, in our study the organic carbon content of the sediment was lower at the seep sites (Artur Fink, personal communication), which may contribute to explaining these divergent findings.

The dominant archaeal taxon, *Candidatus* Nitrosopumilus, has previously been described in PNG to increase in abundance as pH decreases (Raulf *et al.* 2015). Its role as ammonia oxidizer may contribute to maintain nitrification in reef sediment under reduced bacterial ammonia oxidation (Laverock *et al.* 2013; Raulf *et al.* 2015). We also detected an increase in *Candidatus* Nitrosopumilus at decreased pH, which was, however, restricted to high HI sites and may therefore be less likely to occur under future OA.

In summary, we were able to confirm the majority of the trends in differentially abundant taxa, which were previously observed either in PNG or at other naturally CO_2-rich sites. However, in specific instances, we detected taxa, which have not been identified in OA research before, or which did not display the same trends as reported previously. These inconsistencies with previous studies may have several reasons: (I) The distinction between medium and high HI sites allowed us to identify taxa only changing in abundance towards sites exhibiting conditions that may be less likely under future OA scenarios. The most drastic changes in microbial community composition were observed at the high HI sites and thus are likely correlated with parameters other than pH. (II) In many instances, pH may not be the primary factor limiting the distribution of a microbial taxon even at medium HI sites. Other factors, such as oxygen availability, temperature, organic carbon content, or the presence of alternative electron acceptors, may be equally or more likely to explain the differential abundance of microbial taxa between hydrothermal influence categories. (III) It is important to consider the taxonomic resolution when analyzing microbial communities. Especially in physiologically highly diverse taxa, a comparison at low taxonomic resolution levels might be insufficient to recover more detailed patterns in microbial community composition. (IV) As already suggested by Raulf *et al.* (2015) the sampling area in PNG may be subject to a large

temporal variation in microbial community composition. To better account for this phenomenon and to resolve inconsistencies with previous results, repeated monitoring studies, as conducted here, would be necessary.

Conclusion

We conclude that naturally CO_2-rich sites, such as the CO_2 seeps in PNG, may continue to be used for OA research on sediment microbial communities under the premise that the environmental conditions in the sediment are well documented. Furthermore, we recommend caution in attributing changes in microbial communities to acidification without a careful consideration of other environmental parameters. Thus, for future research on the impact of OA on sediment microbial communities, we strongly recommend performing a detailed assessment of the environmental conditions in the sediment and of other parameters than those of the carbonate system. This will enable a more reliable selection of naturally CO_2-rich sites as analogues for OA scenarios and will also improve the comparability between studies from different naturally CO_2-rich sites.

Funding

This work was part of the BIOACID II project that was supported by the German Federal Ministry of Education and Research [FKZ 03F0655].

Acknowledgements

Foremost we would like to thank the cruise leader Katharina Fabricius, all cruise participants and the crew and captain of the MS Chertan during the cruise to Papua New Guinea in 2013 and 2014. Further, we thank Pier Luigi Buttigieg, Christian Quast and Jan Gerken for their advice on the bioinformatic and statistical analysis, Martina Alisch for TA, DIC and nutrient measurements and Massimiliano Molari for extended discussions about CO_2 seeps.

References

Amann RI, Binder BJ, Olson RJ *et al.* Combination of 16S rRNA-Targeted Oligonucleotide Probes with Flow Cytometry for Analyzing Mixed Microbial Populations. *Appl Environ Microbiol* 1990;**56**:1919–25.

Asker D, Beppu T, Ueda K. Zeaxanthinibacter enoshimensis gen. nov., sp. nov., a novel zeaxanthin-producing marine bacterium of the family Flavobacteriaceae, isolated from seawater off Enoshima Island, Japan. *Int J Syst Evol Microbiol* 2007;**57**:837–43.

Beman JM, Chow C-E, King AL *et al.* Global declines in oceanic nitrification rates as a consequence of ocean acidification. *Proc Natl Acad Sci U S A* 2011;**108**:208–13.

Benjamini Y, Hochberg Y. Controlling the False Discovery Rate: a Practical and Powerful Approach to Multiple Testing. *J R Statist Soc B* 1995;**57**:289–300.

Bernardet J-F, Nakagawa Y, Holmes B. Proposed minimal standards for describing new taxa of the family Flavobacteriaceae and emended description of the family. *Int J Syst Evol Microbiol* 2002;**52**:1049–70.

Bolger AM, Lohse M, Usadel B. Trimmomatic: A flexible trimmer for Illumina sequence data. *Bioinformatics* 2014;**30**:2114–20.

Bourne DG, van der Zee MJJ, Botté ES *et al.* Sulfur-oxidizing bacterial populations within cyanobacterial dominated coral disease lesions. *Environ Microbiol Rep* 2013;**5**:518–24.

Braeckman U, Van Colen C, Guilini K *et al.* Empirical Evidence Reveals Seasonally Dependent Reduction in Nitrification in Coastal Sediments Subjected to Near Future Ocean Acidification. *PLoS One* 2014;**9**:e108153.

Burrell TJ, Maas EW, Hulston DA *et al.* Bacterial abundance, processes and diversity responses to acidification at a coastal CO_2 vent. *FEMS Microbiol Ecol* 2015, DOI: 10.1093/femsle/fnv154.

Egan S, Harder T, Burke C *et al.* The seaweed holobiont: understanding seaweed-bacteria interactions. *FEMS Microbiol Rev* 2013;**37**:462–76.

Fabricius KE, Langdon C, Uthicke S *et al.* Losers and winners in coral reefs acclimatized to elevated carbon dioxide concentrations. *Nat Clim Chang* 2011;**1**:165–9.

Fernandes AD, Reid JN, Macklaim JM *et al.* Unifying the analysis of high-throughput sequencing datasets: characterizing RNA-seq, 16S rRNA gene sequencing and selective growth experiments by compositional data analysis. *Microbiome* 2014;**2**:15.

Fisher MM, Triplett EW. Automated Approach for Ribosomal Intergenic Spacer Analysis of Microbial Diversity and Its Application to Freshwater Bacterial Communities Automated Approach for Ribosomal Intergenic Spacer Analysis of Microbial Diversity and Its Application to Freshwater. *Appl Environ Microbiol* 1999;**65**:4630–6.

Gazeau F, Van Rijswijk P, Pozzato L *et al.* Impacts of ocean acidification on sediment processes in shallow waters of the Arctic Ocean. *PLoS One* 2014;**9**, DOI: 10.1371/journal.pone.0094068.

German CR, von Damm KL. Hydrothermal Processes. *Treatise on Geochemistry* 2003;**6**:181–222.

Giovannelli D, d'Errico G, Manini E *et al.* Diversity and phylogenetic analyses of bacteria from a shallow-water hydrothermal vent in Milos island (Greece). *Front Microbiol* 2013;**4**:1–13.

Hall-Spencer JM, Rodolfo-Metalpa R, Martin S *et al.* Volcanic carbon dioxide vents show ecosystem effects of ocean acidification. *Nature* 2008;**454**:96–9.

Hanson CA, Fuhrman JA, Horner-Devine MC *et al.* Beyond biogeographic patterns: processes shaping the microbial landscape. *Nat Rev Microbiol* 2012;**10**:497–506.

Hofmann GE, Barry JP, Edmunds PJ *et al.* The Effect of Ocean Acidification on Calcifying Organisms in Marine Ecosystems: An Organism-to-Ecosystem Perspective. *Annu Rev Ecol Evol Syst* 2010;**41**:127–47.

Husson F, Josse J, Le S *et al.* FactoMineR: Multivariate Exploratory Data Analysis and Data Mining. R package version 1.29. 2015. http://CRAN.R-project.org/package=FactoMineR.

Iino T, Mori K, Uchino Y *et al.* Ignavibacterium album gen. nov., sp. nov., a moderately thermophilic anaerobic bacterium isolated from microbial mats at a terrestrial hot spring and proposal of Ignavibacteria classis nov., for a novel lineage at the periphery of green sulfur bacteria. *Int J Syst Evol Microbiol* 2010;**60**:1376–82.

IPCC. Climate Change 2013: the Physical Science Basis. Cambridge: Cambridge University Press, 2013.

Joint I, Doney SC, Karl DM. Will ocean acidification affect marine microbes? *ISME J* 2011;**5**:1–7.

Kawaichi S, Ito N, Kamikawa R *et al.* Ardenticatena maritima gen. nov., sp. nov., a ferric iron- and nitrate-reducing bacterium of the phylum "Chloroflexi" isolated from an iron-rich coastal hydrothermal field, and description of Ardenticatenia classis nov. *Int J Syst Evol Microbiol* 2013;**63**:2992–3002.

Kerfahi D, Hall-Spencer JM, Tripathi BM *et al.* Shallow Water Marine Sediment Bacterial Community Shifts Along a Natural CO_2 Gradient in the Mediterranean Sea Off Vulcano, Italy. *Microb Ecol* 2014, DOI: 10.1007/s00248-014-0368-7.

Kitidis V, Laverock B, McNeill LC *et al.* Impact of ocean acidification on benthic and water column ammonia oxidation. *Geophys Res Lett* 2011;**38**:L21603, DOI:10.1029/2011GL049095.

Klindworth A, Pruesse E, Schweer T *et al.* Evaluation of general 16S ribosomal RNA gene PCR primers for classical and next-generation sequencing-based diversity studies. *Nucleic Acids Res* 2013;**41**:e1.

Koch M, Bowes G, Ross C *et al.* Climate change and ocean acidification effects on seagrasses and marine macroalgae. *Glob Chang Biol* 2013;**19**:103–32.

Koschorreck M. Microbial sulphate reduction at a low pH. *FEMS Microbiol Ecol* 2008;**64**:329–42.

Krause E, Wichels A, Giménez L *et al.* Small changes in pH have direct effects on marine bacterial community composition: a microcosm approach. *PLoS One* 2012;**7**:e47035.

Krumbein WE, Giele C. Calcification in a coccoid cyanobacterium associated with the formation of desert stromatolites. *Sedimentology* 1979;**26**:593–604.

Kuever J, Rainey FA, Widdel F. Family I. Desulfobacteraceae. In: Brenner DJ, Krieg NR, Staley JT, Garrity GM (eds). Bergey's Manual of Systematic Bacteriology, 2nd edn, vol. 2 (The Proteobacteria), part C (The Alpha-, Beta-, Delta-, and Epsilonproteobacteria). New York: Springer, 2005, 959–60.

Laverock B, Kitidis V, Tait K *et al.* Bioturbation determines the response of benthic ammonia-oxidizing microorganisms to ocean acidification. *Philos Trans R Soc Lond B Biol Sci* 2013;**368**:20120441.

Lindh M V., Riemann L, Baltar F *et al.* Consequences of increased temperature and acidification on bacterioplankton community composition during a mesocosm spring bloom in the Baltic Sea. *Environ Microbiol Rep* 2013;**5**:252–62.

Liu J, Weinbauer M, Maier C *et al.* Effect of ocean acidification on microbial diversity and on microbe-driven biogeochemistry and ecosystem functioning. *Aquat Microb Ecol* 2010;**61**:291–305.

Liu Z, Frigaard NU, Vogl K *et al.* Complete genome of Ignavibacterium album, a metabolically versatile, flagellated, facultative anaerobe from the phylum Chlorobi. *Front Microbiol* 2012;**3**:1–15.

Lomas M, Hopkinson B, Losh J *et al.* Effect of ocean acidification on cyanobacteria in the subtropical North Atlantic. *Aquat Microb Ecol* 2012;**66**:211–22.

Mahé F, Rognes TT, Quince C *et al.* Swarm: robust and fast clustering method for amplicon-based studies. *PeerJ* 2014;**2**:e593, DOI:10.7717/peerj.593.

Martin M. Cutadapt removes adapter sequences from high-throughput sequencing reads. *EMBnet.journal* 2011;**17**:10.

Maszenan AM, Seviour RJ, Patel BKC *et al.* Defluvicoccus vanus gen. nov., sp. nov., a novel Gram-negative coccus/coccobacillus in the "Alphaproteobacteria" from activated sludge. *Int J Syst Evol Microbiol* 2005;**55**:2105–11.

Maugeri TL, Lentini V, Gugliandolo C *et al.* Bacterial and archaeal populations at two shallow hydrothermal vents off Panarea Island (Eolian Islands, Italy). *Extremophiles* 2009;**13**:199–212.

Meron D, Atias E, Iasur Kruh L *et al.* The impact of reduced pH on the microbial community of the coral Acropora eurystoma. *ISME J* 2011;**5**:51–60.

Meyer-Dombard DR, Price RE, Pichler T *et al.* Prokaryotic Populations in Arsenic-Rich Shallow-Sea Hydrothermal Sediments of Ambitle Island, Papua New Guinea. *Geomicrobiol J* 2012;**29**:1–17.

Miroshnichenko ML, Kolganova TV, Spring S *et al.* Caldithrix palaeochoryensis sp. nov., a thermophilic, anaerobic, chemo-organotrophic bacterium from a geothermally heated sediment, and emended description of the genus Caldithrix. *Int J Syst Evol Microbiol* 2010;**60**:2120–3.

Miroshnichenko ML, Kostrikina NA, Chernyh NA *et al.* Caldithrix abyssi gen. nov., sp. nov., a nitrate-reducing, thermophilic, anaerobic bacterium isolated from a Mid-Atlantic ridge hydrothermal vent, represents a novel bacterial lineage. *Int J Syst Evol Microbiol* 2003;**53**:323–9.

Morrow KM, Bourne DG, Humphrey C *et al.* Natural volcanic CO_2 seeps reveal future trajectories for host-microbial associations in corals and sponges. *ISME J* 2014;**2**:1–15.

Munday PL, Cheal AJ, Dixson DL *et al.* Behavioural impairment in reef fishes caused by ocean acidification at CO 2 seeps. *Nat Clim Chang* 2014;**4**:487–92.

Newbold LK, Oliver AE, Booth T *et al.* The response of marine picoplankton to ocean acidification. *Environ Microbiol* 2012;**14**:2293–307.

Oksanen J, Blanchet FG, Kindt R *et al.* vegan: Community Ecology Package. R package version 2.3-0. 2015. http://CRAN.R-project.org/package=vegan

Oliver AE, Newbold LK, Whiteley AS *et al.* Marine bacterial communities are resistant to elevated carbon dioxide levels. *Environ Microbiol Rep* 2014;**6**:574–82.

Piontek J, Lunau M, Händel N *et al.* Acidification increases microbial polysaccharide degradation in the ocean. *Biogeosciences* 2010;**7**:1615–24.

Pruesse E, Peplies J, Glöckner FO. SINA: Accurate high-throughput multiple sequence alignment of ribosomal RNA genes. *Bioinformatics* 2012;**28**:1823–9.

Ramette A. Quantitative community fingerprinting methods for estimating the abundance of operational taxonomic units in natural microbial communities. *Appl Environ Microbiol* 2009;**75**:2495–505.

Raulf FF, Fabricius KE, Uthicke S *et al.* Changes in microbial communities in coastal sediments along natural CO_2 gradients at a volcanic vent in Papua New Guinea. *Environ Microbiol* 2015;**17**:3678–91.

Rippka R, Deruelles J, Waterbury JB *et al.* Generic Assignments, Strain Histories and Properties of Pure Cultures of Cyanobacteria. *J Gen Microbiol* 1979;**111**:1–61.

Roy A-S, Gibbons SM, Schunck H *et al.* Ocean acidification shows negligible impacts on high-latitude bacterial community structure in coastal pelagic mesocosms. *Biogeosciences* 2013;**10**:555–66.

Schöttner S, Pfitzner B, Grünke S *et al.* Drivers of bacterial diversity dynamics in permeable carbonate and silicate coral reef sands from the Red Sea. *Environ Microbiol* 2011;**13**:1815–26.

Straub KL, Rainey FA, Widdel F. Marine Phototrophic Ferrous-Iron-Oxidizing Purple Bacteria. *Int J Syst Bacteriol* 1999;**49**:729–35.

Sunagawa S, Coelho LP, Chaffron S *et al.* Structure and function of the global ocean microbiome. *Science* 2015;**348**:1–10.

Tait K, Laverock B, Widdicombe S. Response of an Arctic Sediment Nitrogen Cycling Community to Increased CO_2. *Estuaries and Coasts* 2013, DOI: 10.1007/s12237-013-9709-x.

Tait K, Laverock B. Minor impact of ocean acidification to the composition of the active microbial community in an Arctic sediment. *Environ Microbiol Rep* 2013, DOI: 10.1111/1758-2229.12087.

Taylor JD, Ellis R, Milazzo M *et al.* Intertidal epilithic bacteria diversity changes along a naturally occurring carbon dioxide and pH gradient. *FEMS Microbiol Ecol* 2014, DOI: 10.1111/1574-6941.12368.

Van den Boogaart KG, Tolosana R, Bren M. compositions: Compositional Data Analysis. R package version 1.40-1. 2014. http://CRAN.R-project.org/package=compositions.

Vandieken V, Thamdrup B. Identification of acetate-oxidizing bacteria in a coastal marine surface sediment by RNA-stable isotope probing in anoxic slurries and intact cores. *FEMS Microbiol Ecol* 2013;**84**:373–86.

Vizzini S, Di Leonardo R, Costa V *et al.* Trace element bias in the use of CO_2-vents as analogues for low-pH environments: Implications for contamination levels in acidified oceans. *Estuar Coast Shelf Sci* 2013;**134**:19–30.

Wenzhöfer F, Holby O, Glud RN *et al.* In situ microsensor studies of a shallow water hydrothermal vent at Milos , Greece. *Mar Chem* 2000;**69**:43–54.

Witt V, Wild C, Anthony KRN *et al.* Effects of ocean acidification on microbial community composition of, and oxygen fluxes through, biofilms from the Great Barrier Reef. *Environ Microbiol* 2011;**13**:2976–89.

Yamada T, Sekiguchi Y, Hanada S *et al.* Anaerolinea thermolimosa sp. nov., Levilinea saccharolytica gen. nov., sp. nov. and Leptolinea tardivitalis gen. nov., sp. nov., novel filamentous anaerobes, and description of the new classes Anaerolineae classis nov. and Caldilineae classis nov. *Int J Syst Evol Microbiol* 2006;**56**:1331–40.

Zhang J, Kobert K, Flouri T *et al.* PEAR: A fast and accurate Illumina Paired-End reAd mergeR. *Bioinformatics* 2014;**30**:614–20.

Supporting information

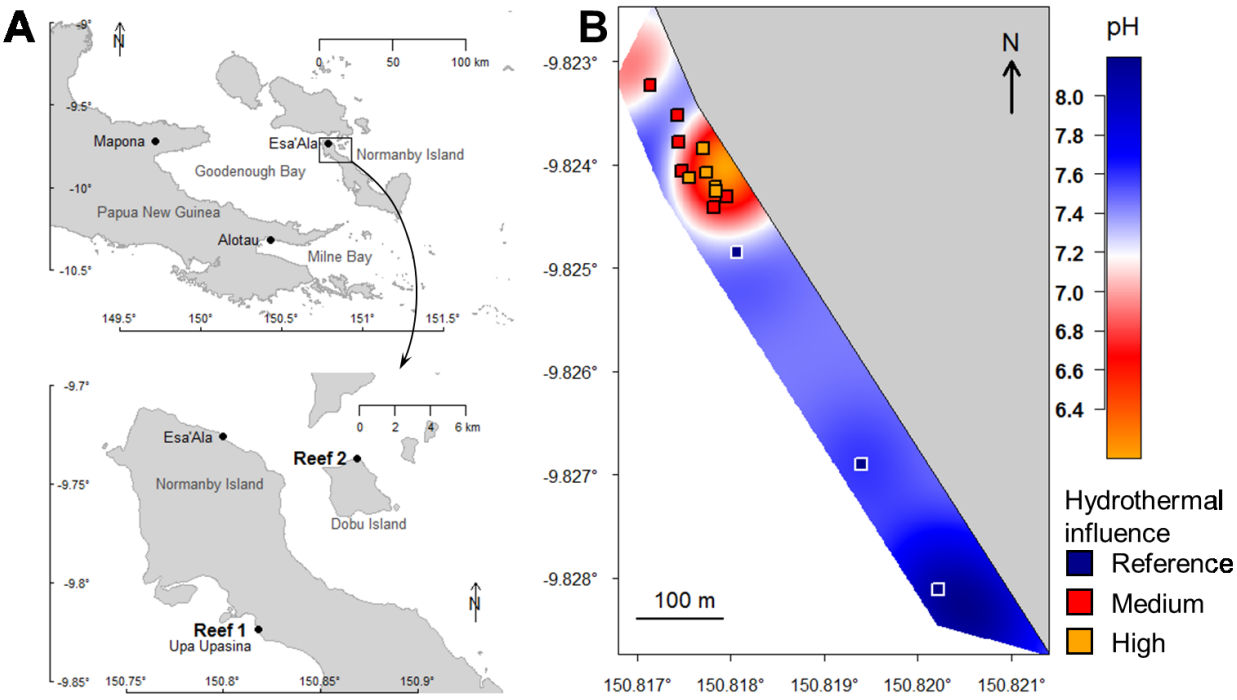

SI figure 1: Map of the sampling area in Papua New Guinea (A). Location of the sampling sites at Reef 1 colored by hydrothermal influence category (B); background colored by median pH in the upper 2 cm of the sediment. The reference sites at Reef 2 were approximately 2 km distant from the seep sites.

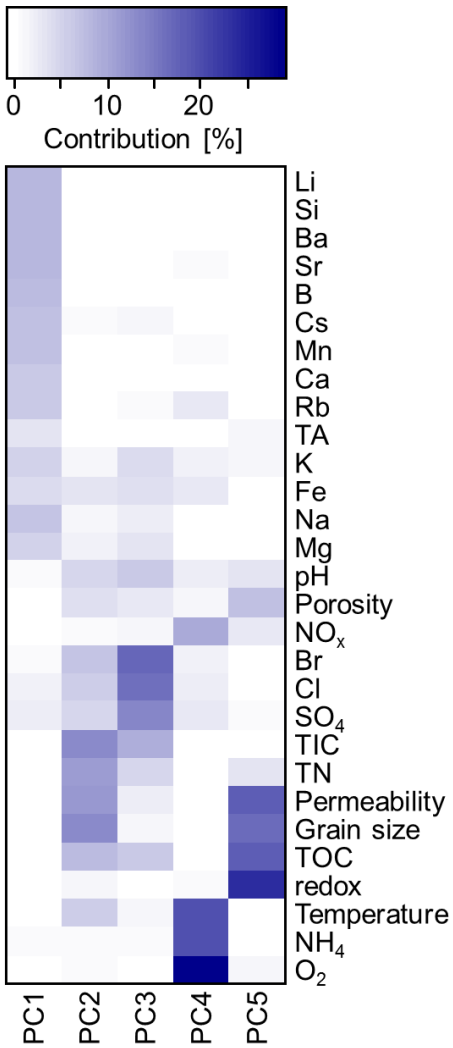

SI figure 2: Heatmap showing the contribution of the environmental parameters to the principal components (Figure 1). TIC: total inorganic carbon, TOC: total organic carbon, DIC: dissolved inorganic carbon, TN: total nitrogen, TA: total alkalinity.

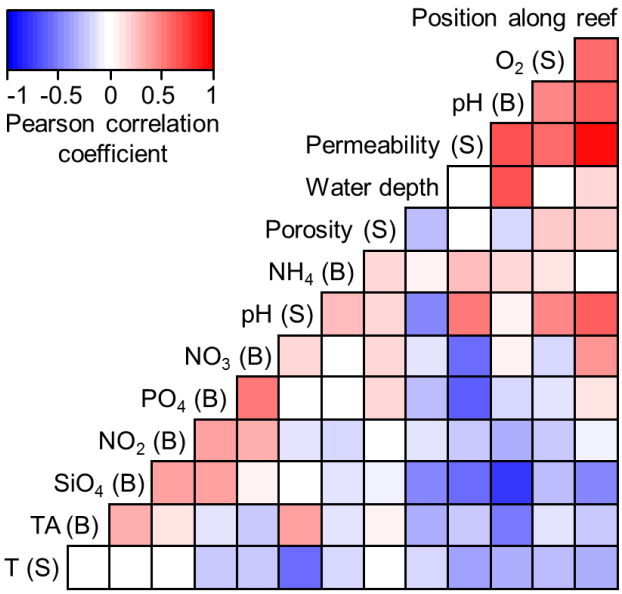

SI figure 3: Heatmap of the correlation between the environmental parameters that were used in the redundancy analysis (RDA) models (Table 2) to explain the variation in microbial community structure. Sediment and bottom water parameters are marked with (S) and (B), respectively.

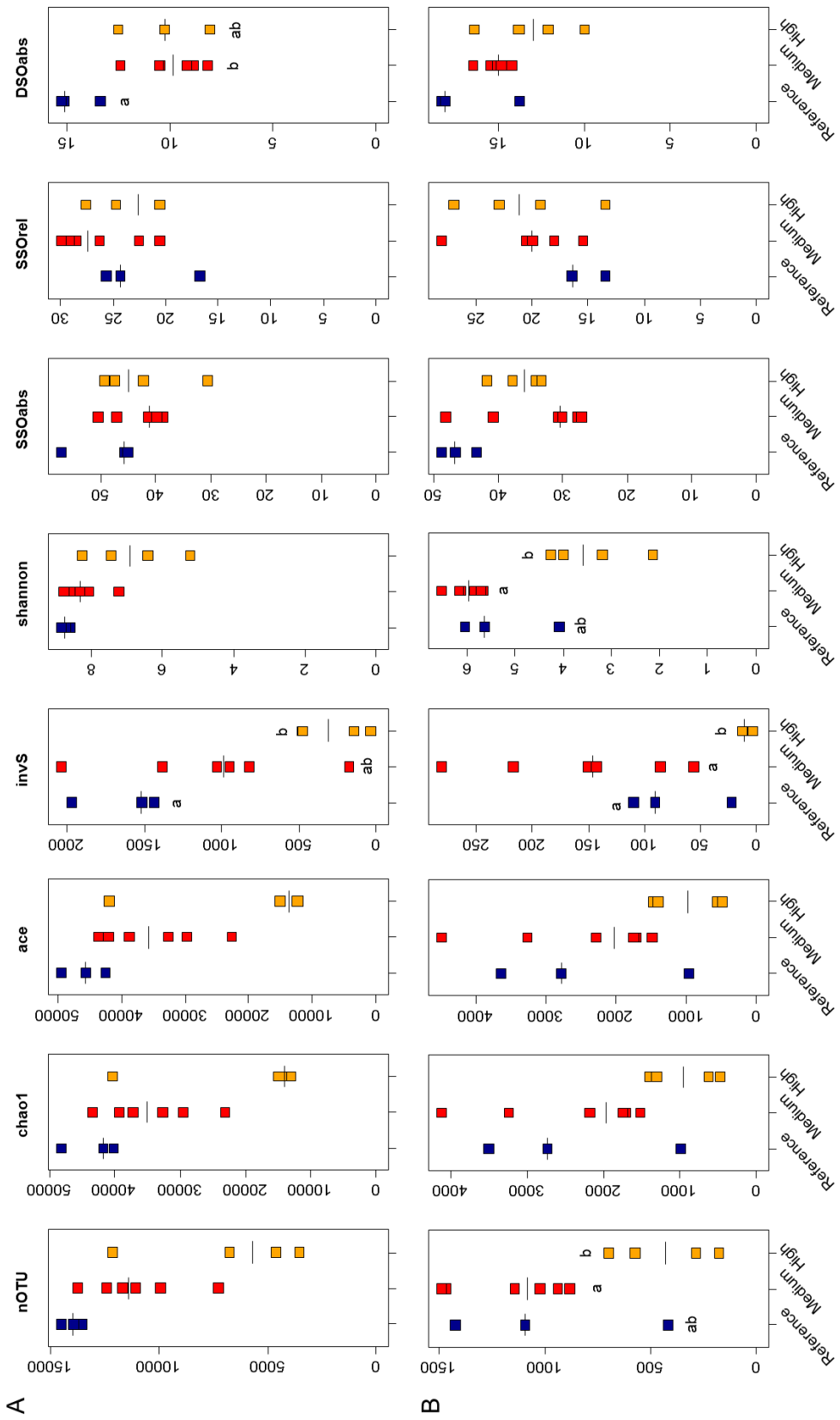

SI figure 4: Alpha diversity of the bacterial (A) and archaeal (B) community at reference, medium and high HI (hydrothermal influence) sites. Values based on repeated random subsampling (100×) to the lowest number of sequences per sample (bacteria: 32 534, archaea: 4728). Alpha diversity indices: OTU number, Chao1 and abundance-based coverage estimator (ACE), inverse Simpson index (invS), Shannon index, percentage absolute (SSOabs) and relative singletons (SSOrel) and absolute doubletons (DSOabs) per sample. The black line shows the median per group. Significant differences based on the Benjamini-Hochberg (BH)-adjusted p-values of permutation tests marked by lowercase letters.

SI table 1: Overview of the sampling design and the measured parameters at Reef 1 at Normanby and Reef 2 at Dobu Island, Papua New Guinea. HI: hydrothermal influence, TA: total alkalinity, DIC: dissolved inorganic carbon, TIC: total inorganic carbon, TOC: total organic carbon, TN: total nitrogen. Sample size still including missing samples and failed measurements.

Parameters	*Reef 1*	*Reef 2*
Spatial		
Position along the reef, water depth	14 sites (3 reference, 6 medium HI, 5 high HI)	6 sites (2 reference, 2 medium HI, 2 high HI)
Bottom water		
pH, TA, DIC, SiO_4, PO_4, NO_x, NH_4	14 sites (3 reference, 6 medium HI, 5 high HI) 3 replicates per site	6 sites (2 reference, 2 medium HI, 2 high HI) 3 replicates per site
Pore water *in-situ* measurements[a]		
pH, temperature, O_2, redox potential	8 sites (2 reference, 4 medium HI, 2 high HI) microsensor profiles down to 10 cm sediment depth 2 – 3 replicate profiler runs per site	
Pore water geochemistry[a]		
TA, cations (Fe, Mg, K, Na, Ca, Si, Mn, Li, B, Rb, Ba, Sr, Cs), anions (SO_4, Cl, Br)	3 sites (1 medium HI, 2 high HI) pore water geochemistry down to > 10 cm sediment depth 2 replicate cores per site	
Sediment[a]		
Porosity, grain size, permeability, TIC, TOC, TN	8 sites (2 reference, 4 medium HI, 2 high HI) 3 sediment layers (0 – 2 cm, 2 – 4 cm, 4 – 6 cm) 2 – 4 replicates per site	
ARISA (ITSF / ITSReub)[b]	14 sites (3 reference, 6 medium HI, 5 high HI) 2 sediment layers (0 – 2 cm, 2 – 4 cm) 3 replicate cores per site	6 sites (2 reference, 2 medium HI, 2 high HI) 2 sediment layers (0 – 2 cm, 2 – 4 cm) 3 replicate cores per site
Amplicon sequencing		
Bacteria (S-D-Bact-0341-b-S-17 / S-D-Bact-0785-a-A-21)[b] Archaea (Arch349F / Arch915R)[b]	13 sites (3 reference, 6 medium HI, 4 high HI) 0 – 2 cm sediment depth 1 replicate per site	

[a] These parameters were analyzed from separate sediment cores taken at the same sampling sites as the cores for the molecular analysis

[b] Primer pair

SI table 2: Analysis of similarity (ANOSIM) of the microbial community based on Bray-Curtis dissimilarity. ANOSIM R of non-significant results after Benjamini-Hochberg (BH)-adjustment not reported. Values in parentheses: mean percentage of shared OTUs of any two samples between hydrothermal influence categories.

Sediment layer	*Reef*	*Comparison*	*ARISA complete*		*16S Bacteria*		*16S Archaea*	
0 – 2 cm	Reef 1		0.691		0.875		0.761	
		Reference – Medium	0.727	(41%)	0.821	(28%)	0.481	(19%)
		Reference – High	0.823	(36%)	1	(13%)	1	(12%)
		Medium – High	0.651	(39%)	0.865	(25%)	0.861	(17%)
	Reef 2		0.735					
		Reference – Medium	0.741	(35%)				
		Reference – High	0.956	(31%)				
		Medium– High	0.454	(33%)				
2 – 4 cm	Reef 1		0.717					
		Reference – Medium	0.796	(41%)				
		Reference – High	0.807	(35%)				
		Medium– High	0.676	(38%)				
	Reef 2		0.519					
		Reference – Medium	1	(34%)				
		Reference – High	0.460	(25%)				
		Medium– High	0.312	(28%)				

SI table 3: Number of differentially abundant taxa between hydrothermal influence categories. Numbers in parentheses indicate the numbers of taxa that were differentially abundant between reference and medium HI (hydrothermal influence) sites.

Taxonomic level	*Bacteria*	*Archaea*
Phylum	7 (2)	2 (2)
Class	16 (2)	2 (0)
Order	38 (7)	5 (0)
Family	52 (14)	6 (0)
Genus	81 (26)	6 (0)
OTU	438 (97)	48 (19)

SI tables 4 and 5: Bacterial (SI table 4) and archaeal (SI table 5) taxa detected as differentially abundant between hydrothermal influence categories. Please refer to the online supporting information to the published manuscript at FEMS Microbiology Ecology (http://femsec.oxfordjournals.org/content/92/5/fiw027.long).

Chapter 3

Metatranscriptomic and biogeochemical investigations of sediment microbial processes at a shallow-water hydrothermal CO_2 vent in Papua New Guinea

Christiane Hassenrück[1], Artur Fink[1]*, Pierre Offre[1], Pier Luigi Buttigieg[1], Halina E. Tegetmeyer[2], Alban Ramette[1,3], Dirk de Beer[1]

[1] Max Planck Institute for Marine Microbiology, Celsiusstraße 1, 28359 Bremen, Germany

[2] University of Bielefeld, Center for Biotechnology – CeBiTec, Universitätsstraße 27, 33615 Bielefeld, Germany

[3] Institute of Social and Preventive Medicine, Bern University, Finkenhubelweg 11, 3012 Bern, Switzerland

Frontiers in Aquatic Microbiology (in preparation).

Abstract: Microbial processes are crucial for element cycling in permeable sediments of tropical coral reefs, and contribute to maintaining the high productivity of these reefs. Coral reefs are threatened by ocean acidification (OA), however very little is known about OA effects on microbial processes and element cycling in reef sediments. Since the effects of long-term exposure to OA in an ecosystem context are of particular interest to scientists, natural OA analogues, such as shallow-water hydrothermal CO_2 vents, are increasingly being studied. Here, we used a metatranscriptomic approach combined with metabolic rate measurements to investigate gene expression and functional rates related to a broad range of microbial processes involved in major element cycles in reef sediments at a CO_2 vent in Papua New Guinea. Photosynthetic primary production and carbohydrate degradation did not seem to be strongly affected by the CO_2 vent, although the taxonomic composition of the microorganisms performing these functions was altered. Sulfate reduction rates and gene expression were severely decreased at the CO_2 vent. Nitrogen fixation, nitrification and denitrification also seemed to be strongly affected by the CO_2 venting, although further rate measurements are necessary to confirm the observed trends. Additionally, trace elements, such as arsenic, may be increasingly used as energy source by microorganisms. We provide an overview of microbial processes involved in major element cycles and how they may be affected at the CO_2 vents. Furthermore, we present hypotheses for future research on microbial processes at shallow-water hydrothermal CO_2 vents as OA analogues.

Keywords: hydrothermal vent, CO_2 seep, microbial processes, photosynthesis, remineralization, metatranscriptomics, active community

Introduction

Tropical coral reefs constitute a highly productive ecosystem in an otherwise nutrient-depleted marine desert. Microbial processes play a crucial role in maintaining the high productivity of coral reefs by facilitating efficient element cycling. In particular permeable reef sediments, which can cover areas up to ten times those of the coral reef framework, host microbial communities that are involved in element cycling and the remineralization of organic matter (Gattuso et al., 1998; Rasheed et al., 2002). For instance, microphytobenthic communities consisting mainly of cyanobacteria and small eukaryotes, such as diatoms, contribute to primary production via photosynthetic carbon fixation (Boucher et al., 1998; Werner et al., 2008). Other carbon fixation pathways are unique to prokaryotes (Hügler and Sievert, 2011), although their contribution to bulk carbon fixation in coral reef sediments remains unknown. Microbial remineralization processes include, but are not restricted to, the degradation of organic matter via hydrolytic enzymes, and subsequent respiration either aerobically in the oxygenated layer of the sediment, or anaerobically in deeper, anoxic sediment layers coupled to nitrate, manganese, iron and sulfate reduction (Fenchel and Jorgensen, 1977). Prokaryotic microbes are key players in all steps of the marine nitrogen cycle, an element which is usually depleted on coral reefs and requires rapid recycling (Rusch and Gaidos, 2013). Because of their involvement in major element cycles, changes to microbial processes in the sediment can have profound effects on reef maintenance and health (Ainsworth et al., 2010; Garren and Azam, 2012).

Ocean acidification (OA) is a major threat to coral reefs, yet little is known about long-term OA effects on microbial processes in reef sediments and their consequences for coral reef ecosystem functioning (Liu et al., 2010b). Currently, there are three main hypotheses regarding OA effects on microbial communities and their functions: (1) Microbial communities and their functions will not be affected by OA, (2) changes in microbial communities due to OA will not affect community functions, but will only result in a replacement of the organisms performing a particular function (functional redundancy), and (3) OA will affect microbial processes and ecosystem functioning (Joint et al., 2011; Liu et al., 2010b; O'Brien et al., 2016). So far there is no consensus as

to which of these hypotheses pertains to OA effects on microbial communities and processes in coral reef sediments.

The majority of previous observations are limited to short-term laboratory and mesocosm experiments that mainly focused on water column microbial communities and functions. Overall, these studies indicated rather small effects of OA on planktonic microbial communities (Lindh et al., 2013; Newbold et al., 2012; Oliver et al., 2014; Roy et al., 2013; Zhang et al., 2012). Regarding microbial functions, such as carbon and nitrogen fixation rates and hydrolytic carbon degradation, OA effects were often not the most dominant cause of observed changes (Allgaier et al., 2008; Arnosti et al., 2011; Endres et al., 2014; Grossart et al., 2006; Piontek et al., 2013), and may further depend on changes in other environmental parameters (Fu et al., 2008). First studies on OA effects on microbial communities and their function in other marine environments, such as sediments, suggest that their response to OA may differ in magnitude to that of planktonic microbial communities (Tait and Laverock, 2013), indicating that OA effects may be environment-specific.

Unlike short-term laboratory and mesocosm experiments, the use of natural analogues for OA provides the opportunity to study long-term OA effects on sediment microbial communities in an ecosystem that has been exposed to reduced pH/increased pCO_2 conditions for several decades (Fabricius et al., 2011; Hall-Spencer et al., 2008). Shallow-water hydrothermal CO_2 vents associated with tropical coral reefs constitute such OA analogues (Fabricius et al., 2011). Most previous studies investigated the composition and diversity of the total microbial community in the sediment using DNA-based molecular techniques, further using changes in community composition as proxy for changes in microbial processes (Hassenrück et al., 2016; Kerfahi et al., 2014; Raulf et al., 2015). However, the taxonomic composition of the total microbial community can at best act as rough estimate of microbial functions and may at worst be severely biased, since it does not provide information on microbial activity (Gaidos et al., 2011; Lanzen et al., 2011; Moeseneder et al., 2005). Very little data are available on direct measurements of microbial processes in the sediment at shallow-water hydrothermal CO_2 vents. Studies from the Mediterranean and Papua New Guinea reported decreases in sulfate reduction and oxygen consumption rates at the CO_2 vent (Fink et al., submitted; Molari et al., in

preparation), whereas nitrification rates remained largely unaffected (Kitidis et al., 2011). Nonetheless, the range of microbial functions investigated in coral reef sediments at shallow-water hydrothermal CO_2 vents remains severely limited.

Here, we investigated the active microbial community and major microbial processes in the sediment at a shallow-water hydrothermal CO_2 vent in a coral reef in Papua New Guinea (PNG). There, the hydrothermal CO_2 venting has changed the environmental conditions and characteristics of the sediment with the potential to alter microbially mediated element cycling (Fink et al., submitted). The aim of this study was (I) to provide an overview of the active microbial community and a broad range of major microbial processes in the sediment, and how these may be affected by long-term CO_2 venting, and (II) to formulate more specific hypotheses for further investigations into microbial processes in reef sediments at shallow-water CO_2 vents used as natural analogues for OA. We focused on RNA-based molecular techniques conducting a 16S rRNA fingerprinting and a metatranscriptomic screening of the composition and function of the active microbial community. This we compared to the total microbial community and its genetic functional potential based on metagenomics. Furthermore, the results of the metagenomic and metatranscriptomic analysis were complemented with additional data on physico-chemical environmental parameters, microbial community composition and metabolic rates based on a replicated sampling design (Fink et al., submitted; Hassenrück et al., 2016; Lichtschlag et al., in preparation).

Methods

Sampling area

The sampling sites for this study were located along a pH gradient created by a shallow-water hydrothermal CO_2 vent within a coral reef at Upa Upasina, Normanby Island, Papua New Guinea (S 9.82, W 150.82; Figure S1). These sampling sites were previously investigated to characterize the physico-chemical conditions in the sediment (Fink et al., submitted; Lichtschlag et al., in preparation) as well as the diversity and composition of the total microbial community (Hassenrück et al., 2016).

At the CO_2 vent, the physico-chemical conditions in the sediment were profoundly different from ambient conditions at a reference site approximately 500 m distant from the vent (Fink et al., submitted; Lichtschlag et al., in preparation). In the sediment at the CO_2 vent, pH values of < 6 and temperatures of more than 37°C could be reached, especially in deeper sediment layers (Fink et al., submitted). Grain size and permeability as well as organic carbon and total nitrogen were reduced (Fink et al., submitted). Pore water element composition further showed an enrichment of signature elements for hydrothermal fluids such as silicon, manganese, lithium and iron, whereas magnesium and sodium were depleted (Lichtschlag et al., in preparation). Based on their physico-chemical properties the sampling sites were grouped into three categories of hydrothermal influence (HI): reference sites, medium HI and high HI sites (see Hassenrück et al., 2016).

Data for the physico-chemical characterization of the sampling sites, the molecular characterization of the benthic microbial communities, and metabolic rate measurements were collected in two consecutive years (May 2013 and April 2014). An overview of the available data is provided in Table S1. Due to logistic constraints, data are not available for all parameters at all sampling sites for both years.

Molecular analysis

For the molecular analyses of the microbial communities, sediment was collected from the upper 2 cm and preserved in RNAlater (Ambion) as described previously

(Hassenrück et al., 2016). DNA was extracted using the UltraClean Soil DNA extraction kit (MoBio Laboratories Inc., Carlsbad, CA, USA) according to the manufacturer's instructions. RNA was extracted from 4 g sediment from triplicate sediment cores from one sampling site per HI category, where most data were available (Figure S1, Table S1), using the PowerSoil RNA extraction kit (MoBio Laboratories Inc., Carlsbad, CA, USA) according to the manufacturer's instructions. Prior to the RNA extraction the RNAlater-preserved sediment was washed twice with 4 ml sterile 1× PBS at 2500× g at 4°C for 10 min to remove the RNAlater. After the RNA extraction, excess DNA was removed in a DNase digest. The DNA-free RNA solution was cleaned-up using the RNeasy MinElute Clean-up kit (Qiagen, Hilden, Germany). Metagenomic and metatranscriptomic TruSeq libraries of one replicate core were prepared for sequencing with Illumina MiSeq paired-end and HiSeq single-end technology (CeBiTec, Bielefeld). Due to a low amount of starting material, the library preparation included five amplification steps.

For TRFLP fingerprinting of the bacterial community, 15 µL RNA template were reverse transcribed into first-strand cDNA. TRFLP fingerprinting was conducted on the 16S rRNA and the 16S rRNA gene using the primer combination 27F and 907R. To screen the microbial community involved in sulfate reduction, of which previous measurements were available (Fink et al., submitted), TRFLP was also performed on the dissimilatory sulfite reductase gene subunit A (*dsrA*) using the primer set 3 (PS3) described in (Santillano et al., 2010). TRFLP PCRs were run in triplicates for each primer combination. The PCR products were purified using the QiaQuick Gel extraction kit (Qiagen, Hilden, Germany). Both 16S and *dsrA* fragments were digested with AluI (New England BioLabs GmbH, Frankfurt am Main, Germany). Restriction fragment lengths were analyzed on a capillary sequencer. Custom R scripts were used to bin forward fragments into OTUs and to merge the OTU profiles of replicate PCRs into one OTU profile per sample (http://www.mpi-bremen.de/en/Software_4.html). Restriction fragments longer than the expected PCR amplicon were removed from the analysis. Further information on the molecular analyses is provided in Tables S2-S4.

Metagenomic and metatranscriptomic sequence processing

Sequencing controls and adapters were removed from the metagenomic and metatranscriptomic data sets with *bbduk* v34.00 (Bushnell, 2015). Sequences were quality trimmed with *trimmomatic* v0.32 (Bolger et al., 2014) and in case of the metagenomic libraries merged using *PEAR* v0.9.5 (Zhang et al., 2014). rRNA sequences were filtered from non-rRNA sequences using *sortmerna* v2.0 (Kopylova et al., 2012) with the SILVA ssu and lsu rRNA, and RFAM databases as reference (Quast et al., 2013). rRNA sequences were then taxonomically classified with *SINA* v1.2.10 (Pruesse et al., 2012) using the SILVA ssu reference database release 119 (Quast et al., 2013). Coding sequences (CDS) on non-rRNA sequences were predicted with *fraggenescan* v1.19 (Rho et al., 2010) and annotated with *interproscan* v5.13-52.0 including gene ontology (GO) annotations (Jones et al., 2014). For the metagenomic sequences the CDS prediction and annotation were conducted using the EBI metagenomics portal (Hunter et al., 2014). GO networks were constructed in *Cytoscape* v3.2.1 (Shannon et al., 2003) using *OntoFox* (Xiang et al., 2010) to extract the subset of the full gene ontology specific to our dataset. Based on the InterPro annotation, functional marker genes of specific microbial processes (Table S5) were further curated using NCBI blastp (*blast+* v2.2.30; (Camacho et al., 2009). The taxonomic composition of these marker genes was extracted from the best blast hit using efetch from the NCBI e-utils package *edirect* v2.70 (Kans, 2013). Differences in the abundance of the marker genes and taxonomic groups between samples are shown as centered log ratio transformed sequence counts, with the difference between values representing log2-fold changes. Further information on the parameter setting of the programs used for the processing of sequences is provided in Table S6.

Pigment analysis

Sediment cores (3.5 cm inner diameter) were analyzed for photopigment concentrations using the HPLC method after Wright (1991). Within 2 h after sampling sediment cores were sliced at 0 - 0.5, 0.5 - 1, 1 - 2, 2 – 4 and 4 - 6 cm depth intervals, homogenized and stored frozen at -20°C. Samples were freeze-dried, vortexed (5 sec), sonicated (3 min) in ice-cold acetone and pigments were extracted at -20°C for 24 h. The

extract was filtered (Acrodisc CR 4 mm syringe filters, 0.45 µm pore size, PALL Life Sciences, USA) and injected into a reverse-phase HPLC (Waters, MA, USA). Separation and detection of the pigments occurred on a Waters 2695 separation module and a Waters 9996 photo diode array detector, respectively. Pigment standards (DHI Water and Environment, Denmark) for chlorophyll a, chlorophyll b, pheophythin a, fucoxanthin, diatoxanthin, diadinoxanthin, zeaxanthin and ß-carotene were used for identification and quantification of these pigments.

Net photosynthesis and primary production

Microphytobenthic activity was investigated *ex situ* using oxygen microsensors (tip size 50 - 60 µm, measuring surface 5 µm). The microsensors were built as described in Revsbech (1989) and two-point calibrated using air-saturated water and anoxic sediment pore water. Three sediment cores per site were obtained with acrylic core liners (8 cm inner diameter) and were incubated in the dark or in the light (220 µmol photons m^{-2} s^{-1}) at 28 - 29°C. Light intensity was measured at the sediment surface using a LI-190 quantum sensor (LI-COR, Lincoln, Nebraska, USA). A thin air stream provided by an air pump stirred the water overlaying the sediment creating a diffusive boundary layer. Steady-state microprofiles (n = 1 - 3 per core) of the upper 10 mm of the sediment were obtained after a pre-incubation of approximately 30 minutes.

Diffusive oxygen fluxes (J) were calculated according to Fick's first law of diffusion (1) where DO_2 is the diffusion coefficient, $[O_2]$ is the oxygen concentration and z is the depth.

$$J = DO_2 * d[O_2]/dz \qquad (1)$$

Oxygen fluxes through the diffusive boundary layer (J_{DBL}) were measured in the dark and in the light. The downward oxygen flux from the base of the euphotic zone (J_{EUPH}) in the light was calculated taking into account porosity (φ), and the diffusion coefficient was corrected for tortuosity ($DO_2' = DO_2/\theta^2$) adjusted for sands ($\theta^2 = \varphi^{1-m}$, m = 2; (Boudreau, 1997). Gross primary production (GPP) was calculated as

$J_{GPP}(light) = J_{EUPH}(light) - J_{DBL}(light) + J_{DBL}(dark)$, assuming the same oxygen consumption in the light as in the dark.

Extracellular enzymatic activity

Sediment samples from 0 – 2 cm sediment depth were stored at -20°C for the measurement of extracellular enzymatic activity. Potential extracellular enzymatic activity of α- and β-glucosidases was measured fluorometrically via the release of the fluorochrome methylumbelliferone (MUF) during the cleavage of an artificial substrate (Boetius and Lochte, 1994). The artificial substrates for α- and β-glucosidases were 4-MUF-α-D-glucopyranoside and 4-MUF-β-D-glucopyranoside, respectively. A volume of 100 µL substrate (100 µM) was added to 0.5 ml sediment diluted with 4.5 ml sterile-filtered artificial seawater. Samples were then incubated at 28°C and MUF concentration was measured after 1 h, 3 h and 5 h with an excitation wavelength of 365 nm and an emission wavelength of 445 nm. For each sample triplicate incubations were set up. Enzymatic activity was calculated as the amount of MUF released over 1 h per gram dry sediment. Separate calibration curves were measured for reference samples (high amount of calcium carbonate), and medium and high HI samples (silicate sands, low amount of calcium carbonate).

Results and Discussion

Total and active microbial community

The microbial community along the pH gradient at the CO_2 vent at Upa Upasina was previously investigated using community fingerprinting and amplicon sequencing of the same samples (Hassenrück et al., 2016). While this approach gave valuable information on the composition and diversity of the total bacterial and archaeal community, no data were so far available on the active fraction of the microbial community. Here we used TRFLP fingerprinting to compare the composition of the active and total bacterial community, using 16S rRNA as indicator for activity, whereas the total bacterial community was represented by the 16S rRNA gene pool.

We observed a shift in the composition of the total and active bacterial community between HI categories with the strongest change towards high HI sites (Figure 1A). The change in the composition of the total bacterial community was consistent with previous observations (Hassenrück et al., 2016). Although highly similar patterns were observed with both DNA and RNA-based methods (Mantel test based on Bray-Curtis dissimilarity, $r = 0.857$, $p < 0.001$), there was a pronounced offset between the active and total community (Figure 1A). Per sample about 45% of the OTUs were shared between the active and total community, a value comparable to the OTU turnover between HI categories. Such strong differences between active and total community composition are not uncommon in natural systems, where the most dominant members of a microbial community are not necessarily the most active (Lanzen et al., 2011; Moeseneder et al., 2005; Shi et al., 2011).

To reduce the bias of PCR-based methods and to further include information on functional genes, the metagenome and metatranscriptome of one sample per HI category was sequenced. Approximately 5 million metagenomic and 40 million total RNA metatranscriptomic reads were generated, of which 0.5% and 97% were assigned to rRNA, respectively. Of small subunit rRNA and rRNA gene sequences, the majority were classified as *Bacteria* (> 67%), followed by *Eukaryota* (3 – 30%) and *Archaea* (0.3 – 6%; Table S7). Generally, the composition of the microbial community in each domain of life was as expected for shallow-water marine sediments and comparable to

previous data from PNG, with the bacterial community dominated by *Proteobacteria* (α, γ and δ), *Bacteroidetes*, *Chloroflexi* and *Cyanobacteria*, the eukaryotic community dominated by *Diatomea*, and the archaeal community dominated by *Halobacteria*, *Marine Group* I and *Thermoplasmata* (Figure S2; Hassenrück et al., 2016; Raulf et al., 2015; Werner et al., 2008).

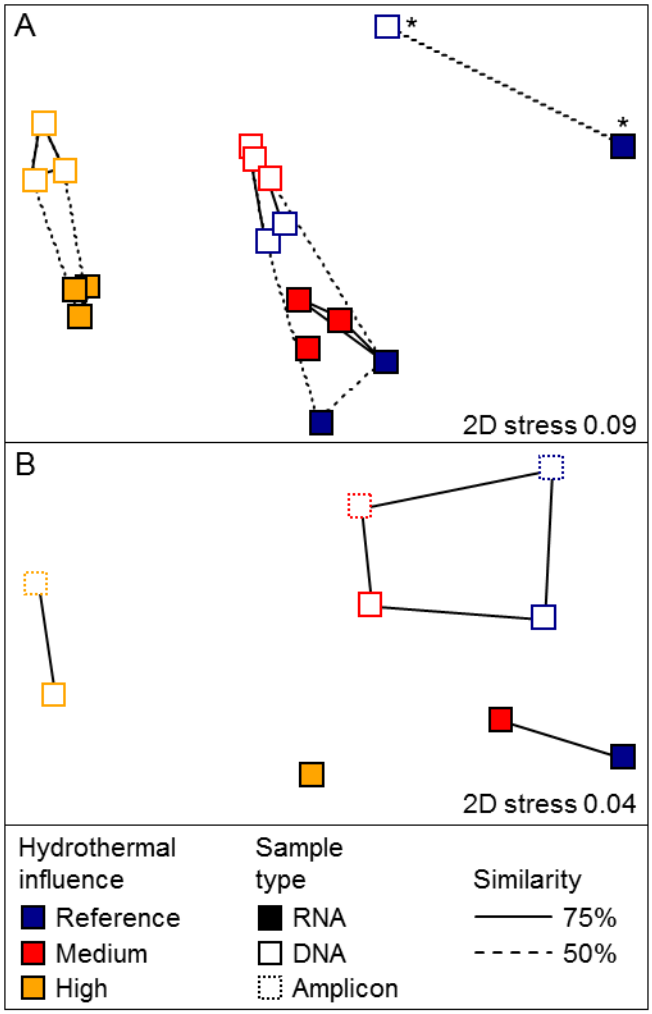

Figure 1: Non-metric multidimensional scaling plot of bacterial 16S TRFLP (A) and class-level taxonomy of bacterial 16S metagenomic, metatranscriptomic and amplicon sequences (B). Calculated based on Bray-Curtis dissimilarity of relative sequence abundances. The asterisk marks an outlier replicate which was not used for metagenomic and metatranscriptomic analyses.

Non-metric multidimensional scaling of the relative abundance of bacterial classes in previously obtained 16S amplicon (Hassenrück et al., 2016), metagenomic and metatranscriptomic data sets of the same samples showed that a similar pattern with HI category could be recovered with the sequencing approaches compared to TRFLP, and

that metagenomes and amplicon data were more similar to each other than to the metatranscriptomes (Figure 1B). The differences towards metatranscriptomic 16S were already detectable among the most abundant bacterial classes, with a larger proportion of *Cyanobacteria* in the reference sample, and a smaller proportion of *Chlorobi* and *Deferribacteres* in the high HI sample of the metatranscriptomic data set (Figure S2A). A more detailed comparison between the different sequencing approaches based on 16S and 18S classification is included in the SI text.

The difference between metagenomic and metatranscriptomic data was also apparent in the functional profile of the microbial community. To investigate patterns among dominant functional genes, gene ontology (GO) networks of the 20 most abundant GO terms per sample and GO namespace (molecular function, biological process, cellular component) were created (Figure S3). The GO networks showed an enrichment of photosynthesis and photosynthesis-related carbon and energy metabolism in the metatranscriptomic data sets, whereas the metagenomes were enriched in genes related to more general GO terms such as membrane, ribosome, metabolic process, transport and catalytic activity as well as house-keeping functions. Furthermore, the abundance of dominant metagenomic GO terms was very similar between samples, suggesting that the pool of functional genes is similar between HI categories. Among highly expressed genes, several GO terms were enriched at least two-fold in medium and high HI samples compared to the reference sample: photosynthesis-related GO terms, proton transport coupled to energy generation, carbon fixation via the Calvin cycle, membrane-related GO terms such as thylakoid membrane, and aerobic respiration possibly related to increased metabolic rates of photosynthetic organisms. The common denominator of these GO terms was photosynthesis, suggesting that this process may be of increased importance in the sediment at the CO_2 vent.

Key microbial processes in the sediment

Further analyses focused on specific metabolic pathways that play crucial roles in element cycling on coral reefs: photosynthesis, selected carbon fixation pathways, degradation of organic matter by carbohydrate active enzymes, sulfate reduction, nitrogen fixation, nitrification, and nitrate reduction to ammonia and N_2. The prevalence of each

process was assessed by the expression of functional marker genes in each sample of the three HI categories. To support the findings of the marker gene analysis, replicated biogeochemical measurements of metabolic rates were available from previous work (sulfate reduction rates; Fink et al. submitted) and were extended here to include photosynthesis, carbon and nitrogen fixation, and hydrolytic carbon degradation rates. Furthermore, photopigment concentrations were used as proxy to assess the composition of the microphytobenthic community. Moreover, trends in microbial processes were discussed in the context of changes in known environmental parameters in the sediment at the CO_2 vents (Fink et al., submitted; Lichtschlag et al., in preparation). An overview of the metabolic pathways of interest and corresponding marker genes as well as other parameters that were measured to characterize the environment and microbial processes in sediment is provided in Table S1 and Figure S4. Absolute sequence counts of functional marker genes are shown in Table S8.

Photosynthesis

As apparent from the GO networks, the majority of the sequences affiliated with functional genes in the metatranscriptomic data set were related to photosynthesis. For a more detailed investigation of photosynthetic gene expression the following marker genes were selected: photosystem I reaction center (*psa*), photosystem II reaction center (oxygenic photosynthesis: *psb*, anoxygenic photosynthesis: *puf*) and light harvesting antenna proteins, as well as carbonic anhydrase as representative for carbon concentrating mechanisms (Bryant and Frigaard, 2006; Kranz et al., 2009). Only transcripts of genes for oxygenic photosynthesis (*psa* and *psb*) were detected in the metatranscriptomes. The expression of *psa* was similar in all three samples with a slight decrease in the high HI sample. In contrast, *psb* expression increased approximately 2 and 5-fold in medium and high HI samples, respectively (Figure 2). Assuming that gene expression is a valid proxy for photosynthesis rates, the decoupled trends in *psa* and *psb* expression were unexpected since both genes are required for oxygenic photosynthesis in cyanobacteria and phototrophic eukaryotes (Bryant and Frigaard, 2006).

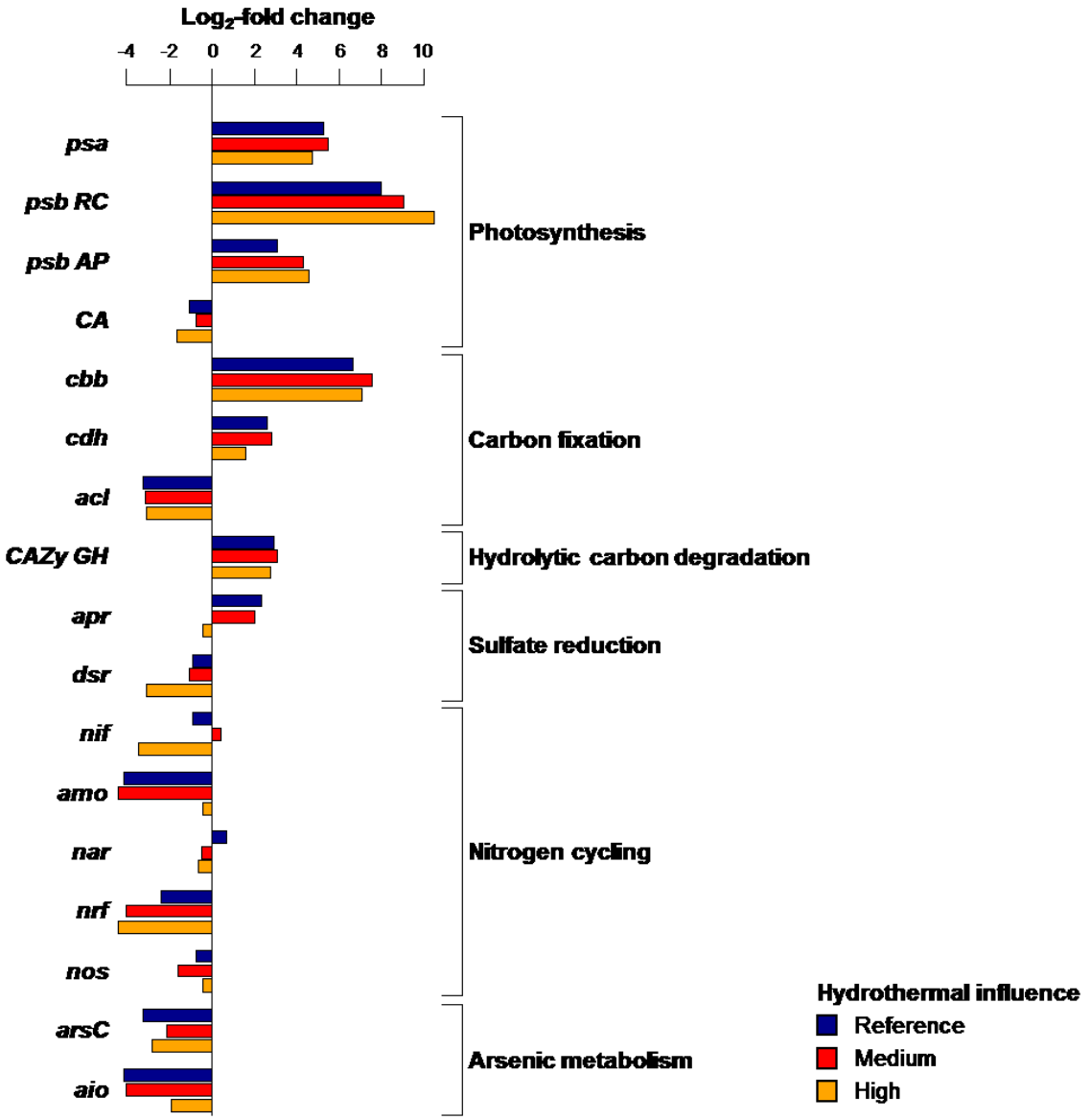

Figure 2: Expression patterns of functional marker genes. Sequence abundance displayed as log2-fold change relative to the geometric mean (zero value) of all genes per sample (centered log-ratio transformation). Photosynthesis: photosystem I reaction center (*psa*), photosystem II reaction center (*psb RC*) and antenna proteins (*psb AP*), carbonic anhydrase (*CA*). Carbon fixation: ribulose-bisphosphate carboxylase/oxygenase (*cbb*), bifunctional carbon monoxide dehydrogenase/acetyl-CoA synthase (*cdh*), ATP-dependent citrate lyase (*acl*). Hydrolytic carbon degradation: carbohydrate active enzymes, glycoside hydrolase families (*CAZy GH*). Sulfate reduction: adenylylsulfate reductase (*apr*), dissimilatory sulfite reductase (*dsr*). Nitrogen cycling: nitrogenase (*nif*), ammonia monooxygenase (*amo*), nitrate reductase (*nar*), ammonifying nitrite reductase (*nrf*), nitrous oxide reductase (*nos*). Arsenic metabolism: arsenate reductase (*arsC*), arsenite oxidase (*aio*). The relative sequence abundance of these functional marker genes in the metagenomic data sets is provided in Figure S5.

The large majority of *psa* and *psb* transcripts were affiliated with diatoms followed by cyanobacteria and other phototrophic eukaryotes. The relative abundance of 18S and 16S transcripts affiliated with diatoms and cyanobacteria showed opposite trends between HI categories. Whereas diatoms were increased 1.6 to 3.8-fold in medium and high HI samples compared to the reference sample, cyanobacteria decreased 2.9 to 9.6-fold, respectively (Figure 3A). A similar trend was observed in the metagenomic and amplicon data sets, although it was less pronounced for diatoms (Figure 3B+C). The change in the relative contribution of diatoms and cyanobacteria to photosynthesis was further supported by photopigment concentrations, which showed a significant decrease in the ratio of zeaxanthin to fucoxanthin concentrations towards the vent sites in 2013. Fucoxanthin and zeaxanthin (in the absence of chlorophyll b) are considered marker pigments for diatoms and cyanobacteria, respectively (Werner et al., 2008; Wright, 1991). However, chlorophyll b was detected in low concentrations indicating that the usage of zeaxanthin as marker pigment for cyanobacteria may be potentially biased. An increased prevalence of diatoms at the vent sites may be related to the increased availability of silicate (Hassenrück et al., 2016; Lichtschlag et al., in preparation), which is required by diatoms for the construction of their silicate skeleton (Martin-Jézéquel et al., 2000). Additionally, the elevated amount of dissolved CO_2 at the vent may reduce the need to enzymatically convert bicarbonate to CO_2 for photosynthesis and thus lower the energetic costs of photosynthesis (Koch et al., 2013). The expression of carbonic anhydrase was slightly reduced in the high HI sample (Figure 2) and further contained less sequences affiliated with eukaryotic phototrophs compared to cyanobacteria than in the reference sample. The carbonic anhydrase of cyanobacteria, which are generally adapted to low CO_2 concentrations, is known to be more efficient than the carbonic anhydrase of eukaryotic phototrophs (Kranz et al., 2009). Therefore an increase in dissolved CO_2 may be more beneficial to eukaryotic phototrophs such as diatoms, which may outcompete cyanobacteria in natural communities (Koch et al., 2013).

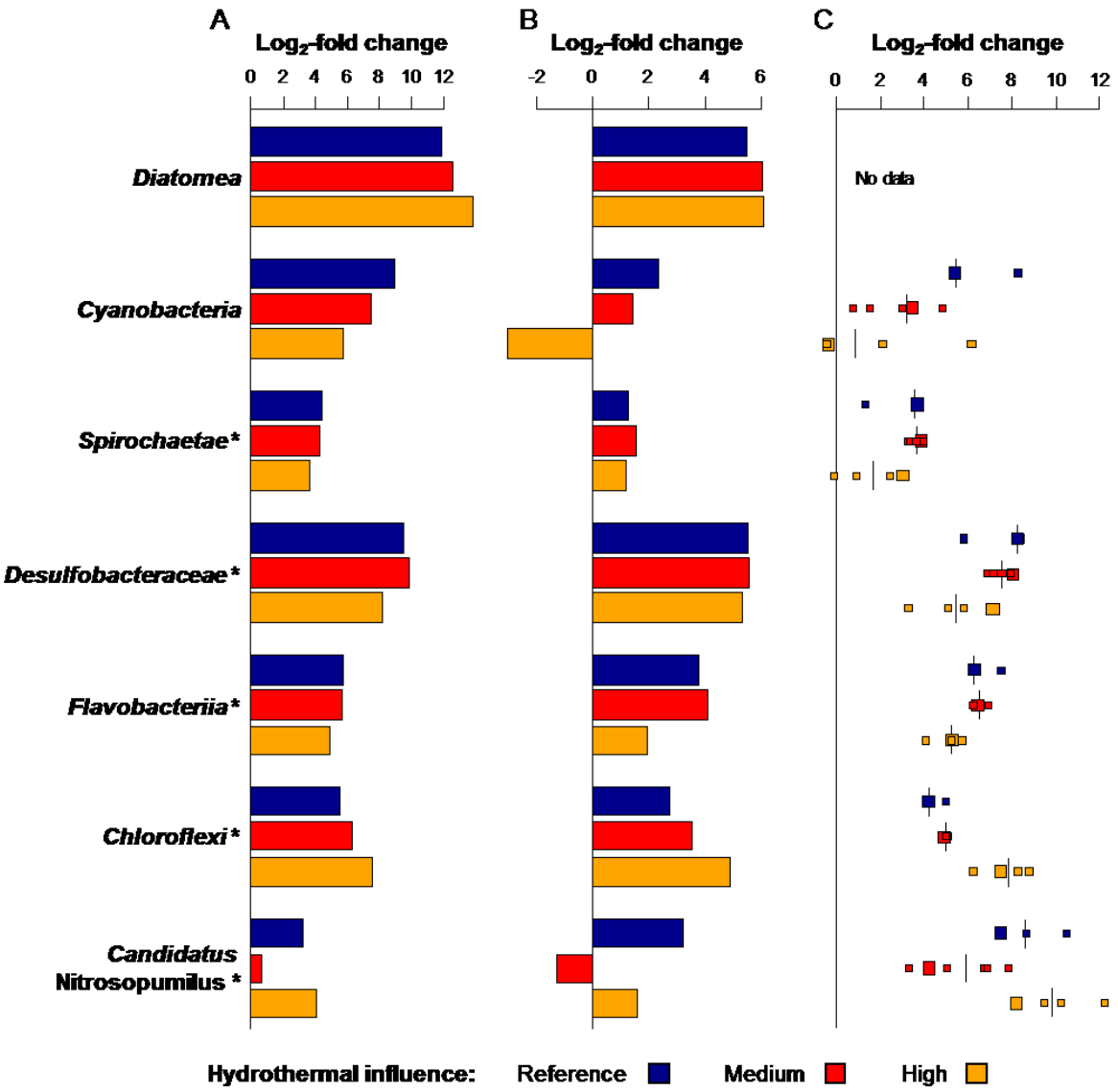

Figure 3: Abundance of key taxa involved in carbon, sulfur and nitrogen cycling based on 16S and 18S sequences in metatranscriptomic (A), metagenomic (B) and amplicon libraries from reference, medium and high hydrothermal influence (HI) sites. Sequence abundance displayed as log2-fold change relative to the geometric mean (zero value) of all taxa per sample (centered log-ratio transformation). Asterisks indicate significant differences between HI categories in the amplicon data set. Larger squares in the amplicon data set (C) mark samples that were used for the construction of metatranscriptomic and metagenomic libraries.

So far our results suggest a shift in the relative contribution of cyanobacteria and diatoms to the photosynthetic community at the CO_2 vent. However, assuming that marker pigment concentrations can be used as abundance proxy, it is likely that this shift is rather caused by an extreme decline of cyanobacteria than an increase in the abundance of diatoms, especially at medium HI sites. Absolute zexanthin concentrations in 2013 decreased steeply from median values of 0.08 µg gdw^{-1} at reference to 0.01 µg gdw^{-1} and less at medium and high HI sites (Figure 4A). Fucoxanthin concentrations in 2013 were significantly lower at medium compared to reference sites with median values of 0.6 and 1.0 µg gdw^{-1}, respectively (Figure 4A). At high HI sites, fucoxanthin concentrations exhibited a large range of values (0.7 to 2.2 µg gdw^{-1}), and although fucoxanthin concentrations from the high HI site with metatranscriptomic data available were among the highest within the data set, no significant differences could be detected between reference and high HI sites in general (Figure 4A). A similar, although less pronounced pattern in fucoxanthin and zeaxanthin concentrations was also observed in 2014, suggesting a weak temporal variability, the exact degree and scale of which needs to be further investigated. It still remains unclear to which degree favorable silicate and CO_2 conditions as well as reduced grazing pressure (Fink et al., submitted) may allow diatoms to thrive, or to merely persist under otherwise presumably adverse environmental conditions at the vent sites.

For estimates of net and gross benthic photosynthesis rates, oxygen fluxes at the sediment-water interface were calculated. Both net and gross photosynthesis rates were not significantly different between HI categories with values ranging from 0.7 to 3.4 and 0.9 to 4.5 mmol O_2 m^{-2} h^{-1}, respectively (Figure 4B). These estimates were consistent with previous observations on photosynthesis rates in permeable reef sediment (Rao et al., 2012; Werner et al., 2008). Compared to photosystem gene expression and pigment concentrations the pattern observed in the photosynthesis rates most closely resembled *psa* expression, although this congruence may also be coincidental since no replication was available for *psa* expression data, and furthermore estimates of photosynthesis rates were only available for 2014. Chlorophyll a concentrations, as marker for phototrophic organisms in general, did not show a consistent pattern with photosynthesis rates (Figure 4A+B). It is likely that in the system investigated here, proxy variables for photosynthesis

such as *psb* expression and chlorophyll a concentration are confounded by other variables. Preliminary data on the light conditions suggested a change in light quality between reference and vent sites (Laurie Hofmann, personal communication). Since photosystem I and II have different light absorption spectra, a change in light quality may cause a shift in the ratio of photosystem I and II expression to avoid an electron imbalance in the photosynthetic electron transport chain (Chow et al., 1990; Cunningham et al., 1990). Additionally, UVB seemed to penetrate deeper into the water at the CO_2 vent (Laurie Hofmann, personal communication). Since photosystem II is more vulnerable to UVB radiation than photosystem I (Sass et al., 1997; Tyystjärvi, 2008), the increased *psb* expression in medium and high HI samples may indicate a higher turnover of the protein rather than increased photosynthesis rates. Furthermore, sediments at the CO_2 vent exhibited increased concentrations of toxic substances such as arsenic (Lichtschlag et al. in preparation), which is known to inhibit photosynthesis in diatoms (Barral-Fraga et al., 2015; Wängberg and Blanck, 1990). In summary, although there may be a shift in the phototrophic microbial community, photosynthesis rates appear to remain stable under the environmental conditions at the CO_2 vent.

Carbon fixation

Based on transcript abundance, the Calvin cycle was the major carbon fixation pathway in the sediment in PNG. Similar to *psa* expression, the transcription of ribulose-bisphosphate carboxylase/oxygenase (*cbb*) as marker gene for the Calvin cycle did not show a clear pattern by HI category (Figure 2), suggesting that carbon fixation via the Calvin cycle may not vary much between reference and vent sites, and further supporting the hypothesis of similar photosynthesis rates at the CO_2 vent. The taxonomic affiliation of *cbb* transcripts was consistent with the taxonomic composition of transcripts related to photosynthesis marker genes with mostly diatoms, showing the same inverse relationship between diatom and cyanobacteria activity, which was observed in 16S and 18S sequences as well as photopigments.

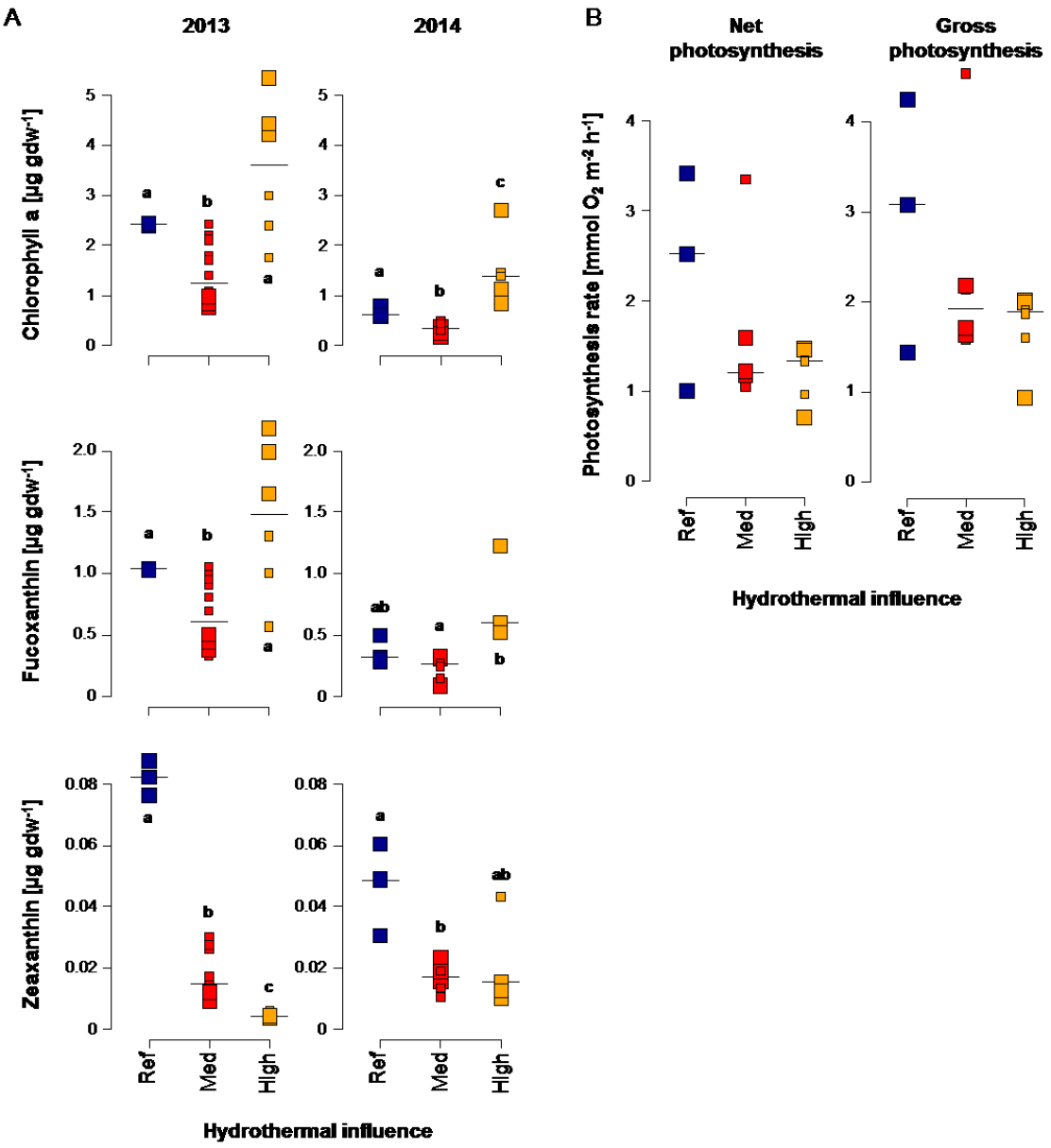

Figure 4A: Marker pigment concentrations in the upper 2 cm of the sediment in May 2013 and April 2014. B: Net and gross photosynthesis rates measured in May 2013. Lower case letters indicate significant differences based on Kruskal-Wallis and fdr-adjusted Wilcoxon post-hoc tests. Larger squares mark data from sampling sites with metatranscriptomic and metagenomic data available.

Prokaryotes possess other pathways for autotrophic carbon fixation than the Calvin cycle (Hügler and Sievert, 2011). Here, we focus on the reductive Acetyl-CoA (rAcetyl-CoA) pathway (Ljungdhal, 1986), and the reductive tricarboxylic acid (rTCA) cycle (Buchanan and Arnon, 1990). The bifunctional carbon monoxide dehydrogenase/ acetyl-CoA synthase (*cdh*) as marker gene for the rAcetyl-CoA pathway (Ragsdale and Wood, 1985) showed a two-fold decrease in the high HI sample compared to medium HI and reference samples (Figure 2). The rAcetyl-CoA pathway is mostly known from acetogenic bacteria and autotrophic sulfate reducers (Hügler and Sievert, 2011). Most of the *cdh* transcripts were affiliated with *Spirochaetae* and *Deltaproteobacteria*, which include known acetogenic and sulfate reducing bacteria, respectively (Hügler and Sievert, 2011; Montoya et al., 2012). Similar to *cdh* expression, the relative abundance of 16S transcripts affiliated with *Spirochaetae* and *Deltasulfobacteraceae*, a deltaproteobacterial family consisting mostly of sulfate reducers, was reduced in the high HI sample (Figure 3A). Comparable trends were also observed in the amplicon data set, where significant differences in the relative sequence abundance of these taxa were detected between HI categories (Figure 3C). Known organisms capable of the rAcetyl-CoA pathway for carbon fixation are anaerobes (Hügler and Sievert, 2011). However, since the oxygen penetration depth was lowest at high HI sites (Fink et al., submitted), it is likely that factors other than the presence of oxygen determine the expression of this pathway in the sediment at the CO_2 vent. Only very few transcripts were annotated to the ATP-dependent citrate lyase (*acl*) as the marker gene for the rTCA cycle (Hügler and Sievert, 2011 and references therein). The rTCA cycle is known to play a major role in carbon fixation at deep-sea hydrothermal vents (Campbell and Cary, 2004). However, our results suggest that its importance at shallow-water hydrothermal vents may be minor.

Unfortunately, no information is yet available on carbon fixation rates at the sampling sites in PNG, apart from photosynthetic carbon fixation based on estimates of gross photosynthesis rates. Pending measurements based on ^{13}C incubation experiments may give better estimates of carbon fixation rates. Nevertheless, our results so far suggest that the majority of carbon is fixed by phototrophic organisms, and that these carbon fixation rates may not vary between reference and vent conditions. Regarding biomass production, it is likely that photoautotrophic far outweigh chemoautotrophic processes in

reef sediments given the unlimited supply of light energy compared to chemical compounds as energy source for carbon fixation (Hügler and Sievert, 2011). Therefore, changes in the rAcetyl-CoA pathway or the rTCA cycle may not relevantly alter bulk carbon fixation.

Carbohydrate degradation

There are a multitude of enzymes to degrade complex carbohydrate molecules such as those that make up the majority of the particulate and dissolved organic matter (DOM) pool. These enzymes are referred to as carbohydrate active enzymes (CAZy). According to type of catalyzed reaction CAZys are grouped into different categories (Lombard et al., 2014). Here, we focused on glycoside hydrolases, which catalyze the hydrolytic cleavage of the glycosidic bond between carbohydrate monomers. The samples from all three HI categories showed similar expression levels of glycoside hydrolases, suggesting that the glycosidic degradation of carbohydrates may not be affected by the CO_2 vent. Taxonomically, the majority of the glycoside hydrolase transcripts were affiliated with *Bacteroidetes*, *Gammaproteobacteria*, *Chloroflexi* and *Firmicutes*. There was an opposite trend in the relative abundance of glycoside hydrolase transcripts affiliated with *Bacteroidetes*, which declined slightly from reference to medium and high HI samples, and *Chloroflexi*, which was increased 1.5 and 2.5-fold in the medium and high HI sample compared to the reference, respectively. This shift in the taxonomic composition of carbohydrate degraders was also visible in 16S metatranscriptomic, metagenomic and amplicon sequences affiliated with *Flavobacteriia*, as major carbon degrading group among the *Bacteroidetes* (Bernardet et al., 2002), and *Chloroflexi*. Based on the amplicon data, it was hypothesized that anaerobic carbon degraders among the *Chlorobi*, *Deferribacteres* and *Chloroflexi* may replace aerobic carbon degraders such as *Flavobacteriia* at the CO_2 vent (Hassenrück et al., 2016). Our results support this hypothesis and further identify *Chloroflexi* as more likely to replace *Flavobacteriia* compared to *Chlorobi* and *Deferribacteres*, which did not appear to contribute much to carbohydrate degradation.

Carbohydrates such as polysaccharides from algal cell walls and storage compounds, starch and smaller oligosaccharides are degraded by α- and β-glucosidases,

which accounted for a large proportion of the glycoside hydrolase transcripts. Measurements of the potential extracellular enzymatic activity of α- and β-glucosidases were not significantly different between HI categories (Figure 5), thus supporting the results from the marker gene analysis. These results contradict previous studies, which have so far mostly detected an increased degradation potential of microbial communities under elevated CO_2 conditions (Burrell et al., 2015; Maas et al., 2013; Piontek et al., 2010). However, the lower availability of degradable material because of a lower organic carbon input in the sediment at the CO_2 vent (Fink et al., submitted) may have further modified the expression of glucoside hydrolases.

At the reference site, the enzymatic activity of β-glucosidases was approximately ten times higher than that of α-glucosidases, which was consistent with previous observations on the contribution of α- and β-glucosidase activity to carbohydrate degradation in marine sediments (Böer et al., 2009). However, at high HI sites, where the lowest activities of β-glucosidases were measured, the ratio of α-glucosidases and β-glucosidases was almost equal (Figure 5). This change in the contribution of α- and β-glucosidases to carbohydrate degradation may indicate a change in the available degradable organic material at the CO_2 vent. Differences in the composition of organic matter further have the potential to alter the light absorption properties of water (Sulzberger and Durisch-Kaiser, 2009), and may thus lead to differences in light quality and UVB penetration that were observed at the CO_2 vent. Raulf et al. (2015) hypothesized that a change in benthic cover (Fabricius et al., 2011) may cause a shift in DOM composition from coral to seagrass and macroalgae-derived DOM. However, since so far there is no direct evidence that the composition of the organic matter differs between reference and vent sites, this hypothesis is still tenuous. Furthermore, no pCO_2 effect on DOM composition was detected in mesocosm experiments (Zark et al., 2015), although at the CO_2 vent other factors that pCO_2 may influence DOM composition. Additionally, since the enzymatic activity measurements were conducted with frozen samples, the results may be biased and should be re-evaluated using fresh sediment material. Moreover, the samples for enzymatic activity measurements were collected in 2014, whereas the molecular and UV data were only available for 2013. Since the degree and scale of the temporal variability of the measured parameters within the sampling area

is still unknown, it remains to be determined whether the consistent patterns between gene expression and enzymatic activity can be reproduced.

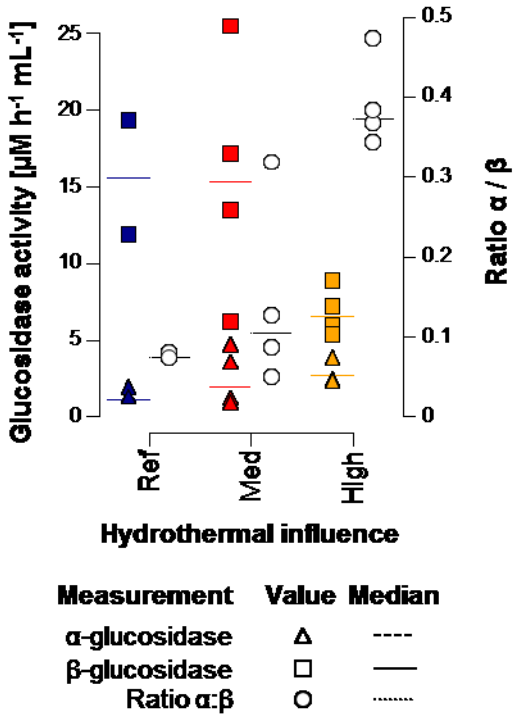

Figure 5: Potential extracellular α- and β-glucosidase activity measured in sediment samples from 0 – 2 cm sediment depth.

Sulfate reduction

Previous observations at the CO_2 vent in PNG documented a steep decrease in sulfate reduction rates (Fink et al., submitted). Here, we observed a similar pattern in two functional marker genes for sulfate reduction, adenylylsulfate reductase (*apr*) and dissimilatory sulfite reductase (*dsr*; Meyer and Kuever, 2007; Santillano et al., 2010), which were both decreased approximately 5-fold in the high HI sample (Figure 2). As previously noted, 16S sequences affiliated with known sulfate reducers such as *Desulfobacteraceae* also showed a decrease at high HI sites (Figure 3). Since sulfate reduction can be coupled to carbon fixation via the rAcetyl-CoA pathway (Hügler and Sievert, 2011; Montoya et al., 2012), the decrease in sulfate reduction rates may further support the decrease observed in the expression of *cdh*. Additionally, TRFLP

fingerprinting of the *dsr* gene showed that there was a shift in the composition of sulfate reducing community between HI categories (Figure 6). A decrease of sulfate reduction rates has been observed at other CO_2 vents as well (Bayraktarov et al., 2013; Molari et al., in preparation; Sievert et al., 1999), and is strongly supported here. Most likely the low sulfate reduction rates are related to the decrease in pH/increase in pCO_2 at the vent, a reduced availability of organic matter and changes in sediment characteristics such as permeability (Fink et al., submitted).

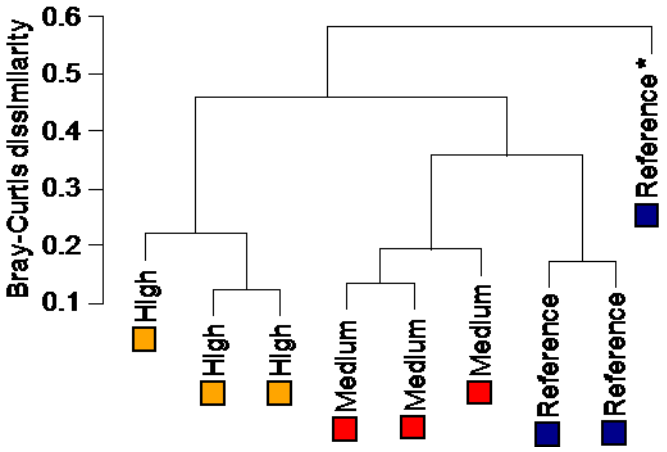

Figure 6: Cluster diagram of sulfate reducing bacteria from reference, medium and high hydrothermal influence (HI) sites based on TRFLP analysis of the *dsrA* gene. Complete linkage clustering based on Bray-Curtis dissimilarity calculated from the relative abundance of TRFLP-OTUs. The asterisk marks an outlier replicate which was not used for metagenomic and metatranscriptomic analyses.

Nitrogen cycle

Nitrogen fixation, i.e. the conversion of N_2 into NH_3, is mediated by the enzyme nitrogenase (*nif*; Zehr et al., 2003). In the open surface ocean, cyanobacteria are considered to be responsible for the majority of nitrogen fixation (Foster et al., 2009). In sediments, other microbial organisms such as deltaproteobacterial sulfate reducers also contribute to nitrogen fixation (Werner et al., 2008; Zehr et al., 2003). We observed the highest *nif* expression in the medium HI sample, which was about 2.5-fold higher than in the reference sample. In the high HI sample there was an almost 6-fold decrease in *nif* expression compared to the reference (Figure 2). Assuming that medium HI sites most

closely resemble conditions used in ocean acidification experiments, the increase in *nif* expression would be consistent with previous studies, which reported increased nitrogen fixation rates for cyanobacterial strains at reduced pH (Fu et al., 2008; Hutchins et al., 2007). The severe decrease of *nif* expression at the high HI site may be related to the decrease in cyanobacteria and sulfate reducers such as *Desulfobacteraceae* (Figure 3). Additionally, nitrogen fixation rates are considered to be lower in silicate compared to carbonate sediments (Bednarz et al., 2015), which are found here at the CO_2 and reference sites, respectively (Fink et al., submitted). An increased availability of ammonium at the CO_2 vent may also lead to a down-regulation of nitrogen fixation (Artur Fink, personal communication; Ohmori and Hattori, 1974). However, these conclusions are so far only based on molecular data and need to be further validated by direct measurement of nitrogen fixation rates (pending).

Nitrification refers to the oxidation of ammonium to nitrate. The first step in this process is catalyzed by the ammonia monooxygenase (*amo*; Ward et al., 2011 and references therein). We detected a more than 10-fold increase in *amo* expression in the high HI sample (Figure 2). The increase of archaeal *amo* expression at elevated pCO_2 has been observed before in an experiment, where sediment was incubated at 3000 ppm CO_2, comparable to the pCO_2 at high HI sites (Tait et al., 2014). Almost all *amo* transcripts were affiliated with archaea, most likely the candidate genus Nitrosopumilus, which also dominated the archaeal 16S amplicon sequences at high HI sites (Figure 3C). Both previous studies on the archaeal community in the sediment in PNG observed an increase in the relative abundance of 16S sequences affiliated with *Candidatus* Nitrosopumilus at the CO_2 vent (Hassenrück et al., 2016; Raulf et al., 2015), which was also observed in metatranscriptomic and metagenomic 16S here, although the reference sample also contained a high proportion of 16S sequences affiliated with *Candidatus* Nitrosopumilus (Figure 3C).

It has been hypothesized that archaeal nitrifiers such as *Candidatus* Nitrosopumilus may replace bacterial nitrifiers such as *Nitrosococcus* at the CO_2 vent (Raulf et al., 2015). However, here only one *amo* transcript from the high HI sample was affiliated with ammonia oxidizing bacteria. Instead, we suggest that even at reference sites, mainly archaea are responsible for nitrification in the sediment, and that at high HI sites archaeal

nitrification is strongly increased. It is possible that an increased supply of ammonium from the CO_2 vent (Artur Fink, personal communication) is fueling archaeal nitrification. This hypothesis contradicts previous suggestions about nitrification rates under reduced pH conditions, where the chemical equilibrium between ammonia and ammonium is shifted towards a reduced availability of ammonia that is used by ammonia oxidizers (Beman et al., 2011; Huesemann et al., 2002). On the other hand, observations from other natural systems, where microbial communities have been adapted to reduced pH conditions for a long time, support our findings (Fulweiler et al., 2011; Kitidis et al., 2011). Furthermore, archaeal nitrification appears to be less sensitive to low pH (Lehtovirta-Morley et al., 2011; Nicol et al., 2008). Yet, since no direct measurements of nitrification rates are so far available, our hypothesis needs further validation.

Nitrate reduction processes were also assessed based only on marker gene expression, since no data on biogeochemical rates were available. We focused on two nitrate reduction processes that either result in a loss of biologically available nitrogen, i.e. denitrification to N_2, or retain nitrogen, i.e. the dissimilatory nitrate reduction to ammonium (DNRA). As marker genes nitrate reductase (*nar*), ammonifying nitrite reductase (*nrf*) and nitrous oxide reductase (*nos*) were selected, catalyzing the reduction of nitrate to nitrite, the reduction of nitrite to ammonium during DNRA and the reduction of nitrous oxide to N_2, respectively (Rusch and Gaidos, 2013). Expression of *nar* and *nrf* were both more than 2-fold decreased in the medium and high HI samples compared to the reference sample (Figure 2). On the other hand, *nos* expression was only decreased in the medium, but not the high HI sample (Figure 2). However, since nitrous oxide reductase is known to be vulnerable to reduced pH (Liu et al., 2010a), its increased expression level in the high HI sample may also indicate a high protein turnover. The contribution of DNRA and denitrification to N_2 to denitrification processes in reef sediments are considered to be similar, although in some cases DNRA was reported to be the dominant denitrification process (Dong et al., 2011; Erler et al., 2014). So far our results are not conclusive regarding how the importance of these two processes will be affected by the CO_2 vent, although it appears that denitrification in general may be reduced, possibly related to the lower permeability and decreased availability of organic

material at the CO_2 vent (Fink et al., submitted). Further direct measurements of denitrification rates are needed to confirm the results of this study.

Arsenic metabolism

During the characterization of the environmental conditions in the sediment, an enrichment of arsenic in the pore water and solid phase was detected at the CO_2 vent (Lichtschlag et al., in preparation). High concentrations of arsenic are not uncommon at hydrothermal vents in PNG, where arsenic mainly occurs as arsenate (As(V)) and arsenite (As(III); Price and Pichler, 2005; Price et al., 2007). Both forms of arsenic are toxic to most microorganisms and require active detoxification (Achour et al., 2007). Alternatively, some bacteria are able to use arsenate and arsenite in their energy metabolism (Akerman et al., 2011). Here, we focused on the arsenate reductase subunit of the arsenic detoxification protein complex (*arsC*; Achour et al., 2007), and the arsenite oxidase (*aio*) involved in the energy metabolism (Lebrun et al., 2003). The expression of *arsC* was increased 2-fold in the medium HI sample compared to the reference sample (Figure 2), consistent with the increase in arsenic concentrations at this site. However, in the high HI sample *arsC* expression was only marginally higher than in the reference sample, although arsenic concentrations exceeded those at medium HI sites. The expression of *aio* was only increased in the high HI sample, which showed an almost 6-fold higher expression compared to the medium HI and reference samples (Figure 2). It is likely that in the immediate vicinity of the CO_2 vents arsenite constitutes the majority of arsenic species, as observed at another hydrothermal vent in PNG (Price et al., 2007). Furthermore, arsenite oxidation has a higher energy yield than arsenate reduction (Akerman et al., 2011), suggesting that it may be the dominating process in arsenic energy metabolism at high HI the CO_2 vents. We propose that arsenic detoxification is a valid metabolic strategy for microorganisms at medium HI sites, whereas at high HI sites microorganisms that can exploit high arsenite concentration for energy generation have a competitive advantage.

Table 1: Potential effects of hydrothermal CO_2 venting on microbial processes (function) and the organisms involved in these processes (taxa) in the sediment. HI: hydrothermal influence, increase (↑), decrease (↓), no change (−), no conclusive information available (?). Processes marked with an asterisk were assessed without data on actual functional rates.

	Medium HI		High HI	
	Function	Taxa	Function	Taxa
Carbon cycle				
Photosynthesis	No change	*Diatomea* ↑− *Cyanobacteria* ↓	No change	*Diatomea* ↑− *Cyanobacteria* ↓
Carbon fixation*	No change	*Diatomea* ↑− *Cyanobacteria* ↓	Calvin cycle – rAcetyl-CoA ↓	*Diatomea* ↑− *Cyanobacteria* ↓ *Spirochaeatae* ↓ *Desulfobacteraceae* ↓
Carbohydrate degradation	No change	*Chloroflexi* ↑−	No change, but increased ratio of α:β glucosidase activity	*Chloroflexi* ↑ *Flavobacteriia* ↓
Sulfur cycle				
Sulfate reduction	Decrease	Shift in TRFLP fingerprint	Decrease	*Desulfobacteraceae* ↓ Shift in TRFLP fingerprint
Nitrogen cycle				
Nitrogen fixation*	Increase	No change	Decrease	*Cyanobacteria* ↓ *Desulfobacteraceae* ↓
Ammonia oxidation*	No change	No change	Increase	*Candidatus* Nitrosopumilus ↑
Denitrification to ammonia*	Decrease	?	Decrease	?
Denitrification to N_2*	Decrease	?	?	?
Other elements				
Arsenate reduction*	Increase	?	No change	?
Arsenite oxidation*	No change	?	Increase	?

Conclusion

We provided an overview of major microbial processes involved in element cycling in the sediment at a shallow-water hydrothermal CO_2 vent in PNG that is used as natural analogue in OA research. Some functions, such as photosynthesis and carbohydrate degradation, did not seem to be strongly affected by the CO_2 vent, although the taxonomic composition of the microorganisms performing these functions was altered, suggesting functional redundancy among microbial taxa (Table 1). On the other hand, sulfate reduction and nitrogen cycling seemed to be impacted at the CO_2 vent, suggesting that among the microorganisms involved in these processes no functional redundancy applied (Table 1). Furthermore, altered sediment characteristics such as reduced permeability at the CO_2 vent may largely explain the decrease in remineralization rates. The challenge of using hydrothermal CO_2 vents to investigate OA effects on microbial processes in the sediment is to differentiate between potential OA effects and the influence of other environmental variables at the CO_2 vent (Hassenrück et al., 2016; Vizzini et al., 2013). Assuming that medium HI sites may constitute a more realistic OA scenario than high HI sites (Hassenrück et al., 2016), changes in microbial processes, which were only observed at high HI sites, may not represent responses to future ocean acidification (Table 1).

Besides, many microbial processes could not be fully assessed with the methods at our disposal. Despite the power of meta-omics approaches, such as metatranscriptomic sequencing, to provide information on the active microbial community and function, such techniques remain limited in their ability to assess actual metabolic rates. Here, we observed consistent patterns in gene expression and metabolic rate measurements in some cases, whereas in other cases gene expression deviated strongly from the actual metabolic rate. Gene expression data may therefore be used to generate hypotheses regarding microbial functions, but should not be used on its own to draw conclusions about functional rates. Since functional rate measurements were not available for all microbial processes investigated by metatranscriptomic marker gene analysis, further quantitative validation of our results is necessary. For future research we propose to focus on the following objectives:

- Is the beneficial effect of increased CO_2 concentrations on photosynthesis rates at the CO_2 vent counteracted by otherwise adverse physico-chemical conditions such as potentially increased UV irradiance and arsenic concentrations? How likely are such adverse conditions under future OA?
- What is the contribution of different carbon fixation pathways to primary production in the sediment, and how are they affected by the CO_2 vent?
- Is the composition of DOM directly or indirectly affected by the CO_2 vent, and is this in turn influencing the expression of carbohydrate degrading enzymes?
- Are the changes in gene expression related to the nitrogen cycle representative of nitrogen fixation, nitrification and denitrification rates at the CO_2 vent?
- How are metals and trace elements, which are enriched in vent fluids, used in the microbial energy metabolism? Will the decrease in pH due to OA result in a similar leeching of metals and trace elements?
- How stable are the patterns observed in microbial processes at the CO_2 vent at different temporal scales?

Such questions will help to better understand microbial processes in the sediment at hydrothermal CO_2 vents associated with coral reefs, as well as to better predict long-term OA effects based on the study of such natural analogues.

Acknowledgements

Foremost we would like to thank the cruise leader Katharina Fabricius, all cruise participants and the crew and captain of the MV Chertan during the cruise to Papua New Guinea in 2013 and 2014. Further, we thank Antonio Fernandez-Guerra, Bert Möhlmann and the team of the EBI metagenomics portal for their advice on the bioinformatic and statistical analysis, Nataly Guevara for her support with the TRFLP analysis and Laurie Hofmann for providing information on the light conditions at the sampling sites. Special thanks to Anna Lichtschlag for sharing her data on pore water geochemistry and for long discussions about the vent system in PNG. The study was part of the BIOACID II project that was supported by the German Federal Ministry of Education and Research [FKZ 03F0655].

References

Achour, A. R., Bauda, P., and Billard, P. (2007). Diversity of arsenite transporter genes from arsenic-resistant soil bacteria. *Res. Microbiol.* 158, 128–37. doi:10.1016/j.resmic.2006.11.006.

Ainsworth, T. D., Vega Thurber, R., and Gates, R. D. (2010). The future of coral reefs: a microbial perspective. *Trends Ecol. Evol.* 25, 233–40. doi:10.1016/j.tree.2009.11.001.

Akerman, N. H., Price, R. E., Pichler, T., and Amend, J. P. (2011). Energy sources for chemolithotrophs in an arsenic- and iron-rich shallow-sea hydrothermal system. *Geobiology* 9, 436–45. doi:10.1111/j.1472-4669.2011.00291.x.

Allgaier, M., Riebesell, U., Vogt, M., Thyrhaug, R., and Grossart, H. P. (2008). Coupling of heterotrophic bacteria to phytoplankton bloom development at different pCO_2 levels: a mesocosm study. *Biogeosciences Discuss.* 5, 317–359. doi:10.5194/bgd-5-317-2008.

Arnosti, C., Grossart, H. P., Mühling, M., Joint, I., and Passow, U. (2011). Dynamics of extracellular enzyme activities in seawater under changed atmospheric pCO_2: A mesocosm investigation. *Aquat. Microb. Ecol.* 64, 285–298. doi:10.3354/ame01522.

Barral-Fraga, L., Morin, S., Rovira, M. D. M., Urrea, G., Magellan, K., and Guasch, H. (2015). Short-term arsenic exposure reduces diatom cell size in biofilm communities. *Environ. Sci. Pollut. Res. Int.* 23, 4257–4257. doi:10.1007/s11356-015-4894-8.

Bayraktarov, E., Price, R. E., Ferdelman, T. G., and Finster, K. (2013). The pH and pCO_2 dependence of sulfate reduction in shallow-sea hydrothermal CO_2-venting sediments (Milos Island, Greece). *Front. Microbiol.* 4, 1–10. doi:10.3389/fmicb.2013.00111.

Bednarz, V., van Hoytema, N., Cardini, U., Naumann, M., Al-Rshaidat, M., and Wild, C. (2015). Dinitrogen fixation and primary productivity by carbonate and silicate reef sand communities of the Northern Red Sea. *Mar. Ecol. Prog. Ser.* 527, 47–57. doi:10.3354/meps11224.

Beman, J. M., Chow, C.-E., King, A. L., Feng, Y., Fuhrman, J. A., Andersson, A., et al. (2011). Global declines in oceanic nitrification rates as a consequence of ocean acidification. *Proc. Natl. Acad. Sci. U. S. A.* 108, 208–213. doi:10.1073/pnas.1011053108.

Bernardet, J.-F., Nakagawa, Y., and Holmes, B. (2002). Proposed minimal standards for describing new taxa of the family Flavobacteriaceae and emended description of the family. *Int. J. Syst. Evol. Microbiol.*, 1049–1070. doi:10.1099/ijs.0.02136-0.02136.

Böer, S. I., Arnosti, C., Van Beusekom, J. E. E., and Boetius, A. (2009). Temporal variations in microbial activities and carbon turnover in subtidal sandy sediments. *Biogeosciences* 6, 1149–1165. doi:10.5194/bg-6-1149-2009.

Boetius, A., and Lochte, K. (1994). Regulation of microbial enzymatic degradation of organic matter in deep-sea sediments. *Mar. Ecol. Prog. Ser.* 104, 299–307. doi:10.3354/meps104299.

Bolger, A. M., Lohse, M., and Usadel, B. (2014). Trimmomatic: A flexible trimmer for Illumina sequence data. *Bioinformatics* 30, 2114–2120. doi:10.1093/bioinformatics/btu170.

Boucher, G., Clavier, J., Hily, C., and Gattuso, J. P. (1998). Contribution of soft-bottoms to the community metabolism (primary production and calcification) of a barrier reef flat (Moorea, French Polynesia). *J. Exp. Mar. Bio. Ecol.* 225, 269–283. doi:10.1016/S0022-0981(97)00227-X.

Boudreau, B. P. (1997). *Diagenetic Models and Their Implementation*. Berlin; Heidelberg; New York; Barcelona; Budapest; Hong Kong; London; Milan; Paris; Santa Clara; Singapore; Tokyo: Springer.

Bryant, D. A., and Frigaard, N. U. (2006). Prokaryotic photosynthesis and phototrophy illuminated. *Trends Microbiol.* 14, 488–496. doi:10.1016/j.tim.2006.09.001.

Buchanan, B. B., and Arnon, D. I. (1990). A reverse KREBS cycle in photosynthesis: consensus at last. *Photosynth. Res.* 24, 47–53.

Burrell, T. J., Maas, E. W., Hulston, D. A., and Law, C. S. (2015). Bacterial abundance , processes and diversity responses to acidification at a coastal CO_2 vent. *FEMS Microbiol. Lett.* doi:http://dx.doi.org/10.1093/femsle/fnv154.

Bushnell, B. (2015). BBMap: A fast, accurate, splice-aware aligner. Available at: sourceforge.net/projects/bbmap/.

Camacho, C., Coulouris, G., Avagyan, V., Ma, N., Papadopoulos, J., Bealer, K., et al. (2009). BLAST+: architecture and applications. *BMC Bioinformatics* 10, 421. doi:10.1186/1471-2105-10-421.

Campbell, B. J., and Cary, S. C. (2004). Abundance of Reverse Tricarboxylic Acid Cycle Genes in Free-Living Microorganisms at Deep-Sea Hydrothermal Vents. *Appl. Environ. Microbiol.* 70, 6282–6289. doi:10.1128/AEM.70.10.6282.

Chow, W. S., Melis, a, and Anderson, J. M. (1990). Adjustments of photosystem stoichiometry in chloroplasts improve the quantum efficiency of photosynthesis. *Proc. Natl. Acad. Sci. U. S. A.* 87, 7502–7506. doi:10.1073/pnas.87.19.7502.

Cunningham, F. X., Dennenberg, R. J., Jursinic, P. a, and Gantt, E. (1990). Growth under Red Light Enhances Photosystem II Relative to Photosystem I and Phycobilisomes in the Red Alga Porphyridium cruentum. *Plant Physiol.* 93, 888–895. doi:10.1104/pp.93.3.888.

Dong, L. F., Sobey, M. N., Smith, C. J., Rusmana, I., Phillips, W., Stott, A., et al. (2011). Dissimilatory reduction of nitrate to ammonium, not denitrification or anammox, dominates benthic nitrate reduction in tropical estuaries. *Limnol. Oceanogr.* 56, 279–291. doi:10.4319/lo.2011.56.1.0279.

Endres, S., Galgani, L., Riebesell, U., Schulz, K. G., and Engel, A. (2014). Stimulated bacterial growth under elevated pCO_2: Results from an off-shore mesocosm study. *PLoS One* 9, 1–8. doi:10.1371/journal.pone.0099228.

Erler, D. V., Santos, I. R., and Eyre, B. D. (2014). Inorganic nitrogen transformations within permeable carbonate sands. *Cont. Shelf Res.* 77, 69–80. doi:10.1016/j.csr.2014.02.002.

Fabricius, K. E., Langdon, C., Uthicke, S., Humphrey, C., Noonan, S., De'ath, G., et al. (2011). Losers and winners in coral reefs acclimatized to elevated carbon dioxide concentrations. *Nat. Clim. Chang.* 1, 165–169. doi:10.1038/nclimate1122.

Fenchel, T., and Jorgensen, B. B. (1977). Detritus food chains of aquatic ecosystems: the role of bacteria. *Adv. Microb. Ecol.* 1, 1–57. doi:10.1007/978-1-4615-8219-9_1.

Fink, A., Guilini, K., Hassenrück, C., Lichtschlag, A., Borisov, S., de Beer, D. (submitted). Sediment biogeochemistry at hydrothermal CO_2 seeps within a coral reef. *Limnol. Oceanogr.*

Foster, R. A., Subramaniam, A., and Zehr, J. P. (2009). Distribution and activity of diazotrophs in the Eastern Equatorial Atlantic. *Environ. Microbiol.* 11, 741–50. doi:10.1111/j.1462-2920.2008.01796.x.

Fu, F., Mulholland, M. R., Garcia, N. S., Beck, A., Bernhardt, P. W., Warner, M. E., et al. (2008). Interactions between changing pCO_2, N_2 fixation, and Fe limitation in the marine unicellular cyanobacterium Crocosphaera. *Limnol. Oceanogr.* 53, 2472–2484. doi:10.4319/lo.2008.53.6.2472.

Fulweiler, R. W., Emery, H. E., Heiss, E. M., and Berounsky, V. M. (2011). Assessing the Role of pH in Determining Water Column Nitrification Rates in a Coastal System. *Estuaries and Coasts* 34, 1095–1102. doi:10.1007/s12237-011-9432-4.

Gaidos, E., Rusch, A., and Ilardo, M. (2011). Ribosomal tag pyrosequencing of DNA and RNA from benthic coral reef microbiota: community spatial structure, rare members and nitrogen-cycling guilds. *Environ. Microbiol.* 13, 1138–52. doi:10.1111/j.1462-2920.2010.02392.x.

Garren, M., and Azam, F. (2012). New directions in coral reef microbial ecology. *Environ. Microbiol.* 14, 833–844. doi:10.1111/j.1462-2920.2011.02597.x.

Gattuso, J.-P., Frankignoulle, M., and Wollast, R. (1998). Carbon and the carbonate metabolism in coastal aquatic ecosystems. *Annu. Rev. Ecol. Evol. Syst.* 29, 405–434. doi:10.1146/annurev.ecolsys.29.1.405.

Grossart, H. P., Allgaier, M., Passow, U., and Riebesell, U. (2006). Testing the effect of CO_2 concentration on the dynamics of marine heterotrophic bacterioplankton. *Limnol. Oceanogr.* 51, 1–11. doi:10.4319/lo.2006.51.1.0001.

Hall-Spencer, J. M., Rodolfo-Metalpa, R., Martin, S., Ransome, E., Fine, M., Turner, S. M., et al. (2008). Volcanic carbon dioxide vents show ecosystem effects of ocean acidification. *Nature* 454, 96–9. doi:10.1038/nature07051.

Hassenrück, C., Fink, A., Lichtschlag, A., Tegetmeyer, H. E., Beer, D. de, and Ramette, A. (2016). Quantification of the effects of ocean acidification on sediment microbial communities in the environment: the importance of ecosystem approaches. *FEMS Microbiol. Ecol.* 92. doi:10.1093/femsec/fiw027.

Huesemann, M. H., Skillman, A. D., and Crecelius, E. A. (2002). The inhibition of marine nitrification by ocean disposal of carbon dioxide. *Mar. Pollut. Bull.* 44, 142–148. doi:10.1016/S0025-326X(01)00194-1.

Hügler, M., and Sievert, S. M. (2011). Beyond the Calvin Cycle: Autotrophic Carbon Fixation in the Ocean. *Ann. Rev. Mar. Sci.* 3, 261–289. doi:10.1146/annurev-marine-

120709-142712.

Hunter, S., Corbett, M., Denise, H., Fraser, M., Gonzalez-Beltran, A., Hunter, C., et al. (2014). EBI metagenomics - A new resource for the analysis and archiving of metagenomic data. *Nucleic Acids Res.* 42, 600–606. doi:10.1093/nar/gkt961.

Hutchins, D. A., Fu, F.-X., Zhang, Y., Warner, M. E., Feng, Y., Portune, K., et al. (2007). CO_2 control of Trichodesmium N_2 fixation, photosynthesis, growth rates, and elemental ratios: Implications for past, present, and future ocean biogeochemistry. *Limnol. Oceanogr.* 52, 1293–1304. doi:10.4319/lo.2007.52.4.1293.

Joint, I., Doney, S. C., and Karl, D. M. (2011). Will ocean acidification affect marine microbes? *ISME J.* 5, 1–7. doi:10.1038/ismej.2010.79.

Jones, P., Binns, D., Chang, H. Y., Fraser, M., Li, W., McAnulla, C., et al. (2014). InterProScan 5: Genome-scale protein function classification. *Bioinformatics* 30, 1236–1240. doi:10.1093/bioinformatics/btu031.

Kans, J. (2013). Entrez Direct: E-utilities on the UNIX Command Line. *NCBI*.

Kerfahi, D., Hall-Spencer, J. M., Tripathi, B. M., Milazzo, M., Lee, J., and Adams, J. M. (2014). Shallow Water Marine Sediment Bacterial Community Shifts Along a Natural CO_2 Gradient in the Mediterranean Sea Off Vulcano, Italy. *Environ. Microbiol.* doi:10.1007/s00248-014-0368-7.

Kitidis, V., Laverock, B., McNeill, L. C., Beesley, A., Cummings, D., Tait, K., et al. (2011). Impact of ocean acidification on benthic and water column ammonia oxidation. *Geophys. Res. Lett.* 38, 1–5. doi:10.1029/2011GL049095.

Koch, M., Bowes, G., Ross, C., and Zhang, X.-H. (2013). Climate change and ocean acidification effects on seagrasses and marine macroalgae. *Glob. Chang. Biol.* 19, 103–32. doi:10.1111/j.1365-2486.2012.02791.x.

Kopylova, E., Noé, L., and Touzet, H. (2012). SortMeRNA: Fast and accurate filtering of ribosomal RNAs in metatranscriptomic data. *Bioinformatics* 28, 3211–3217. doi:10.1093/bioinformatics/bts611.

Kranz, S. A., Sültemeyer, D., Richter, K.-U., and Rost, B. (2009). Carbon acquisition by *Trichodesmium*: the effect of pCO_2 and diurnal changes. *Limnol. Oceanogr.* 54, 548–559. doi:10.4319/lo.2009.54.2.0548.

Lanzen, A., Jorgensen, S. L., Bengtsson, M. M., Jonassen, I., Ovreas, L., and Urich, T. (2011). Exploring the composition and diversity of microbial communities at the Jan Mayen hydrothermal vent field using RNA and DNA. *FEMS Microbiol. Ecol.* 77, 577–589. doi:10.1111/j.1574-6941.2011.01138.x.

Lebrun, E., Brugna, M., Baymann, F., Muller, D., Lièvremont, D., Lett, M. C., et al. (2003). Arsenite oxidase, an ancient bioenergetic enzyme. *Mol. Biol. Evol.* 20, 686–693. doi:10.1093/molbev/msg071.

Lehtovirta-Morley, L. E., Stoecker, K., Vilcinskas, A., Prosser, J. I., and Nicol, G. W. (2011). Cultivation of an obligate acidophilic ammonia oxidizer from a nitrifying acid soil. *Proc. Natl. Acad. Sci.* 108, 15892–15897. doi:10.1073/pnas.1107196108.

Lindh, M. V, Riemann, L., Baltar, F., Romero-Oliva, C., Salomon, P. S., Granéli, E., et

al. (2013). Consequences of increased temperature and acidification on bacterioplankton community composition during a mesocosm spring bloom in the Baltic Sea. *Environ. Microbiol. Rep.* 5, 252–262. doi:10.1111/1758-2229.12009.

Liu, B., Mørkved, P. T., Frostegård, Å., and Bakken, L. R. (2010a). Denitrification gene pools, transcription and kinetics of NO, N_2O and N_2 production as affected by soil pH. *FEMS Microbiol. Ecol.* 72, 407–417. doi:10.1111/j.1574-6941.2010.00856.x.

Liu, J., Weinbauer, M., Maier, C., Dai, M., and Gattuso, J.-P. (2010b). Effect of ocean acidification on microbial diversity and on microbe-driven biogeochemistry and ecosystem functioning. *Aquat. Microb. Ecol.* 61, 291–305. doi:10.3354/ame01446.

Ljungdhal, L. G. (1986). The Autotrophic Pathway of Acetate Synthesis in Acetogenic Bacteria. *Annu. Rev. Microbiol.* 40, 415–450.

Lombard, V., Golaconda Ramulu, H., Drula, E., Coutinho, P. M., and Henrissat, B. (2014). The carbohydrate-active enzymes database (CAZy) in 2013. *Nucleic Acids Res.* 42, 490–495. doi:10.1093/nar/gkt1178.

Maas, E., Law, C., Hall, J., Pickmere, S., Currie, K., Chang, F., et al. (2013). Effect of ocean acidification on bacterial abundance, activity and diversity in the Ross Sea, Antarctica. *Aquat. Microb. Ecol.* 70, 1–15. doi:10.3354/ame01633.

Martin-Jézéquel, V., Hildebrand, M., and Brzezinski, M. A. (2000). Silicon metabolism in diatoms: Implications for growth. *J. Phycol.* 36, 821–840. doi:10.1046/j.1529-8817.2000.00019.x.

Meyer, B., and Kuever, J. (2007). Molecular analysis of the diversity of sulfate-reducing and sulfur-oxidizing prokaryotes in the environment, using aprA as functional marker gene. *Appl. Environ. Microbiol.* 73, 7664–7679. doi:10.1128/AEM.01272-07.

Moeseneder, M. M., Arrieta, J. M., and Herndl, G. J. (2005). A comparison of DNA- and RNA-based clone libraries from the same marine bacterioplankton community. *FEMS Microbiol. Ecol.* 51, 341–352. doi:10.1016/j.femsec.2004.09.012.

Molari, M., Guilini, K., Weber, M., Ramette, A., Lott, C., Wenzhöfer, F., et al. Effects of high CO_2 leakage on biogeochemical functions of submarine sandy sediment communities.

Montoya, L., Celis, L. B., Razo-Flores, E., and Alpuche-Solis, A. G. (2012). Distribution of CO_2 fixation and acetate mineralization pathways in microorganisms from extremophilic anaerobic biotopes. *Extremophiles* 16, 805–817. doi:10.1007/s00792-012-0487-3.

Newbold, L. K., Oliver, A. E., Booth, T., Tiwari, B., Desantis, T., Maguire, M., et al. (2012). The response of marine picoplankton to ocean acidification. *Environ. Microbiol.* 14, 2293–307. doi:10.1111/j.1462-2920.2012.02762.x.

Nicol, G. W., Leininger, S., Schleper, C., and Prosser, J. I. (2008). The influence of soil pH on the diversity, abundance and transcriptional activity of ammonia oxidizing archaea and bacteria. *Environ. Microbiol.* 10, 2966–2978. doi:10.1111/j.1462-2920.2008.01701.x.

O'Brien, P. A., Morrow, K. M., Willis, B. L., and Bourne, D. G. (2016). Implications of

Ocean Acidification for Marine Microorganisms from the Free-Living to the Host-Associated. *Front. Mar. Sci.* 3. doi:10.3389/fmars.2016.00047.

Ohmori, M., and Hattori, A. (1974). Effect of ammonia on nitrogen fixation by the blue-green alga Anabaena cylindrica. *Plant Cell Physiol.* 15, 131–142. Available at: http://pcp.oxfordjournals.org/content/15/1/131.short.

Oliver, A. E., Newbold, L. K., Whiteley, A. S., and van der Gast, C. J. (2014). Marine bacterial communities are resistant to elevated carbon dioxide levels. *Environ. Microbiol. Rep.* 6, 574–582. doi:10.1111/1758-2229.12159.

Piontek, J., Borchard, C., Sperling, M., Schulz, K. G., Riebesell, U., and Engel, A. (2013). Response of bacterioplankton activity in an Arctic fjord system to elevated pCO_2: Results from a mesocosm perturbation study. *Biogeosciences* 10, 297–314. doi:10.5194/bg-10-297-2013.

Piontek, J., Lunau, M., Händel, N., Borchard, C., Wurst, M., and Engel, A. (2010). Acidification increases microbial polysaccharide degradation in the ocean. *Biogeosciences* 7, 1615–1624. doi:10.5194/bg-7-1615-2010.

Price, R. E., Amend, J. P., and Pichler, T. (2007). Enhanced geochemical gradients in a marine shallow-water hydrothermal system: Unusual arsenic speciation in horizontal and vertical pore water profiles. *Appl. Geochemistry* 22, 2595–2605. doi:10.1016/j.apgeochem.2007.06.010.

Price, R. E., and Pichler, T. (2005). Distribution, speciation and bioavailability of arsenic in a shallow-water submarine hydrothermal system, Tutum Bay, Ambitle Island, PNG. *Chem. Geol.* 224, 122–135. doi:10.1016/j.chemgeo.2005.07.017.

Pruesse, E., Peplies, J., and Glöckner, F. O. (2012). SINA: Accurate high-throughput multiple sequence alignment of ribosomal RNA genes. *Bioinformatics* 28, 1823–1829. doi:10.1093/bioinformatics/bts252.

Quast, C., Pruesse, E., Yilmaz, P., Gerken, J., Schweer, T., Yarza, P., et al. (2013). The SILVA ribosomal RNA gene database project: improved data processing and web-based tools. *Nucleic Acids Res.* 41, D590–6. doi:10.1093/nar/gks1219.

Ragsdale, S. W., and Wood, H. G. (1985). Acetate biosynthesis by acetogenic bacteria. Evidence that carbon monoxide dehydrogenase is the condensing enzyme that catalyzes the final steps of the synthesis. *J. Biol. Chem.* 260, 3970–3977.

Rao, A. M. F., Polerecky, L., Ionescu, D., Meysman, F. J. R., and de Beer, D. (2012). The influence of pore-water advection, benthic photosynthesis, and respiration on calcium carbonate dynamics in reef sands. *Limnol. Oceanogr.* 57, 809–825. doi:10.4319/lo.2012.57.3.0809.

Rasheed, M., Badran, M. I., Richter, C., and Huettel, M. (2002). Effect of reef framework and bottom sediment on nutrient enrichment in a coral reef of the Gulf of Aqaba, Red Sea. *Mar. Ecol. Prog. Ser.* 239, 277–285. doi:10.3354/meps239277.

Raulf, F. F., Fabricius, K. E., Uthicke, S., de Beer, D., Abed, R. M. M., and Ramette, A. (2015). Changes in microbial communities in coastal sediments along natural CO_2 gradients at a volcanic vent in Papua New Guinea. *Environ. Microbiol.* 17, 3678–3691. doi:doi:10.1111/1462-2920.12729.

Revsbech, N. P. (1989). An oxygen microsensor with a guard cathode. *Limnol. Oceanogr.* 34, 474–478.

Rho, M., Tang, H., and Ye, Y. (2010). FragGeneScan: Predicting genes in short and error-prone reads. *Nucleic Acids Res.* 38, 1–12. doi:10.1093/nar/gkq747.

Roy, A.-S., Gibbons, S. M., Schunck, H., Owens, S., Caporaso, J. G., Sperling, M., et al. (2013). Ocean acidification shows negligible impacts on high-latitude bacterial community structure in coastal pelagic mesocosms. *Biogeosciences* 10, 555–566. doi:10.5194/bg-10-555-2013.

Rusch, A., and Gaidos, E. (2013). Nitrogen-cycling bacteria and archaea in the carbonate sediment of a coral reef. *Geobiology* 11, 472–84. doi:10.1111/gbi.12048.

Santillano, D., Boetius, A., and Ramette, A. (2010). Improved dsrA-based terminal restriction fragment length polymorphism analysis of sulfate-reducing bacteria. *Appl. Environ. Microbiol.* 76, 5308–11. doi:10.1128/AEM.03004-09.

Sass, L., Spetea, C., Mate, Z., Nagy, F., and Vass, I. (1997). Repair of UV-B induced damage of photosystem II via de novo synthesis of the D1 and D2 reaction subunits of Synechocystis sp. PCC 6803. *Photosynth. Res.* 54, 55–62.

Shannon, P., Markiel, A., Ozier, O., Baliga, N. S., Wang, J. T., Ramage, D., et al. (2003). Cytoscape: a software environment for integrated models of biomolecular interaction networks. *Genome Res.* 13, 2498–2504. doi:10.1101/gr.1239303.

Shi, Y., Tyson, G. W., Eppley, J. M., and DeLong, E. F. (2011). Integrated metatranscriptomic and metagenomic analyses of stratified microbial assemblages in the open ocean. *ISME J.* 5, 999–1013. doi:10.1038/ismej.2010.189.

Sievert, S. M., Brinkhoff, T., Muyzer, G., Ziebis, W., and Kuever, J. (1999). Spatial Heterogeneity of Bacterial Populations along an Environmental Gradient at a Shallow Submarine Hydrothermal Vent near Milos Island (Greece). *Appl. Environ. Microbiol.* 65, 3834–3842.

Sulzberger, B., and Durisch-Kaiser, E. (2009). Chemical characterization of dissolved organic matter (DOM): A prerequisite for understanding UV-induced changes of DOM absorption properties and bioavailability. *Aquat. Sci.* 71, 104–126. doi:10.1007/s00027-008-8082-5.

Tait, K., and Laverock, B. (2013). Minor impact of ocean acidification to the composition of the active microbial community in an Arctic sediment. *Environ. Microbiol. Rep.* doi:10.1111/1758-2229.12087.

Tait, K., Laverock, B., and Widdicombe, S. (2014). Response of an Arctic Sediment Nitrogen Cycling Community to Increased CO_2. *Estuaries and Coasts* 37, 724–735. doi:10.1007/s12237-013-9709-x.

Tyystjärvi, E. (2008). Photoinhibition of Photosystem II and photodamage of the oxygen evolving manganese cluster. *Coord. Chem. Rev.* 252, 361–376. doi:10.1016/j.ccr.2007.08.021.

Vizzini, S., Di Leonardo, R., Costa, V., Tramati, C. D., Luzzu, F., and Mazzola, A. (2013). Trace element bias in the use of CO_2-vents as analogues for low-pH environments: Implications for contamination levels in acidified oceans. *Estuar.*

Coast. Shelf Sci. 134, 19–30. doi:10.1016/j.ecss.2013.09.015.

Wängberg, S.-A., and Blanck, H. (1990). Arsenate sensitivity in marine periphyton communities established under various nutrient regimes. *J. Exp. Mar. Bio. Ecol.* 139, 119–134. doi:10.1016/0022-0981(90)90042-B.

Ward, B. B., Arp, D. J., and Klotz, M. G. (2011). *Nitrification*. Washington,DC: American Society for Microbiology (ASM).

Werner, U., Blazejak, A., Bird, P., Eickert, G., Schoon, R., Abed, R. M. M., et al. (2008). Microbial photosynthesis in coral reef sediments (Heron Reef, Australia). *Estuar. Coast. Shelf Sci.* 76, 876–888. doi:10.1016/j.ecss.2007.08.015.

Wright, S. W. (1991). Improved HPLC method for the analysis of chlorophylls and carotenoids from marine phytoplankton. *Mar. Ecol. Prog. Ser.* 77, 183–196. doi:10.3354/meps077183.

Xiang, Z., Courtot, M., Brinkman, R. R., Ruttenberg, A., and He, Y. (2010). OntoFox: web-based support for ontology reuse. *BMC Res. Notes* 3, 1–12. doi:10.1186/1756-0500-3-175.

Zark, M., Riebesell, U., and Dittmar, T. (2015). Effects of ocean acidification on marine dissolved organic matter are not detectable over the succession of phytoplankton blooms. *Sci. Adv.* 1, e1500531–e1500531. doi:10.1126/sciadv.1500531.

Zehr, J. P., Jenkins, B. D., Short, S. M., and Steward, G. F. (2003). Nitrogenase gene diversity and microbial community structure : a cross-system comparison. *Environ. Microbiol.* 5, 539–554. doi:10.1046/j.1462-2920.2003.00451.x.

Zhang, J., Kobert, K., Flouri, T., and Stamatakis, A. (2014). PEAR: A fast and accurate Illumina Paired-End reAd mergeR. *Bioinformatics* 30, 614–620. doi:10.1093/bioinformatics/btt593.

Zhang, R., Xia, X., Lau, S. C. K., Motegi, C., Weinbauer, M. G., and Jiao, N. (2012). Response of bacterioplankton community structure to an artificial gradient of pCO_2 in the Arctic Ocean. *Biogeosciences Discuss.* 9, 10645–10668. doi:10.5194/bgd-9-10645-2012.

Supporting information

SI text: Comparison between metagenomic, metatranscriptomic and amplicon sequencing approaches

Rarefaction analysis showed that more bacterial classes were detected in metatranscriptomic 16S than in amplicon sequences at the same sequencing depth (Figure S2B). The beginning of the metagenomic rarefaction curves indicated an equal or higher diversity than in metatranscriptomic 16S, suggesting that a primer bias may cause the reduced richness of the amplicon data set. However, a more comprehensive comparison between the richness of bacterial classes in metagenomic and metatranscriptomic 16S was difficult, because the sequencing depth of metagenomic 16S was insufficient to saturate rarefaction curves. Among eukaryotes and archaea, the comparison between the different sequencing approaches generally showed similar trends (Figure S2C-F), although the number of 16S/18S sequences in the metagenomic data set was often very low (Table S7), and no 18S amplicon data were available for a detailed comparison. Still, the composition of metagenomic and metatranscriptomic 18S was markedly different, especially in two samples with metagenomes dominated by metazoan rRNA genes that only contained low amounts of metazoan rRNA (Figure S2C), suggesting that the sediment samples probably contained dead metazoan material. DNA-based methods would not have been able to distinguish between dead and live material, which further highlights the importance of RNA-based approaches.

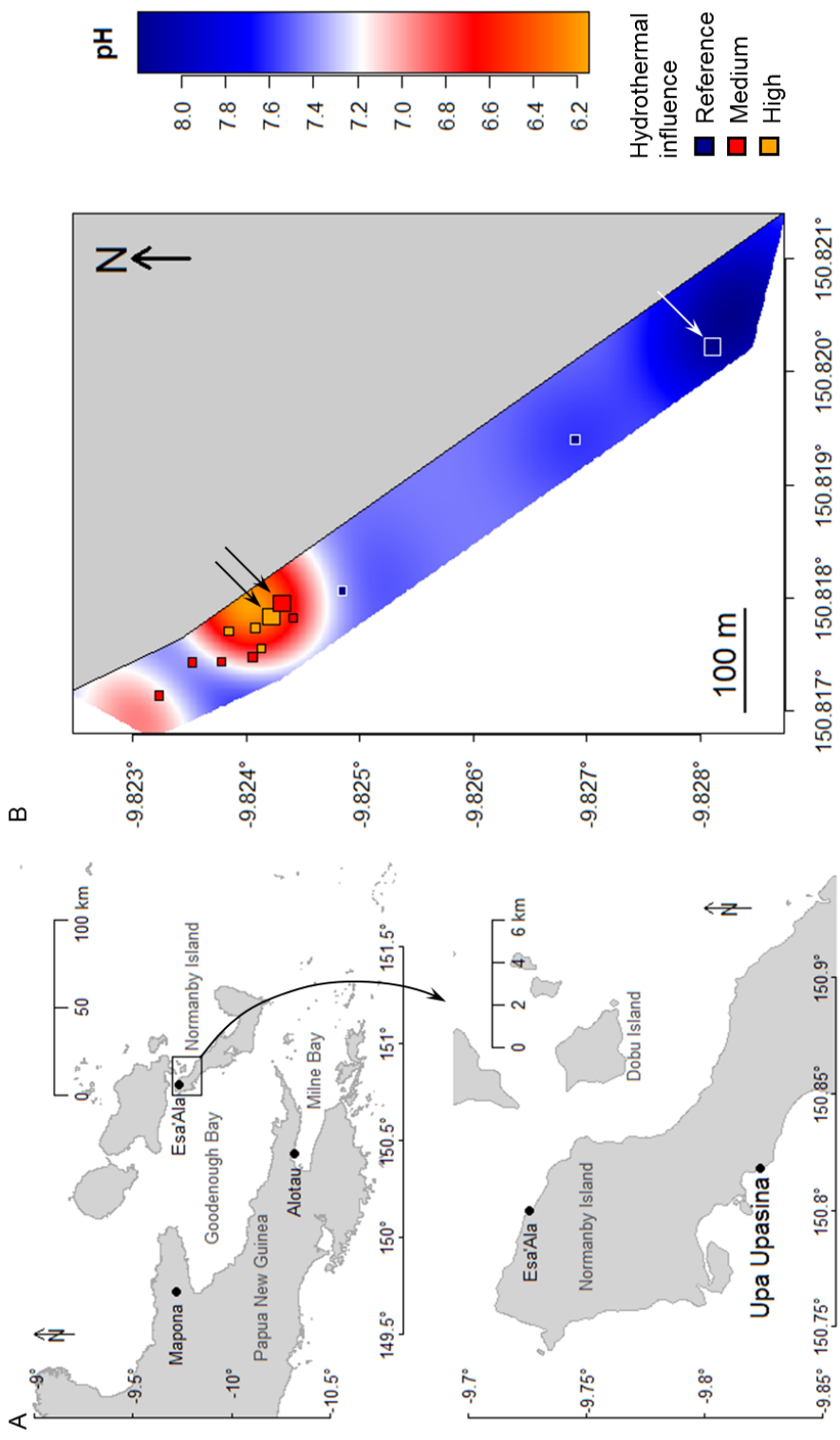

Figure S1A: Map of the sampling area in Papua New Guinea. B: Location of the sampling sites at Upa Upasina colored by hydrothermal influence category. Background colored by median pH in the upper 2 cm of the sediment. Larger symbols and arrows mark sampling sites with metatranscriptomic and metagenomic data available.

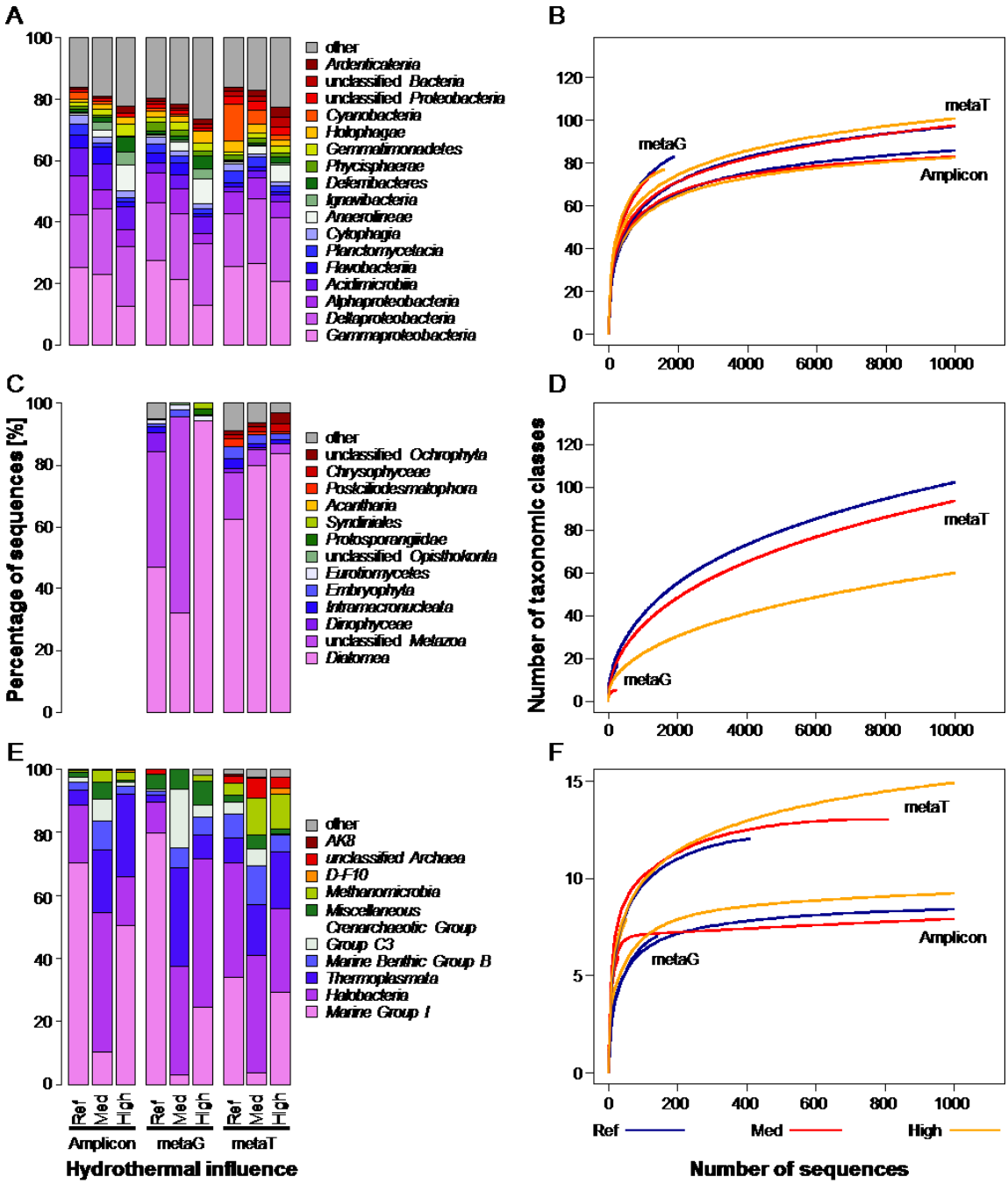

Figure S2: Taxonomic composition and diversity of metatranscriptomic (metaT), metagenomic (metaG) and amplicon sequencing libraries based on class-levels affilation of 16S and 18S sequences. Dominant classes among *Bacteria* (A), *Eukaryota* (C) and *Archaea* (E). Rarefaction analysis for *Bacteria* (B), *Eukaryota* (D) and *Archaea* (F).

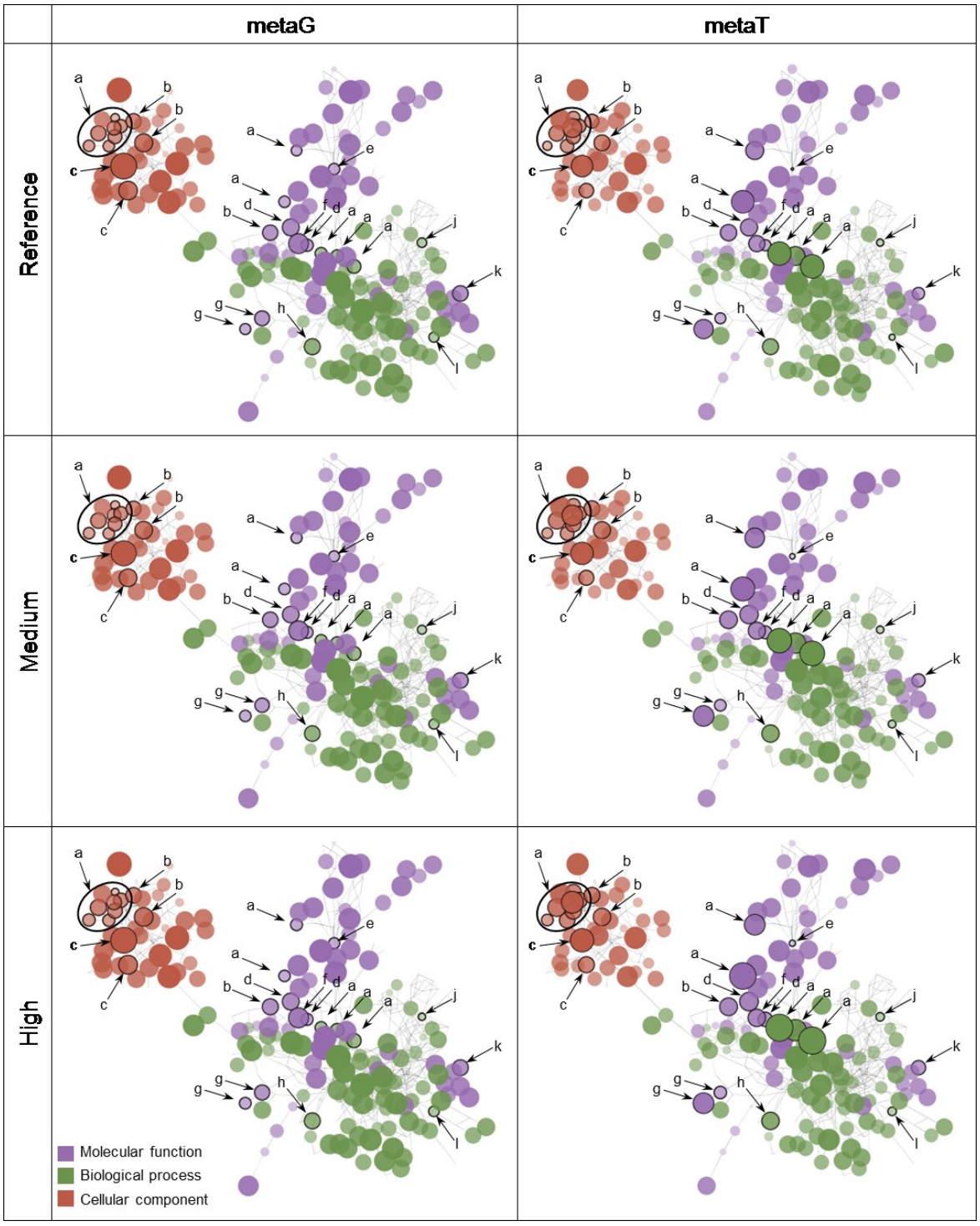

Figure S3: Gene ontology (GO) network of the dominant functions in the metagenomic (metaG) and metatranscriptomic (metaT) data sets from reference, medium and high hydrothermal influence (HI) sites. Nodes: GO terms, edges: connections between GO terms. Node size, transparency and z-location indicate abundance of GO terms. Node color indicates GO namespace. Arrows indicate GO terms associated with transcripts which at least doubled between reference and vent samples. a: photosynthesis-related, b: proton transport coupled to energy generation, c: membrane-related including thylakoid membrane, d: oxidoreductase related to proton transport, e: binding, f: transporter, g: carboxylase such as ribulose-bisphosphate carboxylase/oxygenase, h: aerobic respiration, j: nucleotide metabolism, k: phosphotransferase, l: carbohydrate metabolism.

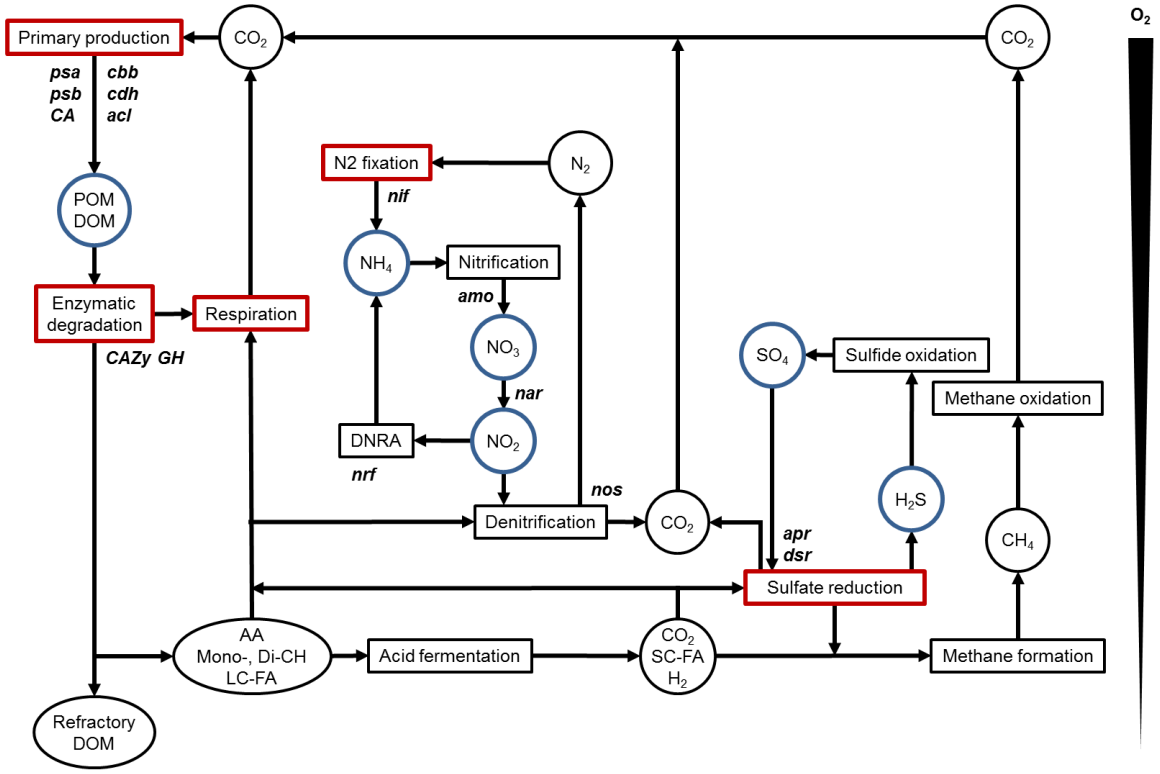

Figure S4: Microbial processes involved in carbon, nitrogen and sulfur cycling in marine sediments (modified after Fenchel and Jorgensen, 1977). Red frame: data available on metabolic rates, blue circle: concentration measurements, in italics: marker genes for microbial functions. AA: amino acids, CH: carbohydrates, LC-FA: long chain fatty acids, SC-FA: short chain fatty acids, DNRA: dissimilatory nitrate reduction to ammonium. Photosynthesis: photosystem I (*psa*), photosystem II (*psb*), carbonic anhydrase (*CA*). Carbon fixation: ribulose-bisphosphate carboxylase/oxygenase (*cbb*), bifunctional carbon monoxide dehydrogenase/acetyl-CoA synthase (*cdh*), ATP-dependent citrate lyase (*acl*). Hydrolytic carbon degradation: carbohydrate active enzymes - glycoside hydrolase families (*CAZy GH*). Sulfate reduction: adenylylsulfate reductase (*apr*), dissimilatory sulfite reductase (*dsr*). Nitrogen cycling: nitrogenase (*nif*), ammonia monooxygenase (*amo*), nitrate reductase (*nar*), ammonifying nitrite reductase (*nrf*), nitrous oxide reductase (*nos*).

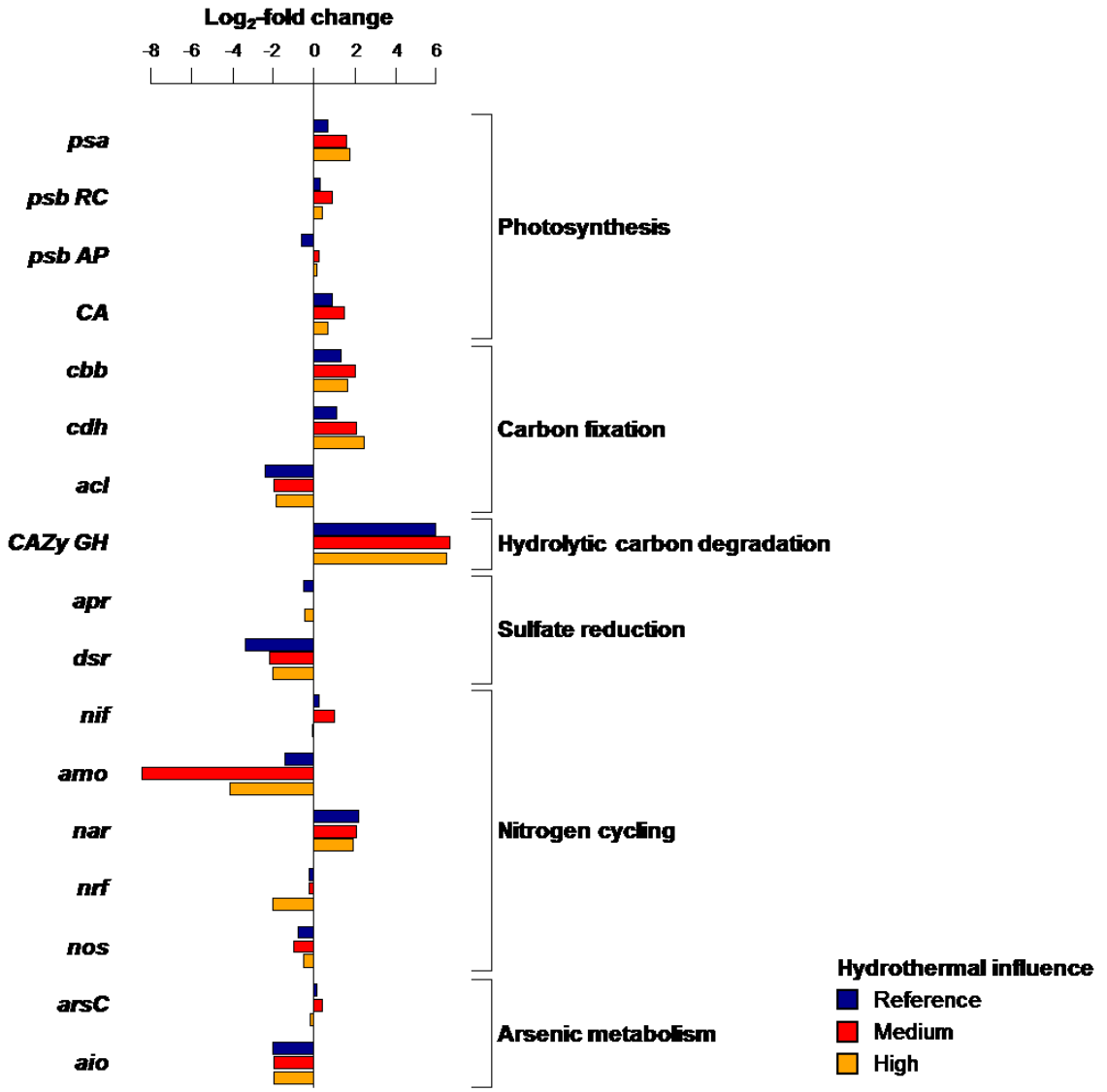

Figure S5: Relative abundance of functional marker genes in metagenomes of samples from reference, medium and high hydrothermal influence (HI) sites. Sequence abundance displayed as log2-fold change relative to the geometric mean (zero value) of all genes per sample (centered log-ratio transformation). Photosynthesis: photosystem I reaction center (*psa*), photosystem II reaction center (*psb RC*) and antenna proteins (*psb AP*), carbonic anhydrase (*CA*). Carbon fixation: ribulose-bisphosphate carboxylase/oxygenase (*cbb*), bifunctional carbon monoxide dehydrogenase/acetyl-CoA synthase (*cdh*), ATP-dependent citrate lyase (*acl*). Hydrolytic carbon degradation: carbohydrate active enzymes - glycoside hydrolase families (*CAZy GH*). Sulfate reduction: adenylylsulfate reductase (*apr*), dissimilatory sulfite reductase (*dsr*). Nitrogen cycling: nitrogenase (*nif*), ammonia monooxygenase (*amo*), nitrate reductase (*nar*), ammonifying nitrite reductase (*nrf*), nitrous oxide reductase (*nos*). Arsenic metabolism: arsenate reductase (*ars*), arsenite oxidase (*aio*).

Table S1: Overview of the data available from the sampling sites at the CO_2 vent at Upa Upasina, Normanby Island, Papua New Guinea. HI: hydrothermal influence.

	Method	N sites	N replicates	Sampling time	Reference
Physico-chemical characterization					
Sediment profiles (oxygen, pH, temperature, H_2S, redox)	*In situ* microprofiles	2 reference 4 medium HI 2 high HI	2 – 3	2013	Fink et. al (submitted)
Total organic and inorganic carbon, total nitrogen	CN elemental analyzer	2 reference 4 medium HI 2 high HI	2 – 4	2013	Fink et. al (submitted)
Nutrient fluxes	Chamber incubations	1 reference 1 medium HI 2 high HI	3	2013	Artur Fink, personal communication
Pore water geochemistry (major and trace element concentrations)	Optical Emission Spectroscopy	1 medium HI 2 high HI	2	2013	Lichtschlag et al. (in preparation)
Light conditions		1 reference 1 high HI	1	2013	Laurie Hofmann, personal communication
Pigment concentrations	Reverse-phase HPLC	1 reference 4 medium HI 2 high HI	2 – 3	2013, 2014[a]	This study
Molecular data[b]					
Total and active bacterial community profiles	16S rRNA and 16S rRNA gene TRFLP	1 reference 1 medium HI 1 high HI	3	2013	This study
Total sulfate reducing community profiles	*dsrA* TRFLP	1 reference 1 medium HI 1 high HI	3	2013	This study
Total bacterial and archaeal communities	16S rRNA gene amplicons sequencing	3 reference 6 medium HI 4 high HI	1	2013	Hassenrück et al. (2016)

	Method	N sites	N replicates	Sampling time	Reference
Total microbial community and genetic functional potential	Metagenomic sequencing	1 reference 1 medium HI 1 high HI	1	2013	This study
Active microbial community and expressed functional genes	Metatranscriptomic sequencing	1 reference 1 medium HI 1 high HI	1	2013	This study
Metabolic rates					
Photosynthesis	*Ex situ* O_2 microsensor profiles	1 reference 2 medium HI 2 high HI	3	2014	This study
Carbon fixation rates	^{13}C tracer incubations	1 reference 2 medium HI 2 high HI	3	2014	pending
Oxygen consumption rates	*Ex situ* planar oxygen optodes	1 reference 4 medium HI 1 high HI	3	2013	Fink et al. (submitted)
Potential extracellular enzymatic activity	Fluorometric, using artificial substrates	2 reference 2 medium HI 2 high HI	1 – 2	2014	This study
Sulfate reduction rates	^{35}S tracer incubations	1 reference 4 medium HI 2 high HI	2 – 3	2013	Fink et al. (submitted)
Nitrogen fixation rates	^{15}N tracer incubations	1 reference 2 medium HI 2 high HI	3	2014	pending

[a] For 2014 only two medium HI sites were sampled.
[b] DNA and RNA- based analyses were performed on the same sediment cores.

Table S2: Ingredients and reaction conditions for the DNase digest and the reverse transcription of RNA samples.

DNase digest		**Amount**	**Final concentration**
Reagents			
	Dnase I recombinant (Roche, Basel, Switzerland)	10 µL	1.45 units µL $^{-1}$
	Dnase incubation buffer (Roche, Basel, Switzerland)	7 µL	1×
	RNasin Plus RNase Inhibitor (Promega, WI, USA)	2 µL	1.16 units µL $^{-1}$
	RNA template	50 µL	
Incubation conditions			
	20 min at 37°C		
	10 min at 56°C		
Reverse transcription		**Amount**	**Final concentration**
Reagents			
	Random Primers (Promega, WI, USA)	1 µL	20 ng µL $^{-1}$
	M-MLV Reverse Transcriptase RNase H minus (Promega, WI, USA)	2 µL	16 units µL $^{-1}$
	Reverse transcriptase incubation buffer (Promega, WI, USA)	5 µL	1×
	dNTPs (PeqLab Biotechnology GmbH, Erlangen, Germany)	1.25 µL	each 0.5 nmol µL $^{-1}$
	RNasin Plus RNase Inhibitor (Promega, WI, USA)	1 µL	1.6 units µL $^{-1}$
	RNA template	15 µL	
Incubation conditions			
	Annealing (addition of random primers to RNA template):		
	10 min 70°C		
	15 min 4°C		
	Reverse transcription (addition of remaining reagents):		
	10 min 20°C		
	60 min 45°C		

Table S3: Ingredients and reaction conditions for the PCRs of the 16S and *dsrA* TRFLP.

16S	**Reagents**		**Amount**	**Final concentration**
		H_2O	24.525 µL	
		Reaction buffer S (PeqLab Biotechnology GmbH, Erlangen, Germany)	3.5 µL	1×
		Bovine serum albumin	1.05 µL	0.13 g L^{-1}
		dNTPs (PeqLab Biotechnology GmbH, Erlangen, Germany)	0.875 µL	each 0.25 mmol L^{-1}
		27F (5'-AGAGTTTGATCMTGGCTCAG-3')	0.35 µL	0.5 µmol L^{-1}
		907R (5'-CCGTCAATTCCTTTRAGTTT-3')	0.35 µL	0.5 µmol L^{-1}
		Taq polymerase (PeqLab Biotechnology GmbH, Erlangen, Germany)	0.35 µL	0.05 units μL^{-1}
		DNA template	4 µL	
	PCR conditions			
		5 min 94°C		
		(1 min 94°C, 1 min 60°C, 1 min 72°C) × 30		
		10 min 72°C		
dsrA	**Reagents**		**Amount**	**Final concentration**
		H_2O	25.575 µL	
		Reaction buffer S (PeqLab Biotechnology GmbH, Erlangen, Germany)	3.5 µL	1×
		dNTPs (PeqLab Biotechnology GmbH, Erlangen, Germany)	0.875 µL	each 0.25 mmol L^{-1}
		DSR1Fmix (see Santillano et al. 2010)	0.35 µL	each 0.5 µmol L^{-1}
		DSR1R (5'-TYT TCC ATC CAC CAR TCC-3')	0.35 µL	0.5 µmol L^{-1}
		Taq polymerase (PeqLab Biotechnology GmbH, Erlangen, Germany)	0.35 µL	0.05 units μL^{-1}
		DNA template	4 µL	
	PCR conditions			
		3 min 94°C		
		(40 sec 94°C, 40 sec 54°C, 2 min 72°C) × 30		
		8 min 72°C		

Table S4: Ingredients and reaction conditions for the restriction digest of the 16S and *dsrA* TRFLP.

AluI	**Reagents**	**Final concentration (20 µL)**
	H_2O	
	Restriction buffer (New England BioLabs GmbH, Frankfurt am Main, Germany)	1×
	AluI (New England BioLabs GmbH, Frankfurt am Main, Germany)	0.5 units μL^{-1}
	DNA template	150 ng
	Incubation conditions	
	4 h 37°C	
	20 min 80°C	

Table S5: InterPro annotation of marker genes. Accession numbers in parentheses represent unspecific InterPro entries with hits to more than the gene of interest. All InterPro hits to marker genes were further curated using blastp against the NCBI nr database.

Gene name	Process	Abbreviation	Interpro annotation
Photosystem I reaction center	Photosynthesis	*psa*	IPR001280 (IPR000484)
Photosystem II reaction center	Photosynthesis	*psb RC*	IPR000484 (IPR001280)
Photosystem II antenna proteins	Photosynthesis	*psb AP*	IPR000932
Carbonic anhydrase	Carbon concentration	*CA*	IPR018338, IPR001148, IPR001765, IPR015892
Ribulose bisphosphate carboxylase/oxygenase	Carbon fixation (Calvin cycle)	*cbb*	IPR000685, IPR020878, IPR017443, IPR024681, IPR000894, IPR024680
Bifunctional carbon monoxide dehydrogenase/acetyl-CoA synthase	Carbon fixation (rAcetyl-CoA pathway)	*cdh*	IPR004461, IPR016041 (IPR016101)
ATP-dependent citrate lyase	Carbon fixation (rTCA cycle)	*acl*	(IPR016142, IPR016143, IPR002020, IPR005811, IPR016102)
Carbohydrate active enzymes, glycoside hydrolase families	Carbohydrate degradation	*CAZy GH*	IPR000111, IPR000125, IPR000322, IPR000334, IPR000400, IPR000490, IPR000514, IPR000556, IPR000602, IPR000726, IPR000743, IPR000757, IPR000805, IPR000852, IPR000933, IPR001000, IPR001088, IPR001137, IPR001139, IPR001223, IPR001286, IPR001360, IPR001382, IPR001524, IPR001547, IPR001554, IPR001579, IPR001661, IPR001701, IPR001722, IPR001764, IPR002037, IPR002053, IPR002196, IPR002241, IPR002252, IPR002594, IPR002772, IPR003385, IPR003469, IPR004185, IPR004193, IPR004197, IPR004300, IPR005154, IPR005192, IPR005194, IPR005195, IPR005196, IPR005197, IPR005198, IPR005199, IPR005201, IPR006047, IPR006101, IPR006102, IPR006103, IPR006104, IPR006710, IPR008270, IPR010383, IPR010905, IPR011099, IPR011100, IPR011613, IPR011682, IPR011683, IPR012878, IPR012939, IPR013148, IPR013189, IPR013190, IPR013191, IPR013319, IPR013529, IPR013780, IPR013781, IPR013812, IPR014718, IPR015341,

Gene name	Process	Abbreviation	Interpro annotation
			IPR015883, IPR018053, IPR018087, IPR018120, IPR018208, IPR018221, IPR018232, IPR018238, IPR019800, IPR019801, IPR019834, IPR022616, IPR022790, IPR023099, IPR023226, IPR023230, IPR023232, IPR023296, IPR024745, IPR024746, IPR025092, IPR025887, IPR027291, IPR030458
Adenylylsulfate reductase	Sulfate reduction	*apr*	IPR011802, IPR022738 (IPR004511)
Dissimilatory sulfite reductase	Sulfate reduction	*dsr*	IPR014793
Nitrogenase	Nitrogen fixation	*nif*	IPR000510, IPR000318, IPR024564 (IPR000392, IPR030655)
Ammonia monooxygenase	Nitrification	*amo*	IPR003393, IPR024656
Nitrate reductase (respiratory)	Nitrate reduction	*nar*	IPR028189, IPR029263 (IPR006656, IPR006657, IPR006963, IPR006655, IPR027467)
Ammonifying nitrite reductase	Dissimilatory nitrate reduction to ammonium	*nrf*	IPR003321, IPR017571
Nitrous oxide reductase	Denitrification to N_2	*nos*	(IPR002429, IPR008972)
Arsenate reductase	Arsenic detoxification	*arsC*	IPR006659, IPR014064, IPR006660 (IPR006656, IPR006657)
Arsenite oxidase	Arsenite oxidation (energy metabolism)	*aio*	IPR014067 (IPR006656, IPR006657, IPR006963)

Table S6: Bioinformatic programs and parameter settings for the analysis of metagenomic and metatranscriptomic sequences.

Step	Program	Parameter settings
Removal of sequencing controls (phiX)	*bbduk* v34.00	k=31
Removal of sequencing adapters (TruSeq)	*bbduk* v34.00	k=27 ktrim=r (repeat with ktrim=l) mink=12
Removal of low quality bases	*trimmomatic* v0.32	HEADCROP:5 SLIDINGWINDOW:4:15 MINLEN:100
Merging of paired end reads	*PEAR* v0.9.5	-v 10
rRNA filtering	*sortmerna* v2.0	--best 1
16S classification	*SINA* v1.2.10	--outtype fasta --search --meta-fmt csv --overhang remove --insertion forbid --filter none --fs-kmer-no-fast --fs-kmer-len 10 --fs-req 2 --fs-req-full 1 --fs-min 40 --fs-max 40 --fs-weight 1 --fs-full-len 1400 --fs-msc 0.7 --match-score 1 --mismatch-score -1 --pen-gap 5 --pen-gapext 2 --search-cover query --search-iupac optimistic --search-min-sim 0.9 --turn all --lca-quorum 0.7 --lca-fields tax_slv
Coding sequence prediction	*fraggenescan* v1.19	-complete=0 -train=illumina_10
Gene annotation	*interproscan* v5.13-52.0	-appl PRINTS Gene3D Pfam TIGRFAM ProSitePatterns --goterms -dp --pathways
Curation of gene annotation	*blastp*+ v2.2.30	-evalue 1e-5 -max_target_seqs 10

Table S7: Metagenomic (metaG) and metatranscriptomic (metaT) sequence libraries generated from the sediment samples at reference, medium and high hydrothermal influence (HI) sites.

	metaG (PE)			**metaT (SE)**		
	Reference	Medium HI	High HI	Reference	Medium HI	High HI
Raw reads	6,576,971	4,102,526	4,551,438	41,416,222	41,590,474	38,137,516
Good quality[a]	7,031,584	4,476,036	4,755,483	38,234,030	39,075,387	36,589,145
non-rRNA reads	6,992,753	4,454,163	4,739,321	1,194,507	1,242,684	1,228,778
pCDS[b]	7,934,624	4,909,540	5,321,400	1,025,252	1,075,358	1,060,667
annotated	3,377,780	2,009,575	2,238,310	188,546	210,361	308,894
rRNA reads[c]	38,831	21,873	16,162	369,155	377,752	353,919
16S[d]	2,350	1,636	1,788	124,745	132,362	117,531
Bacteria	1,945	1,372	1,682	99,933	102,476	79,212
Eukaryotes	262	232	53	24,402	29,070	37,269
Archaea	143	32	53	410	816	1,050

[a] Metagenomic sequences include merged reads and single reads, which either could not be merged or were not paired anymore after quality trimming.
[b] If more than one coding sequence was predicted per input sequence, the sequence was split, which resulted in a higher number of pCDS reads than good quality reads.
[c] Input for the taxonomic classification with SINA. Metatranscriptomic rRNA reads were subsampled to 1% of the total number of rRNA reads.
[d] Sequences classified as 16S reads with SINA, excluding mitochondrial and chloroplast sequences.

Table S8: Absolute sequence counts of functional marker genes in metagenomic (metaG) and metatranscriptomic (metaT) data sets.

Gene name	**Abbreviation**	**metaG**			**metaT**		
		Reference	Medium HI	High HI	Reference	Medium HI	High HI
Photosystem I reaction center	*psa*	613	522	813	2,994	3,301	2,566
Photosystem II reaction center	*psb RC*	473	322	313	20,234	39,379	136,459
Photosystem II antenna proteins	*psb AP*	253	211	267	702	1,464	2,205
Carbonic anhydrase	*CA*	721	489	392	37	44	29
Ribulose bisphosphate carboxylase/oxygenase	*cbb*	974	727	774	7,915	14,412	13,034
Bifunctional carbon monoxide dehydrogenase/acetyl-CoA synthase	*cdh*	811	746	1,316	493	543	276
ATP-dependent citrate lyase	*acl*	73	46	67	8	8	11
Carbohydrate active enzymes, glycoside hydrolase families	*CAZy GH*	23,718	17,860	20,983	621	636	624
Adenylylsulfate reductase	*apr*	273	172	181	396	305	70
Dissimilatory sulfite reductase	*dsr*	37	38	58	43	35	11
Nitrogenase	*nif*	465	359	223	42	101	8
Ammonia monooxygenase	*amo*	141	0	13	4	3	70
Nitrate reductase (respiratory)	*nar*	1801	745	907	132	54	61
Ammonifying nitrite reductase	*nrf*	315	145	59	15	4	4
Nitrous oxide reductase	*nos*	232	88	170	48	24	72
Arsenate reductase	*arsC*	438	227	207	8	16	13
Arsenite oxidase	*aio*	94	46	61	4	4	25

Chapter 4

Seagrass biofilm communities at a naturally CO_2-rich vent

Christiane Hassenrück[1], Laurie C. Hofmann[2], Kai Bischof[2], Alban Ramette[1]

[1] Max Planck Institute for Marine Microbiology, Celsiusstraße 1, 28359 Bremen, Germany

[2] University of Bremen, Leobener Str. NW2, 28359 Bremen, Germany

Environmental Microbiology Reports 7: 516–525.

Summary: Seagrass meadows are a crucial component of tropical marine reef ecosystems. Seagrass plants are colonized by a multitude of epiphytic organisms that contribute to broadening the ecological role of seagrasses. To better understand how environmental changes like ocean acidification might affect epiphytic assemblages, the microbial community composition of the epiphytic biofilm of *Enhalus acroides* was investigated at a natural CO_2 vent in Papua New Guinea using molecular fingerprinting and next generation sequencing of 16S and 18S rRNA genes. Both bacterial and eukaryotic epiphytes formed distinct communities at the CO_2-impacted site compared with the control site. This site-related CO_2 effect was also visible in the succession pattern of microbial epiphytes. We further found an increased relative sequence abundance of bacterial types associated with coral diseases at the CO_2-impacted site (Fusobacteria, *Thalassomonas*), whereas eukaryotes, such as certain crustose coralline algae, commonly related to healthy reefs were less diverse. These trends in the epiphytic community of *E. acroides* suggest a potential role of seagrasses as vectors of coral pathogens and may support previous predictions of a decrease in reef health and prevalence of diseases under future ocean acidification scenarios.

Keywords: ocean acidification, natural CO_2 vents, seagrass, epiphytes, microbial community composition, coral reef ecology

Introduction

Tropical marine reef ecosystems are hotspots of biodiversity and productivity in an otherwise desert-like marine system. Apart from corals, seagrass meadows are a crucial component of these reef ecosystems. As fish nurseries, nutrient cyclers, organic carbon producers and sediment stabilizers, seagrass meadows contribute substantially to ecosystem functioning (Orth et al., 2006). Similar to corals (Mouchka et al., 2010), seagrasses are colonized by microorganisms that form epiphytic biofilms on the seagrass leaves (Michael et al., 2008). These biofilms have been shown to affect seagrass physiology as well as their interactions with other reef organisms by e.g. regulating light availability (Sand-Jensen, 1977), influencing the settlement of secondary epibionts and biofouling (Wahl, 1989) or the production of antimicrobial substances (Marhaeni et al., 2011). As such, a seagrass plant and its epiphytic biofilm can be referred to as a seagrass holobiont.

Ocean acidification (OA), defined as a decrease in ocean water pH caused by increased atmospheric CO_2 concentrations, is among the most worrisome threats to coral reef ecosystems (Hoegh-Guldberg et al., 2007). The impacts of OA on corals range from a decrease of skeletal integrity (Hoegh-Guldberg et al., 2007) to changes in the composition of the microbial biofilm associated with the coral, reducing larval settlement and probably coral health (Meron et al., 2011; Webster et al., 2013). Seagrasses, on the other hand, are generally thought to benefit from OA because of the increased availability of CO_2 and bicarbonate for photosynthesis (Koch et al., 2013; Brodie et al., 2014). However, data on how the epiphytic biofilm on seagrass leaves might respond to OA and on the behavior of the seagrass holobiont in future OA scenarios are still sparse.

Several studies have investigated the epiphytic community on seagrass leaves giving detailed information on the composition of bacterial or eukaryotic epiphytes (Uku et al., 2007; Medina-Pons et al., 2009; Hamisi et al., 2013). The effect of OA on epiphytic communities on seagrass leaves is far less well documented. Previous studies reported a decrease of calcifying epiphytes such as crustose coralline algae (Martin et al., 2008; Donnarumma et al., 2014) as already seen elsewhere in coral reefs (Fabricius et al., 2011). Donnarumma and colleagues (2014) also highlighted a decrease in epiphyte diversity with decreasing pH. However, both studies only visually identified epiphytes by

using light microscopy and did not address the multitude of cryptic epiphytes detectable only with the increased sensitivity and taxonomic resolution provided by molecular tools. Our study aims (i) to provide a first overview of both bacterial and eukaryotic epiphytes at a molecular level and (ii) to estimate how the epiphytic community on seagrass leaves may change in response to OA. This may help to increase our understanding of the part the seagrass holobiont may play in the reef ecosystem under future OA scenarios.

Recent research has turned to naturally CO_2-rich systems as models for future OA scenarios (Hall-Spencer et al., 2008; Fabricius et al., 2011; Lidbury et al., 2012; Kerfahi et al., 2014). Unlike laboratory experiments, which are usually restricted to short-term studies, natural sites offer the opportunity to predict OA effects in long-term adapted systems that can be studied in their entirety without the need for experimental manipulation (Hall-Spencer et al., 2008). However, the inherent complexity of natural systems can also confound OA effects, and caution is needed in selecting natural CO_2-rich sites for OA research (Vizzini et al., 2013).

Here, the epiphytic biofilm on the leaves of the seagrass *Enhalus acroides* was investigated at a natural CO_2 vent and a control site in Papua New Guinea (PNG; Fig. S1). The sites were previously described as potential sites to study long-term effects of OA on coral reef communities because the prevailing environmental conditions are assumed to have been stable for up to 100 years (Fabricius et al., 2011). The diversity and composition of both bacterial and eukaryotic microbial epiphytic communities were assessed using molecular community fingerprinting and next generation sequencing of amplicon libraries. Besides the site-related CO_2 impact, the factor leaf age was included in the analysis to account for different developmental stages of the epiphytic biofilm as well as potential interactions of biofilm development with OA effects. To further characterize the seagrass leaves and their epiphytes, additional data were collected on total epiphyte cover, and carbon and nitrogen content of the seagrass leaves.

Results and Discussion

Logger deployments over approximately 44 h at the vent site at Dobu Island (Fig. S1) recorded median pH values of 7.8 in the water column (K. Fabricius, pers. comm.). At the control site, pH values of 8.3 were measured. These values were consistent with previous data on the carbonate system at Dobu Island (Fabricius et al., 2011). Apart from the carbonate system, the physicochemical characteristics of the water at the two sampling sites were very similar, suggesting that changes in the carbonate system between the vent and the control site were not confounded by any other of the observed parameters (Fabricius et al., 2011).

18S ribosomal DNA sequences confirmed that the seagrass shoots belonged to one species and did not show any pattern by sampling site (data not shown). Each shoot consisted of three to five leaf pairs that were ranked by their order of budding, i.e. leaf age, with the youngest leaf pair being assigned the first rank. When possible, we sampled ranks one to four (youngest to oldest). On average, *E. acroides* is expected to produce a new pair of leaves approximately every month (Johnstone, 1979; Brouns and Heijs, 1986; Agawin et al., 2001). The time covered in this study would then amount to 4–5 months of settlement, although it is possible that growth rates were higher under low pH conditions (Koch et al., 2013). During that time, carbon (C) content of the seagrass leaves decreased with leaf age from approximately 33% to 26% dry weight (analysis of variance (ANOVA), $F_{1,38} = 25.986$, $p < 0.001$) and nitrogen (N) content from 2% to almost 1% (Kruskal-Wallis, $\chi 2 = 21.262$, df = 3, $p < 0.001$; Table 1). Carbon and nitrogen measurements matched previous measurements of leaves of *E. acroides* (Yamamuro et al., 2004) and were not affected by sampling site, suggesting that the substrate type, i.e. the seagrass leaf, was not confounded between sampling sites.

Epiphyte cover increased with leaf age (Table 1). At the vent site, this increase reached only about threefold lower values than under control conditions, most likely due to a lower abundance of pH-sensitive organisms such as crustose coralline algae (Corlett and Jones, 2007; Martin et al., 2008; Fabricius et al., 2015). However, regardless of the trend in epiphyte cover, at the high taxonomic resolution provided by 16S and 18S amplicon sequencing, epiphyte communities seemed to be as diverse at the vent site than at the control site (Table 1).

Table 1: Carbon (C) and nitrogen (N) content in percentage dry weight, C:N ratio and epiphyte cover of the leaves of *E. acroides*, the number of bacterial and eukaryotic OTUs obtained through ARISA and amplicon sequencing (Bacteria: 16S rRNA gene, Eukaryota: 18S rRNA gene); values constitute mean +/- standard error where applicable; for the bacterial sequencing dataset Chao1 richness estimates are given in italics with lower confidence interval/upper confidence interval in brackets.

					ARISA		Amplicon sequencing	
	N [%]	C [%]	C:N ratio	Epiphyte cover [%]	Bacteria	Eukaryota	Bacteria (16S)	Eukaryota (18S)
Control								
All ages	1.42 ± 0.08	28.87 ± 0.8	20.98 ± 0.71	18.08 ± 2.45	96.52 ± 3.27	86.14 ± 2.56	507.5 ± 31.45 *917.31 ± 49.13*	520.75 ± 84.25
Youngest	1.98 ± 0.18	34.63 ± 2.21	17.89 ± 2.5	3.25 ± 3.25	111.25 ± 6.02	72.5 ± 3.8	585 *913.76 (822.52/1040.05)*	277
2nd youngest	1.54 ± 0.1	29.68 ± 0.73	19.56 ± 0.88	14.3 ± 5.5	96.83 ± 7.49	86.67 ± 4.97	532 *991.53(863.52/1168.96)*	664
3rd youngest	1.2 ± 0.04	28.07 ± 0.8	23.47 ± 0.42	22.33 ± 2.72	94.83 ± 2.4	93.17 ± 3.36	462 *984.34 (827.90/1207.66)*	561
Oldest	1.19 ± 0.04	25.83 ± 0.89	21.87 ± 1.31	22.54 ± 3.56	86.4 ± 6.31	88 ± 4.69	451 *779.63 (680.69 /921.19)*	581
Vent								
All ages	1.41 ± 0.12	26.93 ± 1.8	19.96 ± 0.79	6.61 ± 1.6	135.95 ± 2.82	89.68 ± 2.71	619.67 ± 48.22 *1044.09 ± 187.94*	517.75 ± 23.24
Youngest	2.05 ± 0.05	32.02 ± 0.42	15.68 ± 0.42	2.5 ± 1.5	139.6 ± 7.64	97.4 ± 7.06	594 *933.61 (839.61/1063.58)*	459
2nd youngest	1.25 ± 0.21	24.87 ± 3.83	20.15 ± 0.74	8.7 ± 2.2	133.5 ± 5.94	87.33 ± 4.36	NA	553
3rd youngest	1.07 ± 0.18	24.26 ± 3.91	22.65 ± 1.3	8.55 ± 3.84	133.83 ± 2.7	84.33 ± 3.19	552 *788.18 (718.60 /886.80)*	502
Oldest	1.29 ± 0.04	28.36 ± 0.1	22.04 ± 0.76	3.75 ± 0.75	140.5 ± 7.5	93.5 ± 7.5	713 *1410.49 (1240.43/1635.38)*	557
Total	1.41 ± 0.07	27.92 ± 0.97	20.48 ± 0.53	12.81 ± 1.77	408	329	2179 *3811.43 ± 142.83*	3928

Molecular Fingerprinting using Automated Ribosomal Intergenic Spacer Analysis (ARISA)

As a first step to assessing the composition of the epiphytic biofilm of *E. acroides*, the epiphytic community was screened using the molecular fingerprinting technique ARISA (Ramette, 2009; Wolf et al., 2013). ARISA identified 408 bacterial and 321 eukaryotic operational taxonomic units (OTUs). Non-metric multidimensional scaling ordination plots based on Bray-Curtis dissimilarity coefficients revealed three prominent patterns in the bacterial and eukaryotic community structure (Fig. 1).

First, there was a strong separation of the communities sampled at the vent and the control site, which tended to cluster away from each other (bacteria: analysis of similarity (ANOSIM), $R = 0.775$, $p < 0.05$; eukaryotes: $R = 0.692$, $p < 0.05$; Table S1). Only about 30% of the bacterial and eukaryotic OTUs were shared between any two samples from the vent and the control site. Redundancy analysis further confirmed that both sampling site and leaf age significantly explained part of the variation in the microbial community structure (Table S2). Of the observed parameters, sampling site was the dominant factor responsible for the patterns in epiphytic community structure (bacteria: adjusted $R^2 = 27.3\%$; eukaryotes: adjusted $R^2 = 12.4\%$), with about four times more variation being explained by sampling site than leaf age (Table S2). This pronounced shift in the epiphytic community structure on seagrass leaves between vent and control site further supports previous results, which found a response of bacterial as well as eukaryotic microbes to OA in other habitats (Johnson et al., 2011; Lidbury et al., 2012; Kerfahi et al., 2014).

Second, at each site, there appeared to be a successive shift in epiphyte communities from the youngest to older leaves (Table S1). Despite the differences in epiphytic community composition between the vent and the control site, a successional pattern in community composition from younger to older leaves was observed at both sites regardless of CO_2 impact (Fig. 1). Because organic matter has been shown to be transferred from the seagrass leaves to the epiphytes (Michael et al., 2008), changes in carbon and nitrogen content with leaf age, as documented here, may contribute to the influence of leaf age in shaping epiphyte communities.

Third, apart from the general response to the factors sampling site and leave age, patterns in community structure between samples, i.e. the pairwise similarity between samples, correlated strongly between the bacterial and eukaryotic data sets (Mantel test, $r = 0.64$, $p < 0.05$). The strong correlation seemed unlikely to be caused exclusively by changes in abiotic parameters. A more likely explanation may be that both communities influence and shape each other as previously suggested by Steele and colleagues (2011) and Sawall and colleagues (2012).

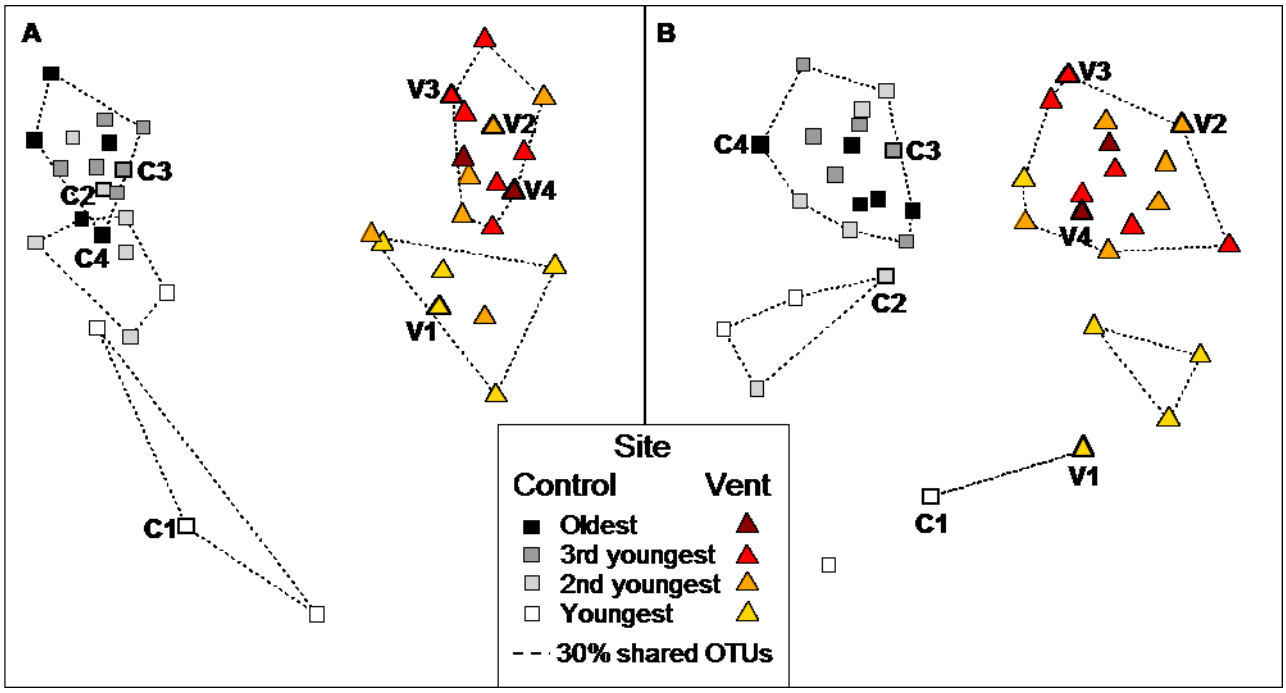

Figure 1: Non-metric multidimensional scaling (NDMS) plot based on the Bray-Curtis dissimilarity matrix for bacteria (A) and on the Jaccard dissimilarity matrix for eukaryotes (B) on leaves of *E. acroides*; both bacterial and eukaryotic communities were assessed using ARISA; dashed hulls representing a minimum of 30% shared OTUs between samples within the hull; labeled points: samples selected for 16S/18S amplicon sequencing.

Amplicon sequencing of epiphytic communities

To taxonomically classify the epiphytic communities on *E. acroides*, eight samples were selected for amplicon sequencing of 16S and 18S rRNA genes for bacterial and eukaryotic communities respectively (ENA accession PRJEB7181). From each sampling site, one sample was chosen for each leaf age. OTU clustering was performed at 97% sequence identity, and SILVAngs was used for the taxonomic classification of the OTUs (Quast et al., 2013). A more detailed description of the sequence processing workflow can be found in Text S1.

Amplicon sequencing of the V4-V6 variable region of the bacterial 16S rRNA gene recovered 2179 OTUs with about 600 OTUs per sample. Approximately 62% of the OTUs were singletons (47%) or doubletons (15%), which accounted for 8 - 16% of the total sequence counts per sample. This percentage of rare bacterial types did not significantly vary between sampling sites (Welch's t-test, $t = -0.944$, $df = 3.817$, $p > 0.05$). The Chao1 index of total OTU richness yielded estimates almost twice as high as the raw counts. There was no significant difference in OTU richness between the sampling sites (Welch's t-test, $t = -0.819$, $df = 2.204$, $p > 0.05$; Table 1). Previous reports on bacterial richness and rare bacterial types using next generation sequencing technology showed inconsistent responses to OA (Kerfahi et al., 2014; Raulf et al., 2015), which might be explained by the difference in environments being investigated. As such, the lack of change in bacterial richness and rare bacterial types on seagrass leaves at the vent site should not be generalized beyond the scope of this study.

Amplicon sequencing of the V4 variable region of the eukaryotic 18S rRNA gene recovered 3928 OTUs. OTU number per sample ranged from 277 (C1) to 664 (C2; Table 1). Similar to the bacterial OTU richness, there was no significant trend in the OTU number between sampling sites (Welch's t-test, $t = 0.034$, $df = 3.454$, $p > 0.05$). This result was consistent with that of Lidbury and colleagues (2012), who did not detect a response of eukaryotic microbial richness on settlement tiles to OA using a molecular fingerprinting technique. However, the scarcity of OA studies on eukaryotic microbes applying next generation sequencing technology does not allow for a more comprehensive discussion on how eukaryotic epiphyte richness may respond to OA.

Taxonomic composition of bacterial epiphytes

Most of the bacterial sequences belonged to the phylum Proteobacteria (51%), with Gammaproteobacteria (38%) and Alphaproteobacteria (11%) constituting the majority. The next most abundant phyla were Cyanobacteria (30%, chloroplast sequences 27%), Bacteroidetes (12%, Flavobacteria: 8%) and Fusobacteria (4%), which were especially abundant on older leaves at the vent site (Fig. 2A). The high percentage of Gammaproteobacteria and Alphaproteobacteria was consistent with previous observations on bacterial epiphytes of tropical seagrasses (Weidner et al., 2000; Uku et al., 2007). The high percentage of chloroplast sequences may be explained by the origin of the samples, which were taken in the photic zone from a chloroplast-containing substratum that was also colonized by algae. We identified several taxa that may potentially be influenced by sampling site and/or age of the seagrass leaves (Table S3). Notice that taxa that seemed to be predominantly affected by leaf age are not further discussed here, because the main objective of our study was to describe potential OA effects on epiphytic microbes.

Cyanobacteria appeared to have a higher relative abundance at the control site than at the CO_2-impacted vent site. Predictions of OA effects on free-living cyanobacteria are controversial and range from no effect on metabolic rates (Gradoville *et al*., 2014) to an increase in carbon and nitrogen fixation (Hutchins *et al*., 2007; Lomas *et al*., 2012). In microbial biofilms, OA seemed to lead to a decrease in cyanobacterial abundance and diversity (Witt *et al*., 2011; Russell *et al*., 2013). In complex assemblages, Cyanobacteria are supposed to benefit less from OA than other photosynthetic organisms such as chlorophytes, and may thus be outcompeted by them (Low-Décarie *et al*., 2014). In agreement with this hypothesis, cyanobacteria seemed to decrease in relative abundance with decreasing pH in this study: e.g. the two nitrogen fixing genera *Leptolyngbya* and *Lyngbya*, which are known epiphytes of seagrasses (Uku *et al*., 2007; Hamisi *et al*., 2013), were more abundant at the control site, the latter even being unique to the control site. In the case of *Leptolyngbya*, this response has been documented before in a temperate system (Russell *et al*., 2013), whereas *Lyngbya* is expected to react more to changes in temperature and nutrient availability than to OA (Paerl and Huisman, 2009).

Contrarily to Cyanobacteria, Deltaproteobacteria, Bacilli, Fusobacteria and Clostridia seemed to increase in relative abundance at the vent site. Within the Deltaproteobacteria, this increase was mostly due to an increase in the relative abundance of OTUs of the order Bdellovibrionales at the vent site, as also observed by Raulf and colleagues (2015) in sediments from PNG. The responses of Bacilli and Fusobacteria were mostly due to an increase in the relative abundance of only one OTU belonging to the genus *Paenibacillus* and to the family Leptotrichiaceae, respectively. For *Paenibacillus*, this response has previously been observed in sediments under elevated pCO_2 (Kerfahi et al., 2014). The fusobacterial OTU was among the most abundant OTUs in the data set (3.5% of all sequences) and was further identified as a relative of *Propionigenium* sp. with a sequence identity of 93% to the latter (NCBI accession number KC918186). Fusobacteria are a group of strictly anaerobic bacteria, which have been associated with tidal flat sediments, where they contribute to organic matter degradation (Graue et al., 2012), and are present in the gut microflora of marine invertebrates (Li et al., 2012; Dishaw et al., 2014; Rungrassamee et al., 2014) and coral biofilm (Morrow et al., 2012). There is evidence that Fusobacteria associated with corals increase in abundance under OA (Vega Thurber et al., 2009), which might support our results; although the exceptionally high sequence abundance of Fusobacteria at the vent site was restricted to the two oldest leaves. Noticeably, Fusobacteria as well as Clostridia have been implicated in coral diseases (Vega Thurber et al., 2009; Sweet et al., 2013).

Alphaproteobacteria, Gammaproteobacteria and Flavobacteria did not show a response to sampling site on class level. However, at a higher level of taxonomic resolution, several taxa appeared to be affected by sampling site (Table S3). Among the most abundant OTUs in the data set, those potentially influenced by sampling site belonged to the Gammaproteobacteria, i.e. *Thalassomonas* (1.6%) and *Marinomonas* (3.8%), which were more abundant at the vent site, and *Reinekea* (7.2%) and *Melitea* (2.3%), which were more abundant at control site. Sequence comparison of the OTU belonging to *Thalassomonas* showed a high sequence identity (99%) to the sequence retrieved by Webster and colleagues (2013; NCBI accession number JQ178640), which was associated with the crustose coralline algae *Hydrolithon* at low pH. It was further closely related (96% sequence identity) to *Thalassomonas loyana* (NCBI accession

number NR043066), the causative agent of white plague-like disease in corals (Thompson et al., 2006), suggesting a potentially pathogenic role. The OTU of *Marinomonas* was related to *Marinomonas poseidonica* (99% sequence identity, NCBI accession number NR074719), which has been reported to be beneficial to seagrass (Celdrán et al., 2012) and may contribute to increased growth rates at the vent site. *Reinekea* is a genus that might play an important role in the degradation of organic matter after phytoplankton blooms (Teeling et al., 2012). Its reduced abundance at the vent site may be caused by the decreased availability of degradable material presumably due to the lower percentage of epiphyte cover. However, it also belongs to the order Oceanospirillales, which are common in coral biofilms and expected to decrease in abundance in diseased corals (Mouchka et al., 2010). Hardly anything is known about the genus *Melitea*, and, although it has been mentioned before in OA research, its response to elevated pCO_2 remains largely unknown (Meron et al., 2011).

The direction of potential changes (i.e. the increase or decrease) in relative OTU abundance from control to vent site or vice versa appeared to be related to total OTU abundance. Whereas approximately equal numbers of abundant OTUs (defined by more than 1% total sequence abundance) increased towards either the vent or control site, more OTUs of intermediate abundance level (defined by more than two sequence occurrences, but less than 1% total sequence abundance) tended to increase towards the vent site than towards the control site (Table S4). Although not seen in the rare bacterial types as previously discussed, this trend might be comparable with the increase in rare types with decreasing pH observed in marine sediments at PNG (Raulf et al., 2015).

Among these increasing OTUs, sulfur oxidizers were overrepresented, some of which - but not all - were unique to the vent site. This suggests that a higher concentration of sulfur compounds that can be metabolized by bacteria might be present in the water column at the vent compared to the control site, although so far, no direct evidence exists for that matter (Fabricius et al., 2011). H_2S was detected in the sediment (A. Fink, pers. comm.) and gas, but H_2S levels in the water column did not exceed values typically observed for seawater (Fabricius et al., 2011). On the other hand, sulfur-oxidizing bacteria might also constitute a contamination from the sediment and might not even be active on the seagrass leaves. Furthermore, apart from their biogeochemical

function, sulfur-oxidizing bacteria have also been associated with coral diseases (Frias-Lopez et al., 2002; 2004; Bourne et al., 2013). Their increased relative abundance may therefore not only be attributable to sulfide seepage. Other OTUs of intermediate abundance, which increased at the vent site, belonged to genera such as *Shewanella* and *Vibrio*, which again have been related to coral diseases (Mouchka et al., 2010; Meron et al., 2011; Garcia et al., 2013; Sweet et al., 2013). This general trend of an increase in disease-associated bacterial OTUs at the vent site has also been observed at PNG in corals (Morrow *et al*., 2014).

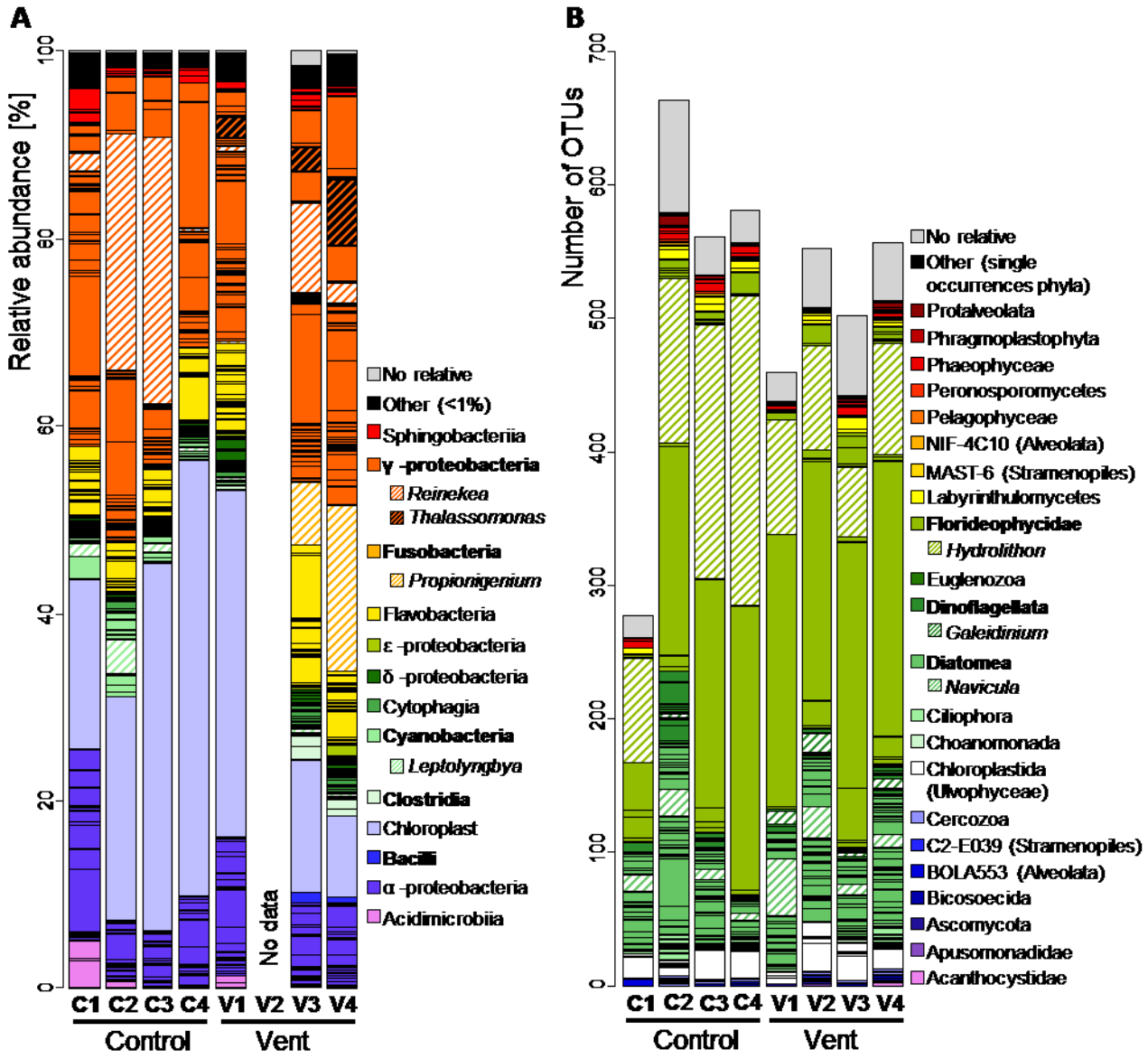

Figure 2: Taxonomic composition of the epiphytic biofilm on leaves of *E. acroides*, A: bacterial community based on the relative abundance of OTUs (16S rRNA gene sequences, 454 sequencing); B: eukaryotic community based on the presence/absence of OTUs (18S rRNA gene sequences, Illumina). Bars are colored by bacterial class or eukaryotic phylum, separated by genus. Hatched areas: examples of genera potentially influenced by site and/or leaf age. Bold: bacterial classes or eukaryotic phyla potentially influenced by sampling site (Tables S3 and S5). Samples are ordered by leaf age (left: youngest, right: oldest) within sampling site.

Taxonomic composition of eukaryotic epiphytes

Eukaryotic OTUs were dominated by Florideophycidae, which mostly consisted of crustose coralline algae (Corallinophycidae, 2282 OTUs) and Rhodymeniophycidae (235 OTUs), followed by diatoms (695 OTUs), Ulvophyceae (171 OTUs) and dinoflagellates (145 OTUs, Fig. 2B). This composition conforms with the findings of microscopy-based work on tropical seagrasses, which also reported a prevalence of crustose coralline algae (Corlett and Jones, 2007; Martin et al., 2008).

Potential changes in OTU richness were related to genera of the taxa Corallinophycidae, Dinoflagellata and Diatomea (Table S5). Corallinophycidae were slightly less diverse at the vent site, especially on the older leaves where they only retained about 65% of their OTUs. As calcifying organisms, crustose coralline algae are likely to suffer from OA (Martin et al., 2008; Fabricius et al., 2011; Donnarumma et al., 2014). However, some genera appear to be more vulnerable to elevated pCO_2 than others. Here, *Hydrolithon* the most diverse genus of crustose coralline algae on the leaves of *E. acroides* lost about two thirds of its OTUs, and *Lithophyllum*, which disappeared completely at the vent site, seemed especially susceptible to acidified conditions. Severe declines in *Hydrolithon* have also been observed on settlement tiles in PNG (Fabricius et al., 2015). The calcite deposits of *Hydrolithon* and *Lithophyllum* contain a high percentage of magnesium, whereas e.g. *Spongites*, which was the only crustose coralline algae unique to the vent site, deposits calcite with little magnesium content - a form that is less susceptible to reduced pH than high-Mg calcite (Smith et al., 2012). These differences in calcite composition may contribute to the resilience of crustose coralline algae under OA (Ries, 2011; Ragazzola et al., 2013).

The genus *Galeidinium* (Dinoflagellata) was more diverse at the vent compared with the control site. However, the impacts of OA on dinoflagellates, in general, and *Galeidinium*, in particular, are not very well studied so that potential implications of an increased diversity of *Galeidinium* under elevated pCO_2 cannot yet be predicted.

Diatoms showed a variable response to sampling site with *Navicula* and *Grammatophora* being more diverse at the vent, and *Cyclophora* and *Cylindrotheca* at the control site. These changes in the diversity of diatoms largely concurred with previous findings, which predicted an increase in the genera *Grammatophora* and

Navicula under OA with a coinciding decrease of *Cyclophora* and *Cylindrotheca* (Johnson *et al*., 2011; Singh and Singh, 2014), which was also the case here. Although photosynthetic organisms in general are expected to benefit from OA, species-specific responses depend on the respective ability of each organism to utilize inorganic carbon during photosynthesis and on their comparative competitiveness (Koch *et al*., 2013).

Conclusion: Does epiphyte composition change due to OA?

We detected a highly diverse bacterial and eukaryotic community on the leaves of *E. acroides*. Although OTU richness seemed unaffected, our results overall suggest a pronounced and interconnected shift in bacterial and eukaryotic community composition of the epiphytic biofilm of *E. acroides* with changes in the carbonate system of the surrounding water. Besides organisms well known to respond to elevated pCO_2, this shift may also include taxa that have not been identified in OA research before. In some cases, a potential response to elevated pCO_2 was only visible at a very high level of taxonomic resolution. We further detected an increased prevalence of microbial sequence types associated with coral diseases at the vent site under elevated pCO_2 conditions. This agrees with the hypothesis that coral reefs experiencing elevated pCO_2 levels will be more susceptible to diseases than reefs not yet exposed to OA (Hoegh-Guldberg *et al*., 2007). It further highlights the potential of seagrasses as vectors of coral pathogens (Sweet *et al*., 2013) and stresses the point that seagrasses should be viewed as a holobiont when making predictions about OA effects and ecological consequences in coral reefs. Given the high diversity of the epiphytic community on seagrass leaves, an accurate assessment of the interaction of seagrasses with other components of reef ecosystems will also require further knowledge of their epiphytic community composition.

Acknowledgements

We thank the scientists and crew of the cruise to Papua New Guinea for their support during the sampling, especially Katharina Fabricius (AIMS, Australia), Dirk de Beer and Artur Fink (both MPI for Marine Microbiology, Bremen) for their continued advice. The research was funded by the German Federal Ministry of Education and Research (BMBF) in the framework of the BIOACID II project, the Max Planck Society and the University of Bremen.

References

Agawin, N.S.R., Duarte, C.M., Fortes, M.D., Uri, J.S., and Vermaat, J.E. (2001) Temporal changes in the abundance, leaf growth and photosynthesis of three co-occurring Philippine seagrasses. *J. Exp. Mar. Bio. Ecol.* **260**: 217–239.

Bourne, D.G., van der Zee, M.J.J., Botté, E.S., and Sato, Y. (2013) Sulfur-oxidizing bacterial populations within cyanobacterial dominated coral disease lesions. *Environ. Microbiol. Rep.* **5**: 518–524.

Brodie, J., Williamson, C.J., Smale, D. A., Kamenos, N. A., Mieszkowska, N., Santos, R., et al. (2014) The future of the northeast Atlantic benthic flora in a high CO_2 world. *Ecol. Evol.* **4**: 2787–2798.

Brouns, J.J.W.M. and Heijs, F.M.L. (1986) Production and biomass of the seagrass Enhalus acoroides (L.f.) Royle and its epiphytes. *Aquat. Bot.* **25**: 21–45.

Celdrán, D., Espinosa, E., Sánchez-Amat, A., and Marín, A. (2012) Effects of epibiotic bacteria on leaf growth and epiphytes of the seagrass Posidonia oceanica. *Mar. Ecol. Prog. Ser.* **456**: 21–27.

Corlett, H. and Jones, B. (2007) Epiphyte communities on Thalassia testudinum from Grand Cayman, British West Indies: Their composition, structure, and contribution to lagoonal sediments. *Sediment. Geol.* **194**: 245–262.

Dishaw, L.J., Flores-Torres, J., Lax, S., Gemayel, K., Leigh, B., Melillo, D., et al. (2014) The gut of geographically disparate Ciona intestinalis harbors a core microbiota. *PLoS One* **9**: e93386.

Donnarumma, L., Lombardi, C., Cocito, S., and Gambi, M.C. (2014) Settlement pattern of Posidonia oceanica epibionts along a gradient of ocean acidification: an approach with mimics. *Mediterr. Mar. Sci.* **15**: 498–509.

Fabricius, K.E., Kluibenschedl, A., Harrington, L., Noonan S. and De'ath, G. (2015) In situ changes of tropical crustose coralline algae along carbon dioxide gradients. *Scientific Reports* **5**: 9537. doi: 10.1038/srep09537.

Fabricius, K.E., Langdon, C., Uthicke, S., Humphrey, C., Noonan, S., De'ath, G., et al. (2011) Losers and winners in coral reefs acclimatized to elevated carbon dioxide concentrations. *Nat. Clim. Chang.* **1**: 165–169.

Frias-Lopez, J., Klaus, J.S., Bonheyo, G.T., and Fouke, B.W. (2004) Bacterial Community Associated with Black Band Disease in Corals. *Appl. Environ. Microbiol.* **70**: 5955–5962.

Frias-Lopez, J., Zerkle, A.L., Bonheyo, G.T., and Fouke, B.W. (2002) Partitioning of Bacterial Communities between Seawater and Healthy, Black Band Diseased, and Dead Coral Surfaces. *Appl. Environ. Microbiol.* **68**: 2214–2228.

Garcia, G.D., Gregoracci, G.B., Santos, E.D.O., Meirelles, P.M., Silva, G.G.Z., Edwards, R., et al. (2013) Metagenomic analysis of healthy and white plague-affected Mussismilia braziliensis corals. *Microb. Ecol.* **65**: 1076–1086.

Gradoville, M.R., White, A.E., Bo, D., Church, M.J., and Letelier, R.M. (2014) Diversity trumps acidification : Lack of evidence for carbon dioxide enhancement of Trichodesmium community nitrogen or carbon fixation at Station ALOHA. *Limnol. Oceanogr.* **59**: 645–659.

Graue, J., Engelen, B., and Cypionka, H. (2012) Degradation of cyanobacterial biomass in anoxic tidal-flat sediments: a microcosm study of metabolic processes and community changes. *ISME J.* **6**: 660–669.

Hall-Spencer, J.M., Rodolfo-Metalpa, R., Martin, S., Ransome, E., Fine, M., Turner, S.M., et al. (2008) Volcanic carbon dioxide vents show ecosystem effects of ocean acidification. *Nature* **454**: 96–99.

Hamisi, M., Díez, B., Lyimo, T., Ininbergs, K., and Bergman, B. (2013) Epiphytic cyanobacteria of the seagrass Cymodocea rotundata: diversity, diel nifH expression and nitrogenase activity. *Environ. Microbiol. Rep.* **5**: 367–376.

Hoegh-Guldberg, O., Mumby, P.J., Hooten, A.J., Steneck, R.S., Greenfield, P., Gomez, E., et al. (2007) Coral reefs under rapid climate change and ocean acidification. *Science* **318**: 1737–1742.

Hutchins, D.A., Fu, F.-X., Zhang, Y., Warner, M.E., Feng, Y., Portune, K., et al. (2007) CO_2 control of Trichodesmium N_2 fixation, photosynthesis, growth rates, and elemental ratios: Implications for past, present, and future ocean biogeochemistry. *Limnol. Oceanogr.* **52**: 1293–1304.

Johnson, V.R., Brownlee, C., Rickaby, R.E.M., Graziano, M., Milazzo, M., and Hall-Spencer, J.M. (2011) Responses of marine benthic microalgae to elevated CO_2. *Mar. Biol.* **160**: 1813–1824.

Johnstone, I.M. (1979) Papua New Guinea seagrasses and aspects of the biology and growth of Enhalus acoroides (L.f.) Royle. *Aquat. Bot.* **7**: 197–208.

Kerfahi, D., Hall-Spencer, J.M., Tripathi, B.M., Milazzo, M., Lee, J., and Adams, J.M. (2014) Shallow Water Marine Sediment Bacterial Community Shifts Along a Natural CO_2 Gradient in the Mediterranean Sea Off Vulcano, Italy. *Microb. Ecol.* **67**: 819–828.

Koch, M., Bowes, G., Ross, C., and Zhang, X.-H. (2013) Climate change and ocean acidification effects on seagrasses and marine macroalgae. *Glob. Chang. Biol.* **19**: 103–132.

Li, S., Sun, L., Wu, H., Hu, Z., Liu, W., Li, Y., and Wen, X. (2012) The intestinal microbial diversity in mud crab (Scylla paramamosain) as determined by PCR-DGGE and clone library analysis. *J. Appl. Microbiol.* **113**: 1341–1351.

Lidbury, I., Johnson, V., Hall-Spencer, J.M., Munn, C.B., and Cunliffe, M. (2012) Community-level response of coastal microbial biofilms to ocean acidification in a natural carbon dioxide vent ecosystem. *Mar. Pollut. Bull.* **64**: 1063–1066.

Lomas, M., Hopkinson, B., Losh, J., Ryan, D., Shi, D., Xu, Y., and Morel, F. (2012) Effect of ocean acidification on cyanobacteria in the subtropical North Atlantic. *Aquat. Microb. Ecol.* **66**: 211–222.

Low-Décarie, E., Fussmann, G.F., and Bell, G. (2014) Aquatic primary production in a high-CO_2 world. *Trends Ecol. Evol.* **29**: 223–232.

Marhaeni, B., Radjasa, O.K., Khoeri, M.M., Sabdono, A., Bengen, D.G., and Sudoyo, H. (2011) Antifouling Activity of Bacterial Symbionts of Seagrasses against Marine Biofilm-Forming Bacteria. *J. Environ. Prot. (Irvine,. Calif).* **02**: 1245–1249.

Martin, S., Rodolfo-Metalpa, R., Ransome, E., Rowley, S., Buia, M.-C., Gattuso, J.-P., and Hall-Spencer, J. (2008) Effects of naturally acidified seawater on seagrass calcareous epibionts. *Biol. Lett.* **4**: 689–692.

Medina-Pons, F.J., Terrados, J., López-López, A., Yarza, P., and Rosselló-Móra, R. (2009) Evaluation of the 18S rRNA clone library approach to study the diversity of the macroeukaryotic leaf-epiphytic community of the seagrass Posidonia oceanica (L.) Delile. *Mar. Biol.* **156**: 1963–1976.

Meron, D., Atias, E., Iasur Kruh, L., Elifantz, H., Minz, D., Fine, M., and Banin, E. (2011) The impact of reduced pH on the microbial community of the coral Acropora eurystoma. *ISME J.* **5**: 51–60.

Michael, T.S., Shin, H.W., Hanna, R., and Spafford, D.C. (2008) A review of epiphyte community development: Surface interactions and settlement on seagrass. *J. Environ. Biol.* **29**: 629–638.

Morrow, K.M., Bourne, D.G., Humphrey, C., Botté, E.S., Laffy, P., Zaneveld, J., et al. (2014) Natural volcanic CO_2 seeps reveal future trajectories for host-microbial associations in corals and sponges. *ISME J.* **2**: 1–15.

Morrow, K.M., Moss, A.G., Chadwick, N.E., and Liles, M.R. (2012) Bacterial associates of two Caribbean coral species reveal species-specific distribution and geographic variability. *Appl. Environ. Microbiol.* **78**: 6438–6449.

Mouchka, M.E., Hewson, I., and Harvell, C.D. (2010) Coral-associated bacterial assemblages: current knowledge and the potential for climate-driven impacts. *Integr. Comp. Biol.* **50**: 662–674.

Orth, R.J., Carruthers, T.J.B., Dennison, W.C., Duarte, C.M., Fourqurean, J.W., Heck Jr, K.L., et al. (2006) A Global Crisis for Seagrass Ecosystems. *Bioscience* **56**: 987–996.

Paerl, H.W. and Huisman, J. (2009) Climate change: a catalyst for global expansion of harmful cyanobacterial blooms. *Environ. Microbiol. Rep.* **1**: 27–37.

Quast, C., Pruesse, E., Yilmaz, P., Gerken, J., Schweer, T., Yarza, P., et al. (2013) The SILVA ribosomal RNA gene database project: improved data processing and web-based tools. *Nucleic Acids Res.* **41**: D590–D596.

Ragazzola, F., Foster, L.C., Form, A.U., Büscher, J., Hansteen, T.H., and Fietzke, J. (2013) Phenotypic plasticity of coralline algae in a High CO 2 world. *Ecol. Evol.* **3**: 3436–3446.

Ramette, A. (2009) Quantitative community fingerprinting methods for estimating the abundance of operational taxonomic units in natural microbial communities. *Appl. Environ. Microbiol.* **75**: 2495–2505.

Raulf, F.F., Fabricius, K.E., Uthicke, S., de Beer, D., Abed, R.M.M., and Ramette, A. (2015) Changes in microbial communities in coastal sediments along natural CO_2 gradients at a volcanic vent in Papua New Guinea. *Environ. Microbiol.* doi: 10.1111/1462-2920.12729.

Ries, J.B. (2011) Skeletal mineralogy in a high-CO_2 world. *J. Exp. Mar. Bio. Ecol.* **403**: 54–64.

Rungrassamee, W., Klanchui, A., Maibunkaew, S., Chaiyapechara, S., Jiravanichpaisal, P., and Karoonuthaisiri, N. (2014) Characterization of intestinal bacteria in wild and domesticated adult black tiger shrimp (Penaeus monodon). *PLoS One* **9**: e91853.

Russell, B.D., Connell, S.D., Findlay, H.S., Tait, K., Widdicombe, S., and Mieszkowska, N. (2013) Ocean acidification and rising temperatures may increase biofilm primary productivity but decrease grazer consumption. *Philos. Trans. R. Soc. Lond. B. Biol. Sci.* **368**: 20120438.

Sand-Jensen, K. (1977) Effect of epiphytes on eelgrass photosynthesis. *Aquat. Bot.* **3**: 55–63.

Sawall, Y., Richter, C., and Ramette, A. (2012) Effects of eutrophication, seasonality and macrofouling on the diversity of bacterial biofilms in equatorial coral reefs. *PLoS One* **7**: e39951.

Singh, S.P. and Singh, P. (2014) Effect of CO_2 concentration on algal growth: A review. *Renew. Sustain. Energy Rev.* **38**: 172–179.

Smith, A.M., Sutherland, J.E., Kregting, L., Farr, T.J., and Winter, D.J. (2012) Phylomineralogy of the coralline red algae: correlation of skeletal mineralogy with molecular phylogeny. *Phytochemistry* **81**: 97–108.

Steele, J.A., Countway, P.D., Xia, L., Vigil, P.D., Beman, J.M., Kim, D.Y., et al. (2011) Marine bacterial, archaeal and protistan association networks reveal ecological linkages. *ISME J.* **5**: 1414–1425.

Sweet, M.J., Bythell, J.C., and Nugues, M.M. (2013) Algae as reservoirs for coral pathogens. *PLoS One* **8**: e69717.

Teeling, H., Fuchs, B.M., Becher, D., Klockow, C., Gardebrecht, A., Bennke, C.M., et al. (2012) Substrate-controlled succession of marine bacterioplankton populations induced by a phytoplankton bloom. *Science* **336**: 608–611.

Thompson, F.L., Barash, Y., Sawabe, T., Sharon, G., Swings, J., and Rosenberg, E. (2006) Thalassomonas loyana sp. nov., a causative agent of the white plague-like disease of corals on the Eilat coral reef. *Int. J. Syst. Evol. Microbiol.* **56**: 365–368.

Uku, J., Björk, M., Bergman, B., and Díez, B. (2007) Characterization and Comparison of Prokaryotic Epiphytes Associated With Three East African Seagrasses. *J. Phycol.* **43**: 768–779.

Vega Thurber, R., Willner-Hall, D., Rodriguez-Mueller, B., Desnues, C., Edwards, R.A., Angly, F., et al. (2009) Metagenomic analysis of stressed coral holobionts. *Environ. Microbiol.* **11**: 2148–2163.

Vizzini, S., Di Leonardo, R., Costa, V., Tramati, C.D., Luzzu, F., and Mazzola, A. (2013) Trace element bias in the use of CO_2-vents as analogues for low-pH environments: Implications for contamination levels in acidified oceans. *Estuar. Coast. Shelf Sci.* **134**: 19–30.

Wahl, M. (1989) Marine epibiosis. I. Fouling and antifouling: some basic aspects. *Mar. Ecol. Prog. Ser.* **58**: 175–189.

Webster, N.S., Uthicke, S., Botté, E.S., Flores, F., and Negri, A.P. (2013) Ocean acidification reduces induction of coral settlement by crustose coralline algae. *Glob. Chang. Biol.* **19**: 303–315.

Weidner, S., Arnold, W., Stackebrandt, E., and Pu, A. (2000) Phylogenetic Analysis of Bacterial Communities Associated with Leaves of the Seagrass Halophila stipulacea by a Culture-Independent Small-Subunit rRNA Gene Approach. *Microb. Ecol.* **39**: 22–31.

Witt, V., Wild, C., Anthony, K.R.N., Diaz-Pulido, G., and Uthicke, S. (2011) Effects of ocean acidification on microbial community composition of, and oxygen fluxes through, biofilms from the Great Barrier Reef. *Environ. Microbiol.* **13**: 2976–2989.

Wolf, C., Frickenhaus, S., Kilias, E.S., Peeken, I., and Metfies, K. (2013) Regional variability in eukaryotic protist communities in the Amundsen Sea. *Antarct. Sci.* **11**: 1–11.

Yamamuro, M., Umezawa, Y., and Koike, I. (2004) Internal variations in nutrient concentrations and the C and N stable isotope ratios in leaves of the seagrass Enhalus acoroides. *Aquat. Bot.* **79**: 95–102.

Supporting information

Text S1: 16S sequence processing workflows.

Sequencing was performed at Research and Testing Laboratories (Lubbock, Texas, USA). For the bacteria the V4-V6 hypervariable region of the 16S gene was sequenced on the Roche 454 FLX+ system (Roche, Basel, Switzerland); for the eukaryotes the V4 hypervariable region of the 18S rRNA gene was sequenced on the Illumina MiSeq platform. Raw sequences were denoised (only 454 sequencing data) and quality trimmed in mothur v.1.33.3 (Schloss et al. 2009) and submitted to SILVAngs (Quast et al. 2013) for taxonomic classification. Clustering of OTUs was performed at 97% sequence identity and taxonomic classification at 93% sequence identity on genus level. Sequence counts were adjusted to the minimum number of sequences per sample (454 sequencing: 5249, Illumina sequencing: 19474). Single OTU occurrences and sequence contaminations from animals and *E. acroides* were removed prior to the analysis of the eukaryotic dataset (Logares et al. 2014). Sample C1 was dominated by OTUs assigned to an annelid worm. After the removal of contaminating sequences, OTU richness in sample C1 was much lower than in the other samples presumably due to the compositional character of DNA samples, i.e. because of the presence of a highly dominant OTU, DNA belonging to rare organisms was less likely to be sequenced than in samples with a more even distribution. The larger number of eukaryotic OTUs in comparison to the bacterial dataset was due to the increased sequencing effort with the Illumina technology. After rarefying the eukaryotic sequences to the minimum of the bacterial sequence counts and accounting for the large proportion of rare bacterial OTUs, i.e. comparing the number of eukaryotic OTUs to the Chao1 estimated bacterial OTU richness, there were approximately twice as many bacterial as eukaryotic OTUs. The eukaryotic community data were further converted to presence/absence to account for multicellularity and variations in rRNA gene copy number per genome (Prokopowich et al. 2003; Logares et al. 2014).

References:

Logares, R. et al., 2014. Patterns of rare and abundant marine microbial eukaryotes. *Current biology*, 24(8), pp.813–821.

Prokopowich, C.D., Gregory, T.R. & Crease, T.J., 2003. The correlation between rDNA copy number and genome size in eukaryotes. *Genome*, 46, pp.48–50.

Quast, C. et al., 2013. The SILVA ribosomal RNA gene database project: improved data processing and web-based tools. *Nucleic acids research*, 41(Database issue), pp.D590–6.

Schloss, P.D. et al., 2009. Introducing mothur: open-source, platform-independent, community-supported software for describing and comparing microbial communities. *Applied and environmental microbiology*, 75(23), pp.7537–41.

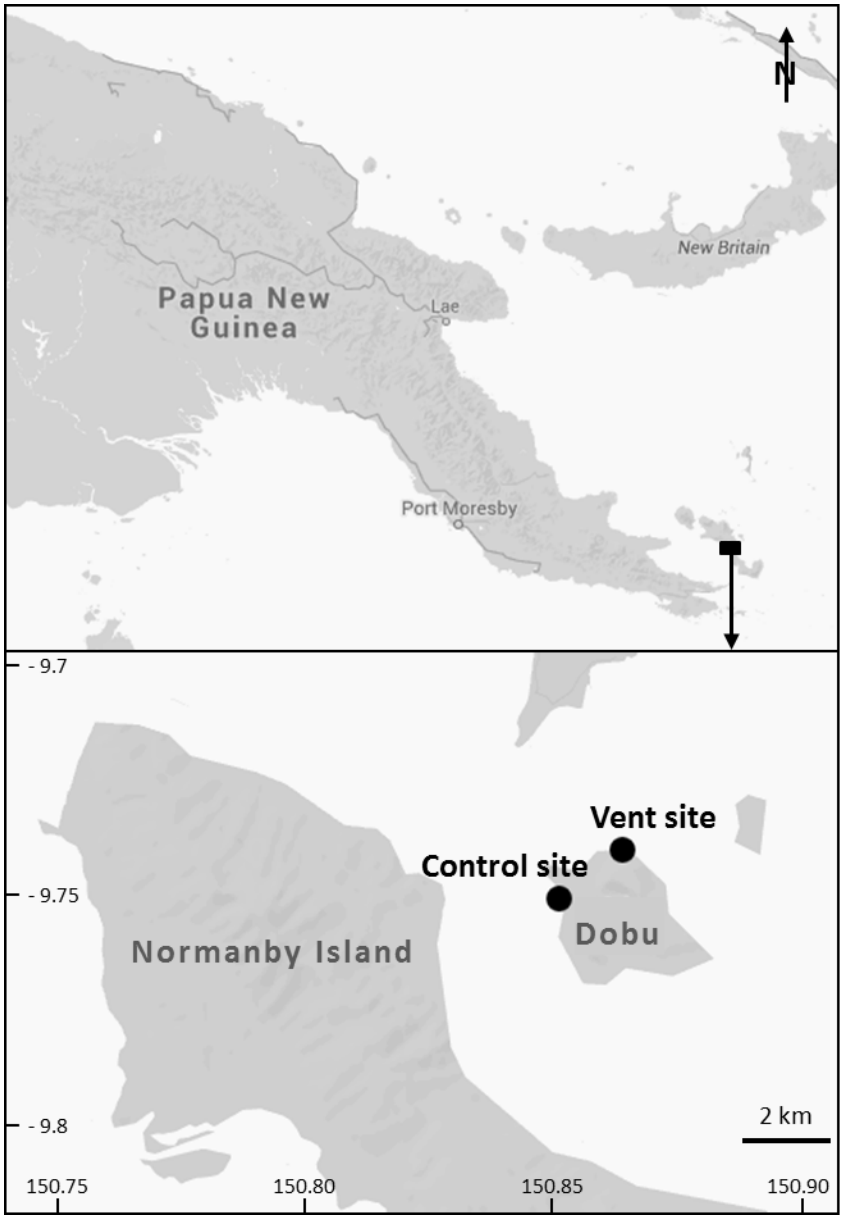

Figure S1: Sampling area in Papua New Guinea showing the two sampling sites, which were approximately 2 km apart (control site: S9.752, E150.854, vent site: S9.737, E150.869).

Table S1: Analysis of similarities (ANOSIM) results to test the influence of sampling site and leaf age on the similarity of bacterial and eukaryotic communities based on ARISA; upper panel: ANOSIM R based on Bray-Curtis dissimilarity coefficient, lower panel: ANOSIM R based on Jaccard dissimilarity coefficient. 1 - 4 representing leaf ages from youngest to oldest. Fdr-adjusted p-values < 0.1 (°), < 0.05 (*), < 0.01 (**), < 0.001 (***), ANOSIM R of non-significant results not reported.

		Bacterial communities		Eukaryotic communities	
		Control	Vent	Control	Vent
Bray-Curtis	All ages	0. 775 ***		0.731 ***	
	1	0.606 *		0.606 *	
	2	0.861 *		0.835 *	
	3	0.989 *		0.781 *	
	4[a]	0.982 °		1°	
	1-2	0.270 °	0.360 *	0.242 °	0.239 °
	1-3	0.583 *	0.752 *	0.520 *	0.253 °
	1-4[a]	0.338 *		0.438 *	
	2-3				
	2-4[a]				
	3-4[a]				
Jaccard	All ages	0.870 ***		0.692 ***	
	1	0.906 *		0.775 *	
	2	0.987 *		0.835 **	
	3	1 *		0.907 *	
	4[a]	1°		1 °	
	1-2	0.393 *	0.480 *	0.397 *	0.501 **
	1-3	0.877 *	0.805 *	0.639 *	0.592 *
	1-4[a]	0.831 *		0.563 *	
	2-3	0.161 °			
	2-4[a]				
	3-4[a]				

[a] only 2 samples available for oldest leaves from the vent site

Table S2: RDA results to identify factors significantly explaining the variation in bacterial and eukaryotic communities based on ARISA; results shown for RDA based on hellinger-transformed relative abundances and presence/absence (binary) data.

	Source of variation	Sample size	R^2 unadjusted	R^2 adjusted	df	F	Significance
Bacteria							
Hellinger							
	Site (CO_2 level)	24	0.305	0.273	1,22	9.631	$p < 0.05$
	Leaf age	40	0.103	0.066	3,25	1.860	$p < 0.05$
Binary							
	Site (CO_2 level)	24	0.240	0.206	1,22	6.961	$p < 0.05$
	Leaf age	40	0.092	0.044	3,25	1.521	$p < 0.05$
Eukaryotes							
Hellinger							
	Site (CO_2 level)	24	0.251	0.217	1,22	7.365	$p < 0.05$
	Leaf age	40	0.089	0.040	3,25	1.484	$p < 0.05$
Binary							
	Site (CO_2 level)	24	0.162	0.124	1,22	4.265	$p < 0.05$
	Leaf age	40	0.092	0.036	3,25	1.391	$p < 0.05$

Table S3: Bacterial taxa potentially affected by sampling site based on relative OTU abundance; information is given on the abundance of the respective taxa (high: > 1% total abundance, rare: singletons and doubletons), the number of taxa of the next lower taxonomic level (subtaxa), taxa that cumulatively contributed to 70% of the dissimilarity between sampling sites (SIMPER analysis based on Bray-Curtis dissimilarity coefficient), factors potentially affecting abundance based on an uncorrected significance threshold of 0.05 and 0.1 (effect), evaluation of the response of potentially impacted taxa (response to sampling site and/or leaf age, minor response), direction of potential change in abundance and whether taxa were exclusive to either sampling site. SI table 3 is not included in the PhD thesis. Please refer to the online supporting information to the published manuscript at EMIR (http://onlinelibrary.wiley.com/wol1/doi/10.1111/1758-2229.12282/abstract).

Table S4: Number of bacterial (upper panel) and eukaryotic (lower panel) taxa potentially affected by sampling site and the direction of that effect (increase in abundance/diversity); in brackets: number of taxa unique to that site.

			Phylum	Class	Order	Family	Genus	OTU
Bacteria								
	Site							
		Vent	4	5 (1)	7 (1)	7 (3)	28 (9)	48 (34)
		Control	1	1	2	0	3 (1)	9 (6)
	Leaf age							
		Young	2	2	4	4	7	7
		Intermediate	0	0	0	0	2	4
		Old	1	1	1	1	3	0
		Old-young	0	0	0	0	1	1
Eukaryotes								
	Site							
		Vent	0	1			9 (3)	
		Control	1	1			6 (1)	
	Leaf age							
		Young	0	0			1	
		Old	1	0			2	
		Intermediate	1	1			1	

Table S5: Eukaryotic taxa potentially affected by sampling site based on the presence/absence of OTUs; information is given on the number of taxa of the next lower taxonomic level (subtaxa), factors potentially affecting OTU number (diversity) based on an uncorrected significance threshold of 0.15, evaluation of the response of potentially impacted taxa (response to sampling site and/or leaf age, minor response), direction of potential change in diversity and whether taxa were exclusive to either sampling site. SI table 5 is not included in the PhD thesis. Please refer to the online supporting information to the published manuscript at EMIR (http://onlinelibrary.wiley.com/wol1/doi/10.1111/1758-2229.12282/abstract).

Chapter 5

Short report*:
Bacterial biofilm composition on settlement tiles along natural pH gradients at two CO_2 seeps in Papua New Guinea

Christiane Hassenrück[1], Katharina Fabricius[2], Alban Ramette[1,3]

[1] Max Planck Institute for Marine Microbiology, Celsiusstraße 1, 28359 Bremen, Germany
[2] Australian Institute of Marine Science, PMB 3, Townsville, Queensland 4810, Australia
[3] Institute of Social and Preventive Medicine, Bern University, Finkenhubelweg 11, 3012 Bern, Switzerland

* This report will not be submitted to a scientific journal in its current form, but will be integrated in a manuscript by Katharina Fabricius et al. about coral recruitment along natural pH gradients at which time the further co-authors of the manuscript will be determined.

Abstract: Bacterial biofilms provide cues for the settlement of marine invertebrates, such as coral larvae, and are therefore important for the resilience and recovery of coral reefs. To better understand how ocean acidification may affect microbial life, we investigated the community composition and diversity of bacterial biofilms on settlement tiles exposed to naturally reduced pH conditions. Settlement tiles were deployed in Papua New Guinea along natural pH gradients created by two CO_2 seeps. Automated Ribosomal Intergenic Spacer Analysis was used to characterize the bacterial community on the settlement tiles 5 and 13 months after deployment. The bacterial biofilm community was very heterogeneous (25% shared OTUs between samples). Among the observed environmental parameters, pH alone only had a very weak effect on community composition (R^2 = 1%) and did not affect community richness and evenness. Our results suggest that ocean acidification does not have a strong impact on the development of bacterial biofilms on settlement tiles. Other abiotic and biotic factors, such as light exposure or close interactions with other organisms on the settlement tiles, may be more important in shaping bacterial biofilms than changes in seawater pH.

Introduction

The colonization of bare substrate by reef organisms is a crucial process in the resilience and recovery of tropical coral reefs. Especially the settlement of coral larvae is important to sustain as well as replenish coral cover in case of damage to the reef (Webster et al. 2004, Witt, Wild, Anthony, et al. 2011) and to prevent a shift from coral to algae dominated reefs (Hughes et al. 2003, Hoegh-Guldberg et al. 2007). Crustose coralline algae (CCA) and their adherent bacterial biofilms play a major role in the mediation of coral larval settlement (Negri et al. 2001, Harrington et al. 2004). Bacterial biofilms can also enhance settlement rates in the absence of CCA (Webster et al. 2004). Certain bacterial strains, e.g. *Pseudoalteromonas* or *Roseobacter*, produce chemical compounds that trigger the settlement process in coral larvae (Negri et al. 2001, Tebben et al. 2011, 2015, Sneed et al. 2014). Therefore, changes in the community composition of the bacterial biofilm, specifically those related to settlement-inducing bacteria, have the potential to affect the rate and success of coral larval settlement (Webster et al. 2011, Sneed et al. 2015).

Ocean acidification (OA), one of the major threats to coral reefs, can alter the composition of bacterial biofilms on various reef substrates (Witt, Wild, Anthony, et al. 2011, Webster et al. 2012, 2013). In incubation experiments, Witt et al. (2011) showed that bacterial biofilms on glass slides differ in community composition after exposure to CO_2-enriched seawater, with decreases in the relative abundance of *Roseobacter*. Webster et al. (2012) detected an effect of reduced pH treatments on the bacterial community associated with natural reef substrates, including CCA. After further experiments, Webster et al. (2013) hypothesized that declines in settlement rates with decreasing pH may be a result of changes in the composition of the bacterial community associated with CCAs. First observations from naturally CO_2-rich systems supported the development of distinct bacterial biofilm communities under reduced pH conditions (Lidbury et al. 2012). However, data from naturally CO_2-rich systems are still scarce and potential interactions between coral larval settlement, bacterial biofilm composition and the occurrence of macroorganisms, such as algae and macroinvertebrates, during community development are underexplored.

Here we studied the development of bacterial biofilms in a reef system, where natural CO_2 seeps locally reduce seawater pH, thus mimicking conditions expected under OA (Fabricius et al. 2011). This project was part of a larger experiment to investigate the impact of OA on the development of the whole community on artificial settlement tiles. In addition to sampling bacterial biofilms, data were collected on tile colonization by e.g. algae and macroinvertebrates, on the abundance and composition of CCAs (Fabricius et al. 2015), and on the number and species of coral recruits. This short report focuses on the effects of reduced pH on the composition and diversity of bacterial biofilm communities, which were investigated by molecular fingerprinting with Automatic Ribosomal Intergenic Spacer Analysis (ARISA).

Methods

PVC settlement tiles (11.5 cm × 11.5 cm) were deployed along pH gradients created by CO_2 seeps at two coral reefs at Upa Upasina on Normanby Island and on Dobu Island, Papua New Guinea. In December 2011, 45 tiles were placed at each reef, of which 30 tiles per reef were sampled for the analysis of bacterial biofilms. More information on the experimental set-up is provided in Fabricius et al. (2015). The pH gradients ranged from pH_T (pH total scale) 7.6 to 8.0 (Upa Upasina) and from pH_T 7.4 to 8.0 (Dobu Island). At Upa Upasina the tiles covered the whole range of pH values, whereas at Dobu Island pH values were either lower than 7.8 at the CO_2 seeps or approximately 8.0 and higher at the reference site. To analyze the bacterial biofilm communities on the settlement tiles a 2 cm × 2 cm square area was scraped off of the lower and upper side of each settlement tile 5 and 13 months after deployment. In total more than 200 biofilm samples were analyzed. Biofilm samples were stored in RNAlater (Ambion) for later DNA extraction using the UltraClean Soil DNA extraction kit (MoBio) following the manufacturer's instructions. ARISA was conducted as previously described (Ramette 2009, Hassenrück et al. 2015, 2016). ARISA fragments were binned into operational taxonomic units (OTUs) using custom R scripts available at http://www.mpi-bremen.de/en/Software_4.html.

Non-metric multidimensional scaling (NMDS) plots were calculated based on the Bray-Curtis dissimilarity matrix of relative OTU abundances. Analysis of similarity (ANOSIM) was conducted to test for differences in community composition between groups of samples defined by pH_T values of more than 7.95 ('reference'), between 7.95 and 7.80 ('intermediate'), and less than 7.80 ('low') at each reef. At Dobu Island, no sample was available for the intermediate pH category. Pairwise comparisons were corrected for multiple testing (Benjamini & Hochberg 1995). The contribution of pH to explaining variation in community composition, while accounting for other parameters (reef, tile side, and sampling time), was tested using redundancy analysis (RDA) and variation partitioning. Water column parameters that were highly correlated with pH, i.e. dissolved organic carbon concentration (DIC), pCO_2, calcite and aragonite saturation state, were excluded from the RDA models. Total alkalinity (TA) did not strongly correlate with pH but did not improve the RDA model. Prior to the RDA the bacterial

community table was corrected for compositionality effects using a centered log ratio transformation (Fernandes et al. 2014). The significance of the individual parameters was assessed using restricted permutation tests. Richness (based on OTU number) and evenness (based on the inverse Simpson index) were tested with the same models. All statistical analyses were conducted in R using the package vegan (Oksanen et al. 2015).

Results

The biofilm material collected from 4 cm² of the settlement tiles varied considerably in amount, shape and composition (Figure 1). Some samples only contained very little material, whereas others were filled with approximately 0.5 ml of brown, red or green algal material with occasional traces of calcareous substances.

ARISA of the bacterial communities on the settlement tiles detected a total of 451 OTUs with an average of 143 OTUs per sample (25^{th} percentile: 127 OTUs, 75^{th} percentile: 163). We did not detect an effect of pH, tile side or sampling time on OTU number or evenness. However, the bacterial communities were slightly more diverse at Dobu Island with 147.6 ± 2.5 OTUs and an inverse Simpson of 48.1 ± 1.4 compared to 139.7 ± 2.6 and 33.7 ± 1.3 at Upa Upasina, respectively (Table 1).

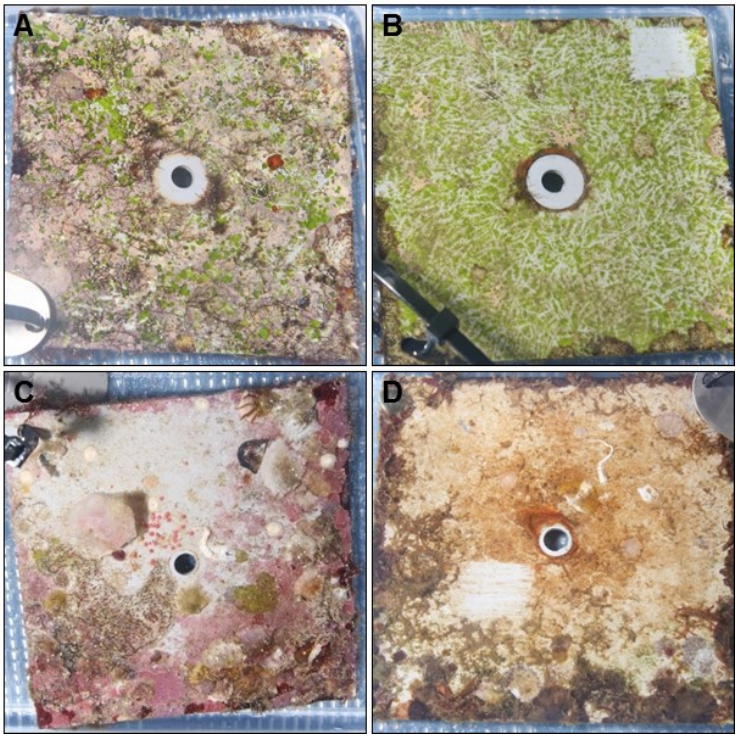

Figure 1: Settlement tiles after 5 months of deployment at Dobu Island reference (A + C) and CO_2 seep (B + D). A + B: upper tile side; C + D: lower tile side. The photographs of the tile at the CO_2 seep (B + D) were taken after the sampling of the 2 × 2 cm square for bacterial biofilm analysis. Photographs courtesy of Katharina Fabricius.

Table 1: Contribution and significance of observed environmental factors to explaining the variation in bacterial richness (OTU number), evenness (inverse Simpson index) and community composition on settlement tiles based on redundancy analysis and variation partitioning. Significance was assessed using restricted permutations; ns: not significant.

	Richness		Evenness		Community composition	
Source of variation	**adjusted R^2**	**p**	**adjusted R^2**	**p**	**adjusted R^2**	**p**
Complete model	0.030	0.030	0.181	0.001	0.088	0.001
Reef	0.021	0.041	0.131	0.001	0.012	0.001
pH	-0.004	ns	0.002	ns	0.010	0.001
Tile side	0.006	ns	0.000	ns	0.051	0.001
Sampling time	-0.002	ns	-0.004	ns	0.013	0.001

NMDS showed a highly heterogeneous composition of the bacterial community with only 25 - 30% shared OTUs between any two samples (Figure 2). In the first two NMDS dimensions the strongest visible patterns were between upper and lower tile sides and the two sampling times. A weak pattern by pH was mainly recognizable in the NMDS dimensions two and three (Figure 2). ANOSIM confirmed that at a given sampling time and tile side the bacterial communities were different between pH categories (Table 2). However, the separation of the bacterial communities between pH categories was very weak, especially at Upa Upasina, with ANOSIM R values of less than 0.5. The differences in bacterial community composition between reference and low pH categories at Dobu Island were more pronounced with an ANOSIM R between 0.51 and 0.88 except for samples from the lower tile side after 13 months deployment (Table 2).

The observed environmental parameters pH, reef, tile side and sampling time were only able to explain a small, yet significant, fraction of the variation in bacterial community composition (R^2 = 8.8%; Table 1). Among these parameters, tile side was the most important parameters explaining 5% of the variation compared to less than 1.5% attributed to the other observed parameters, including pH (Table 1).

Table 2: ANOSIM of the bacterial communities to test for the effect of pH category (reference: pH > 7.95, intermediate: 7.95 > pH > 7.8, low: pH < 7.8). ANOSIM performed separately for each reef, tile side and sampling time. For Upa Upasina, values in bold show the results of the omnibus test; subsequent pairwise comparisons corrected for multiple testing.

	Upa Upasina		Dobu	
	ANOSIM R	**p**	**ANOSIM R**	**p**
Upper tile side 5 months	**0.14**	**0.010**		
reference - intermediate	0.09	ns		
reference - low	0.34	0.006	0.71	0.001
intermediate - low	-0.01	ns		
Lower tile side 5 months	**0.36**	**0.001**		
reference - intermediate	0.48	0.002		
reference - low	0.48	0.002	0.88	0.001
intermediate - low	0.06	ns		
Upper tile side 13 months	**0.18**	**0.001**		
reference - intermediate	0.13	0.039		
reference - low	0.27	0.003	0.51	0.001
intermediate - low	0.15	0.024		
Lower tile side 13 months	**0.30**	**0.001**		
reference - intermediate	0.22	0.003		
reference - low	0.44	0.003	0.23	0.018
intermediate - low	0.26	0.003		

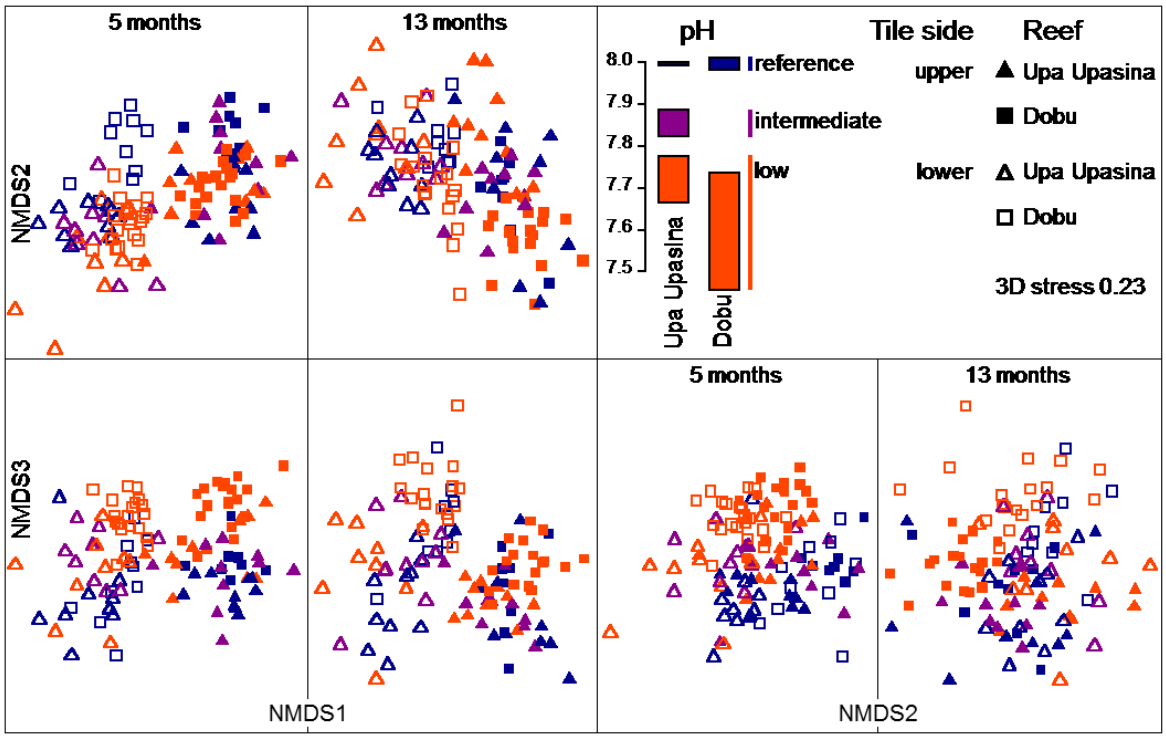

Figure 2: Non-Metric Multidimensional Scaling (NMDS) plot of the bacterial communities on the settlement tiles based on Bray-Curtis dissimilarity. Average percentage of shared OTUs for each tile side, pH category and sampling time: 25 - 30%.

Discussion

As part of a larger study on colonization patterns and coral recruitment on artificial settlement tiles along natural pH gradients, we investigated the diversity and composition of the bacterial biofilm on these settlement tiles. The most striking feature of the bacterial communities was their highly heterogeneous composition. This high degree of heterogeneity has also been observed in a similar experiment in a temperate system (personal observation) and made the detection of patterns in community composition difficult. The amount of variation explained by the observed environmental parameters here was below average for studies on microbial community composition (Hanson et al. 2012). However, our model only included few environmental parameters, and it is likely that other biotic or abiotic factors, which were not observed here, may be better suited to explain patterns in the composition of the bacterial community on the settlement tiles. It is also possible that a largely random settlement process led to the establishment of very different bacterial communities on each tile (Maignien et al. 2014, Roguet et al. 2015).

Of the observed environmental parameters, tile side was the most important factor in explaining patterns in community composition. Tile side can act as proxy for various environmental parameters, predominantly light exposure and grazing pressure, but also current velocities or proximity to the substrate that the settlement tiles were attached to. That light exposure has a major influence on community development in settlement experiments has been documented before (Sawall et al. 2012, Lidbury et al. 2012). The increased light availability on the upper tile side favors the growth of photosynthetic primary producers, such as algae and cyanobacteria, potentially resulting in a different trophic structure and therefore a different community composition (Ylla et al. 2009, Sawall et al. 2012).

There was only a minor effect of pH on bacterial community composition. Although the pH effect was statistically significant, its biological relevance is questionable since pH only explained 1% of community variation. These results were supported by the weak separation of bacterial communities between pH categories, with ANOSIM R values either not statistically significant or below values that are considered to show a strong separation of bacterial communities (Shade et al. 2007, Zinger et al. 2011). At Dobu Island the distinction between reference and low pH communities was

stronger than at Upa Upasina. However, it is possible that at Dobu Island the pH effect is enhanced by the larger geographic distance between reference and CO_2 seep sites of approximately 2 km compared to 500 m at Upa Upasina. Our results do not agree with the majority of previous observations on ocean acidification effects on bacterial biofilm development and composition, including those from naturally CO_2-rich systems, which so far pointed to a rather strong effect of pH on bacterial communities (Witt, Wild, Anthony, et al. 2011, Lidbury et al. 2012, Webster et al. 2012). However, the duration of previous experiments was much shorter than the period of deployment here. Therefore, the relative importance of the environmental parameters governing community dynamics may have shifted over time. The weak pH effect that we detected was rather in agreement with ocean acidification studies on planktonic bacteria, which reported only limited effects of reduced pH on bacterial community composition (Newbold et al. 2012, Lindh et al. 2013, Oliver et al. 2014).

We also detected an effect of sampling time on bacterial community composition, which may however not be related to succession during the early establishment of the tile community. The time period between the start of the experiment and the first sampling spanned five months, which was most likely sufficient for the formation of a fully established biofilm community, especially in warm tropical waters (Witt, Wild, & Uthicke 2011, Sawall et al. 2012). Any further changes in community composition may represent the temporal variability of already established bacterial communities. On the other hand, due to the long duration of the experiment, the settlement tiles were also already colonized by macroorganisms, such as algae and macroinvertebrates, whose presence and succession patterns may influence the development of the bacterial biofilm. It is known that different reef organisms host distinct bacterial communities (Barott et al. 2011, Morrow et al. 2012, Sneed et al. 2015), suggesting that there may be strong biotic interactions between biofilm bacteria and other members of the tile community. These biotic interactions may result in the formation of microhabitats, with small-scale environmental conditions unrelated to water column chemistry, and may be more important than large-scale abiotic factors in shaping bacterial community composition. Preliminary results on the correlation between bacterial communities and other components of the tile community using path analysis (Figure S1) appear to support the

hypothesis that the interaction with macroorganisms may be the determining factor of bacterial community composition in established biofilms.

Reef was the only factor that influenced bacterial richness and evenness estimates suggesting that the bacterial biofilm communities at Dobu Island were slightly more diverse. However, the cause behind these differences remains unclear so far. Bacterial communities on the settlement tiles at Dobu Island could have been subject to a higher frequency of disturbances resulting in a higher diversity (Horner-Devine et al. 2004). Anthropogenic impacts due to a higher population on Dobu Island compared to Upa Upasina may constitute a possible source of such disturbances. However, richness and evenness estimates may also have been biased by the insufficient resolution of the molecular fingerprinting technique, and high-resolution techniques such as next generation sequencing should be used to confirm the patterns observed here.

In conclusion, our data from settlement tiles deployed along natural pH gradients in Papua New Guinea do not support strong OA effects on bacterial biofilms. Besides, we have only begun elucidating the factors that shape the development of bacterial communities on the settlement tiles. For further analyses it is crucial to also consider other components of the tile community, as biotic interactions with co-existing macroorganisms on the tiles and the creation of microhabitats may drive the development of the bacterial community and may overshadow pH effects.

Acknowledgements

We would like to thank the scientists at AIMS, foremost Sam Noonan, who supported the field work and sample collection for this study. Further thanks to the captain and crew of the MS Chertan. Many thanks to Erika Weiz-Bersch, Linda Geuer, Silke Wetzel and Sabine Kühn who helped with the DNA extractions, ARISA PCRs and capillary electrophoresis.

References

Barott KL, Rodriguez-brito B, Janouškovec J, Marhaver KL, Smith JE, Keeling P, Rohwer FL (2011) Microbial diversity associated with four functional groups of benthic reef algae and the reef-building coral Montastraea annularis. Environ Microbiol 13:1192–1204

Benjamini Y, Hochberg Y (1995) Controlling the False Discovery Rate: A Practical and Powerful Approach to Multiple Testing. J R Stat Soc Ser B 57:289–300

Fabricius KE, Kluibenschedl A, Harrington L, Noonan S, De'ath G (2015) In situ changes of tropical crustose coralline algae along carbon dioxide gradients. Sci Rep 5:9537

Fabricius KE, Langdon C, Uthicke S, Humphrey C, Noonan S, De'ath G, Okazaki R, Muehllehner N, Glas MS, Lough JM (2011) Losers and winners in coral reefs acclimatized to elevated carbon dioxide concentrations. Nat Clim Chang 1:165–169

Fernandes AD, Reid JN, Macklaim JM, McMurrough T a, Edgell DR, Gloor GB (2014) Unifying the analysis of high-throughput sequencing datasets: characterizing RNA-seq, 16S rRNA gene sequencing and selective growth experiments by compositional data analysis. Microbiome 2:15

Hanson CA, Fuhrman JA, Horner-Devine MC, Martiny JBH (2012) Beyond biogeographic patterns: processes shaping the microbial landscape. Nat Rev Microbiol 10:497–506

Harrington L, Fabricius K, De'ath G, Negri A (2004) Recognition and selection of settlement substrata determine post-settlement survival in corals. Ecology 85:3428–3437

Hassenrück C, Fink A, Lichtschlag A, Tegetmeyer HE, Beer D de, Ramette A (2016) Quantification of the effects of ocean acidification on sediment microbial communities in the environment: the importance of ecosystem approaches. FEMS Microbiol Ecol

Hassenrück C, Hofmann LC, Bischof K, Ramette A (2015) Seagrass biofilm communities at a naturally CO_2-rich vent. Environ Microbiol Rep 7:516–525

Hoegh-Guldberg O, Mumby PJ, Hooten AJ, Steneck RS, Greenfield P, Gomez E, Harvell CD, Sale PF, Edwards a J, Caldeira K, Knowlton N, Eakin CM, Iglesias-Prieto R, Muthiga N, Bradbury RH, Dubi A, Hatziolos ME (2007) Coral reefs under rapid climate change and ocean acidification. Science 318:1737–1742

Horner-Devine MC, Carney KM, Bohannan BJM (2004) An ecological perspective on bacterial biodiversity. Proc Biol Sci 271:113–122

Hughes TP, Baird AH, Bellwood DR, Card M, Connolly SR, Folke C, Grosberg R, Hoegh-Guldberg O, Jackson JBC, Kleypas J, Lough JM, Marshall P, Nyström M, Palumbi SR, Pandolfi JM, Rosen B, Roughgarden J (2003) Climate Change, Human Impacts, and the Resilience of Coral Reefs. Review 3:929–934

Lidbury I, Johnson V, Hall-Spencer JM, Munn CB, Cunliffe M (2012) Community-level response of coastal microbial biofilms to ocean acidification in a natural carbon

dioxide vent ecosystem. Mar Pollut Bull 64:1063–1066

Lindh M V, Riemann L, Baltar F, Romero-Oliva C, Salomon PS, Granéli E, Pinhassi J (2013) Consequences of increased temperature and acidification on bacterioplankton community composition during a mesocosm spring bloom in the Baltic Sea. Environ Microbiol Rep 5:252–262

Maignien L, DeForce EA, Chafee ME, Murat Eren A, Simmons SL (2014) Ecological succession and stochastic variation in the assembly of Arabidopsis thaliana phyllosphere communities. MBio 5

Morrow KM, Moss AG, Chadwick NE, Liles MR (2012) Bacterial associates of two Caribbean coral species reveal species-specific distribution and geographic variability. Appl Environ Microbiol 78:6438–6449

Negri AP, Webster NS, Hill RT, Heyward AJ (2001) Metamorphosis of broadcast spawning corals in response to bacteria isolated from crustose algae. Mar Ecol Prog Ser 223:121–131

Newbold LK, Oliver AE, Booth T, Tiwari B, Desantis T, Maguire M, Andersen G, Gast CJ van der, Whiteley AS (2012) The response of marine picoplankton to ocean acidification. Environ Microbiol 14:2293–2307

Oksanen J, Blanchet FG, Kindt R, Legendre P, Minchin PR, O'Hara RB, Simpson GL, Solymos P, Stevens MHH, Wagner H (2015) vegan: Community Ecology Package. R package version 2.3-0. http://cran.r-project.org/package=vegan.

Oliver AE, Newbold LK, Whiteley AS, Gast CJ van der (2014) Marine bacterial communities are resistant to elevated carbon dioxide levels. Environ Microbiol Rep 6:574–582

Ramette A (2009) Quantitative community fingerprinting methods for estimating the abundance of operational taxonomic units in natural microbial communities. Appl Environ Microbiol 75:2495–505

Roguet A, Laigle GS, Therial C, Bressy A, Soulignac F, Catherine A, Lacroix G, Jardillier L, Bonhomme C, Lerch TZ, Lucas FS (2015) Neutral community model explains the bacterial community assembly in freshwater lakes. FEMS Microbiol Ecol 91:1–11

Sawall Y, Richter C, Ramette A (2012) Effects of eutrophication, seasonality and macrofouling on the diversity of bacterial biofilms in equatorial coral reefs. PLoS One 7:e39951

Shade A, Kent AD, Jones SE, Newton RJ, Triplett EW, McMahon KD (2007) Interannual dynamics and phenology of bacterial communities in a eutrophic lake. Limnol Oceanogr 52:487–494

Sneed JM, Ritson-Williams R, Paul VJ (2015) Crustose coralline algal species host distinct bacterial assemblages on their surfaces. Isme J 9:2527–2536

Sneed JM, Sharp KH, Ritchie KB, Paul VJ (2014) The chemical cue tetrabromopyrrole from a biofilm bacterium induces settlement of multiple Caribbean corals. Proc Biol Sci 281:1–9

Tebben J, Motti CA, Siboni N, Tapiolas DM, Negri AP, Schupp PJ, Kitamura M, Hatta M, Steinberg PD, Harder T (2015) Chemical mediation of coral larval settlement by crustose coralline algae. Sci Rep 5:1–11

Tebben J, Tapiolas DM, Motti CA, Abrego D, Negri AP, Blackall LL, Steinberg PD, Harder T (2011) Induction of larval metamorphosis of the coral Acropora millepora by tetrabromopyrrole isolated from a Pseudoalteromonas bacterium. PLoS One 6:1–8

Webster NS, Negri a. P, Flores F, Humphrey C, Soo R, Botté ES, Vogel N, Uthicke S (2012) Near-future ocean acidification causes differences in microbial associations within diverse coral reef taxa. Environ Microbiol Rep 5:243–251

Webster NS, Smith LD, Heyward AJ, Watts JEM, Webb RI, Blackall LL, Negri AP (2004) Metamorphosis of a Scleractinian Coral in Response to Microbial Biofilms. Appl Environ Microbiol 70:1213–1221

Webster NS, Soo R, Cobb R, Negri AP (2011) Elevated seawater temperature causes a microbial shift on crustose coralline algae with implications for the recruitment of coral larvae. ISME J 5:759–770

Webster NS, Uthicke S, Botté ES, Flores F, Negri AP (2013) Ocean acidification reduces induction of coral settlement by crustose coralline algae. Glob Chang Biol 19:303–315

Witt V, Wild C, Anthony KRN, Diaz-Pulido G, Uthicke S (2011) Effects of ocean acidification on microbial community composition of, and oxygen fluxes through, biofilms from the Great Barrier Reef. Environ Microbiol 13:2976–2989

Witt V, Wild C, Uthicke S (2011) Effect of substrate type on bacterial community composition in biofilms from the Great Barrier Reef. FEMS Microbiol Lett 323:188–195

Ylla I, Borrego C, Romaní AM, Sabater S (2009) Availability of glucose and light modulates the structure and function of a microbial biofilm: Research article. FEMS Microbiol Ecol 69:27–42

Zinger L, Amaral-Zettler L A, Fuhrman J A, Horner-Devine MC, Huse SM, Welch DBM, Martiny JBH, Sogin M, Boetius A, Ramette A (2011) Global patterns of bacterial beta-diversity in seafloor and seawater ecosystems. PLoS One 6:e24570

Supporting information

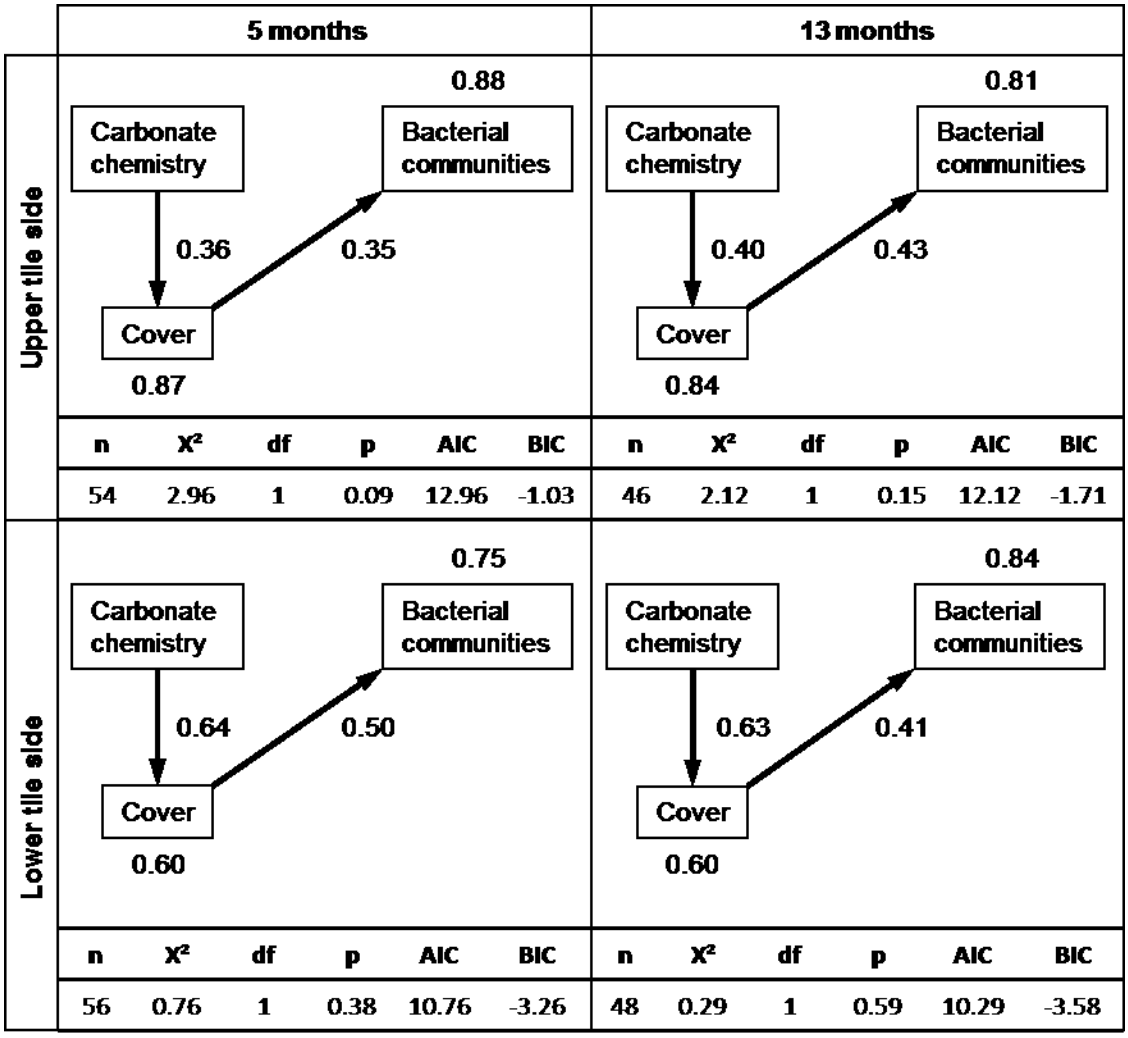

	n	X^2	df	p	AIC	BIC
Upper tile side, 5 months	54	2.96	1	0.09	12.96	-1.03
Upper tile side, 13 months	46	2.12	1	0.15	12.12	-1.71
Lower tile side, 5 months	56	0.76	1	0.38	10.76	-3.26
Lower tile side, 13 months	48	0.29	1	0.59	10.29	-3.58

Figure S1: Final models of the path analysis to test for directional relationships between carbonate chemistry (represented by pH and total alkalinity), bacterial communities and the macroorganisms (represented by percentage tile cover, data from Fabricius et al. 2015) on the settlement tiles for each tile side and sampling time. Values associated with arrows: path coefficients ($p < 0.05$), values associated with factors: unexplained variation. n: number of observations, X^2: goodness-of-fit test statistic, df: degrees of freedom, p: p-value of goodness-of-fit test, AIC: Akaike Information Criterion, BIC: Baysian Information Criterion. Path analysis performed as described previously (Sawall et al. 2012) using z-transformed values for carbonate chemistry, hellinger-transformed percentage tile cover for macroorganisms and clr-transformed relative abundance of bacterial ARISA OTUs. Initial models: carbonate chemistry → cover, carbonate chemistry → bacterial community, cover → bacterial community. In all 4 models, the path coefficient of carbonate chemistry → bacteria was non-significant and excluded from the final model.

3. Discussion and outlook

Ocean acidification (OA) is a major threat to tropical coral reefs. Since microbial communities are involved in multiple aspects of coral reef ecosystem functioning, it is important to understand how OA will affect microbial communities and the services they provide in coral reef systems. To investigate OA effects on microbial communities in an ecosystem context, hydrothermal CO_2 vents have been studied as analogues for future OA scenarios on the entire ecosystem in a natural setting. The previous chapters of this thesis explored the effect of such CO_2 vents on microbial communities in tropical coral reefs in Papua New Guinea. In the following section, I will (3.1) provide an overarching discussion of the influence of the CO_2 vents on microbial communities in various reef environments, (3.2) present hypotheses regarding whole ecosystem effects of CO_2 venting and the role of microbial communities in such effects, (3.3) discuss the challenges of translating vent effects to potential OA effects, and (3.4) give perspectives for future OA research on microbial communities at natural analogues.

3.1 Effect of hydrothermal CO_2 venting on microbial communities in different reef environments

This thesis represents the first in-depth characterization of microbial communities at shallow-water hydrothermal CO_2 vents associated with tropical coral reefs. Molecular, biogeochemical, and statistical methods showed that microbial community composition, activity, functions, and interactions with other reef organisms were fundamentally different at the CO_2 vents compared to reference sites (Table 2). However, the strength of the influence of the CO_2 vent depended on the investigated environment. Of the three environments explored in this thesis, sediment (chapters 2 and 3) and seagrass-associated microbial communities (chapter 4) were most strongly affected by the CO_2 vent, whereas the direct effect of CO_2 venting on microbial communities grown on artificial settlement tiles was negligible (chapter 5). Such environment-specific responses to CO_2 venting have also been observed in another vent system (Molari et al. in preparation).

Table 2: Summary of the observations on microbial community composition and function at the CO_2 vents in Papua New Guinea that were presented in the chapters of this thesis. Arrows indicate increase (↑) or decrease (↓). No effect indicated by a hyphen (–).

Reef environment	Effect at CO_2 vent	Chapter
Sediment		
Bacterial community	Shift in total and active community composition Evenness ↓	2, 3
Archaeal community	Shift in total community composition Evenness ↓	2
Element cycling	Photosynthesis − Carbon fixation − Carbohydrate degradation − Oxygen consumption ↓ Nitrogen fixation[a] (↑)↓ Nitrification ↑ DNRA ↓ Sulfate reduction ↓ Arsenite oxidation ↑	1, 3
Seagrass leaves		
Bacterial biofilm	Shift in community composition Disease-associated ↑	4
Eukaryotic biofilm	Shift in community composition Diversity of crustose coralline algae ↓	4
Settlement tiles		
Bacterial biofilm	Community composition: minor	5

[a] Nitrogen fixation did not show a monotonous decreasing trend from reference to vent sites, but exhibited increased *nif* gene expression levels at medium hydrothermal influence (HI).

In this thesis, the differences in the strength of the vent effect were most likely due to two main factors: exposure time and substrate influence. The sediment has been exposed to the environmental conditions at the CO_2 vent for several decades (Fabricius et al. 2011), whereas the surface of seagrass leaves and settlement tiles was only subject to CO_2 venting for several months depending on growth rate and deployment time, respectively. The long-term exposure to the CO_2 vent has moreover drastically altered sediment characteristics, reducing grain size, calcium carbonate content, and permeability, as well as altering pore water chemistry (chapter 1). These changes further contributed to the differences in sediment microbial communities between reference and vent sites additional to the pure pCO_2/pH effects. The difference in the strength of the vent effect between microbial communities associated with seagrass leaves and settlement tiles appeared to be substrate-related. Seagrass leaves represent a living

substrate that may have the ability to influence the development of its epiphytic biofilm, thus constraining the composition of biofilm communities (Michael et al. 2008). Artificial settlement tiles constitute an inert substrate, where biofilm development is not controlled by biotic interactions with the substrate, and which may therefore host a more heterogeneous macroscopic and microbial community (chapter 5). Although only a limited number of reef environments were investigated in this thesis, coral-associated microbial communities also exhibited environment-specific, i.e. host-specific, vent effects (Morrow et al. 2014). The consideration of the interaction between CO_2 venting and environment-specific conditions in this context is therefore crucial for the assessment of microbial communities at hydrothermal CO_2 vents.

3.2 Whole ecosystem effects of hydrothermal CO_2 venting in a coral reef

Coral reefs constitute a highly complex ecosystem, where changes in microbially mediated processes such as nutrient cycling, remineralization, and larval settlement can have profound effects on the whole reef community (Rasheed et al. 2002, Webster et al. 2004, Webster & Hill 2007, Ainsworth et al. 2010, Garren & Azam 2012). Thereby, it is important to consider that such changes are not unidirectional, and that microbial communities are in turn influenced by changes in reef macroflora and -fauna (Kline et al. 2006, Haas et al. 2011). Given the complex interactions of direct and indirect effects among abiotic and biotic components of coral reef ecosystems, it is difficult to estimate not only consequences of hydrothermal CO_2 venting on individual components of the ecosystems, but also on the interactions between such components, and to identify causal relationships. This thesis has so far mostly focused on the effect on CO_2 venting on microbial communities, as one component of coral reef ecosystems, providing data on microbial diversity, community composition and function, as well as rudimentary information on interactions with other reef organisms. Here, I combined data on microbial communities with the results of previous studies on other reef organisms at the same sampling sites to construct a more comprehensive picture of the coral reef ecosystem at the hydrothermal CO_2 vents in Papua New Guinea, and the role of microbial communities therein (Figure 5).

I propose that direct abiotic effects (e.g. pH, temperature, hydrothermal fluids) and indirect abiotic effects (e.g. permeability, grain size) of the vent activity severely alter the environment in the sediment causing a shift in the microbial community (chapters 1 and 2). In the water column the impact of the hydrothermal activity is diluted so that only the carbonate chemistry is strongly affected (Fabricius et al. 2011). The decrease in water column pH and increased availability of CO_2 has direct effects on the physiology of corals and seagrasses (Strahl, Francis, et al. 2015, Strahl, Stolz, et al. 2015, Takahashi et al. 2015), and may directly or indirectly result in a decline of coral recruitment by reducing the abundance and diversity of crustose coralline algae (Fabricius et al. 2015; chapter 4). Such changes lead to a shift from structurally complex corals to a reef dominated by more massive corals and seagrasses at the CO_2 vent (Fabricius et al. 2011, 2014). An increased prevalence of potential coral pathogens at the CO_2 vent may further contribute to a decline in reef health (chapter 4). The shift in the macroscopic reef community may alter the composition and possibly the amount of released organic material, which is remineralized in the sediment by microbial communities. Due to the reduced permeability, less organic matter is percolated into the sediment, and oxygen penetrates less deep (chapter 1). These conditions may contribute to reduced aerobic and anaerobic remineralization rates, such as oxygen consumption, sulfate reduction, and possibly also nitrate reduction, as well as a shift in the microbial organisms responsible for organic carbon degradation (chapters 1 and 3). The decreased permeability may also lead to decreased nitrogen fixation, i.e. conversion of dinitrogen to ammonium, which is then probably supplied mostly by the hydrothermal vent, and may fuel increased nitrification rates (chapter 3). In conjunction, the changes in remineralization processes may alter the nutrient balance and turnover at the CO_2 vent, and may thus influence reef productivity. Yet, microphytobenthic communities seemed to maintain stable photosynthesis and carbon fixation rates at the CO_2 vent, despite changes in the composition of the photosynthetic microbial community (chapter 3). The stable photosynthesis rates may result from a trade-off between beneficial effects such as reduced meiofaunal grazer abundance (chapter 1) and increased CO_2 availability, and detrimental effects such as UV stress and increased concentrations of toxic trace elements (chapter 3).

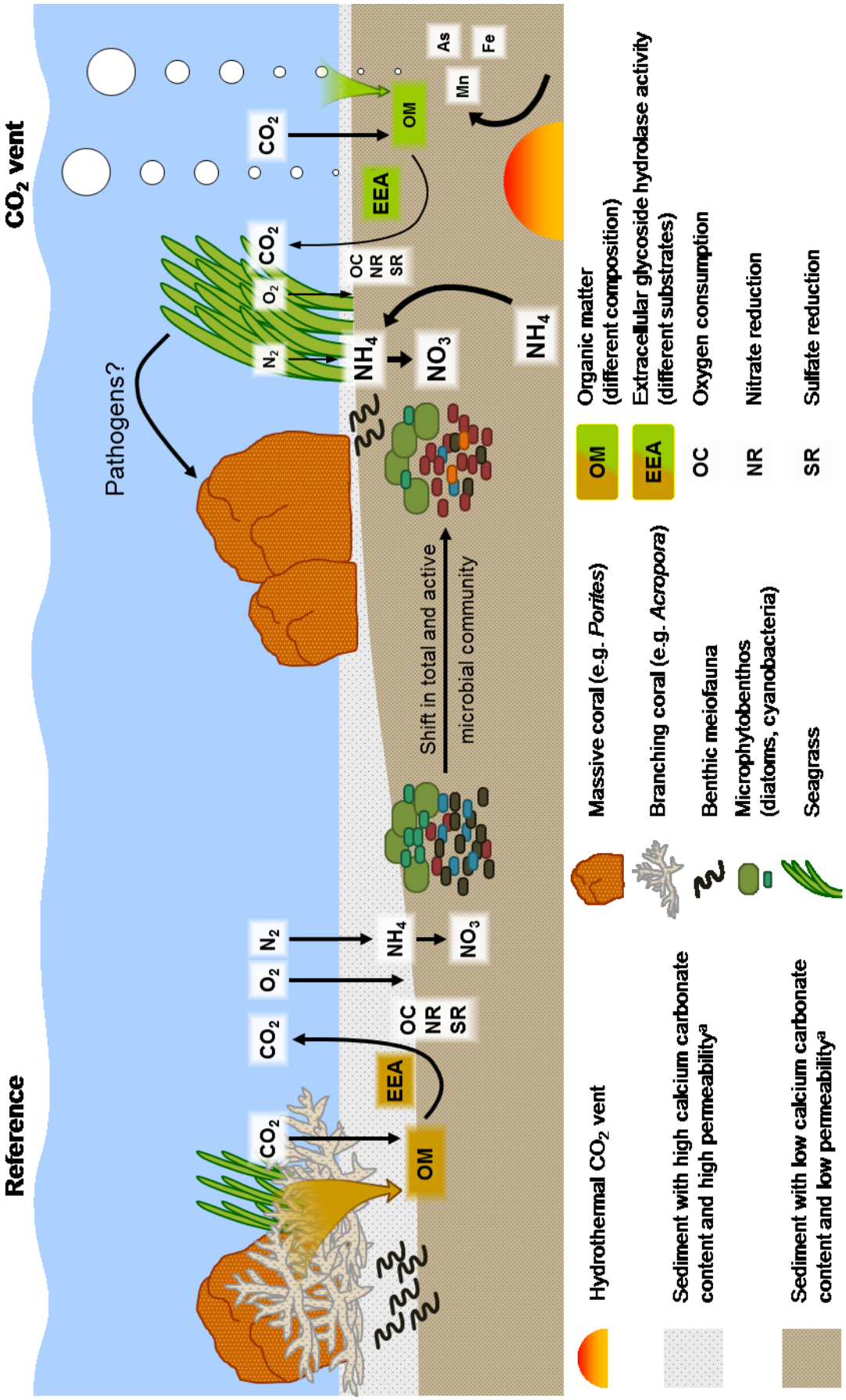

Figure 5: Hypothesized role of microbial communities in the coral reef ecosystem under reference conditions and at the shallow-water hydrothermal CO_2 vents in Papua New Guinea. [a] The shallowing of the oxygen penetration depth is illustrated by the smaller proportion of the light grey area in the figure. However, that does not mean that low calcium carbonate sediment only occurs beneath the oxygen penetration depth. The sediment is well mixed and contains homogeneously less calcium carbonate at the CO_2 vent.

Unlike deep-sea vents, which constitute hotspots of biological productivity and diversity in otherwise desert-like system, hydrothermal CO_2 vents in coral reefs, which on their own are highly productive and diverse ecosystems, may represent an extreme disturbance resulting in a severe decline of the ecosystem. However, our understanding of the complex ecosystem dynamics at the hydrothermal CO_2 vents in Papua New Guinea is still limited, and many of the relationships discussed above are so far only supported by preliminary data. Further studies are necessary to confirm the hypothesized changes in ecosystem functioning at the CO_2 vents.

3.3 Suitability of hydrothermal CO_2 vents as OA analogues

The opportunity to observe ecosystem-wide effects, such as those described in the previous section, makes natural analogues for future OA so attractive to scientists. However, the challenge remains to determine, which conditions at natural analogues still represent realistic scenarios for future ocean conditions. When using hydrothermal CO_2 vents as analogues for OA, OA effects may be confounded by other parameters that are not related to OA, e.g. temperature and hydrothermal fluids (Vizzini et al. 2013; chapters 1 and 2). Often, the knowledge of confounding parameters is limited, and the distinction between realistic and unrealistic conditions for OA in combination with the subsequent selection of study sites as natural OA analogues at hydrothermal CO_2 vents is difficult. An insufficient understanding of the environment at natural OA analogues may result in inconsistent conclusions regarding OA effects on marine life from different studies, which may complicate advising policy makers about consequences of future climate change.

Furthermore, the degree to which OA effects at natural analogues are confounded by other parameters depends on the investigated environment. At the hydrothermal CO_2 vents in Papua New Guinea, the effect of the CO_2 venting appears to be restricted to changes in the carbonate chemistry of the water column as expected under future OA scenarios (Fabricius et al. 2011), whereas the sediment is strongly influenced by additional parameters not related to OA. Even with an extensive environmental characterization (chapter 1), the work here has shown how challenging it is to attribute biotic responses in the sediment to potential OA effects (chapter 2). Therefore, unless a

detailed characterization of the environment is performed, hydrothermal CO_2 vents may be more suitable as OA analogues when investigating organisms exposed to the water column than those in the sediment.

3.4 Future of microbial research at natural OA analogues

Despite the new insights into microbial communities at the shallow-water hydrothermal CO_2 vents in Papua New Guinea, this thesis has shown that there are still many open questions regarding OA effects on microbes in general, and at natural OA analogues in particular, as well as their role in a changing ocean. Many aspects of the impact of OA on microbial life in coral reef ecosystems are not yet or not yet fully understood. Especially, changes in microbial processes and resulting consequences on the ecosystem are still underexplored.

The development of molecular techniques, particularly next generation sequencing, offered a fast and logistically convenient way to screen microbial communities in environmental samples. However, the information provided by sequencing techniques is limited regarding quantitative data on the abundance and functional role of microbial organisms. Sequencing studies that use either taxonomic affiliation or the expression of functional marker genes to assess microbial processes should be supported by biogeochemical measurements of functional rates (chapter 3). Furthermore, when analyzing highly complex environmental microbial communities using meta-omics sequencing approaches, sequencing depths may often not be sufficient for a detailed, high-resolution characterization of microbial communities. Additionally, sequencing techniques only provide relative and not absolute abundance data. Although usually more time-consuming compared to sequencing, quantitative methods, such as qPCR, or classical microscopy-based techniques, such as catalyzed reporter deposition-fluorescence *in situ* hybridization (CARD-FISH), should be used to confirm trends in relative sequence abundance. For a more targeted investigation of the role of specific taxa in microbial processes, more sophisticated methods, such as RNA-stable isotope probing (RNA-SIP) or nanoscale secondary ion mass spectrometry (nanoSIMS), may be applicable. Whereas mostly molecular screening methods were used in this thesis, a combined approach of screening and targeted techniques will be necessary to elucidate

changes in microbial communities and functions at natural OA analogues such as shallow-water hydrothermal CO_2 vents.

At natural analogues, the identification of the effect of interest, i.e. OA-related impacts, on microbial communities is mainly realized by statistical methods (chapter 2). However, to disentangle the influence of environmental parameters on microbial communities in a complex natural setting, a high level of replication and knowledge of a broad range of environmental parameters is necessary. Meeting these requirements of statistical analyses often involves a complex logistic effort during sample collection, which is a limiting factor when research is conducted in remote areas, such as the CO_2 vents investigated in this thesis, but which should be increasingly addressed in future studies. Another issue with studies at natural OA analogues is the lack of replication of the analogue site itself. The two vent systems investigated in this thesis hosted different microbial communities, especially in the sediment (chapter 2). While providing valuable information about a specific analogue site for OA, it is possible that isolated observations might bias more general conclusions about potential OA effects. To gain a broader understanding of OA impacts on microbial communities based on investigations at natural OA analogues, observations should include several analogue sites. Theoretically, such an across-site comparison could be achieved by a meta-analysis of existing data. However, due to inconsistent methodologies between different studies and, more importantly, different sets of recorded environmental parameters, such a comparison may be difficult. Furthermore, the number of known sites that can be used as natural OA analogues is limited. Future research should therefore focus on streamlining the methodology for OA studies at natural analogues, and investigating a larger number of natural analogues. Another aspect that so far has received little attention, but should be further explored, are the effects of temporal variability at natural OA analogues.

In summary, for future work at natural OA analogues I would recommend a dual approach, starting with a combination of deep meta-omics sequencing to screen microbial community composition and functions, and biogeochemical measurements of a broad range of environmental parameters and functional rates in a highly replicated sampling design. Afterwards, more targeted techniques should be used to quantify ecologically relevant microbial groups and to assess their functions in response to changes in OA-

related parameters. Additionally, several natural analogues should be monitored over longer time periods to confirm that observed patterns can be generalized. Furthermore, to provide a holistic picture of coral reef ecosystem functioning at natural OA analogues, data on changes in microbial communities and functions should be interpreted in respect to the whole reef community.

Bibliography

Ainsworth TD, Vega Thurber R, Gates RD (2010) The future of coral reefs: a microbial perspective. Trends Ecol Evol 25:233–240.

Allgaier M, Riebesell U, Vogt M, Thyrhaug R, Grossart HP (2008) Coupling of heterotrophic bacteria to phytoplankton bloom development at different pCO_2 levels: a mesocosm study. Biogeosciences Discuss 5:317–359.

Avaniss-Aghajani E, Jones K, Chapman D, Brunk C (1994) A molecular technique for identification of bacteria using small subunit ribosomal RNA sequences. Biotechniques 17:144–146, 148–149.

Barker S, Ridgwell A (2012) Ocean Acidification. Nat Educ Knowl 3:21.

Beman JM, Chow C-E, King AL, Feng Y, Fuhrman JA, Andersson A, Bates NR, Popp BN, Hutchins DA (2011) Global declines in oceanic nitrification rates as a consequence of ocean acidification. Proc Natl Acad Sci U S A 108:208–213.

Boucher G, Clavier J, Hily C, Gattuso JP (1998) Contribution of soft-bottoms to the community metabolism (primary production and calcification) of a barrier reef flat (Moorea, French Polynesia). J Exp Mar Bio Ecol 225:269–283.

Bourne D, Iida Y, Uthicke S, Smith-Keune C (2008) Changes in coral-associated microbial communities during a bleaching event. ISME J 2:350–363.

Braeckman U, Colen C Van, Guilini K, Gansbeke D Van, Soetaert K, Vincx M, Vanaverbeke J (2014) Empirical Evidence Reveals Seasonally Dependent Reduction in Nitrification in Coastal Sediments Subjected to Near Future Ocean Acidification. PLoS One 9:e108153.

Brussaard CPD, Noordeloos AAM, Witte H, Collenteur MCJ, Schulz K, Ludwig A, Riebesell U (2013) Arctic microbial community dynamics influenced by elevated CO_2 levels. Biogeosciences 10:719–731.

Burrell TJ, Maas EW, Hulston DA, Law CS (2015) Bacterial abundance , processes and diversity responses to acidification at a coastal CO_2 vent. FEMS Microbiol Lett 362.

Caldeira K, Wickett ME (2003) Anthropogenic carbon and ocean pH. Nature 425:365.

Cardigos F, Colaco A, Dando PR, Avila SP, Sarradin PM, Tempera F, Conceicao P, Pascoal A, Santos RS (2005) Shallow water hydrothermal vent field fluids and communities of the D. Joao de Castro Seamount (Azores). Chem Geol 224:153–168.

Chauhan A, Pathak A, Rodolfo-metalpa R, Milazzo M, Green SJ, Hall-spencer JM (2015) Metagenomics Reveals Planktonic Bacterial Community Shifts across a Natural CO 2 Gradient in the Mediterranean Sea. Genome Announc 3:e01543.

Czerny J, Barcelos e Ramos J, Riebesell U (2009) Influence of elevated CO_2 concentrations on cell division and nitrogen fixation rates in the bloom-forming cyanobacterium *Nodularia spumigena*. Biogeosciences Discuss 6:4279–4304.

Dang H, Lovell CR (2000) Bacterial Primary Colonization and Early Succession on Surfaces in Marine Waters as Determined by Amplified rRNA Gene Restriction Analysis and Sequence Analysis of 16S rRNA Genes. Appl Environ Microbiol 66:467–475.

Doney SC, Fabry VJ, Feely RA, Kleypas JA (2009) Ocean Acidification: The Other CO_2 Problem. Ann Rev Mar Sci 1:169–192.

Dupont S, Ortega-Martinez O, Thorndyke M (2010) Impact of near-future ocean acidification on echinoderms. Ecotoxicology 19:449–462.

Edgar RC (2013) UPARSE: highly accurate OTU sequences from microbial amplicon reads. Nat Methods 10:996–998.

Endres S, Galgani L, Riebesell U, Schulz KG, Engel A (2014) Stimulated bacterial growth under elevated pCO_2: Results from an off-shore mesocosm study. PLoS One 9:1–8.

Fabricius KE, De'ath G, Noonan S, Uthicke S (2014) Ecological effects of ocean acidification and habitat complexity on reef-associated macroinvertebrate communities. Proc R Soc B 281:20132479.

Fabricius KE, Kluibenschedl A, Harrington L, Noonan S, De'ath G (2015) In situ changes of tropical crustose coralline algae along carbon dioxide gradients. Sci Rep 5:9537.

Fabricius KE, Langdon C, Uthicke S, Humphrey C, Noonan S, De'ath G, Okazaki R, Muehllehner N, Glas MS, Lough JM (2011) Losers and winners in coral reefs acclimatized to elevated carbon dioxide concentrations. Nat Clim Chang 1:165–169.

Fadrosh DW, Ma B, Gajer P, Sengamalay N, Ott S, Brotman RM, Ravel J (2014) An improved dual-indexing approach for multiplexed 16S rRNA gene sequencing on the Illumina MiSeq platform. Microbiome 2:6.

Fenchel T, Jorgensen BB (1977) Detritus food chains of aquatic ecosystems: the role of bacteria. Adv Microb Ecol 1:1–57.

Fernandes AD, Reid JN, Macklaim JM, McMurrough T a, Edgell DR, Gloor GB (2014) Unifying the analysis of high-throughput sequencing datasets: characterizing RNA-seq, 16S rRNA gene sequencing and selective growth experiments by compositional data analysis. Microbiome 2:15.

Fisher MM, Triplett EW (1999) Automated Approach for Ribosomal Intergenic Spacer Analysis of Microbial Diversity and Its Application to Freshwater Bacterial Communities Automated Approach for Ribosomal Intergenic Spacer Analysis of Microbial Diversity and Its Application to Freshwater. Appl Environ Microbiol 65:4630–4636.

Fu F, Mulholland MR, Garcia NS, Beck A, Bernhardt PW, Warner ME, Sanudo-Wilhelmy SA, Hutchins DA (2008) Interactions between changing pCO_2, N_2 fixation, and Fe limitation in the marine unicellular cyanobacterium Crocosphaera. Limnol Oceanogr 53:2472–2484.

Garren M, Azam F (2012) New directions in coral reef microbial ecology. Environ Microbiol 14:833–844.

Gattuso J-P, Frankignoulle M, Wollast R (1998) Carbon and the carbonate metabolism in coastal aquatic ecosystems. Annu Rev Ecol Evol Syst 29:405–434.

Gazeau F, Quiblier C, Jansen JM, Gattuso JP, Middelburg JJ, Heip CHR (2007) Impact of elevated CO_2 on shellfish calcification. Geophys Res Lett 34:1–5.

Gazeau F, Rijswijk P Van, Pozzato L, Middelburg JJ (2014) Impacts of ocean acidification on sediment processes in shallow waters of the Arctic Ocean. PLoS One 9.

German CR, Damm KL von (2003) Hydrothermal Processes. Treatise on Geochemistry 6:181–222.

Gobet A, Boetius A, Ramette A (2014) Ecological coherence of diversity patterns derived from classical fingerprinting and Next Generation Sequencing techniques. Environ Microbiol 16:2672–2681.

Gradoville MR, White AE, Bo D, Church MJ, Letelier RM (2014) Diversity trumps acidification : Lack of evidence for carbon dioxide enhancement of Trichodesmium community nitrogen or carbon fixation at Station ALOHA. Limnol Oceanogr 59:645–659.

Grossart HP, Allgaier M, Passow U, Riebesell U (2006) Testing the effect of CO_2 concentration on the dynamics of marine heterotrophic bacterioplankton. Limnol Oceanogr 51:1–11.

Haas AF, Nelson CE, Kelly LW, Carlson CA, Rohwer F, Leichter JJ, Wyatt A, Smith JE (2011) Effects of coral reef benthic primary producers on dissolved organic carbon and microbial activity. PLoS One 6:e27973.

Hall-Spencer JM, Rodolfo-Metalpa R, Martin S, Ransome E, Fine M, Turner SM, Rowley SJ, Tedesco D, Buia M-C (2008) Volcanic carbon dioxide vents show ecosystem effects of ocean acidification. Nature 454:96–99.

Hoegh-Guldberg O, Mumby PJ, Hooten AJ, Steneck RS, Greenfield P, Gomez E, Harvell CD, Sale PF, Edwards a J, Caldeira K, Knowlton N, Eakin CM, Iglesias-Prieto R, Muthiga N, Bradbury RH, Dubi A, Hatziolos ME (2007) Coral reefs under rapid climate change and ocean acidification. Science 318:1737–1742.

Huesemann MH, Skillman AD, Crecelius EA (2002) The inhibition of marine nitrification by ocean disposal of carbon dioxide. Mar Pollut Bull 44:142–148.

Hunter S, Corbett M, Denise H, Fraser M, Gonzalez-Beltran A, Hunter C, Jones P, Leinonen R, McAnulla C, Maguire E, Maslen J, Mitchell A, Nuka G, Oisel A, Pesseat S, Radhakrishnan R, Rocca-Serra P, Scheremetjew M, Sterk P, Vaughan D, Cochrane G, Field D, Sansone SA (2014) EBI metagenomics - A new resource for the analysis and archiving of metagenomic data. Nucleic Acids Res 42:600–606.

Hutchins DA, Fu F-X, Zhang Y, Warner ME, Feng Y, Portune K, Bernhardt PW, Mulholland MR (2007) CO_2 control of Trichodesmium N_2 fixation, photosynthesis, growth rates, and elemental ratios: Implications for past, present, and future ocean biogeochemistry. Limnol Oceanogr 52:1293–1304.

Hutchins DA, Mulholland MR, Fu F (2009) Nutrient cycles and Marine Microbes in a CO_2-enriched ocean. Oceanography 22:128–145.

IPCC (2013) Summary for Policymakers. In: Stocker TF, Qin D, Plattner G-K, Tignor K, Allen SK, Boschung J, Nauels A, Xia Y, Bex V, Midgley PM (eds) Climate Change 2013: The Physical Science Basis. Contribution of Working Group I to the Fifth Assessment Report of the Intergovernmental Panel on Climate Change. Cambridge University Press, Cambridge, United Kingdom and New York, NY, USA, p 1–30.

Johnson V, Brownlee C, Milazzo M, Hall-Spencer J (2015) Marine Microphytobenthic Assemblage Shift along a Natural Shallow-Water CO_2 Gradient Subjected to Multiple Environmental Stressors. J Mar Sci Eng 3:1425–1447.

Johnson VR, Brownlee C, Rickaby REM, Graziano M, Milazzo M, Hall-Spencer JM (2011) Responses of marine benthic microalgae to elevated CO_2. Mar Biol 160:1813–1824.

Johnson VR, Russell BD, Fabricius KE, Brownlee C, Hall-Spencer JM (2012) Temperate and tropical brown macroalgae thrive, despite decalcification, along natural CO_2 gradients. Glob Chang Biol 18:2792–2803.

Joint I, Doney SC, Karl DM (2011) Will ocean acidification affect marine microbes? ISME J 5:1–7.

Kerfahi D, Hall-Spencer JM, Tripathi BM, Milazzo M, Lee J, Adams JM (2014) Shallow Water Marine Sediment Bacterial Community Shifts Along a Natural CO_2 Gradient in the Mediterranean Sea Off Vulcano, Italy. Environ Microbiol 67:819–828.

Kim M, Oh HS, Park SC, Chun J (2014) Towards a taxonomic coherence between average nucleotide identity and 16S rRNA gene sequence similarity for species demarcation of prokaryotes. Int J Syst Evol Microbiol 64:346–351.

Kitidis V, Laverock B, McNeill LC, Beesley A, Cummings D, Tait K, Osborn MA, Widdicombe S (2011) Impact of ocean acidification on benthic and water column ammonia oxidation. Geophys Res Lett 38:1–5.

Kline DI, Kuntz NM, Breitbart M, Knowlton N, Rohwer F (2006) Role of elevated organic carbon levels and microbial activity in coral mortality. Mar Ecol Prog Ser 314:119–125.

Koch M, Bowes G, Ross C, Zhang X-H (2013) Climate change and ocean acidification effects on seagrasses and marine macroalgae. Glob Chang Biol 19:103–132.

Krause E, Wichels A, Giménez L, Lunau M, Schilhabel MB, Gerdts G (2012) Small changes in pH have direct effects on marine bacterial community composition: a microcosm approach. PLoS One 7:e47035.

Kroeker KJ, Kordas RL, Crim R, Hendriks IE, Ramajo L, Singh GS, Duarte CM, Gattuso J-P (2013) Impacts of ocean acidification on marine organisms: quantifying sensitivities and interaction with warming. Glob Chang Biol 19:1884–1896.

Laverock B, Kitidis V, Tait K, Gilbert JA, Osborn AM, Widdicombe S (2013) Bioturbation determines the response of benthic ammonia-oxidizing microorganisms to ocean acidification. Philos Trans R Soc B 368:20120441.

Li W, Fu L, Niu B, Wu S, Wooley J (2012) Ultrafast clustering algorithms for metagenomic sequence analysis. Brief Bioinform 13:656–668.

Lidbury I, Johnson V, Hall-Spencer JM, Munn CB, Cunliffe M (2012) Community-level response of coastal microbial biofilms to ocean acidification in a natural carbon dioxide vent ecosystem. Mar Pollut Bull 64:1063–1066.

Lindh M V, Riemann L, Baltar F, Romero-Oliva C, Salomon PS, Granéli E, Pinhassi J (2013) Consequences of increased temperature and acidification on bacterioplankton community composition during a mesocosm spring bloom in the Baltic Sea. Environ Microbiol Rep 5:252–262.

Little TA, Hacker BR, Gordon SM, Baldwin SL, Fitzgerald PG, Ellis S, Korchinski M (2011) Diapiric exhumation of Earth's youngest (UHP) eclogites in the gneiss domes of the D'Entrecasteaux Islands, Papua New Guinea. Tectonophysics 510:39–68.

Liu L, Li Y, Li S, Hu N, He Y, Pong R, Lin D, Lu L, Law M (2012) Comparison of next-generation sequencing systems. J Biomed Biotechnol 2012:1–11.

Liu J, Weinbauer M, Maier C, Dai M, Gattuso J-P (2010) Effect of ocean acidification on microbial diversity and on microbe-driven biogeochemistry and ecosystem functioning. Aquat Microb Ecol 61:291–305.

Lomas M, Hopkinson B, Losh J, Ryan D, Shi D, Xu Y, Morel F (2012) Effect of ocean acidification on cyanobacteria in the subtropical North Atlantic. Aquat Microb Ecol 66:211–222.

Maas E, Law C, Hall J, Pickmere S, Currie K, Chang F, Voyles K, Caird D (2013) Effect of ocean acidification on bacterial abundance, activity and diversity in the Ross Sea, Antarctica. Aquat Microb Ecol 70:1–15.

Mahé F, Rognes TT, Quince C, Vargas C de, Dunthorn M (2014) Swarm: robust and fast clustering method for amplicon-based studies. PeerJ:2:e593.

McMurdie PJ, Holmes S (2014) Waste not, want not: why rarefying microbiome data is inadmissible. PLoS Comput Biol 10:e1003531.

Meron D, Atias E, Iasur Kruh L, Elifantz H, Minz D, Fine M, Banin E (2011) The impact of reduced pH on the microbial community of the coral Acropora eurystoma. ISME J 5:51–60.

Meron D, Buia M-C, Fine M, Banin E (2013) Changes in microbial communities associated with the sea anemone Anemonia viridis in a natural pH gradient. Microb Ecol 65:269–76.

Meron D, Rodolfo-Metalpa R, Cunning R, Baker AC, Fine M, Banin E (2012) Changes in coral microbial communities in response to a natural pH gradient. ISME J 2100:1–11.

Michael TS, Shin HW, Hanna R, Spafford DC (2008) A review of epiphyte community development: Surface interactions and settlement on seagrass. J Environ Biol 29:629–638.

Morrow KM, Bourne DG, Humphrey C, Botté ES, Laffy P, Zaneveld J, Uthicke S, Fabricius KE, Webster NS (2014) Natural volcanic CO_2 seeps reveal future trajectories for host-microbial associations in corals and sponges. ISME J 2:1–15.

Munday PL, Cheal AJ, Dixson DL, Rummer JL, Fabricius KE (2014) Behavioural impairment in reef fishes caused by ocean acidification at CO 2 seeps. Nat Clim Chang 4:487–492.

Newbold LK, Oliver AE, Booth T, Tiwari B, Desantis T, Maguire M, Andersen G, Gast CJ van der, Whiteley AS (2012) The response of marine picoplankton to ocean acidification. Environ Microbiol 14:2293–307.

Oliver AE, Newbold LK, Whiteley AS, Gast CJ van der (2014) Marine bacterial communities are resistant to elevated carbon dioxide levels. Environ Microbiol Rep 6:574–582.

Orr JC, Fabry VJ, Aumont O, Bopp L, Doney SC, Feely RA, Gnanadesikan A, Gruber N, Ishida A, Joos F, Key RM, Lindsay K, Maier-Reimer E, Matear R, Monfray P, Mouchet A, Najjar RG, Plattner G-K, Rodgers KB, Sabine CL, Sarmiento JL, Schlitzer R, Slater RD, Totterdell IJ, Weirig M-F, Yamanaka Y, Yool A (2005) Anthropogenic ocean acidification over the twenty-first century and its impact on calcifying organisms. Nature 437:681–686.

Pelejero C, Calvo E, Hoegh-Guldberg O (2010) Paleo-perspectives on ocean acidification. Trends Ecol Evol 25:332–344.

Piontek J, Borchard C, Sperling M, Schulz KG, Riebesell U, Engel A (2013) Response of bacterioplankton activity in an Arctic fjord system to elevated pCO_2: Results from a mesocosm perturbation study. Biogeosciences 10:297–314.

Piontek J, Lunau M, Händel N, Borchard C, Wurst M, Engel A (2010) Acidification increases microbial polysaccharide degradation in the ocean. Biogeosciences 7:1615–1624.

Prol-Ledesma RM, Canet C, Torres-Vera MA, Forrest MJ, Armienta MA (2004) Vent fluid chemistry in Bahía Concepción coastal submarine hydrothermal system, Baja California Sur, Mexico. J Volcanol Geotherm Res 137:311–328.

Ragazzola F, Foster LC, Form A, Anderson PSL, Hansteen TH, Fietzke J (2012) Ocean acidification weakens the structural integrity of coralline algae. Glob Chang Biol 18:2804–2812.

Rasheed M, Badran MI, Richter C, Huettel M (2002) Effect of reef framework and bottom sediment on nutrient enrichment in a coral reef of the Gulf of Aqaba, Red Sea. Mar Ecol Prog Ser 239:277–285.

Raulf FF, Fabricius KE, Uthicke S, Beer D de, Abed RMM, Ramette A (2015) Changes in microbial communities in coastal sediments along natural CO_2 gradients at a volcanic vent in Papua New Guinea. Environ Microbiol 17:3678–3691.

Roy A-S, Gibbons SM, Schunck H, Owens S, Caporaso JG, Sperling M, Nissimov JI, Romac S, Bittner L, Mühling M, Riebesell U, LaRoche J, Gilbert JA (2013) Ocean acidification shows negligible impacts on high-latitude bacterial community structure in coastal pelagic mesocosms. Biogeosciences 10:555–566.

Rusch A, Gaidos E (2013) Nitrogen-cycling bacteria and archaea in the carbonate sediment of a coral reef. Geobiology 11:472–484.

Russell BD, Connell SD, Uthicke S, Muehllehner N, Fabricius KE, Hall-Spencer JM

(2013) Future seagrass beds: Can increased productivity lead to increased carbon storage? Mar Pollut Bull 73:463–469.

Sala MM, Aparicio FL, Boras JA, Borrull E, Cardelus C, Cros L, Gomes A, Lopez-Sanz A, Malits A, Martinez RA, Mestre M, Movilla J, Sarmento H, Vazquez-Dominguez E, Vaque D, Pinhassi J, Calbet A, Calvo E, Gasol JM, Pelejero C, Marrase C (2016) Contrasting effects of ocean acidification on the microbial food web under different trophic conditions. ICES J Mar Sci 73:670–679.

Sato Y, Willis BL, Bourne DG (2010) Successional changes in bacterial communities during the development of black band disease on the reef coral, Montipora hispida. ISME J 4:203–214.

Schloss PD, Westcott SL, Ryabin T, Hall JR, Hartmann M, Hollister EB, Lesniewski RA, Oakley BB, Parks DH, Robinson CJ, Sahl JW, Stres B, Thallinger GG, Horn DJ Van, Weber CF (2009) Introducing mothur: open-source, platform-independent, community-supported software for describing and comparing microbial communities. Appl Environ Microbiol 75:7537–7541.

Strahl J, Francis DS, Doyle J, Humphrey C, Fabricius KE (2015) Biochemical responses to ocean acidification contrast between tropical corals with high and low abundances at volcanic carbon dioxide seeps. ICES J Mar Sci:1–13.

Strahl J, Stolz I, Uthicke S, Vogel N, Noonan SHC, Fabricius KE (2015) Physiological and ecological performance differs in four coral taxa at a volcanic carbon dioxide seep. Comp Biochem Physiol Part A 184:179–186.

Tait K, Laverock B (2013) Minor impact of ocean acidification to the composition of the active microbial community in an Arctic sediment. Environ Microbiol Rep 5:851–860.

Tait K, Laverock B, Widdicombe S (2014) Response of an Arctic Sediment Nitrogen Cycling Community to Increased CO_2. Estuaries and Coasts 37:724–735

Takahashi M, Noonan SHC, Fabricius KE, Collier CJ (2015) The effects of long-term in situ CO_2 enrichment on tropical seagrass communities at volcanic vents. ICES J Mar Sci:1–11.

Tang K (2013) Microbial Communities in a Shallow-Sea Hydrothermal System. In: Nelson KE (ed) Encyclopedia of Metagenomics.

Tang K, Liu K, Jiao N, Zhang Y, Chen CTA (2013) Functional Metagenomic Investigations of Microbial Communities in a Shallow-Sea Hydrothermal System. PLoS One 8:1–11.

Tarasov VG, Gebruk A V., Mironov AN, Moskalev LI (2005) Deep-sea and shallow-water hydrothermal vent communities: Two different phenomena? Chem Geol 224:5–39.

Taylor JD, Ellis R, Milazzo M, Hall-Spencer JM, Cunliffe M (2014) Intertidal epilithic bacteria diversity changes along a naturally occurring carbon dioxide and pH gradient. FEMS Microbiol Ecol 89:670–678.

Tregoning P, Lambeck K, Stolz A, Morgan P, McClusky SC, Beek P van der, McQueen H, Jackson RJ, Little RP, Laing A, Murphy B (1998) Estimation of current plate motions in Papua New Guinea from Global Positioning System observations. J Geophys Res 103:12181–12203.

Uthicke S, Momigliano P, Fabricius KE (2013) High risk of extinction of benthic foraminifera in this century due to ocean acidification. Sci Rep 3:1769.

Vega Thurber R, Willner-Hall D, Rodriguez-Mueller B, Desnues C, Edwards RA, Angly F, Dinsdale E, Kelly L, Rohwer F (2009) Metagenomic analysis of stressed coral holobionts. Environ Microbiol 11:2148–2163.

Vizzini S, Leonardo R Di, Costa V, Tramati CD, Luzzu F, Mazzola A (2013) Trace element bias in the use of CO_2-vents as analogues for low-pH environments: Implications for contamination levels in acidified oceans. Estuar Coast Shelf Sci 134:19–30.

Vogel N, Fabricius KE, Strahl J, Noonan SHC, Wild C, Uthicke S (2015) Calcareous green alga halimeda tolerates ocean acidification conditions at tropical carbon dioxide seeps. Limnol Oceanogr 60:263–275.

Webster N, Hill R (2007) Vulnerability of marine microbes on the Great Barrier Reef to climate change. In: Johnson J, Marshall P (eds) Climate Change and the Great Barrier Reef: A Vulnerability Assessment. The Great Barrier Reef Marine Park Authority and Australian Greenhouse Office, Australia, p 97–120.

Webster NS, Negri a. P, Flores F, Humphrey C, Soo R, Botté ES, Vogel N, Uthicke S (2012) Near-future ocean acidification causes differences in microbial associations within diverse coral reef taxa. Environ Microbiol Rep 5:243–251.

Webster NS, Smith LD, Heyward AJ, Watts JEM, Webb RI, Blackall LL, Negri AP (2004) Metamorphosis of a Scleractinian Coral in Response to Microbial Biofilms. Appl Environ Microbiol 70:1213–1221.

Webster NS, Uthicke S, Botté ES, Flores F, Negri AP (2013) Ocean acidification reduces induction of coral settlement by crustose coralline algae. Glob Chang Biol 19:303–315.

Wenzhöfer F, Holby O, Glud RN, Nielsen HK, Gundersen JK (2000) In situ microsensor studies of a shallow water hydrothermal vent at Milos, Greece. Mar Chem 69:43–54.

Witt V, Wild C, Anthony KRN, Diaz-Pulido G, Uthicke S (2011) Effects of ocean acidification on microbial community composition of, and oxygen fluxes through, biofilms from the Great Barrier Reef. Environ Microbiol 13:2976–2989.

Wolf C, Frickenhaus S, Kilias ES, Peeken I, Metfies K (2013) Regional variability in eukaryotic protist communities in the Amundsen Sea. Antarct Sci 11:1–11.

Zhang R, Xia X, Lau SCK, Motegi C, Weinbauer MG, Jiao N (2012) Response of bacterioplankton community structure to an artificial gradient of pCO_2 in the Arctic Ocean. Biogeosciences Discuss 9:10645–10668.

Zinger L, Amaral-Zettler L a, Fuhrman J a, Horner-Devine MC, Huse SM, Welch DBM, Martiny JBH, Sogin M, Boetius A, Ramette A (2011) Global patterns of bacterial beta-diversity in seafloor and seawater ecosystems. PLoS One 6:e24570.

Ziveri P, Passaro M, Incarbona A, Milazzo M, Rodolfo-Metalpa R, Hall-Spencer JM (2014) Decline in coccolithophore diversity and impact on coccolith morphogenesis along a natural CO_2 gradient. Biol Bull 226:282–290.

Acknowledgements

This thesis would not have been possible without the help and support of many people.

I want to thank Antje Boetius and Michael Friedrich for advising me during the last three years and reviewing my thesis, as well as being part of my defense committee together with Claudio Richter, Alban Ramette, Pierre Offre and Cedric Hahn.

Many thanks to Alban Ramette for supervising me regardless of geographic distance. Thank you for introducing me to the world of environmental microbiology, multivariate statistics and bioinformatics.

Thank you, Pierre Offre and Pier Buttigieg, for always being there for my questions, and taking the time to answer them. Your support and advice have been invaluable for this thesis.

Furthermore, I want to thank Dirk de Beer and Katharina Fabricius for their advice throughout my PhD thesis and their support during the cruise to Papua New Guinea. Many thanks also to Anna Lichtschlag and the other participants of the cruises to Papua New Guinea, as well as the captain and crew of the MV Chertan.

Artur Fink, without your data and support, and the endless discussion about our respective PhD topics this thesis would not have been possible.

The financial support for this PhD thesis was provided by the BMBF-funded project Biological Impacts of Ocean Acidification II (BIOACID II), as well as the Max Planck Society (MPG).

There were many more colleagues and fellow students, who supported me during the last three years. Thank you Katy Hoffmann, Viola Krukenberg, Gerdhard Jessen, Marianne Jacob, Verena Carvalho, Halina Tegetmeyer, and Massimiliano Molari, as well as the other members of the Deep-Sea Ecology and Technology group and the Microsensor group at the MPI. Many thanks to the technicians, especially Karin Hohmann, Martina Alisch, Erika Weiz-Bersch, Susanne Menger, and Sabine Kühn, and to Christian Quast, Antonio Fernandez-Guerra and Jan Gerken from the Microbial

Genomics and Bioinformatics group for enduring my many questions about bioinformatics.

And last but not least, my family and friends who stayed with me until the very end …

Appendix

Additional co-author publications

Kegler P, Schwieder HF, Gärdes A, Ferse SCA, Alfiansah YR, Lukman M, Hassenrück C, Kunzmann A (in preparation) Different levels of anthropogenic impact influence coral larvae settlement and related bacterial biofilm communities in the Spermonde Archipelago, Indonesia. Mar Ecol Prog Ser.

Abstract: Recruitment of coral larvae is one of the key factors for coral reef recovery. Biological settlement cues emitted from bacterial biofilms play a vital part in larval settlement and metamorphosis. These cues depend largely on the composition of biofilms, which can change drastically with altered environmental conditions and in turn may affect larval settlement behavior. This study investigated bacterial community composition and coral larval settlement at three sites with differing distance from shore, and thus different levels of human impact and water quality, in the Spermonde Archipelago, Indonesia. Bacteria and coral larvae were investigated on natural reef substrate and on artificial ceramic tiles. Results show that the three sites differed in water quality parameters as well as benthic community composition. Bacterial communities on artificial tiles were similar to those on natural substrate and were comprised of *Gammaproteobacteria, Alphaproteobacteria, Cyanobacteria* and *Flavobacteria* as the most dominant classes. The bacterial communities were strongly correlated with the sites as determined by water quality and benthic community composition, and shifted during incubations at increased temperature. Higher numbers of settlement inducing bacteria of the genus *Pseudoalteromonas* were found on the site furthest from shore. No coral recruits were found at the inshore site with the highest anthropogenic impact. Between the other two sites coral recruitment was similar, with differences on a temporal scale. The spatial settlement pattern at both sites was the same with highest numbers of coral spat on the shaded, lower side of the tile. This study shows that negative anthropogenic influences on water quality affect bacterial community compositions and in turn coral larvae recruitment. It also highlights the importance of taking these often neglected factors into account in evaluating the recovery potential of coral reefs.

Hoffmann K, Carvalho V, Hassenrück C, Bienhold C, Harder J, Boetius A
(in preparation) Response of complex benthic bacterial deep-sea communities to changes in detritus composition reaching the ocean floor.

Pop-Ristova P, Hassenrück C, Molari M, Ramette A, Boetius A, Bühring S
(in preparation) Spatial scaling of bacterial community diversity of shallow hydrothermal vents: a global comparison. ISME J.

Conference presentations

Oral presentations

Hassenrück C*, Fink A*, Tegetmeyer H, Hofmann L, Lichtschlag A, Ramette A, de Beer D (2016) Microbial processes in the sediment at a shallow-water hydrothermal vent in a tropical coral reef. International Coral Reef Symposium, Honolulu, Hawaii, USA, June 19-24, 2016. * equal contributions

Hassenrück C, Fink A, Tegetmeyer H, de Beer D, Ramette A (2015) Microbial community composition and functions in sediments of naturally CO_2-rich coral reefs. ASLO Aquatic Sciences Meeting, Granada, Spain, February 22-27, 2015.

Hassenrück C, Hofmann L, Fabricius K, Bischof K, Ramette A (2013) The effect of ocean acidification on microbial biofilms on tropical coral reefs at natural CO_2 vents in Papua New Guinea (BIOACID WP 3.2). BIOACID II meeting, Warnemünde, October 1-2, 2013.

Hassenrück C, Fabricius K, Boetius A, Ramette A (2013) Effect of ocean acidification on biofilm formation on tropical coral reefs. YouMaRes 4.0, Oldenburg, Germany, September 11-13, 2013.

Posters

Hassenrück C, Fink A, Lichtschlag A, Tegetmeyer H, de Beer D, Ramette A (2015) Biogeochemical and microbial characterization of naturally CO_2-rich reef sediments as in-situ laboratories for ocean acidification research. SAME14, Uppsala, Sweden, August 23-28, 2015.

Hassenrück C, Hofmann LC, Bischof K, Ramette A (2014) Bacterial and eukaryotic communities on seagrass leaves exposed to naturally occurring high pCO_2 conditions. BIOACID II meeting, Kiel, Germany, September 10-11, 2014.

Fink A, Hassenrück C, Lichtschlag A, Glas M, Graziani S, Fabricius K, Ramette A, de Beer D (2013) Temporal and spatial habitat characterization, sediment biogeochemistry and microbial community changes along a natural pH/pCO_2 gradient in a tropical coral reef (WP 3.1). BIOACID II meeting, Warnemünde, Germany, October 1-2, 2013.

Appendix

Cruise Participation

MV Chertan 09.05.2013 – 30.05.2013: Research cruise to Normanby and Dobu Island, Papua New Guinea.

Teaching and Tutoring

Tutor of ‘Symbiosis’ lecture series (Nicole Dubilier, Jillian Petersen), MarMic Program, January 2014.

Tutor of ‘Microbial Oceanography’ lecture series (Antje Boetius, Christina Bienhold), MarMic Program, October 2014.

Teaching assistant ‘Microbial Oceanography’ practical course (Antje Boetius, Alban Ramette, Pier Buttigieg), MarMic Program, October 2013, 2014 and 2015.

Supervisor lab rotation ‘Analysis of functional genes of sediment microbial communities along a pH gradient at natural CO_2 seeps’, student: Nataly Guevara, February – April 2014.

Supervisor lab rotation ‘Microbial communities associated with cold water corals’, student: Cedric Hahn, February – April 2016.

Supervisor TA training ‘Biofilm communities on settlement tiles along pH gradients at CO_2 seeps in Papua New Guinea’, trainee: Linda Geuer, June – July 2014.

Supervisor internship ‘Biofilm communities on settlement tiles along a pH/nutrient gradient in the Kieler Förde’, intern: Patrick Schaal, April – May 2014.

Supervisor internship ‘Effect of ocean acidification and warming on the microbiota of Polar and Atlantic cod’, intern: Ann-Kristin Diekmann, January 2015.

Co-supervisor Master thesis ‘Effects of pH and high inorganic nutrients concentration on microbial community and particle formation in situ’, student: Nataly Guevara, September 2014 – August 2015.

Workshop ‘Analysis of 16S Illumina amplicons’, Center for Marine Tropical Ecology, Bremen, 27.05.2015.

Workshop ‘R roundtable on DNA sequence analysis’, Center for Marine Tropical Ecology, Bremen, 21.1.2016.

Micro B3 Marine Metagenomics Bioinformatics (contribution to course material), EMBL-EBI Genome Campus, Hinxton, GB, September 2015.

Contribution to github code repositories and wiki entries on NGS data analysis.

Christiane Hassenrück
Eutiner Straße 33
28219 Bremen

Bremen, 27.04.2016

Erklärung

Hiermit erkläre ich, dass ich die Doktorarbeit mit dem Titel: ”Implications of ocean acidification for microbial life and for microbial interactions” selbstständig verfasst und geschrieben habe und außer den angegeben Quellen keine weiteren Hilfsmittel verwendet habe. Ebenfalls erkläre ich hiermit, dass es sich bei den von mir abgegebenen Arbeiten um drei identische Exemplare handelt.

Christiane Hassenrück